DOKTORSAVHANDLINGAR
VID
CHALMERS TEKNISKA HÖGSKOLA
Nr 25

CONSOLIDATION OF CLAY, WITH SPECIAL REFERENCE TO INFLUENCE OF VERTICAL SAND DRAINS

A Study Made in Connection with
Full-Scale Investigations at Skå-Edeby

by

SVEN HANSBO

STOCKHOLM 1960

DOKTORSAVHANDLINGAR
VID
CHALMERS TEKNISKA HÖGSKOLA
Nr 25

CONSOLIDATION OF CLAY, WITH SPECIAL REFERENCE TO INFLUENCE OF VERTICAL SAND DRAINS

A Study Made in Connection with Full-Scale Investigations at Skå-Edeby

AV

SVEN HANSBO
teknologie licentiat

AKADEMISK AVHANDLING
SOM MED TILLSTÅND AV CHALMERS TEKNISKA HÖGSKOLA FÖR TEKNOLOGIE DOKTORSGRADS VINNANDE TILL OFFENTLIG GRANSKNING FRAMLÄGGES Å FÖRELÄSNINGSSALEN FÖR FYSIK, GIBRALTARGATAN 5 B, GÖTEBORG, MÅNDAGEN DEN 30 MAJ 1960 KL. 10
AVHANDLINGEN FÖRSVARAS PÅ
ENGELSKA OCH SVENSKA

SWEDISH
GEOTECHNICAL INSTITUTE
PROCEEDINGS
No. 18

CONSOLIDATION OF CLAY, WITH SPECIAL REFERENCE TO INFLUENCE OF VERTICAL SAND DRAINS

A Study Made in Connection with Full-Scale Investigations at Skå-Edeby

By

SVEN HANSBO

STOCKHOLM 1960

Printed in Sweden by
Ivar Hæggströms Boktryckeri AB
Stockholm 1960

Contents

Preface

In connection with plans drawn up by the Swedish Board of Civil Aviation for the construction of a new airport near Stockholm, it was considered advisable that the effect of vertical sand drains on consolidation of soft clay should be studied more closely than before. Accordingly in April 1957 the Swedish Geotechnical Institute was ordered by the Government to establish a test field at Skå-Edeby, 25 km west of Stockholm, under the supervision of a Royal Committee composed of the following members: E. Nelander (Chairman), R. Klingberg, J. Osterman, F. Schütz, and S. Haggård (Secretary).

This test field was designed by the Geotechnical Institute under the supervision of Mr. J. Osterman, who was assisted by Mr. S. Hansbo. The measuring equipment to be used in the field was planned in detail by the Mechanical Department of the Institute under the supervision of Mr. T. Kallstenius.

The draining operations and the application of the overload in the field were carried out by the Swedish Board of Roads and Waterways under the supervision of Mr. K. Lekberg. The installation of measuring equipment in the field was supervised by Mr. E. Norén and Mr. I. Ingelson. The measuring and sampling operations in the field were supervised by Mr. Norén.

The calculations and the preliminary investigations in the field and in the laboratory were superintended by Mr. Osterman, with the assistance of Mr. Hansbo, until September 1957. The results obtained up to that time were published by the Committee on September 4th, 1957, and also by Mr. Osterman, in 1959.

The preliminary results indicated some deviations from existing theories, and it was therefore deemed necessary to carry out supplementary laboratory investigations and to follow up the field investigations started before. Furthermore, it was intended to revise, if possible, the old theories in case they proved to

be inadequate. These investigations were made by Mr. Hansbo. The sampling and measuring operations in the field were supervised, as previously, by Mr. Norén.

The special laboratory equipment designed and constructed for the study of certain consolidation phenomena is substantially a result of team work done by Mr. Hansbo, Mr. A. Wallgren, and Mr. J. Goldschmidt. The detailed design of the equipment is mainly due to Mr. Wallgren. The investigations carried out in the laboratory by means of this equipment were made by Mr. Goldschmidt and Mr. Hansbo, and were superintended by Mr. Hansbo. The routine investigations were made at the Consulting Laboratory of the Institute.

The present report was prepared by Mr. Hansbo. In certain parts, it was discussed with Dr. E. Forslind. The English manuscript was touched up by Mr. I. Cyon.

Stockholm, December, 1959.

Swedish Geotechnical Institute

1. Introduction

10. Introductory Remarks

At the end of the Second World War, plans were drawn up for the construction of a new airport near Stockholm, the intention being to replace the present airport at Bromma, where the runways could not be extended to accomodate the heavy intercontinental airplanes which were expected to come into service. Conditions on various sites, such as Väsby, Halmsjön, and Grillby, were investigated, and Halmsjön was found most suitable. The construction of the Halmsjön airport was started in 1946 and a runway was partly completed. However, the work was not finished.

In 1956, when an order had been placed by the Scandinavian Airlines System for Douglas DC 8 jetplanes, the Swedish Board of Civil Aviation found a new modern airport to be necessary. In the meantime it had been suggested that Halmsjön was situated too far away from Stockholm (about 40 km north of Stockholm) and that some other place nearer to Stockholm was wanted. Ultimately, the choice had to be made between Halmsjön and Skå-Edeby, the latter being situated on an island about 25 km west of Stockholm. On April 5th, 1957, a Royal Committee[1] was appointed to investigate the geotechnical and economic conditions for building an airfield either at Halmsjön or at Skå-Edeby. At Halmsjön the settlement of the above-mentioned runway and also of two test areas in the immediate neighbourhood of the runway had been closely followed until the settling was complete. The geotechnical properties of this area were accordingly well known. On the other hand, the properties of the ground at Skå-Edeby were not considered to be sufficiently known, and test areas were planned in order to examine the effect of sand drains on the time-settlement relation. Funds for this test field were granted on April 12th, 1957, and work was started immediately.

The test field was planned in detail, and was provided with measuring equipment, by the Swedish Geotechnical Institute, while the draining operations and the application of overload were carried out by the Swedish Board of Roads and Waterways. This work was completed at the end of July 1957.

Preliminary results obtained from the test field were published in September 1957 (Utlåtande angående Stockholms storflygplats, 1957). Since the test areas had been finished so very recently, no definite conclusions concerning the consolidation time and the final settlement values were drawn from the results obtained at that time. Later, for economic reasons, the Skå-Edeby project had to be abandoned. In spite of this, the great importance of full-scale con-

[1] Members of the Committee:
E. Nelander (Chairman), R. Klingberg, J. Osterman, F. Schütz, and S. Haggård (Secretary).

solidation tests for future similar projects, and particularly for road construction, made it desirable to continue the field tests at Skå-Edeby, and this was consequently done.

The purpose of the present investigation is to make a study of the consolidation problem as a whole, and also to give the results which have so far been obtained from these full-scale tests.

11. Historical Survey of Consolidation Theories

The phenomenon of consolidation which occurs when a load is applied to a clay layer is an extremely important problem in soil mechanics. Two cases of consolidation are of particular interest in this investigation, *viz.*, (1) consolidation of a clay layer drained at one or both sides, and (2) consolidation of a clay layer provided with drain wells. Existing theories of consolidation generally deal with one or both of these two cases, although the solutions of these cases are sometimes given only as special cases of a more general theory.

This historical survey will deal only with some of those papers which present fundamentally new conceptions of the consolidation phenomenon or new consolidation formulas, whereas papers dealing with particular types of loading or with the mathematical treatment of previously known theories will be left out. Papers referring to the above-mentioned case (1) will first be dealt with even where this does not correspond to the chronological order of publication.

The historical survey includes some formulas which have not been applied to the present investigation. This has been done for the sake of completeness and in order to facilitate the study of the different consolidation theories by using consistent symbols.

Consolidation of Clay Layer Drained at One or Both Sides

Long-time settlements of buildings founded on clayey soils were no doubt first observed long ago, and the causes of settlement seem to have been qualitatively known since the beginning of the nineteenth century (*cf.* LEONARDS and RAMIAH, 1959). In Sweden, settlement measurements were carried out by the Geotechnical Commission of the Swedish State Railways in 1914 to 1922 (STATENS JÄRNVÄGAR, 1922). A consolidometer was constructed, Fig. 1, and the explanation of

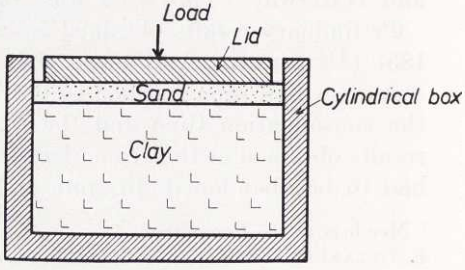

Fig. 1. Consolidometer constructed by the Geotechnical Commission of the Swedish State Railways.

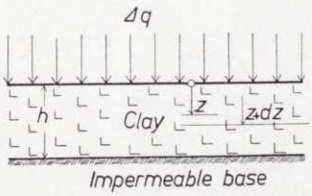

Fig. 2. "Single-drained" clay layer. Location of coordinate z.

the consolidation phenomenon given in the above-mentioned publication is fairly up to date (*cf.* also VIRGIN, 1918).

However, the most important contribution to the solution of this problem was made by TERZAGHI in 1923 and 1925. TERZAGHI's well-known solution is founded on the following basic assumptions:

(1) The clay is saturated and homogeneous.
(2) Pore water flow and deformation take place in one direction only (one-dimensional consolidation).
(3) The clay obeys DARCY's law of permeability. The permeability coefficient k is independent of z.
(4) The pore water and the solids are incompressible as compared with the clay skeleton.
(5) The excess pore water pressure u is equal to the difference between the normal pressure increment $\Delta\sigma$, which is caused by the application of a load, and the corresponding effective intergranular pressure[1] increment $\Delta\bar{\sigma}$.
(6) For a given clay, there is a unique relationship between the effective pressure increment $\Delta\bar{\sigma}$ and the change in void ratio Δe caused by this increment.

For a saturated clay, the change in void ratio in a clay element is equal to the amount of pore water squeezed out of the element as a result of compression. Hence, in the case of a "single-drained" clay layer, Fig. 2, the following equation of one-dimensional consolidation can be deduced

$$c_v \frac{\partial^2 u}{\partial z^2} = \frac{\partial u}{\partial t} \quad \ldots\ldots\ldots\ldots\ldots\ldots\ldots\ldots \quad (1:1)$$

where

c_v = $k\,(1 + e_0)/a_v\,\gamma_w = k/m_v\,\gamma_w$ = coefficient of consolidation,
e_0 = initial void ratio (ratio of volume of voids to volume of mineral grains),
k = DARCY's coefficient of permeability[2],
a_v = $-\Delta e/\Delta\bar{\sigma}$ = coefficient of theoretical compressibility[3], Fig. 3,
m_v = $a_v/(1 + e_0)$ = coefficient of volume compressibility,
γ_w = unit volume weight of pore water,
t = time,
u = excess pore water pressure,
z = distance from the drained surface of the clay layer to the element under consideration, Fig. 2.

[1] In what follows, the latter term is often used in the abbreviated forms »intergranular pressure» or »effective pressure».

[2] TERZAGHI's original consolidation equation gives a different definition of DARCY's coefficient, its value differing from that used in Eq. (1:1) by the factor $(1 + e)$.

[3] The minus sign indicates that e decreases when $\bar{\sigma}$ increases. Strictly, a_v represents the tangent of the slope angle of the compression curve, *i.e.*

$$a_v = -\frac{d\,e}{d\,\bar{\sigma}} = \frac{d\,e}{d\,u}$$

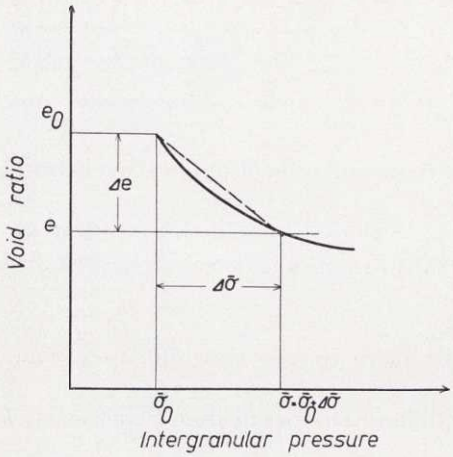

Fig. 3. Void ratio *vs.* vertical intergranular pressure curve for clay. $\bar{\sigma}_0$ represents effective preconsolidation pressure. $a_v = -\Delta e/\Delta\bar{\sigma}$.

An exact solution of Eq. (1: 1) can be obtained if the consolidation index c_v is considered a constant. Thus, in the important case of constant initial excess pore water pressure u_0 throughout the clay layer, we have, for a layer of thickness h, with impermeable base,

$$u = \Delta q \sum_N \frac{2}{N} \sin\left(N\frac{z}{h}\right) \exp\left(-N^2 T_v\right) \ldots\ldots\ldots\ldots \quad (1:2)^1$$

where $T_v = c_v t/h^2 =$ dimensionless factor, called the time factor,
$\Delta q =$ increment of pressure causing consolidation (consolidation load) = initial excess pore water pressure u_0,

$$N = \frac{\pi}{2}, \frac{3\pi}{2}, \frac{5\pi}{2}, \ldots\ldots, \frac{(2m+1)\pi}{2}, \ldots\ldots, \infty$$

The average consolidation ratio of the clay layer

$$\bar{U} = \frac{\delta}{\delta_p} = 1 - \frac{\int_0^h u\, dz}{\int_0^h u_0\, dz} = 1 - \frac{\bar{u}}{\bar{u}_0} \quad \ldots\ldots\ldots\ldots\ldots \quad (1:3)$$

in which

δ = compression at time t,
δ_p = compression of the clay layer obtained when u has finally dissipated

is thus

$$\bar{U} = 1 - \sum_N \frac{2}{N^2} \exp\left(-N^2 T_v\right) \ldots\ldots\ldots\ldots\ldots\ldots \quad (1:4)$$

[1] In Eq. (1: 2) and in what follows e^x is always denoted by the symbol exp x.

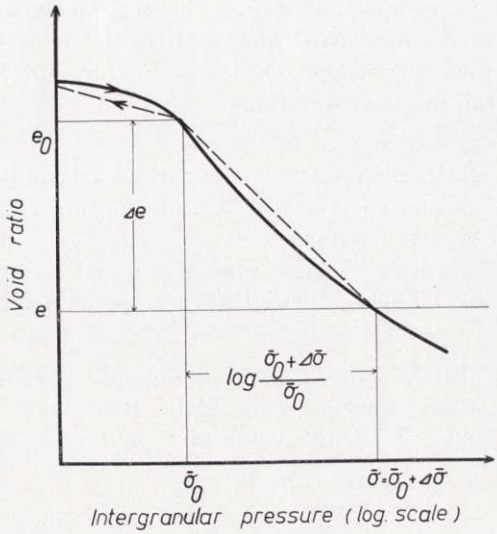

Fig. 4. Void ratio *vs.* logarithm of vertical intergranular pressure curve for clay.

$C_c = -\Delta e / \log \frac{\bar{\sigma}_0 + \Delta\bar{\sigma}}{\bar{\sigma}_0}$.

The final compression $\delta_p = h \frac{a_v}{1 + e_0} \Delta q = h \, m_v \, \Delta q$ is usually computed from the relation between the void ratio and the logarithm of pressure, Fig. 4, which gives

$$\delta_p = h \frac{C_c}{1 + e_0} \log \frac{\bar{\sigma}_0 + \Delta q}{\bar{\sigma}_0} \quad \ldots\ldots\ldots\ldots\ldots\ldots \quad (1{:}5\,a)$$

where C_c is the compression index representing, for a normally consolidated clay, the tangent of the slope angle of the straight part of the e — log $\bar{\sigma}$ curve, the so-called virgin curve, e_0 is the void ratio at the beginning of the consolidation process, and $\bar{\sigma}_0$ is the effective preconsolidation pressure (average for the layer in question)[1].

In Sweden, the laborious void ratio determinations are often avoided by using the relation between strain ε and logarithm of pressure (ODENSTAD, 1954)

$$\delta_p = h \frac{\varepsilon_2}{\log 2} \log \frac{\bar{\sigma}_0 + \Delta q}{\bar{\sigma}_0} \quad \ldots\ldots\ldots\ldots\ldots\ldots \quad (1{:}5\,b)$$

where ε_2 is the compression index representing, for a normally consolidated clay, the additional deformation along the virgin curve due to double load (*cf.* Fig. 60).

Mathematical solutions of TERZAGHI's equation of consolidation for some other important cases of initial excess pore water pressure distribution were given by TERZAGHI and FRÖHLICH in 1936.

[1] It is presupposed that the thickness h of the layer is not too large and that the variation of $\bar{\sigma}_0$ and Δq within the layer is reasonable. Otherwise, it is suggested that the layer should be divided into thinner layers which are studied separately. In particular, this has to be considered when the clay layer is situated just below the dry crust.

A relation taking into account a linear increase in $\bar{\sigma}_0$ with the depth z was deduced by ODENSTAD, 1954.

An important contribution to the elucidation of the consolidation problem was made by BIOT, who treated the case of three-dimensional consolidation for saturated clays[1] (1935) and later also for non-saturated clays (1941) on the following assumptions:

(1) Isotropy of the clay[2].
(2) Reversibility of stress-strain relation under final equilibrium conditions.
(3) Linearity of stress-strain relation (HOOKE's law).
(4) Small strains.
(5) Incompressible pore water and mineral grains.
(6) The clay obeys DARCY's law of permeability. DARCY's coefficient k is independent of z.

In the case of one-dimensional consolidation, *cf.* Fig. 9 a, the general consolidation equation deduced by BIOT may be expressed in the same form as Eq. (1:1). Then, the value of c_v in Eq. (1:1) should be replaced by c'_v defined by

$$\frac{1}{c'_v} = \frac{\alpha_b^2 \gamma_w}{k} \frac{1-2\nu}{2G(1-\nu)} + \frac{\gamma_w}{Q\,k} \quad \ldots\ldots\ldots\ldots\ldots\ldots \quad (1:6)$$

where α_b and Q = coefficients whose values depend on the degree of saturation,
ν = POISSON's ratio,
G = shear modulus of the clay.

When the clay is saturated, $\alpha_b = 1$ and $Q = \infty$, whence

$$c'_v = \frac{k}{\gamma_w} \frac{2G(1-\nu)}{1-2\nu}$$

For a clay layer of depth h, with impermeable base and rectangular initial excess pore pressure distribution, $u_0 = \Delta q$, the solution of BIOT's consolidation equation becomes

$$u = \Delta q \frac{a_f - a_i}{\alpha_b a_f} \sum_N \frac{2}{N} \sin\left(N \frac{z}{h}\right) \exp\left(-N^2 T_v\right) \quad \ldots\ldots\ldots \quad (1:7)$$

where $a_f = \dfrac{1-2\nu}{2G(1-\nu)}$ is called the final compressibility[3], and

$a_i = \dfrac{a_f}{1 + \alpha_b^2 a_f Q}$ is called the instantaneous compressibility.

At the time t, the compression of the clay layer is

$$\delta = h \Delta q \left[a_f - (a_f - a_i) \sum_N \frac{2}{N^2} \exp\left(-N^2 T_v\right)\right] \quad \ldots\ldots\ldots \quad (1:8)$$

[1] This case was also treated by RENDULIC (1936).

[2] According to BIOT, anisotropy could easily be introduced as a refinement.

[3] BIOT's "final compressibility", a_f, corresponds to TERZAGHI's "volume compressibility", m_v.

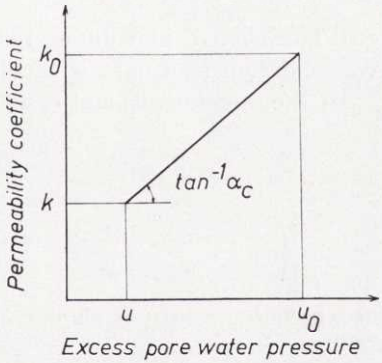

Fig. 5. Relation between coefficient of permeability and excess pore water pressure. (SCHIFFMAN.)

For the solution of more complex consolidation problems, such as consolidation of stratified subsoils and two- or three-dimensional pore water flow, HELENELUND (1951) used the calculus of finite differences. In this way, the consolidation equation can also be solved in the case of varying c_v and for any law of original excess pore pressure distribution. HELENELUND's study is of great practical importance.

The case of varying permeability and time-dependent loading was treated by SCHIFFMAN (1958), who based his equation of consolidation on the following assumptions:

(1) The clay is saturated. Pore water and mineral grains are incompressible.
(2) The clay obeys DARCY's law of permeability instantaneously. The permeability coefficient k is assumed to comply with SCHMID's (1957) relation

$$\overline{k} = \beta\,(n' - n'_0) \quad \ldots\ldots\ldots\ldots\ldots\ldots \quad (1:9)$$

where n' = porosity,
n'_0 = initial porosity,
β = constant,
$\overline{k}$ = average of k.

SCHIFFMAN modified SCHMID's relation as follows:

$$k = k_0 - \nu_c \Delta V_v \quad \ldots\ldots\ldots\ldots\ldots\ldots \quad (1:10)$$

where k_0 = initial value of k,
ν_c = constant,
ΔV_v = change in volume of voids.

Assuming that the relationship between the change in volume of voids and the change in excess pore water pressure is linear, SCHIFFMAN finally obtained, Fig. 5,

$$k = k_0 + \alpha_c(u - u_0) \quad \ldots\ldots\ldots\ldots\ldots\ldots \quad (1:11)$$

where $\alpha_c = \nu_c m_v$ = constant[1],
u_0 = initial value of u.

[1] In SCHIFFMAN's paper, the coefficient of volume compressibility is denoted by m, where $m = -m_v$.

(3) The change in volume due to consolidation bears a linear relation to the consolidation load, and is small as compared with the original volume.

In the one-dimensional case, the equation of consolidation thus becomes

$$\frac{1}{m_v}\frac{\partial}{\partial z}\left(\frac{k}{\gamma_w}\frac{\partial u}{\partial z}\right)+R_u=\frac{\partial u}{\partial t}$$

or

$$\left(c_{v0}-\frac{\alpha_c u_0}{m_v \gamma_w}\right)\frac{\partial^2 u}{\partial z^2}+\frac{\alpha_c}{m_v \gamma_w}u\frac{\partial^2 u}{\partial z^2}+\frac{\alpha_c}{m_v \gamma_w}\left(\frac{\partial u}{\partial z}\right)^2+R_u=\frac{\partial u}{\partial t} \quad \ldots \quad (1:12)$$

in which R_u = rate of change of imposed excess pore water pressure,

$$c_{v0}=\frac{k_0}{m_v \gamma_w}$$

This differential equation is non-linear, and hence complex, but it can be linearized by approximation procedures. One procedure suggested by SCHIFFMAN sets the condition that "the coefficient of permeability is initially constant throughout the soil mass, and that, over a finite increment of time, it is also constant". In other words, this is tantamount to a step-by-step reduction of the consolidation index during the process of consolidation.

SCHIFFMAN also suggested a procedure of approximation in which the following conditions are fulfilled:

$$\begin{cases} k\dfrac{d\,u}{d\,k}=\text{constant}=\dfrac{u_0-u}{\ln\left(\dfrac{k_0}{k}\right)} \\ \dfrac{d\,u}{d\,k}=\dfrac{1}{\alpha_c} \end{cases}$$

This means that u is regarded as a linear function and an exponential function of k at the same time, and that the latter approximates the linear relation.

This approximation leads to a solution of the case of one-dimensional consolidation, which, for a constant initial excess pore water pressure throughout the clay layer and a constant consolidation load, can be presented in the form of Eq. (1:2) if only T_v is replaced by the time factor T_V for variable permeability

$$T_V=\frac{c_V t}{h^2}$$

in which

$$c_V \approx \frac{k_0-k_f}{m_v \gamma_w \ln\left(\dfrac{k_0}{k_f}\right)} \quad \ldots \quad (1:13)$$

SKEMPTON's pore pressure equation[1] (SKEMPTON, 1954; BISHOP and HENKEL, 1957) was applied to the settlement analysis by SKEMPTON and BJERRUM

[1] SKEMPTON's pore pressure equation is usually written

$$\Delta u_w = B\left[\Delta\sigma_3 + A\left(\Delta\sigma_1 - \Delta\sigma_3\right)\right]$$

where Δu_w = pore pressure change (u_w represents total pore water pressure),
$\Delta\sigma_1$ and $\Delta\sigma_3$ = changes in principal stresses,
A and B = "pore pressure coefficients".

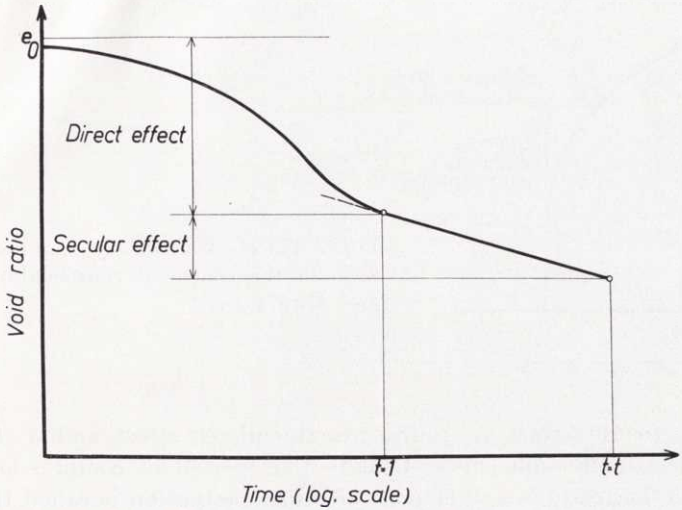

Fig. 6. Consolidation curve for clay. (BUISMAN.)

(1957). The latter authors showed that the consolidation settlement depends on the type and the geological history of the clay, on the thickness of the clay bed, as well as on the shape and the size of the loaded area. The consolidation settlement, as obtained in the conventional oedometer test, should thus be multiplied by a coefficient μ whose value is normally less than unity except for very sensitive clays, where the value of μ may exceed unity. However, if the thickness of the clay bed is small in comparison with the width or the diameter of the loaded area, then, according to the authors, the consolidation settlement can be estimated with reasonable accuracy for any type of clay by a direct application of the oedometer test results.

BRINCH HANSEN (1957) showed on the basis of the theory of elasticity that, among other things, the value of the coefficient A to be used for a given saturated clay is not a constant but depends on the stress history of the clay and on the conditions of deformation.

The consolidation equations presented above give settlement curves which tend asymptotically to finite settlement values, determined by the chosen compressibility values. However, time-settlement curves for buildings founded on clay layers and for laboratory samples submitted to consolidation exhibit in most cases continued settlement even after the end of the given period of settlement. This part of the settlement curve was shown by BUISMAN (1936) to give an approximately straight-line relationship in the e — log t diagram. BUISMAN's formula for the "final settlement" δ_t of a clay layer of depth h is thus time-dependent, and is written, Fig. 6,

$$\delta_t = h \, \Delta q \, (\alpha_p + \alpha_s \log t) \quad \ldots\ldots\ldots\ldots\ldots\ldots \quad (1{:}14)$$

where α_p and α_s are empirically determined constants.

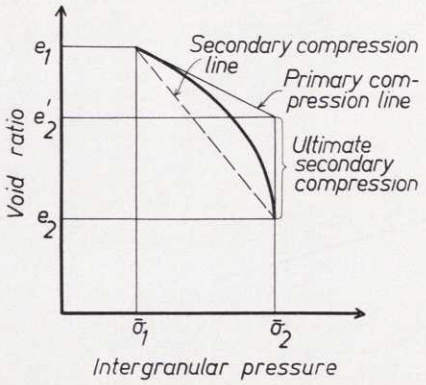

Fig. 7. Effect of secondary compression on void ratio in the course of consolidation. (TAYLOR and MERCHANT.)

According to BUISMAN, α_p represents the direct effect and α_s the secular effect on the compression curve. Usually that period of compression which is considered in TERZAGHI's law of pore pressure dissipation is called the primary or hydrodynamic period, while the subsequent period represents the secondary or secular period.

Formulas combining the results of TERZAGHI's and BUISMAN's investigations were later derived by KOPPEJAN (1948), who gave an expression for the final settlement utilizing Eqs. (1: 5 a) and (1: 14), and by ZEEVAERT (1957), who deduced an expression for the settlement during the complete consolidation process using Eqs. (1: 4) and (1: 14). According to ZEEVAERT, the intersection point of the secondary line and the tangent through the inflection point of the primary settlement curve in the e — log t diagram does not correspond to 100 % primary consolidation as is conventionally assumed, but to a consolidation ratio defined by the time t_a when the rates of settlement $\partial\delta/\partial t$ for primary and secondary consolidation are equal.

BUISMAN's formula was also utilized by ŠUKLJE (1955, 1957), who derived an expression for the pore water pressure at the impermeable base of a "single-drained" layer, u_h, assuming parabolic pore water pressure isochrones and validity of DARCY's law of permeability. Thus, when the time which has passed is so long that u_h has become less than the load increment, he found

$$u_h = \frac{h_s^2 \gamma_w}{4.61\, k} \frac{\alpha_e (1 + \bar{e})}{t} \qquad \text{(1: 15)}$$

where h_s = that part of thickness h which corresponds to solid substance,
$\bar{e}$ = average void ratio at the time t,

$$\alpha_e = \lim_{\Delta t \to 0} \frac{\Delta e}{\log \frac{t + \Delta t}{t}}$$

The first published attempt to determine theoretically the influence of secular effects on the consolidation process was made by TAYLOR and MERCHANT (1940). If the void ratio e is expressed by a function of the effective inter-

granular pressure $\bar{\sigma}$ and the time t, $e = f(\bar{\sigma}, t)$, then the rate of compression is defined by

$$\frac{d\,e}{d\,t} = \frac{\partial e}{\partial t} + \frac{\partial e}{\partial \bar{\sigma}} \frac{d\,\bar{\sigma}}{d\,t} \quad \ldots\ldots\ldots\ldots\ldots\ldots \quad (1:16)$$

Here TAYLOR and MERCHANT postulate that the rate of secular compression is proportional to the yet undeveloped secular compression[1] (*cf.* Fig. 7), *i.e.*

$$\frac{\partial e}{\partial t} = -\mu_c \, \delta'_s \quad \ldots\ldots\ldots\ldots\ldots\ldots \quad (1:17)$$

where μ_c = constant,
δ'_s = undeveloped part of secular compression.

A solution of Eq. (1:16), combined with Eq. (1:17), is given in the special case of constant $\partial e / \partial \bar{\sigma} = -a_v$ [a_v is the coefficient of primary (theoretical) compressibility] and this case is met with if $\mu_c t$ is assumed to be zero. According to the authors, this simplification involves only minor inaccuracies at small values of $\mu_c t$. Introducing the "aggregate consolidation ratio" $\bar{U}_a$ referred to the combination of primary and secondary changes in void ratio, the following solution is obtained:

$$\bar{U}_a = \frac{\delta}{\delta_f} = 1 - \sum_N \frac{1}{N^2} \left\{ \frac{\Phi_1 + \Phi_2}{r_p N^2} (\Phi_3 - 1) \exp\left[(\Phi_1 + \Phi_2) T_v\right] - \right.$$

$$\left. - \frac{\Phi_1 - \Phi_2}{r_p N^2} (\Phi_3 + 1) \exp\left[(\Phi_1 - \Phi_2) T_v\right] \right\} \quad \ldots\ldots\ldots \quad (1:18)$$

where

$$\Phi_1 = -\frac{1}{2}(F_a + N)^2, \; F_a = \frac{\mu_c a_v \gamma_w}{r_p k (1 + e_0)} h^2$$

$$\Phi_2 = \frac{1}{2}\sqrt{(F_a + N^2)^2 - 4 r_p F_a N^2}$$

$$\Phi_3 = \frac{1}{\Phi_2}(\Phi_1 + r_p N^2)$$

r_p = "primary compression ratio" = ratio of the primary compression to the total compression.

The final settlement δ_f is defined by

$$\delta_f = \frac{a_v}{r_p (1 + e_0)} h \, \Delta q \quad \ldots\ldots\ldots\ldots\ldots\ldots \quad (1:19)$$

TAYLOR (1942) also presented another theory which includes effects of plastic structural resistance during the primary portion of compression but does not cover the secondary portion of compression. The plastic structural resistance

[1] This law of compression, with reference to primary instead of secular compression, was shown by HELENELUND (1951) to hold true during the later stage of the hydrodynamic period, as defined by TERZAGHI.

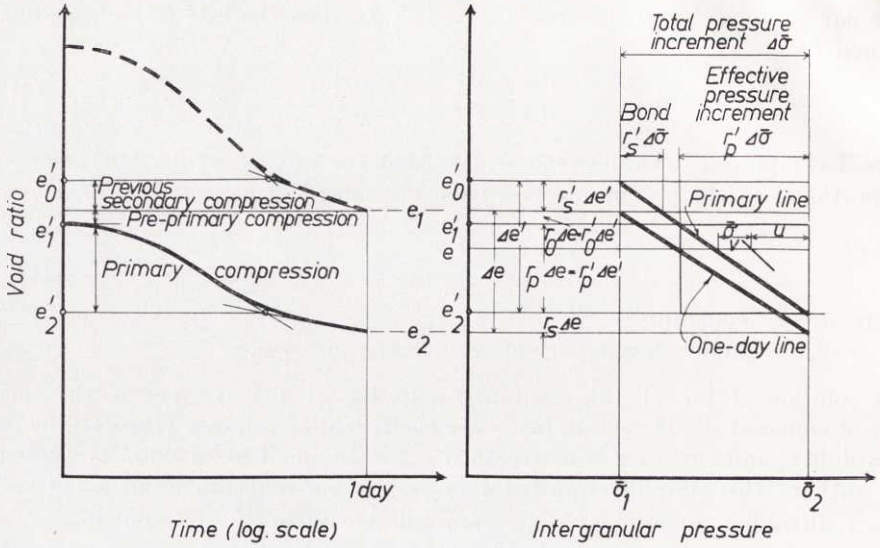

Fig. 8. Primary pressure *vs.* void ratio curve for clay, according to TAYLOR.

of the clay skeleton is resolved into two components, *viz.*, a bond resistance $\bar{\sigma}_b$ and a viscous structural resistance $\bar{\sigma}_v$. The occurrence of bond resistance is ascribed to previous secondary compression during which a structural rearrangement of soil grains into stronger formations has taken place. Therefore, the primary pressure *vs.* void ratio curve based on values obtained in the oedometer test at 100 % primary consolidation (*cf.* CASAGRANDE and FADUM, 1940) at the conventional one-day loading intervals (conventional primary line) practically always involves a certain amount of bond resistance, Fig. 8.

Replacing the coefficient of theoretical compressibility, $a_v = -\frac{\Delta e}{\Delta \bar{\sigma}}$, by

$$e - e'_2 = a\,(u + \bar{\sigma}_v) \quad \ldots\ldots\ldots\ldots\ldots\ldots \quad (1{:}20)$$

where e'_2 = void ratio at the end of primary compression,

$a = \frac{a_v}{r_p}$ = coefficient of total compressibility,

$\bar{\sigma}_v = -\overline{\eta}\frac{\partial e}{\partial t}$

$\overline{\eta}$ = constant of proportionality,

the equation of consolidation, if in other respects founded on TERZAGHI's concepts, becomes

$$\frac{\partial e}{\partial t} - c_p \frac{\partial^2 e}{\partial z^2} - c_p\, a\, \overline{\eta}\, \frac{\partial^3 e}{\partial t\, \partial z^2} = 0 \quad \ldots\ldots\ldots\ldots \quad (1{:}21)$$

where

$$c_p = \frac{k\,(1 + e_0)}{a\,\gamma_w}$$

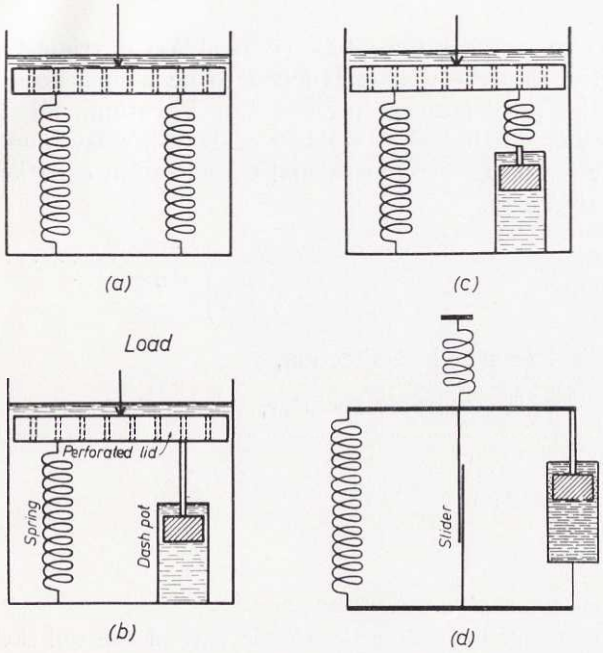

Fig. 9. Rheological models of clay skeleton. (a) BIOT, (b) TAYLOR, (c) TAN, and (d) MURAYAMA and SHIBATA.

The consolidation ratio referred to the primary changes in void ratio, $U = \frac{e'_1 - e}{e'_1 - e'_2}$, differs in this case from the "dissipation ratio", referred to the hydrostatic excess pressure dissipation ratio, $U' = 1 - \frac{u}{r'_p \Delta q}$. Thus, the average consolidation of a single-drained layer of depth h having a rectangular initial excess pore pressure distribution is

$$\bar{U} = 1 - \exp\left(-\frac{T_k}{J}\right) + \sum_N \frac{2}{N^2}\left[\exp\left(-\frac{T_k}{J}\right) - \exp\left(-\frac{T_k}{J + N^{-2}}\right)\right] \quad (1:22)$$

and the dissipation ratio U' is determined by

$$u = r'_p \Delta q \sum_N \frac{2}{N^3 (J + N^{-2})} \sin\left(N \frac{z}{h}\right) \exp\left(-\frac{T_k}{J + N^{-2}}\right) \ldots\ldots\ldots \quad (1:23)$$

where the new variables T_k and J are

$$T_k = \frac{c_p\, t}{h^2}$$

$$J = \frac{c_p\, a\, \bar{\eta}}{h^2}$$

In TAYLOR's consolidation theory, the clay skeleton can be regarded rheologically as a Kelvin body, Fig. 9 b. In order that the secondary after-effects might

also be taken into consideration, TAN (1954, 1957) developed a consolidation theory where the clay skeleton is assumed to be homogeneous and isotropic, and to have the rheological properties of a Poynting and Thomson body, Fig. 9 c. Assuming, furthermore, validity of DARCY's law and incompressible pore water, the following one-dimensional consolidation equation was obtained for a fat saturated clay:

$$\frac{\partial^3 w}{\partial z^3} = \frac{\gamma_w p}{k\left(\Theta + \frac{4}{3}\psi\right)} \frac{\partial w}{\partial z} \quad \ldots\ldots\ldots\ldots\ldots\ldots \quad (1:24)$$

where w = displacement in z-direction,

$p = \frac{\partial}{\partial t}$ = HEAVISIDE's operator,

$\Theta = \frac{2\,G(1+\nu_e)}{3(1-2\nu_e)}$

$\psi = \frac{G\eta p}{\eta p + G}$

G = modulus of shear,

ν_e = POISSON's ratio for the elastic part of the soil skeleton,

η = shear viscosity of the soil skeleton.

The following solution of Eq. (1:24) is obtained for a "single-drained" clay layer of depth h having a rectangular initial excess pore pressure distribution, $u_0 = \Delta q$,

$$\delta = w(0) = \frac{h\,\Delta q}{\Theta} \sum_N \Bigg[1 - (1-g^2) \exp\left(-\frac{g^2 t}{\mu_s}\right) - \frac{2}{N^2} \frac{(1+g^2\omega) \exp\left(\frac{g^2 \omega t}{\mu_s}\right) - (1-g^2) \exp\left(-\frac{g^2 t}{\mu_s}\right)}{\omega + 1} \Bigg] P(\omega, \lambda_s)_{\omega_{1,2}} \ldots \quad (1:25)$$

and

$$u = \Delta q \sum_N \frac{2}{N} \sin\left(N\frac{z}{h}\right) \exp\left(\frac{g^2 t}{\mu_s}\right) P(\omega, \lambda_s)_{\omega_{1,2}} \quad \ldots\ldots \quad (1:26)$$

where $g^2 = \frac{1+\nu_e}{3(1-\nu_e)}$

$\mu_s = \frac{\eta}{G}$

$\lambda_s = -\frac{c'_v \mu_s}{h^2} N^2, \quad c'_v = \frac{k}{\gamma_w} \frac{2\,G(1-\nu_e)}{1-2\nu_e}$

$\omega_{1,2} = \frac{-(1-\lambda_s) \pm \sqrt{(1-\lambda_s)^2 + 4\,g^2\lambda_s}}{2\,g^2}$

$P(\omega, \lambda_s) = \frac{(\omega+1)\,\lambda_s}{g^2\omega^2 + \lambda_s}$

In Eqs. (1:25) and (1:26), δ and u should be computed as the sums of their values for ω_1 and ω_2.

Eq. (1:25) shows that the final settlement determined according to TAN is one to three times that computed according to BIOT.

For the theoretical solution of the case of secondary consolidation MURAYAMA and SHIBATA (1959) applied the rheological model given in Fig. 9 d.

Consolidation of Clay Layer Provided with Drain Wells

According to BARRON (1948), that equation of unsteady flow of heat which is identical with the consolidation equation in the case of symmetrical radial flow in planes at right angles to a drain well, Fig. 10, was first deduced and solved by GLOVER (1930)[1].

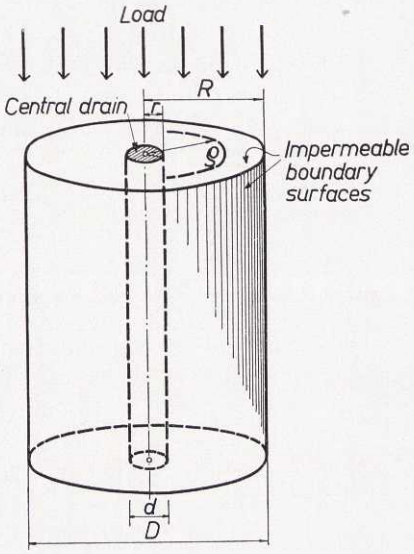

Fig. 10. Zone of influence of drain well in radial consolidation.

BARRON made the following basic assumptions:

(1) The clay is saturated and homogeneous.
(2) All compressive strains within the soil mass occur in a vertical direction.
(3) No vertical pore water flow.
(4) Validity of DARCY's law of permeability. The permeability coefficient k is independent of ϱ.
(5) The pore water and the mineral grains are incompressible in comparison with the clay skeleton.
(6) The load increment is initially carried by excess pore water pressure u.
(7) No excess pressure in the drain well.
(8) The zone of influence of each well is a cylinder.

[1] It has not been possible for the Author to procure a copy of GLOVER's paper.

In cylindrical coordinates the consolidation equation becomes

$$\frac{\partial u}{\partial t} = c_h \left(\frac{1}{\varrho} \frac{\partial u}{\partial \varrho} + \frac{\partial^2 u}{\partial \varrho^2} \right) \quad \ldots\ldots\ldots\ldots\ldots\ldots \quad (1:27)$$

where c_h = consolidation index for horizontal pore water flow,
u = excess pore water pressure at the time t,
ϱ = radius vector from the central axis.

Later Eq. (1:27) was independently deduced and solved by RENDULIC (1935), who also verified the solution experimentally.

A careful analysis of Eq. (1:27) was made by BARRON (1944, 1948), who also investigated the effect of well resistance and smear, *i.e.* influence of a remoulded zone formed around the drains during driving. BARRON showed that the simplified extreme case of equal vertical strains[1] gives almost the same numerical value of the average consolidation as does the more complicated extreme case of free strain. This simplification had also been made previously by KJELLMAN in 1937 (1948; STATENS GEOTEKNISKA INSTITUT, 1949). His solution for radial drainage under the boundary conditions $u = 0$ at $\varrho = d/2$ and $\partial u / \partial \varrho = 0$ at $\varrho = D/2$ may be written[2]

$$\bar{u} = \bar{u}_0 \exp \left[- \frac{8\, T_h}{F\left(\frac{d}{D}\right)} \right] \quad \ldots\ldots\ldots\ldots\ldots\ldots \quad (1:28)$$

in which $T_h = \dfrac{c_h\, t}{D^2}$, $\bar{u}$ = average of u.

Thus, the time of consolidation, t, is

$$t = \frac{D^2}{8\, c_h} F\left(\frac{d}{D}\right) \ln \frac{1}{1 - \bar{U}} \quad \ldots\ldots\ldots\ldots\ldots\ldots \quad (1:29)$$

where $F\left(\dfrac{d}{D}\right) = \dfrac{1}{1 - \left(\dfrac{d}{D}\right)^2} \ln \left(\dfrac{D}{d}\right) - \dfrac{3}{4} + \dfrac{1}{4} \left(\dfrac{d}{D}\right)^2$

c_h = coefficient of consolidation for horizontal pore water flow (assumed to be constant throughout the consolidation process),
D = diameter of zone of influence of a drain well ($= 2R$),
d = diameter of drain well ($= 2r$),
$\bar{U}$ = average consolidation ratio.

In the case of free strain and radial drainage only, and under the previously given boundary conditions, the excess pore water pressure at any point ϱ is (BARRON, 1944)

[1] In this case the left-hand member of Eq. (1:27) should be replaced by $\dfrac{\partial \bar{u}}{\partial t}$, where $\bar{u}$ is the average of u.

[2] A comparison between different methods of solution was made by ODENSTAD in 1947. He compared KJELLMAN's solution with other solutions, *e.g.* that of the corresponding flow-of-heat equation, and found the difference in results to be negligible.

$$u = u_0 \sum_{a_1, a_2, \ldots}^{\infty} \frac{\frac{2}{a}\left[J_1(a)\,Y_0(a) - Y_1(a)\,J_0(a)\right]\left[J_0\left(\frac{a\varrho}{r}\right)Y_0(a) - Y_0\left(\frac{a\varrho}{r}\right)J_0(a)\right]}{\left(\frac{D}{d}\right)^2\left[J_0\left(\frac{aD}{d}\right)Y_0(a) - Y_0\left(\frac{aD}{d}\right)J_0(a)\right]^2 - \left[J_1(a)\,Y_0(a) - Y_1(a)\,J_0(a)\right]^2} \cdot$$

$$\cdot \exp\left[-4\,a^2\left(\frac{D}{d}\right)^2 T_h\right] \quad \ldots\ldots\ldots\ldots\ldots\ldots \quad (1:30)$$

where the initial excess pore pressure u_0 is assumed to be constant throughout the soil,

J_0 ( ) and J_1 ( ) are Bessel functions of first kind of zero and first order, respectively,

Y_0 ( ) and Y_1 ( ) are Bessel functions of second kind of zero and first order, respectively,

$a_1, a_2, \ldots$ are roots of the equation

$$J_1\left(\frac{aD}{d}\right)Y_0(a) - Y_1\left(\frac{aD}{d}\right)J_0(a) = 0$$

The radial consolidation rates at different concentric surfaces obtained in this case for $\frac{D}{d} = 10$ are shown in Fig. 11.

The average degree of consolidation[1] is found from

$$\bar{U} = 1 - \frac{\int_r^R u\,\varrho\,d\varrho}{\int_r^R u_0\,\varrho\,d\varrho} = 1 - \frac{\bar{u}}{\bar{u}_0} \quad \ldots\ldots\ldots\ldots \quad (1:31)$$

As was shown by BARRON (1948), the consolidation time could be considerably increased by smear or well resistance or both. However, according to KJELLMAN (1948), the influence of these factors for a clay without coarse-grained layers is comparatively small.

The calculus of finite differences was applied by RICHART (1957).

SCHIFFMAN (1958) considered the case of equal strain and varying permeability or varying load, or both (*cf.* p. 13).

For constant load, varying permeability, and radial drainage only, the following equation of consolidation is obtained for a saturated clay:

$$\left(c_a\,\frac{\bar{u}}{\bar{u}_0} + c_f\right)\left(\frac{\partial^2 u}{\partial \varrho^2} + \frac{1}{\varrho}\,\frac{\partial u}{\partial \varrho}\right) = \frac{\partial \bar{u}}{\partial t} \quad \ldots\ldots\ldots\ldots \quad (1:32)$$

in which $c_a = \frac{k_0 - k_f}{m_v \gamma_w}$, $\quad c_f = \frac{k_f}{m_v \gamma_w}$

Introducing the boundary conditions

$u = 0$ at $\varrho = r$, and

$\frac{\partial u}{\partial \varrho} = 0$ at $\varrho = R$,

[1] Degree of consolidation = consolidation ratio.

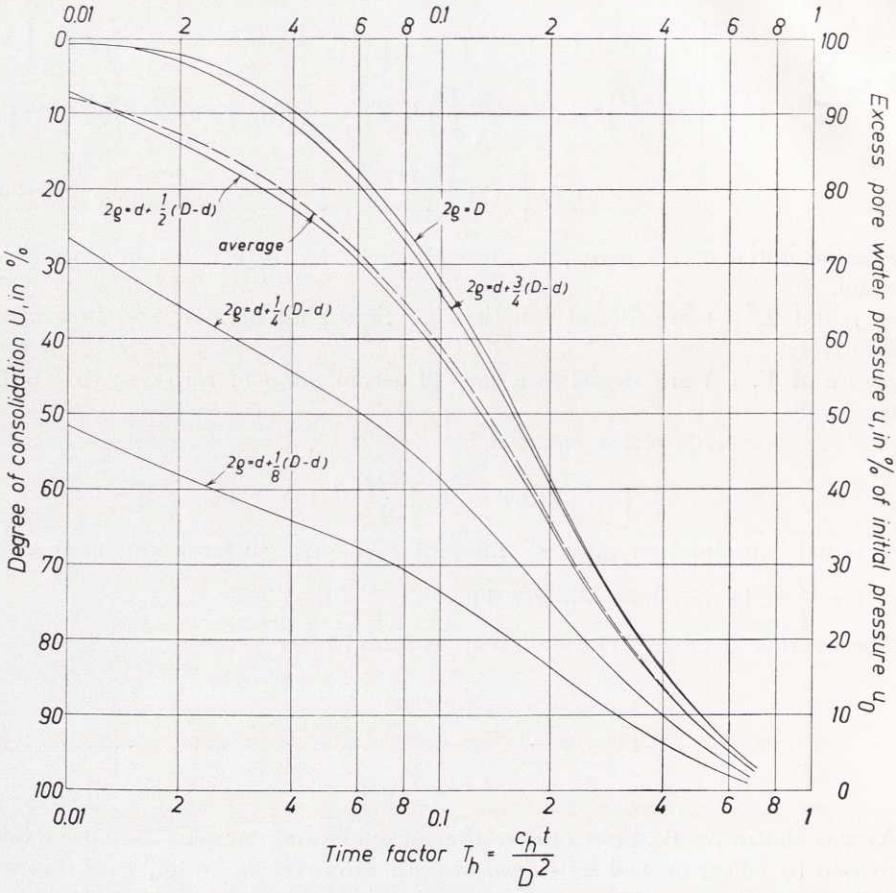

Fig. 11. Radial consolidation rates at different concentric surfaces. (BARRON.)
"Free strain" hypothesis.

we obtain the solution

$$\bar{u} = \frac{\bar{u}_0 \, k_f}{k_f + k_0 \left(\frac{\bar{u}_0}{\bar{u}_2} - 1 \right)} \qquad \text{(1:33)}$$

where $\bar{u}_2 = \bar{u}_0 \exp \left[- \frac{8 \, T_f}{F\left(\frac{d}{D}\right)} \right]$

$F\left(\frac{d}{D}\right)$ as above

$T_f = \frac{c_f \, t}{D^2}$

Eq. (1:33) can be rewritten

$$\bar{U} = 1 - \frac{k_f}{k_f + k_0 \left\{ \exp\left[\frac{8\, T_f}{F\left(\frac{d}{D}\right)} \right] - 1 \right\}} \quad \ldots\ldots\ldots\ldots \quad (1:34)$$

Thus, using SCHIFFMAN's concept of linear variation in average permeability, Fig. 5, a solution is obtained in terms of initial and final permeability coefficients, whose values have to be known.

SCHIFFMAN has also extended his theory so as to include the effect of smear.

If the solutions of Eq. (1:1) and Eq. (1:27) are known, then the solution of the three-dimensional flow equation

$$\frac{\partial u}{\partial t} = c_v \frac{\partial^2 u}{\partial z^2} + c_h \left(\frac{\partial^2 u}{\partial \varrho^2} + \frac{1}{\varrho} \frac{\partial u}{\partial \varrho} \right) \quad \ldots\ldots\ldots\ldots \quad (1:35)$$

is easily found according to CARRILLO (1942). Thus, if under certain specified boundary conditions $u_z/u_0 = f_1(z, t)$ is a solution of Eq. (1:1) and $u_\varrho/u_0 = f_2(\varrho, t)$ is a solution of Eq. (1:27), then under same boundary conditions $u/u_0 = (u_z/u_0)(u_\varrho/u_0)$ is the solution of Eq. (1:35). The latter solution is also applicable to the average excess pore water pressure.

12. Discussion

As regards the mathematical treatment of the consolidation equation, it was generally assumed that the coefficient of consolidation of the clay remains constant throughout the consolidation process. This approach led to the classical solution of the equation of consolidation (TERZAGHI, 1923, 1925; BIOT, 1941). The disagreement between theoretical and actual rate of consolidation was ascribed to difficulties in taking representative and undisturbed samples for consolidometer tests and to visco-elastic phenomena or plastic behaviour of the clay. Theories were thus developed on the basis of visco-elastic concepts (TAYLOR, 1942; TAN, 1954), but these theories resulted in very intricate equations, which are at present almost entirely of academic interest.

The assumption of a constant value of the coefficient of consolidation throughout the consolidation process has been questioned occasionally but is considered to be fairly reasonable for inorganic clays (*cf.* HELENELUND, 1951; BUISSON, 1953).

SCHIFFMAN's approach is equivalent to a decrease in coefficient of consolidation c_v (c_h) with the time of consolidation. This has been noticed in experiments with highly compressible soils, such as mud and peat (HELENELUND, 1951), and in studying results obtained in practice. Experiments indicate, however, that the value of c_v (c_h) increases at a given initial void ratio with increasing magnitude of the load increment that produces the consolidation (TERZAGHI and PECK, 1948), and this phenomenon is not explained by SCHIFFMAN's theory.

One of the reasons for the discrepancy between theoretical and practical results that is at times observed seems to lie in the basic assumption of unlimited validity of DARCY's law of permeability for clays[1]. The possibility of deviations from this law has been suggested by several authors[2] (see *e.g.* BRENNER, 1946; SILFVERBERG, in STATENS GEOTEKNISKA INSTITUT, 1949; BUISSON, 1953). Later experiments on permeability of clay soils have revealed a break-down of DARCY's law for low porosities (WINTERKORN, 1954; SCHMID, 1957) and in the case of low hydraulic gradients (SILFVERBERG, in STATENS GEOTEKNISKA INSTITUT, 1949; BUISSON, 1953; KÉZDI, 1958)[3]. This is of great importance and has to be considered in studying the consolidation phenomenon.

Moreover, thixotropic phenomena may influence the rate of pore pressure dissipation, particularly in the beginning of the consolidation process.

In the Author's opinion the application of the theory of elasticity to the solution of the consolidation problem may give rise to a false and misleading conception of the consolidation phenomenon. As is well known, a certain degree of elasticity of clay does exist, but consolidation is undoubtedly a phenomenon of successive internal shear overstress[4] rather than a phenomenon of pure elasticity. The incongruity of assuming clay to be purely elastic throughout the consolidation process (see *e.g.* BIOT, 1935 and 1941) is made evident by the results obtained by JOSSELIN DE JONG (1957) in the case of a semi-infinite solid loaded uniformly over a circular area of its surface, and also by the results obtained by GIBSON and MCNAMEE (1957) in the case of a rectangular uniformly loaded area on the surface of a semi-infinite solid. Thus assuming a given constant value of the modulus of shear G, the final consolidation settlement will never exceed the instantaneous elastic settlement which is attained only when POISSON's ratio ν tends to zero. Practical results show that an apparent decrease of G is necessary if the result is to hold true, whereas, reasonably, increasing consolidation would cause apparently increasing G.

The final consolidation settlement δ_p, *cf.* Eqs. (1: 5 a–b), is in general considered to represent fairly well the compression obtained in a natural clay deposit under the action of a superimposed load except where the thickness of the clay layer is large in comparison with the diameter of the loaded area (*cf.* BUISSON, 1953; SKEMPTON and BJERRUM, 1957).

The correction factor μ introduced by SKEMPTON and BJERRUM (1957) may be necessary in certain cases when dealing with consolidation of an undisturbed

[1] DARCY's law of permeability (DARCY, 1856) was originally established for saturated silicious sand from the river Saône, having a pore volume of approximately 38 %.

[2] As early as in 1944, DERYAGIN and KRYLOV proved experimentally the non-validity of DARCY's law for ceramic and carbon filters having a maximum average pore diameter of 0.1μ. In some cases they even found the existence of a threshold value of the hydraulic gradient which had to be exceeded before flow took place.

[3] The excellent monograph on flow through porous media presented by SCHEIDEGGER (1957) gives an idea of the present state of knowledge about the physical principles of hydrodynamics in porous media. In his book, SCHEIDEGGER also discusses the chemico-physical causes of anomalies with respect to DARCY's law.

[4] The term "internal shear overstress" is used here to denote the rearrangement of mineral grains occurring as a result of a disturbance of the internal state of equilibrium.

clay layer. However, for a clay layer provided with vertical sand drains, the disturbance due to driving of drains will cause additional settlements, which are not yet accurately known. Therefore, in this case the practical utility of the factor μ may be questioned.

Moreover, in the case of clay of high plasticity μ is difficult to find in the laboratory. Thus, for a saturated clay, μ depends, according to the authors, on (1) SKEMPTON's pore pressure coefficient A (*cf.* p. 14), and (2) the size and the shape of the loaded area.

The value of the coefficient A has been determined by pore pressure measurements in the undrained triaxial test. For a normally consolidated clay, the value of A has generally been found to vary from 0.5 to 1 but A may exceed unity for a quick clay.

However, the pore pressure measurements carried out in the triaxial test are not reliable in dealing with clays of high plasticity. This is partly due to the measuring device. Thus, a relatively large amount of air will be trapped between the rubber membrane and the sample even if great precautions are taken against this (*cf.* BISHOP and HENKEL, 1957, p. 180). Moreover, the capillaries and the filters are filled with water in a way that is not satisfactory because air may be trapped in them. Trapped air can cause considerable errors in pore pressure measurements. In those carried out by the Author (*cf.* Section 21), even a small amount of air trapped in the capillaries made quick and reliable measurements impossible. Nothing but vacuum treatment was sufficient to exhaust the air from the capillaries in the desired degree.

Another cause of the unreliability of the results lies in a possible variation in pore pressure at different points of the specimen. Such a variation might result in considerable errors, particularly below the preconsolidation pressure (*cf.* Section 21).

Other difficulties are also involved (*cf.* BRINCH HANSEN, 1957; SKEMPTON and BISHOP, 1954).

It is evident that the determination of the coefficient A in the laboratory can be impaired by errors, which are difficult to predetermine.

2. Investigation of Consolidation Process by Means of Consolidometer Tests

20. Introduction

Laboratory investigations of the consolidation process are carried out by means of oedometer tests or other similar consolidometer tests. In this paper, "oedometer" will stand for the conventional type of consolidometer with drainage of the sample at top or bottom or both, while "consolidometer" will stand for another type of consolidometer used at the Institute, with drainage by a central cylindrical drain, and for a consolidometer in general.

During a consolidometer test, a clay specimen is subjected to a known axial pressure and to a lateral pressure whose magnitude may be estimated from the condition that no lateral deformations of the specimen are allowed to take place. In reality the axial pressure is affected by "friction"[1] between the sample and the consolidometer ring, whatever precautions are taken to prevent it. However, this source of error may usually be reduced to a negligible order of magnitude.

Of course it is important to know as well as possible the influence of these and other factors in order to be able to interpret the results of consolidometer tests and to use them for practical purposes.

Laboratory research on consolidation of clay, such as pore water pressure investigations, investigations of friction between the sample and the consolidometer ring, investigations of disturbance developed in sample preparation, *etc.*, has been carried out by several authors (RUTLEDGE, 1939; TAYLOR, 1942; VAN ZELST, 1948; MUHS and KANY, 1954; ARAI, 1955; *etc.*). The purpose of the present investigation is to study in the laboratory the excess pore water pressure created in a saturated clay during the oedometer test and to examine the amount of friction between the soil sample and the oedometer ring.

21. Variation of Pore Water Pressure during Consolidation Process

Description of Test Apparatus and Testing Procedure

The pore water pressure measurements were carried out in two different types of apparatus.

In the first type of apparatus, shown in Fig. 12 a, drainage is allowed by a filter disc covering the piston plate of the oedometer, the conditions of consolidation in the sample being in all other respects the same as those in the standard oedometer test. By using a special device, the pore water pressure can be measured at the impermeable base of the sample at three different distances from the centre of the bottom plate. Thus three concentric filter rings made of porous glass are enchased in the bottom plate of the consolidometer, and are connected by means of glass capillaries to a counter-pressure regulator, making it possible to measure the water pressures in the filters when the condition of no pore water flow through the filters is fulfilled. The filter rings are 3 mm in width, and 18, 36, and 54 mm in mean diameter. The capillaries are 0.30 mm in inside diameter, and are provided with millimetre scales and stop cocks. The flow of water through the capillaries can be observed by the travel of a gas bubble produced in them. When the pore water pressure is to be measured in a filter, the stop cock of the capillary belonging of this filter is opened, and the outer counter-pressure is controlled in such a way that the inner end of the gas bubble is kept in a constant position.

In the second type of apparatus, shown in Fig. 12 b, drainage is allowed by a filter disc covering the fixed base of the oedometer, and the pore water pressures

[1] The term "friction" is used here, and in what follows, in the sense of bond rather than in the sense of pure friction.

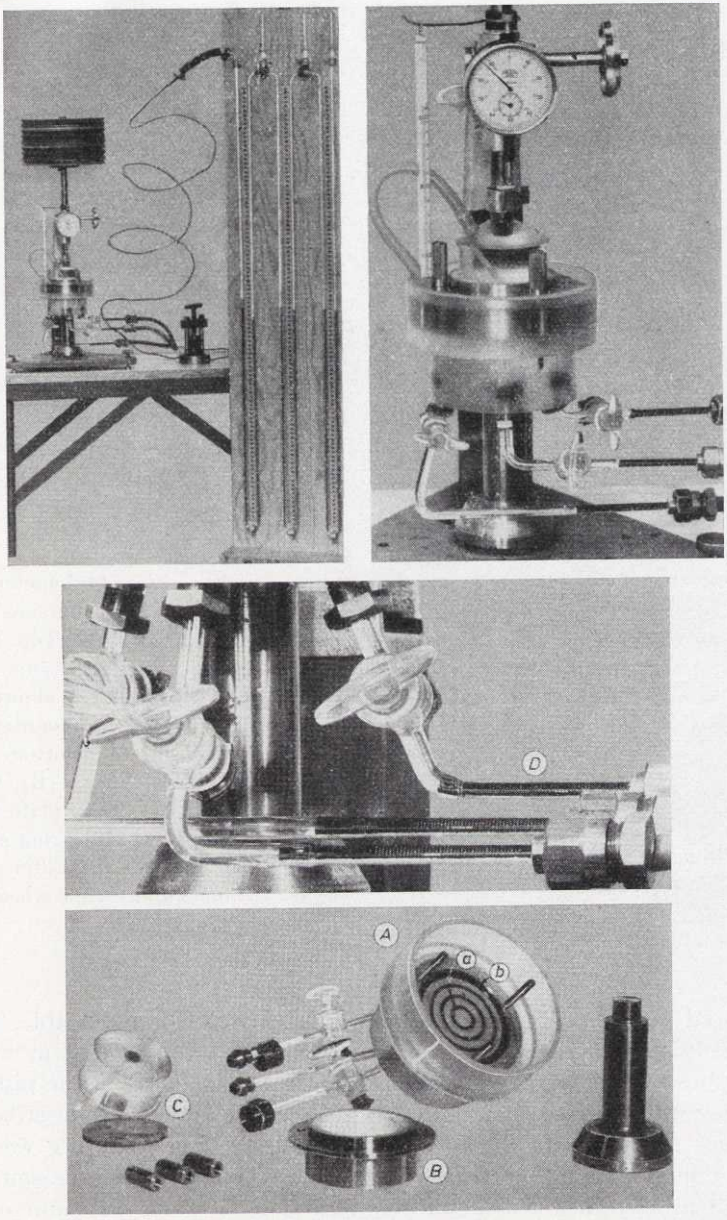

Fig. 12 a. Oedometer used for pore water pressure investigations. Type I. Left-hand top, from left to right: Oedometer, counter-pressure regulator (pressure balance), and mercury manometer. Right-hand top: Oedometer with capillaries, dial gauge, thermometer, and water bath surrounding oedometer ring. Details: (A) Bottom plate with capillaries ("Measuring part"). (a) Filter rings. (b) Enchased rubber ring. (B) Oedometer ring. (C) Piston plate and top filter ("Dewatering part"). (D) Glass capillaries with millimetre scales and stop cocks. Air bubbles visible in graduated part of capillaries.

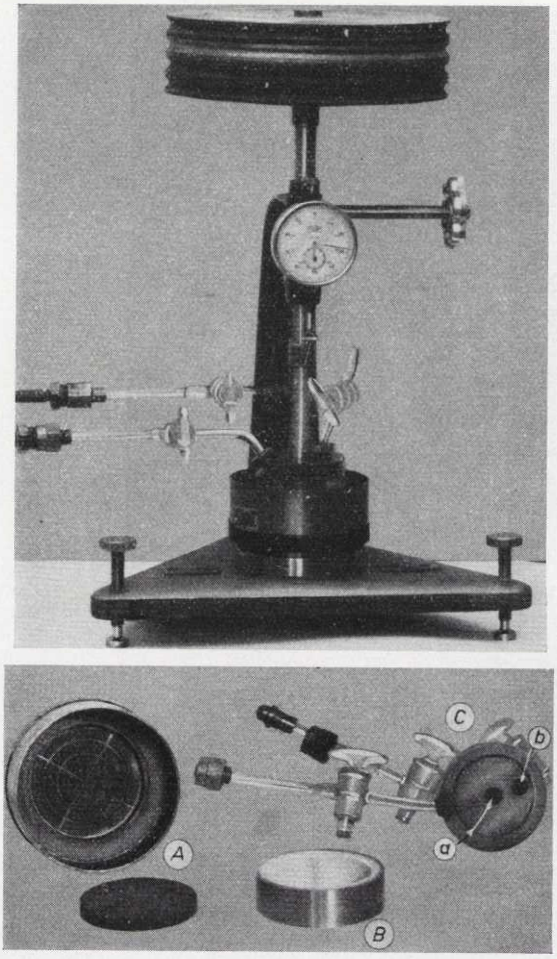

Fig. 12 b. Oedometer used for pore water pressure investigations. Type II. Top: Oedometer with two measuring capillaries and capillary allowing water escape when mounting sample. Bottom: (A) Bottom plate and bottom filter. (B) Oedometer ring. (C) Piston plate with capillaries. (a) Filter ring and central filter disc. (b) Filter disc allowing water escape when mounting sample.

are measured at the piston plate, which is in this case impermeable. A central filter disc, 12 mm in diameter, and an outer filter ring, 2 mm in width and 48 mm in mean diameter, made of porous glass are enchased in the piston plate, and the pore water pressures are studied in the same manner as described above.

To reduce friction between clay and oedometer ring, the ring was greased inside with molybdenum sulphide. Furthermore, for the same reason but also in order to prevent physico-chemical interaction between clay and oedometer ring, its interior part was made of Teflon (polytetrafluorine-ethylene).

The sample was mounted as follows: To begin with, the air was exhausted from the filters and the capillaries. For this purpose, the "measuring part" of the consolidometer, with stop cocks open and glass tubes sealed at their outer ends, and the "dewatering part" of the consolidometer were placed in a vacuum, Fig. 13 a. When vacuum was finally developed, distilled water was poured on

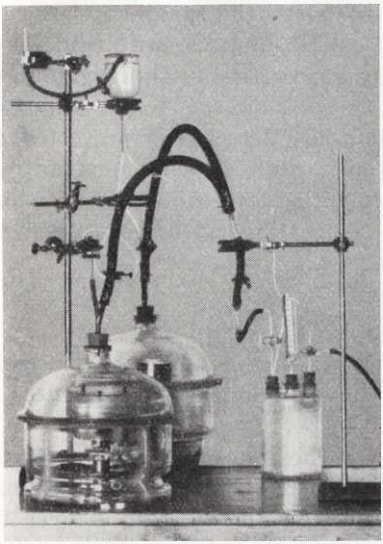

Fig. 13 a. Arrangement for developing vacuum in filters and capillaries. Container at the top, turned upside-down, is used in filling filters and capillaries with water. To the right, a Woulfe vacuum bottle.

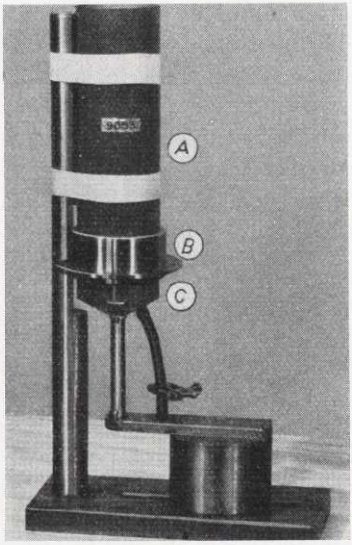

Fig. 13 b. Arrangement for mounting of sample. (A) Sample tube made of glass-fiber-reinforced polyester resin. (B) Oedometer ring. (C) Piston plate.

top of the filters so that, when after this procedure the vacuum container was again filled with air, the water was forced into the filters and the capillaries by the air pressure, and filled them completely.

The sample mounted in the consolidometer ring, the latter being fixed to the piston of the consolidometer during the mounting process, Fig. 13 b, was then brought into contact with the bottom plate, which was covered with water so as to prevent air bubbles from being trapped between the sample and the plate.

Finally, before a capillary was connected with the pressure regulator, the flow-indicating gas bubble was produced in the graduated part of the capillary between the stop cock and the connection point. A length of 4 to 5 mm seemed to be enough for the gas bubble to act as a perfect indicator throughout the test.

Experience showed that the readings had to be taken very swiftly at a large rate of pore water pressure decrease, while at a low rate of decrease, particularly during the secular part of consolidation, every reading required approximately five to ten minutes.

To avoid the influence of varying temperature on the results, the consolidometer ring was surrounded by water whose temperature was kept as nearly constant as possible under the experimental conditions. Thus the observed maximum difference between maximum and minimum temperatures of the water bath was 0.6° C.

Any amount of air, however small, trapped between the sample and the gas bubble in a capillary made it difficult or impossible to take swift readings of the pore water pressure, which were particularly necessary in the beginning of the consolidation process. The presence of entrapped air was to be suspected, especially in the stop cock. However, this was easily detected before a test by varying the counter-pressure with the stop cock shut. If entrapped air was present, then the position of gas bubble varied with the pressure. The vacuum method proved to be the only efficient way of getting rid of entrapped air.

Discussion of Test Results

Some typical results of the measurements are given in Figs. 14 to 16. To facilitate the interpretation of these results they have been partly represented in a more appropriate manner in Figs. 17 and 19 to 20.

The distribution of pore water pressure over the impermeable base of the sample is shown in Fig. 17. When the applied load is below the preconsolidation load, the pore water pressure is fairly uniformly distributed over the central parts of the base, but decreases rapidly towards its periphery, where about zero pressure may occur. The above pore pressure distribution seems to change when the preconsolidation pressure as obtained by CASAGRANDE's method (CASAGRANDE, 1936) is just being exceeded, *cf.* Fig. 18. After this instant the pore pressure is nearly uniformly distributed all over the base. Exceptions to the rule have been found, *e.g.* in the case of Sample 9104. However, for this sample, the preconsolidation pressure is hard to estimate as it has obviously been submitted to considerable disturbance (see Fig. 18).

The results obtained show that the pore pressure distribution over the base of the oedometer is passably representative of that in an infinitely extended and uniformly loaded clay layer submitted to consolidation, only if the preconsolidation load has been exceeded. This should be considered in the case of an overconsolidated clay, where, obviously, the oedometer test may not be representative.

The pore water pressure dissipation obtained above the preconsolidation load from the oedometer test represented in Fig. 14 and that calculated from TERZAGHI's equation of consolidation, Eq. (1: 1)[1], can be compared in Fig. 19. When the load is below the preconsolidation load the dissipation curves given in Fig. 14 bear no resemblance to the theoretical curve, while a certain resemblance is observed when the load is above or equal to the preconsolidation value. However, a decrease in pore water pressure occurs before the instant of decrease determined according to TERZAGHI. The latter phenomenon has always appeared

[1] A better expression for the excess pore water pressure is found if TERZAGHI's equation of consolidation is solved by operational mathematics (see CHURCHILL, 1944). Then, at the impermeable surface, the pore pressure becomes

$$u_h = \Delta q \left[1 - \sum_{m=0}^{\infty} (-1)^m \, 2 \operatorname{erfc} \frac{2m+1}{2\sqrt{T_v}} \right]$$

and this series has a better convergence than has the exponential series, Eq. (1: 2).

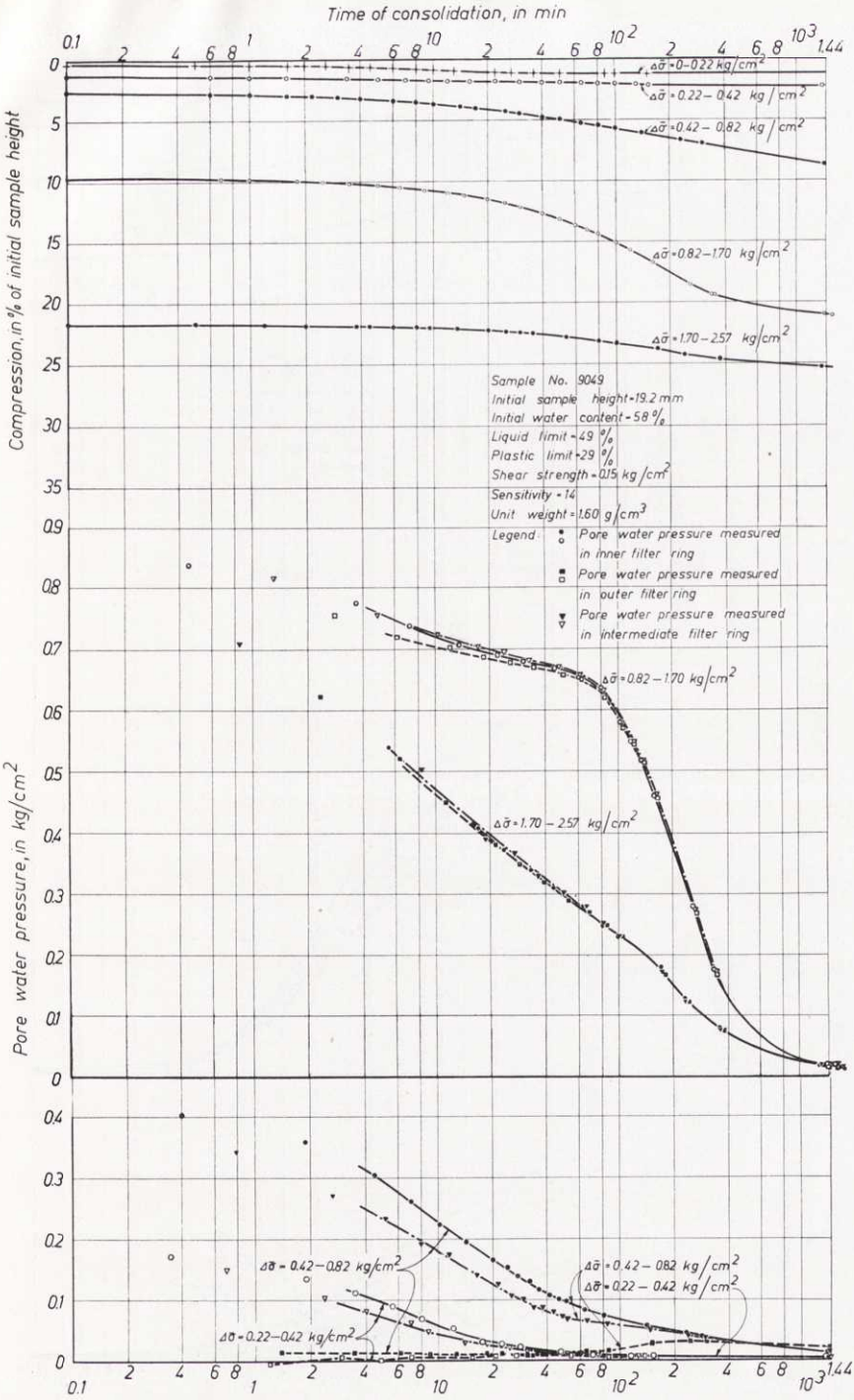

Fig. 14. Pore water pressure dissipation in consolidometer test at impermeable base of clay specimen (or at "midplane" of specimen drained at top and bottom). The respective values of $\Delta\bar{\sigma}$ refer to the loads before and after the application of a new load increment. Observations made by means of oedometer shown in Fig. 12 a. Pore pressures in inner filter ring, full-line curves; in intermediate filter ring, dash-and-dot-line curves; in outer filter ring, dash-line curves.

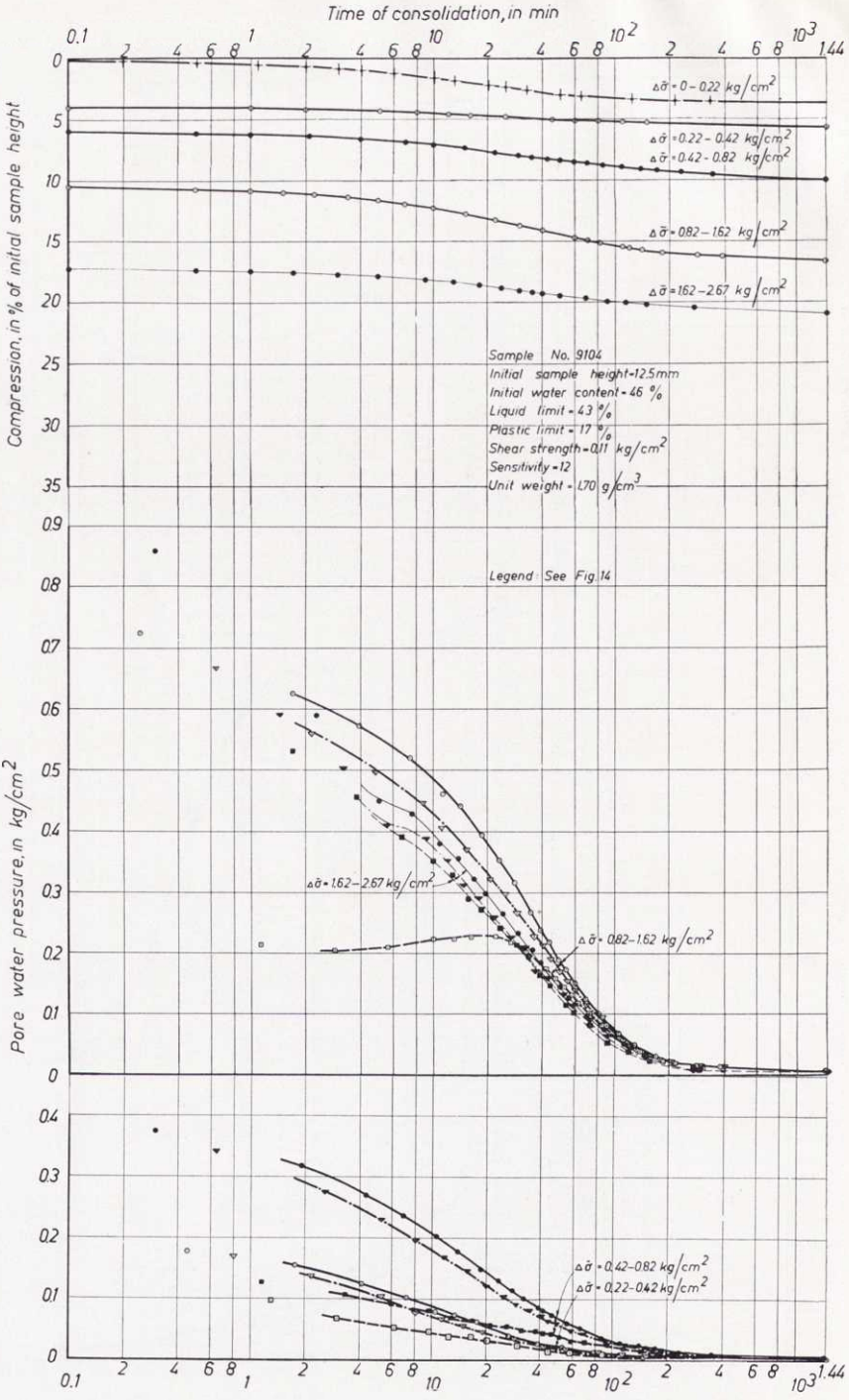

Fig. 15. Pore water pressure dissipation in consolidometer test at impermeable base of clay specimen. The respective values of $\Delta\bar{\sigma}$ refer to the loads before and after the application of a new load increment. Observations made by means of oedometer shown in Fig. 12 a. Pore pressures in inner filter ring, full-line curves; in intermediate filter ring, dash-and-dot-line curves; in outer filter ring, dash-line curves.

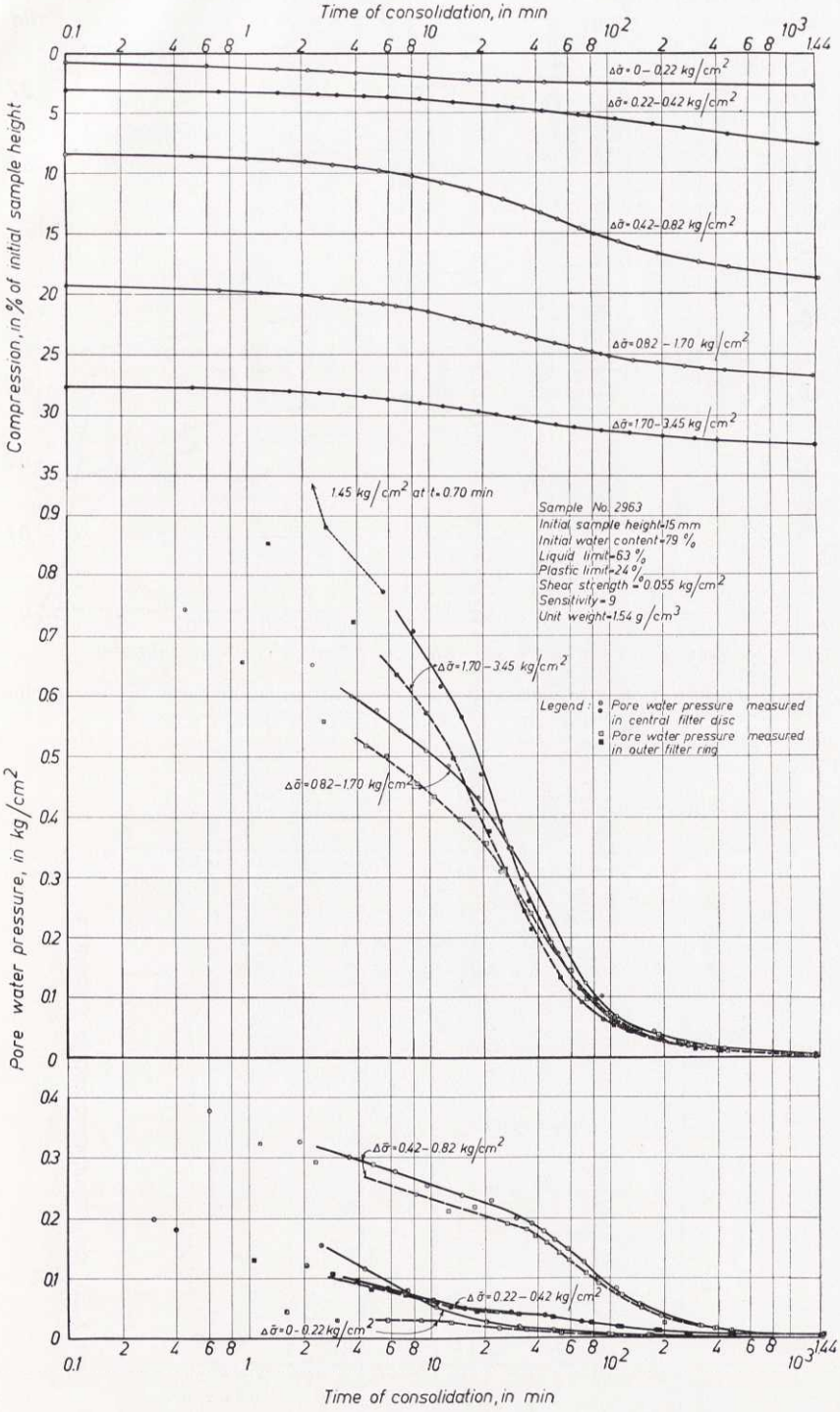

Fig. 16. Pore water pressure dissipation in consolidometer test at impermeable top surface of clay specimen. The respective values of $\Delta\bar{\sigma}$ refer to the loads before and after the application of a new load increment. Observations made by means of oedometer shown in Fig. 12 b. Pore pressures in central filter disc, full-line curves; in outer filter ring, dash-line curves.

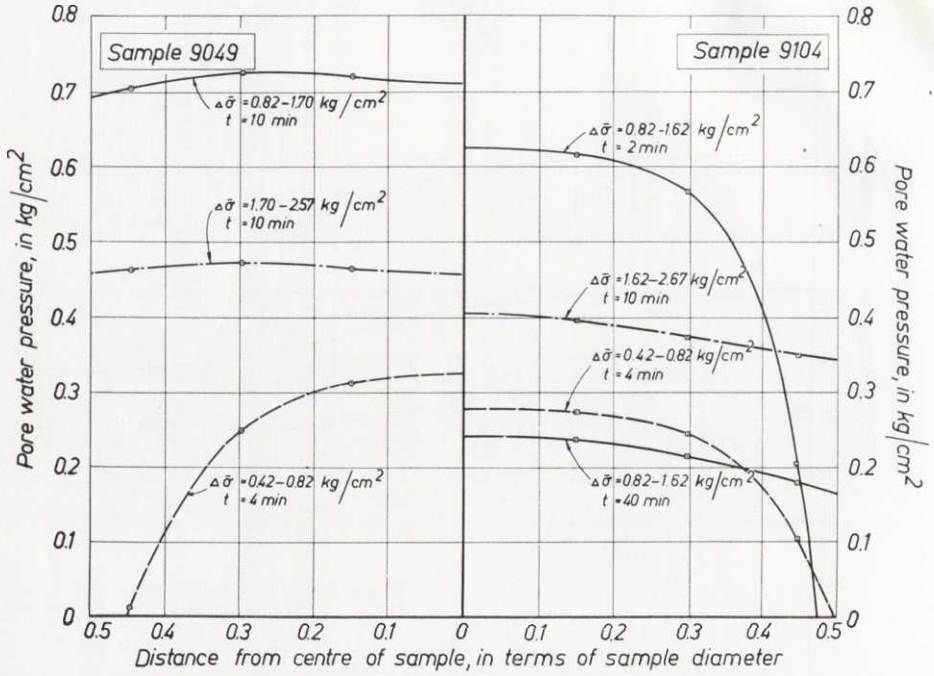

Fig. 17. Distribution of pore water pressure over impermeable base of clay specimen at varying time after beginning of consolidation process.

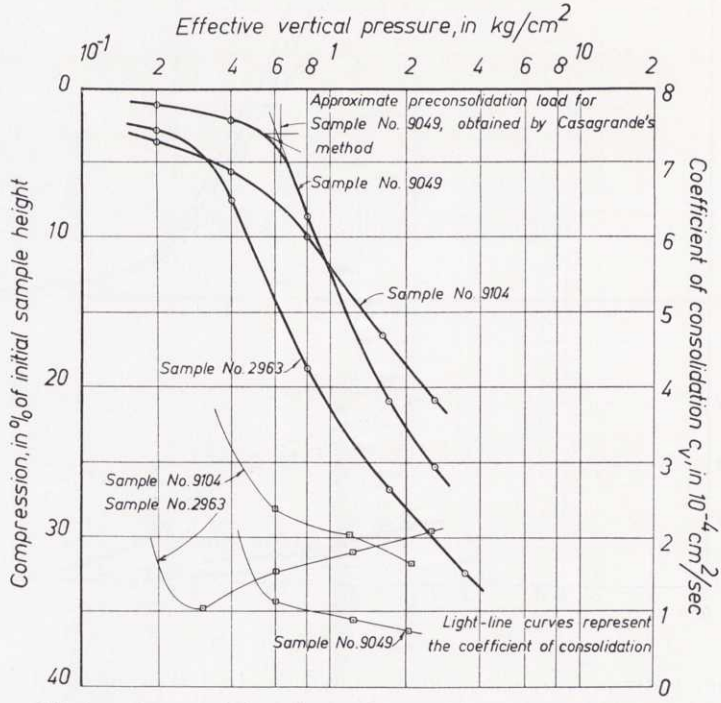

Fig. 18. Consolidation characteristics of samples used in pore water pressure investigations.

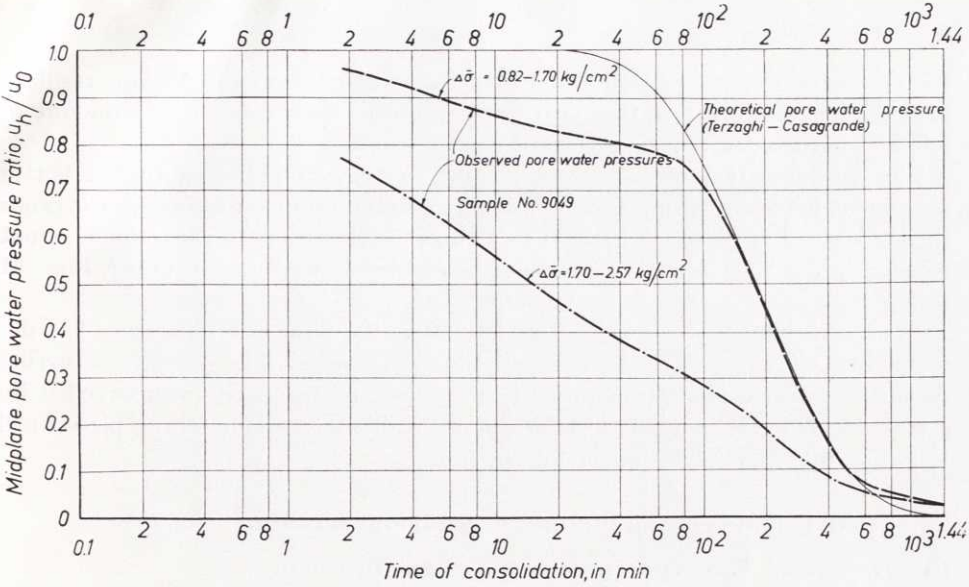

Fig. 19. Observed pore water pressure dissipation compared with that determined from TERZAGHI's consolidation theory.

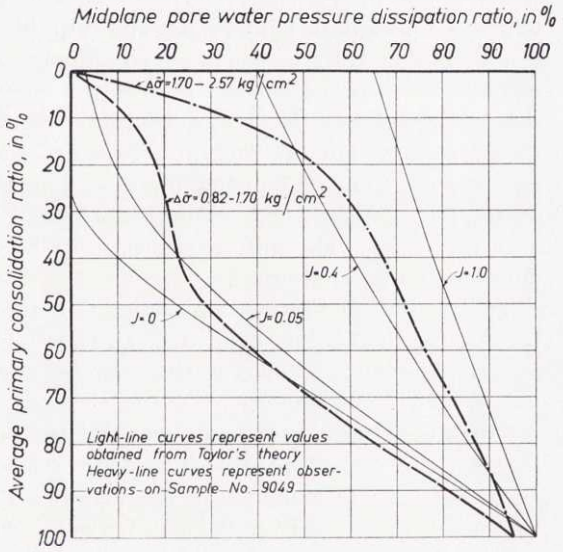

Fig. 20. Observed pore water pressure dissipation compared with that determined from TAYLOR's consolidation theory.

to a greater or less degree in this investigation. Thus it seems as if some of the pore water which is released by the application of the load and whose pressure is consequently measured were bound again to the soil before enough time has passed for it to be expelled (thixotropy). The amount of pore water which may thus be bound ought to be dependent on various factors, *e.g.* the temperature, the load increment, and the initial pore volume of the clay, and ought furthermore to be limited. Thus, for a tested clay, a large amount of pore water released by

the application of the consolidation load (causing a large compression) resulted in a smaller reduction of the pore water pressure than did a small amount of released pore water (causing a small compression).

The interpretation of test results made in Fig. 20 indicates that a better agreement between theory and experiment may be obtained by using TAYLOR's theory instead of TERZAGHI's or TAN's theories. However, the agreement is not so good in our case as in the experiments performed by TAYLOR (1942, Figs. 51 to 53).

At the beginning of secondary consolidation the pore water pressure has decreased to a few per cent of the applied load increment. The pressure occurring during this period is often assumed to be caused by the pore water expelled by a rearrangement of clay particles into more stable formations taking place until the new state of equilibrium is obtained.

22. Friction between Sample and Consolidometer Ring

Description of Test Apparatus and Testing Procedure

The apparatus used in these tests is shown in Fig. 21. It is a conventional oedometer with a floating ring, 60.5 mm in diameter, mounted upon a pressure bellows. The interior part of the oedometer ring is made of Teflon, and this is lubricated inside with molybdenum sulphide. The level of the oedometer ring can be measured by means of two dial gauges, and can be adjusted by a pressure regulator. When the friction is to be measured, the pressure in the regulator is slowly increased until an upward travel of the ring only just begins, indicating with certainty that the friction between ring and sample (and also other friction, *e.g.* between ring and piston plate, and in the loading device) has been overcome. The pressure is then decreased until a corresponding downward travel only just starts. The difference between these two pressures corresponds to the double amount of friction.

The friction in the loading device is reduced to a minimum by using a ball-bearing for the loading axle, and can therefore be neglected. The friction between piston plate and oedometer ring can be studied separately, and the observed values of friction between clay and ring can be corrected accordingly.

In spite of the corrections made and the precautions taken against apparatus friction, the observed values may nevertheless involve some errors. Thus, for example, possible obliquity of the piston plate with reference to the oedometer ring might introduce additional friction. However, such an obliquity is also possible in the conventional oedometer test and in the oedometer used for pore pressure measurements.

Discussion of Test Results

The results of the measurements carried out hitherto are given in Figs. 22 and 23.

At the end of primary compression the observed friction amounted to about 12 % of the vertical load applied in the first load step (below the preconsolidation load), and then decreased to between 8 and 6 % of the load.

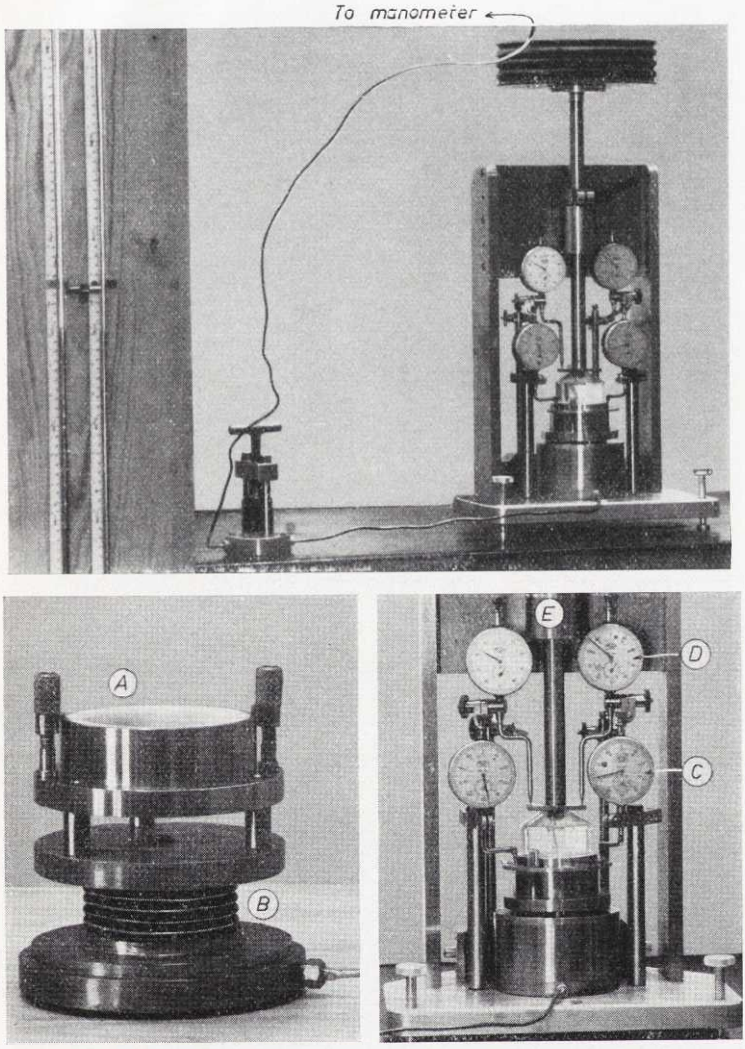

Fig. 21. Apparatus used for "friction" investigations. Top, from left to right: Mercury manometer, pressure regulator, and oedometer with dial gauges and loading plates. Bottom: (A) Oedometer ring mounted on (B) pressure bellows. (C) Dial gauge for observation of oedometer ring displacement. (D) Dial gauge for observation of sample compression. (E) Ball-bearing.

When a new load step was applied, the friction dropped to about half the previous value, corresponding to an average of 2 to 3 % of the applied load. The minimum friction was found to be equal to 1.2 % of the load, and occurred in the test on the more sensitive of the two samples at a load of 1.63 kg/cm^2. No doubt, the observed fall of friction is due to the disturbance of clay structure which is caused by the impact occurring when the load is applied. Thus the results show that the lateral contact pressure between the rigid phase of the

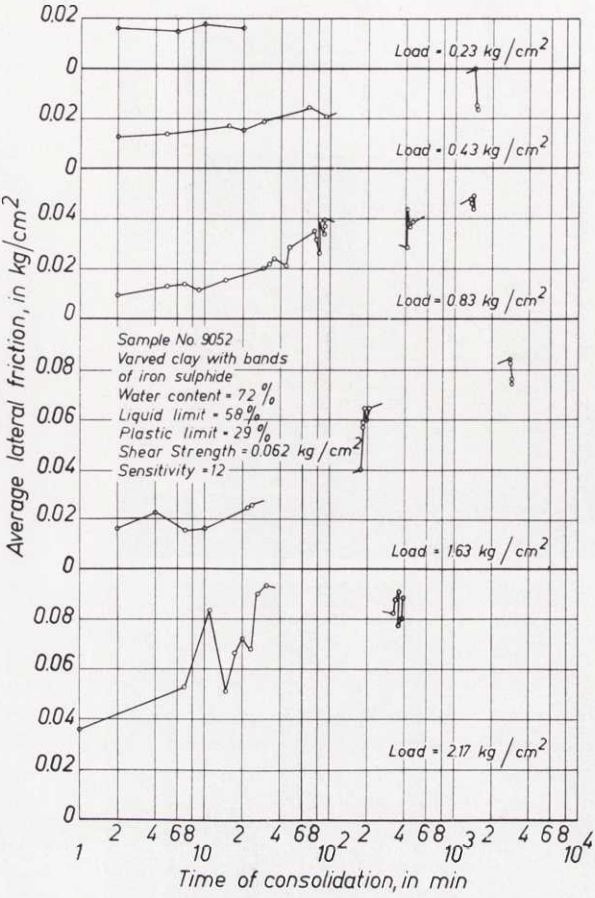

Fig. 22. Observed side "friction" between clay specimen and oedometer ring in consolidometer test. The respective load values represent the successive oedometer loads (from top to bottom in figure).

clay and the oedometer ring was reduced and that, consequently, the intergranular pressure in the clay sample may be reduced at the application of the consolidometer load.

The fall of friction obviously should bear a certain relationship to the sensitivity of the clay. However, the number of tests was too small to determine a quantitative relationship in this case.

In a friction test on a sample, a series of measurements was generally carried out during each period of observation. The observed variation in friction might be caused by occasional obliquity of the piston plate with reference to the oedometer ring, or by a disturbance of the clay in the immediate vicinity of the ring. However, these circumstances do not afford a complete explanation. Thus, after a period of rest, the friction often increased, and this indicates that a bond was formed between ring and clay during this period.

The coefficient of friction during unloading of a sample is considerably higher than that during loading. The friction values observed in the present case varied from 17 to 29 % of the remaining load, Fig. 23.

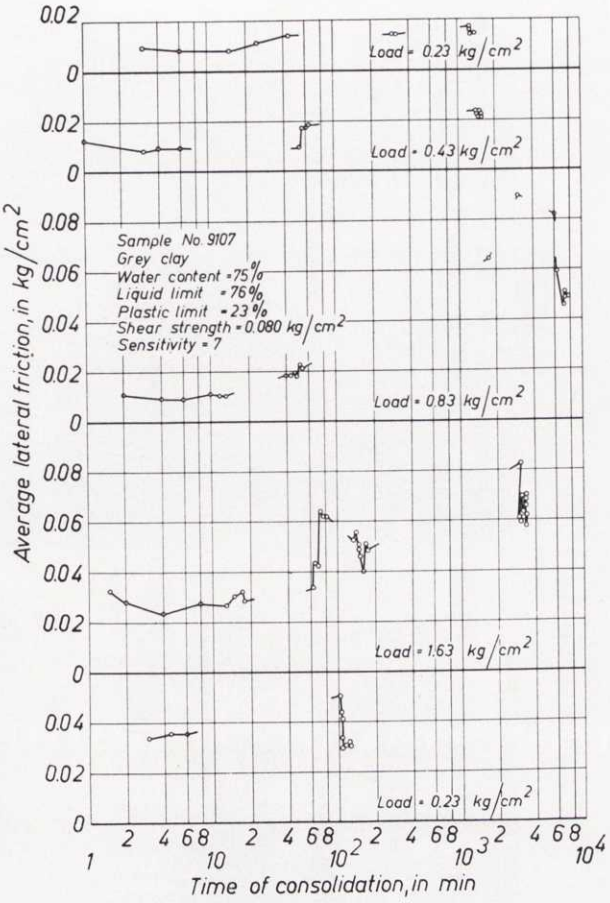

Fig. 23. Observed side "friction" between clay specimen and oedometer ring in consolidometer test. The respective load values represent the successive oedometer loads (from top to bottom in figure).

3. Investigation of Permeability of Clay at Small Hydraulic Gradients

30. Description of Test Apparatus and Testing Procedure

The importance of studying carefully the condition of pore water flow at small hydraulic gradients has already been pointed out in Section 12. For such a study, an extremely accurate apparatus for permeability investigations was constructed at the Institute.

A pressure difference between the top and bottom surfaces of a sample, as shown in Fig. 24 a, is created by the different levels of the free water surfaces in the two containers. The pressure difference causes a flow of water through the sample, and this flow is measured by means of precision capillary tubes,

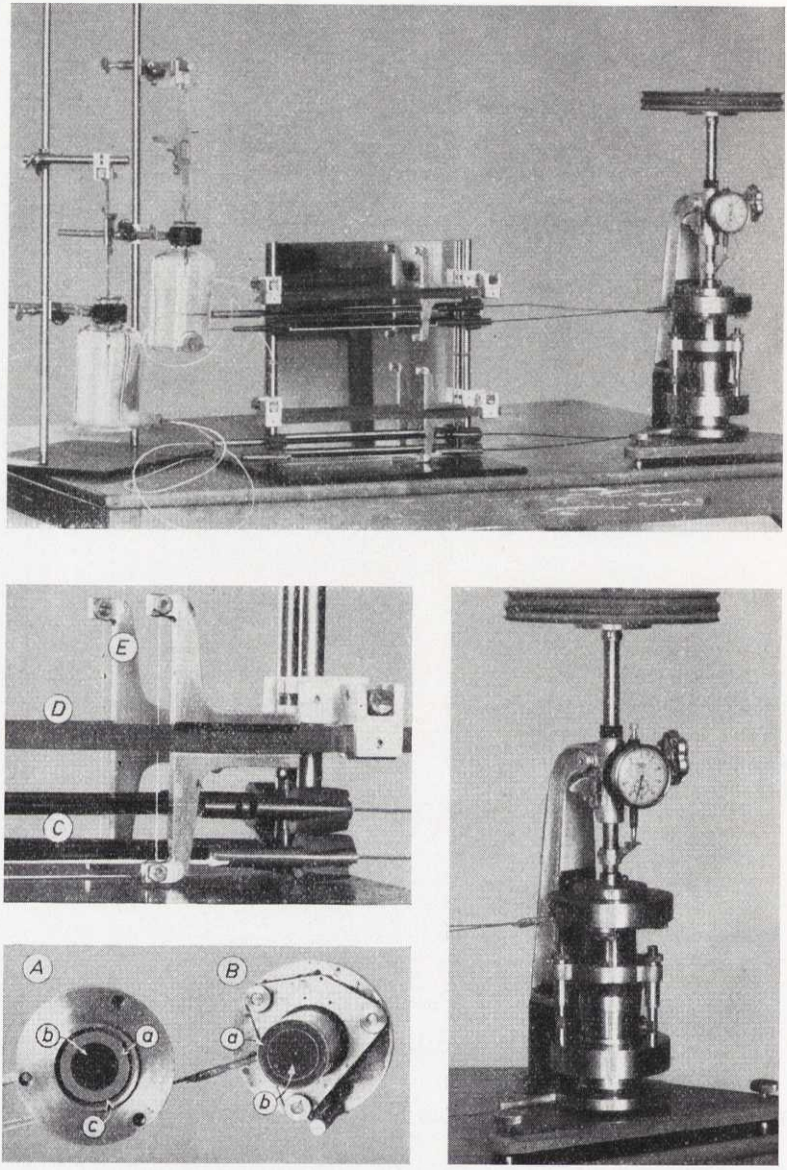

Fig. 24 a. Apparatus used for permeability investigations. Top, from left to right: Two water containers, precision capillary tubes with measuring devices, and "oedometer" containing sample and provided with loading plates and dial gauge for measuring compression of sample. Left-hand bottom: (A) Bottom part. (a) Outer filter ring. (b) Central filter disc. (c) Enchased rubber ring. (B) Top part. (a) Outer filter ring. (b) Central filter disc. (C) Precision capillary tubes with visible air bubbles. (D) Millimetre scale. (E) Reflected image. Right-hand bottom: "Oedometer" with mounted sample.

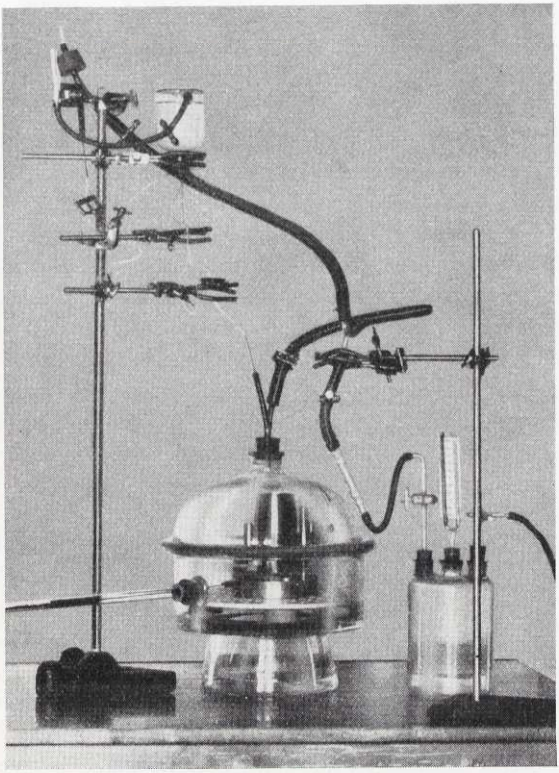

Fig. 24 b. Arrangement for developing vacuum in filters and capillaries. Container at the top, turned upside-down, is used in filling filters and capillaries with water. To the right, a Woulfe vacuum bottle.

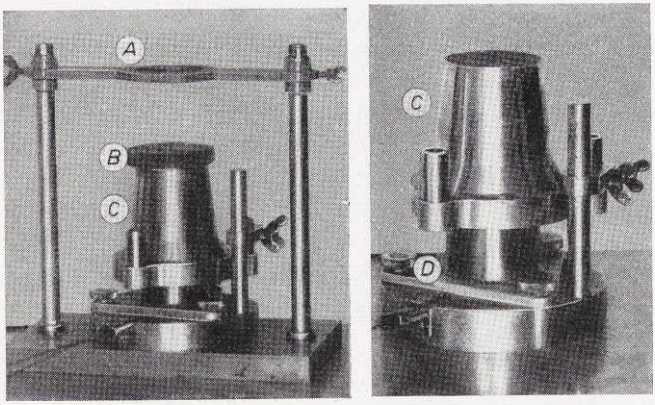

Fig. 24 c. Mounting of clay specimen. Left-hand figure, at the beginning of, and right-hand figure, after completion of, mounting process. (A) Mounting plate. (B) Slice of sample, 20 mm in thickness and 60 mm in diameter. (C) Sample cylinder. (D) Top part of apparatus.

1.00 mm in inner diameter, made of glass. Two such tubes are connected with each one of two glass filters adjoining the top and the bottom of the sample. Each filter consists of an inner, central filter disc, 35 mm in diameter, and an outer concentric filter ring, 6.5 mm in width. The filter disc is separated from the filter ring by a stainless steel wall, 0.5 mm in thickness. Two of the capillary tubes are connected with the central filter discs and the other two with the outer filter rings.

Before a sample is mounted, the air has to be exhausted from the capillaries and the filters. In our case this was done in a vacuum. During this procedure the apparatus was mounted as shown in Fig. 24 b. While the capillaries and the filters were still in a vacuum, water[1] was poured on top of the filters, and was kept at the ensuing water vapour pressure for a period of at least half an hour in order to remove possible remaining air. Air was then allowed to enter into the vacuum container, and the water was consequently forced into capillaries and filters until it filled them completely. Enough water was used to cover entirely the free surfaces of the filters even after filling had been completed.

The clay specimen to be tested was placed between the top filter and a mounting plate, and was squeezed into the sample cylinder, 50 mm in diameter, by pressing this cylinder upwards, *cf.* Fig. 24 c. The top part of the apparatus was then turned upside down, and was placed on the bottom part. The cylinder was finally screwed down until a perfectly tight joint was formed between its edge and the enchased rubber ring. During the mounting process great care was taken that air should not be trapped between the sample and the filters.

To make sure that the sample filled the whole space between the filters, it was consolidated in the permeability meter before the test until it reached a final height equalling 75 to 95 % of the original sample height. Furthermore, owing to this procedure, the pore water in the sample would replace part of the water which originally filled the capillaries and the filters.

After completion of consolidation, air bubbles, at least 10 mm in length, were produced in the capillaries. The two capillaries belonging to the bottom filter were connected with one of the containers, and the other two belonging to the top filter were connected with the other. The travel of the air bubbles in the capillaries observed at a given pressure gradient indicated the permeability of the clay for the gradient in question.

To begin with, measurements were made only of the flow of water through the central filter discs but later also of the flow through the outer filter rings. By thus comparing the travels of the air bubbles in all the different capillaries, it was possible to control the homogeneity of the specimen and a possible in-

[1] To begin with, distilled water was used, but was later replaced by pore water taken from samples having approximately the same characteristics as the specimen under investigation. In the case of distilled water, one could raise the objection that ions could be leached out of the clay specimen during the test, whereas in the case of pore water being pressed out of a similar clay *under high pressure*, the opposite effect, or exchange of ions, might occur. However, the possible influence of these effects on the results of the permeability tests is reduced by the method of testing.

fluence of boundary disturbances, such as remoulding and leakage between the clay and the confining cylindrical wall.

The amount of water allowed to pass through the specimens during the permeability tests was extremely small, and never exceeded 240 mm^3. For comparison it may be mentioned that the pore volume of the least porous specimen at 5 % compression was approximately 24 000 mm^3, or 100 times as great.

The initial sample height chosen in our case was 20 mm so as to reduce a possible influence exerted on the results by the contact surfaces between clay and glass filters.

For comparison of the results of the different permeability tests, they were performed at equal and constant temperatures. Thus, Tests 1 and 2 were performed at a room temperature of 24° C with a maximum variation of ± 0.5° C, and Tests 3 and 4 at 7° C with a maximum variation of ± 1° C. The specimens tested at the latter temperature were taken directly from the site to the test room, and were thus never warmed up.

31. Discussion of Test Results

Permeability investigations, if carefully performed, are time-consuming, and therefore only a restricted number of tests have been carried out. The results of these tests are given in Tables 1 to 4, and are represented in Figs. 25 to 27. For their interpretation it will be necessary to reconsider the inner texture of clay.

According to TAN (1954), clay of illite type is built up of a network of irregular, flaky mineral sheets, mainly with mutual flat surface-edge contacts. A similar picture of the structure of clay was given already in 1926 by GOLDSCHMIDT.

A certain orientation of the grains in the clay skeleton will naturally be caused by the overburden pressure. Thus, as is seen from the results of consolidometer tests, if the pore water is allowed to escape in a horizontal direction (*i.e.* parallel to the clay strata), the coefficient of consolidation is greater than in the case where the pore water is allowed to escape in a vertical direction. This orientation of grains can also be observed by measuring the electrical resistance in horizontal and vertical directions. By this method we generally find, as was to be expected, a smaller resistance in a horizontal direction.

The space left between the mineral grains is assumed to be filled with pore water, consisting of ions and water molecules, which are more or less rigidly bound to the mineral surface. Innermostly, the pore water seems to be fixed in a rigid lattice, and may be regarded as part of the mineral phase. For the water phase, the viscosity was shown by ROSENQVIST (1958) to increase considerably when approaching the mineral surface, from 24 centipoises at 30 % to 153 centipoises at 10 % water content for the clay in question.

When sedimented clay is gradually loaded by overlying sediments, not all grains appear to become part of the load-carrying network (the rigid phase, or "clay skeleton"). Consequently, within this network, the space may be filled

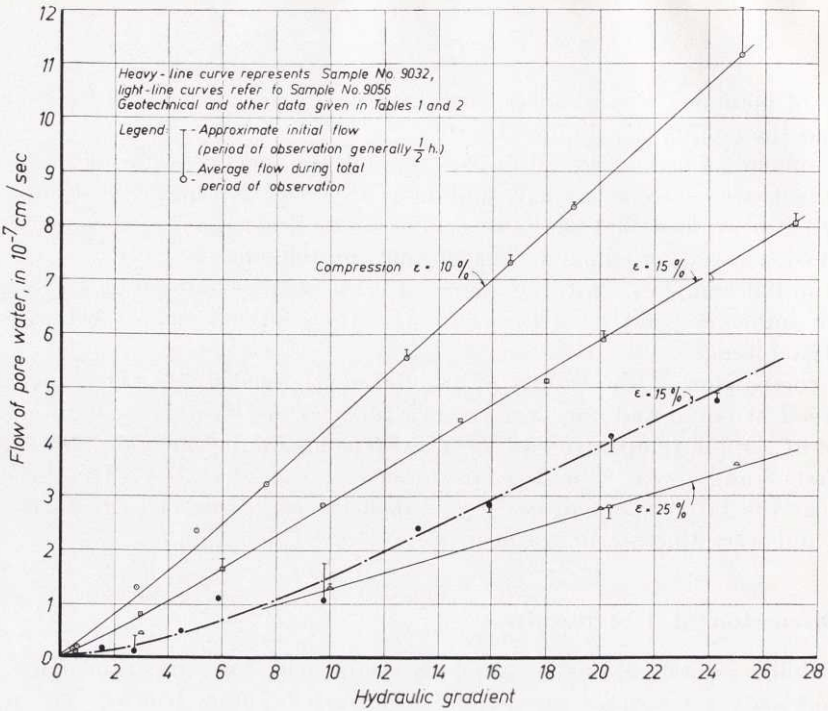

Fig. 25. Results of permeability tests on clay samples taken at depths of 8 m (heavy-line curve) and 5 m (light-line curves) below ground surface. Tests performed at an ambient temperature of $(24 \pm 0.5)^\circ$ C. In drawing the curves which represent the sample taken at a depth of 5 m (Sample No. 9056) stress has been laid on values obtained at high hydraulic gradients.

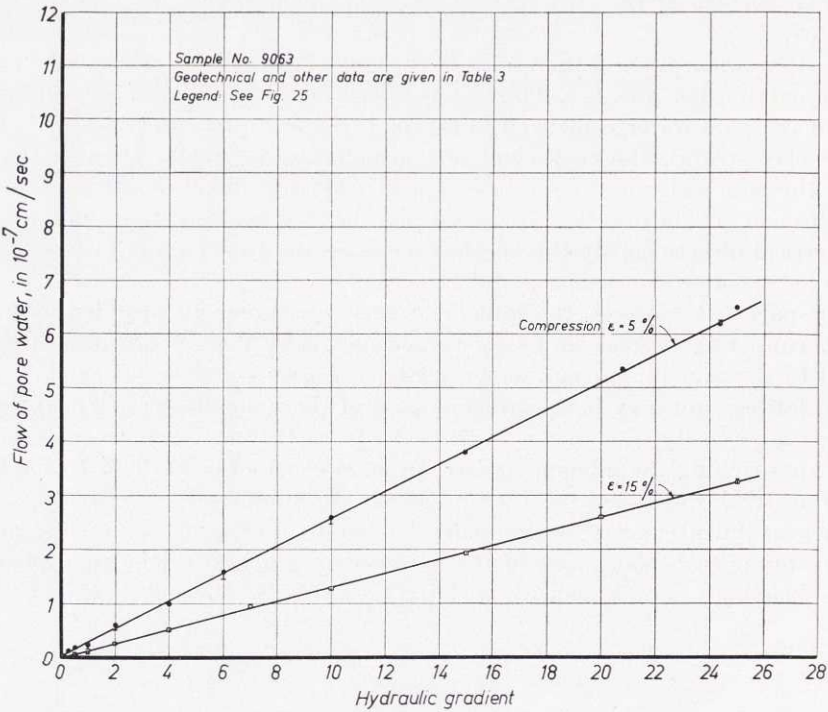

Fig. 26. Results of permeability tests on a clay sample taken at a depth of 2 m below ground surface. Tests performed at an ambient temperature of $(7 \pm 1)^\circ$ C.

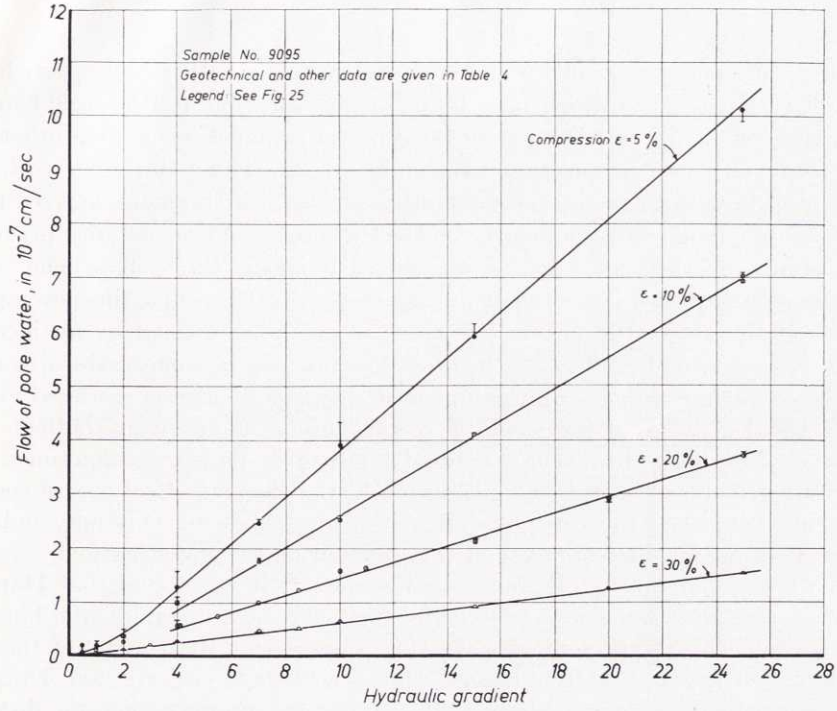

Fig. 27. Results of permeability tests on a clay sample taken at a depth of 6 m below ground surface. Tests performed at an ambient temperature of $(7 \pm 1)°$ C.

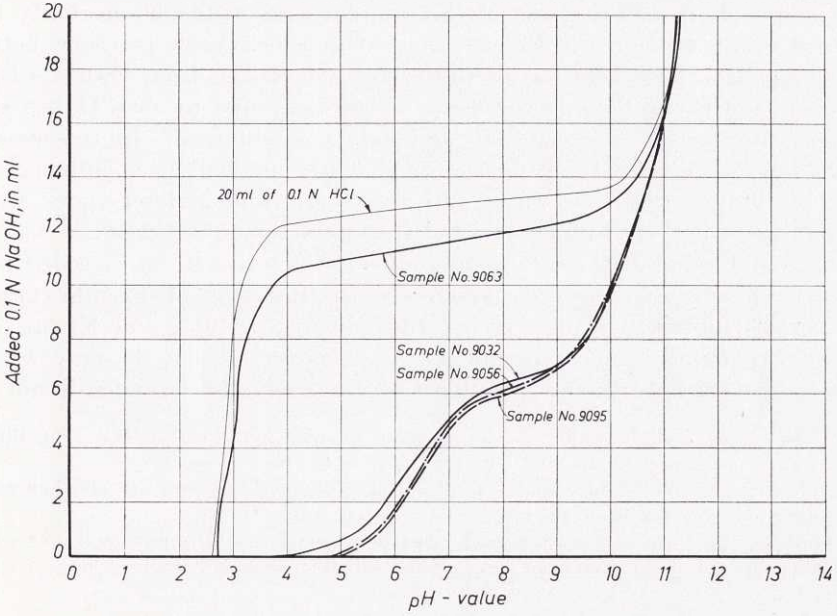

Fig. 28. Titre curves for samples used in permeability investigation: 20 ml of 0.1 N HCl + 1 g of dried, pulverized clay titrated with 0.1 N NaOH.

not only with pore water in its present sense but also with mobile particles of colloidal or greater size which may be bound by sorption and hydrodynamical forces (the mobile phase). This may furnish one explanation, among others, of a phenomenon observed in the permeability tests. Thus, during a test, the direction of flow through the specimen often altered. Furthermore, a given filter sometimes seemingly became nearly blocked during a certain definite period of observation, and then suddenly "re-opened". Obviously, the system behaved as if the mobile particles got meshed during their travel through the pore space, thus clogging part of the pores. The pores would be re-opened by an increase in flow velocity, or by a change in flow direction, or in some cases also after some lapse of time. In general, the apparent clogging effect was rendered visible by a gradual decrease of flow—within certain limits—for a given gradient with the time of action[1]. However, a gradual increase in flow was sometimes also observed, *cf.* Tables 1 to 4. For a given sample, the clogging effect was in general less strongly marked towards the end of the investigation. This may indicate a gradual change in the character of the clay during the investigation.

From results previously obtained (see Section 12) it was found that DARCY's law of permeability is not always valid for small pore pressure gradients. This was also confirmed by the present investigation. Considering the texture of the clay just described, a deviation from DARCY's law is no doubt to be expected. Thus, the forces which bind the mobile phase gradually become stronger when the distance to the rigid phase decreases. As a logical working hypothesis it is therefore suggested that, within certain limits, the clay becomes increasingly porous, *i.e.* permeable, with increasing pore pressure gradient. This deviation from DARCY's law of permeability ought to depend on the interaction between skeleton grains and pore water. In this connection it might be interesting to study the results obtained by pH-metric titration of the samples used in the permeability tests. The titre curves are given in Fig. 28. They show considerable reactions between clay and hydrochloric acid for all the samples deviating from DARCY's law of permeability. Only in Sample No. 9063, which was found to obey DARCY's law, no apparent reaction between clay and acid was obtained[2]. In this case the sample was taken at a small depth (only 2 m), and had been influenced for thousands of years by rain water and vegetation, and in later times also by artificial manuring, *etc.*, which affected the character of the clay[3].

A threshold value of the hydraulic gradient which has to be exceeded before pore water flow takes place (as suggested by *e.g.* BRENNER, 1946, SILFVERBERG, in STATENS GEOTEKNISKA INSTITUT, 1949, BUISSON, 1953, and KÉZDI, 1958) has not been found in our experiments. As a matter of fact, the pore water in the investigated clays was never found to be at a complete stand-still, not even

[1] A decrease in permeability with the time has been recorded by several authors, *e.g.* BODMAN (1937) in the case of packed soils and GRISEL (1936) in the case of concrete.

[2] The different character of this sample, as distinguished from the others, was also indicated by the inconsiderable clogging effect observed in this case, *cf.* Table 3.

[3] The presence of gas in the pore space might also give anomalies with respect to DARCY's law of permeability but gas does not seem to be associated with the anomalies observed here.

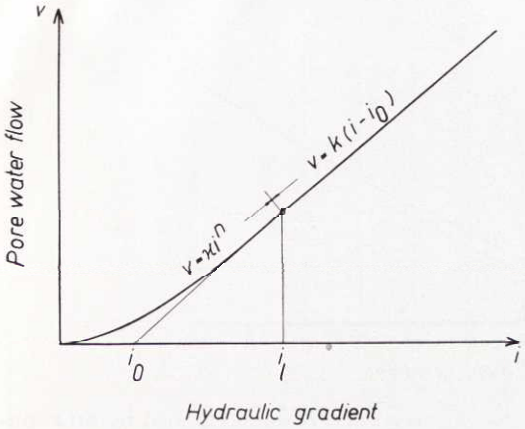

Fig. 29. Assumed equation of pore water flow in a normally consolidated fat clay subjected to small hydraulic gradients.

at hydraulic zero-gradient[1]. However, in practice the pore water flow at zero-gradient was of negligible order of magnitude. In the Author's opinion, a threshold value does not seem probable, at least not for a normally consolidated clay, since the application of a hydraulic gradient, however small, necessarily causes a disturbance of internal equilibrium conditions.

The above-mentioned working hypothesis and the results obtained from our tests lead us to the following equation of rate of pore water flow v (dimensions: LT^{-1}) for a normally consolidated fat clay at *small* hydraulic gradients i, Fig. 29,

$$v = \varkappa i^n \quad \ldots\ldots\ldots\ldots\ldots\ldots\ldots \quad (3:1)$$

where the permeability $\varkappa$ (LT^{-1}) and the exponent n vary with void ratio and temperature but also from one clay to another

$$n \geqq 1$$

When the hydraulic gradient exceeds a certain definite limit i_l, Eq. (3:1) is replaced by the straight-line relationship

$$v = k\,(i - i_0) \quad \ldots\ldots\ldots\ldots\ldots\ldots\ldots \quad (3:2)$$

where $k = n \varkappa i_l^{n-1}$, and $i_0 = i_l\,(n-1)/n$ is the intersection point of the tangent line represented by Eq. (3:2) and the i-axis, Fig. 29[2].

[1] This was later confirmed in a test in which the hydraulic gradient was kept at zero for a period of several months.

[2] In a recent book FLORIN (1959) suggests that, when the applied hydraulic gradient is not high enough for DARCY's law to be valid, then the relation between rate of flow and gradient is represented by a curve bearing a close resemblance to that suggested by the Author. According to FLORIN this curve could be approximately replaced by a straight line intersecting the gradient axis in the same way as the extended tangent line in Fig. 29.

FLORIN's book presents values of i_0 which are as high as 17 to 31.

A shape of the flow *vs.* hydraulic gradient curve similar to that given by the Author would also be obtained by a suitable combination of DARCY's law of permeability and the law of visco-plastic flow which was deduced by SCHIFFMAN (1959) on the basis of the Buckingham-Reiner equation (*cf.* REINER, 1960).

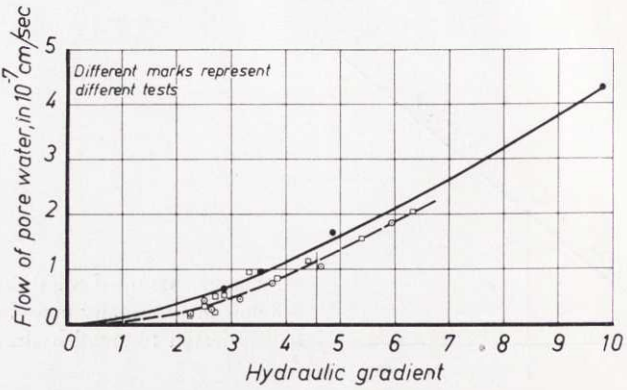

Fig. 30. Results of permeability tests on muddy clay from Väsby performed by SILFVERBERG in 1947. Sample consolidated under a pressure of 0.3 kg/cm^2. Curves drawn by Author.

The gradient i_0 represents the gradient required to overcome the maximum binding energy of mobile pore water.

For the samples investigated here, the coefficient n was found to vary from $n \approx 1$ (Sample 9063) to $n \approx 1.5$ (Sample 9032). In the latter case the gradient $i_l \lessapprox 9$.

It may be interesting to compare these results with those obtained by SILFVERBERG (STATENS GEOTEKNISKA INSTITUT, 1949). By plotting his values of observation in the coordinate system v/i instead of k/i, we find fairly close agreement with our own results[1]. Some of these values are shown in Fig. 30. Obviously, in this case the condition of flow corresponds with good accuracy to Eq. (3: 1) where the coefficient $n \approx 1.5$.

[1] In Figs. 25 to 27 and 30 as well as in Tables 1 to 4 the flow values (or rather rate of flow values) represent discharge velocities and not seepage velocities (*cf.* TERZAGHI, 1944).

[1] It might be interesting to study the magnitude of flow v during a given time interval towards the end of a period of observation at a given hydraulic gradient. This can easily be done by using the values given in Tables 1 to 4. If, for example, v_1 is the flow obtained during a time interval Δt_1 and v_{1+2} is the flow during the time interval $\Delta t_1 + \Delta t_2$, then the flow v_2 during the time interval Δt_2 can be obtained from the equation

$$v_2 = \frac{b\, v_{1+2} - v_1}{b - 1}$$

where

$$b = \frac{\Delta t_1 + \Delta t_2}{\Delta t_1}$$

Example: For Sample No. 9032, we have at a hydraulic gradient of 9.8 a mean flow of $1.55 \cdot 10^{-7}$ cm/sec during an observation period of 267 min and a mean flow of $1.06 \cdot 10^{-7}$ cm/sec during the total period of observation 1 257 min. From the given relation we get during the time interval from 267 to 1 257 min ($b = \frac{1\,257}{267} = 4.71$) the mean flow

$$v = \frac{(4.71 \cdot 1.06 - 1.55)\, 10^{-7}}{3.71} = 0.93 \cdot 10^{-7} \text{ cm/sec}$$

Table 1[1].

Sample No. 9032, taken at a depth of 8 m below ground surface

Data: Shear strength $\tau_f = 1.35$ t/m² (fall-cone test)
Initial water content $w_0 = 65\,\%$
Liquid limit $w_L = 55\,\%$
Plastic limit $w_P = 23\,\%$
Compression $\varepsilon = 15\,\%$

Date	Gradient	Time of flow, in min	Mean flow, in 10^{-7} cm/sec		Direction of flow through sample
			inner filters	outer filters	
13/2	9.8	77	1.74	not measured	downward
		119	1.49		
		202	1.56		
		267	1.55		
		1 257	1.06		
14/2	15.9	79	2.71		downward
		119	2.83		
		130	2.83		
14/2—16/2	2.8	27	0.39		upward
		1 507	0.09		
		2 660	0.11		
16/2	2.8	26	0.19		upward
16/2	20.4	50	3.83		upward
		88	4.01		
		182	4.08		
		222	4.12		
16/2—17/2	5.9	17	1.11		downward
		38	1.11		
		1 037	1.12		
17/2	1.6	37	0.18		downward
		63	0.19		
		93	0.18		
17/2	24.3	31	4.90		downward
		58	4.75		
17/2	13.2	14	2.42		downward
		63	2.42		
17/2	4.5	32	0.49		downward
		56	0.52		
		80	0.50		

Table 2.
Sample No. 9056, taken at a depth of 5 m below ground surface

Data: Shear strength $\tau_f = 0.85$ t/m² (fall-cone test)
Initial water content $w_0 = 63\,\%$
Liquid limit $w_L = 55\,\%$
Plastic limit $w_P = 22\,\%$

A. Compression $\varepsilon = 10\,\%$

Date	Gradient	Time of flow, in min	Mean flow, in 10^{-7} cm/sec		Direction of flow through sample
			inner filters	outer filters	
24/2	25.2	30	12.0	10.6	downward
		60	11.4	10.9	
		90	11.2	11.0	
		120	11.2	11.1	
	19.0	30	8.42	8.71	upward
		60	8.37	8.63	
		90	8.37	8.67	
		120	8.35	8.60	
25/2	12.8	30	5.69	4.98	downward
		60	5.65	5.26	
		90	5.57	5.34	
		120	5.53	5.41	
	7.6	31	3.23	3.36	upward
		61	3.21	3.40	
		91	3.22	3.32	
		121	3.21	3.26	
	5.1	30	2.36	1.69	downward
		60	2.36	1.61	
		90	2.37	1.59	
		120	2.36	1.61	
25/2—26/2	0.48	1 008	0.21	0.06	downward
26/2	2.9	32	1.30	1.01	upward
		62	1.31	0.88	
		92	1.32	0.80	
		122	1.32	0.81	
	0.62	30	0.27	0.33	downward
		60	0.27	0.24	
		90	0.28	0.24	
		120	0.27	0.22	
		150	0.28	0.23	
	16.6	30	7.45	6.50	downward
		60	7.38	6.75	
		90	7.32	6.81	
		120	7.32	6.90	

Sample No. 9056

B. Compression $\varepsilon = 15\,\%$

Date	Gradient	Time of flow, in min	Mean flow, in 10^{-7} cm/sec		Direction of flow through sample
			inner filters	outer filters	
27/2	27.1	30	8.25	9.03	downward
		60	8.13	8.83	
		90	8.05	8.75	
		120	8.06	8.72	
	20.1	30	6.05	6.47	upward
		60	5.98	6.42	
		90	5.92	6.37	
		120	5.92	6.32	
	14.8	30	4.41	4.83	downward
		60	4.44	4.78	
		90	4.40	4.74	
		120	4.40	4.73	
28/2	9.7	30	2.83	3.07	upward
		60	2.82	3.08	
		90	2.84	3.05	
		120	2.83	2.98	
2/3	6.0	30	1.84	1.76	downward
		60	1.79	1.81	
		90	1.69	1.81	
		120	1.65	1.77	
	3.0	30	0.86	0.88	upward
		60	0.86	0.88	
		90	0.85	0.93	
		120	0.84	0.93	
2/3—3/3	0.6	30	0.16	0.23	downward
		60	0.17	0.21	
		90	0.18	0.21	
		120	0.18	0.22	
		1 152	0.11	0.12	
3/3	18.0	30	5.19	5.63	upward
		60	5.13	5.57	
		90	5.08	5.55	
		120	5.10	5.50	

Sample No. 9056

C. Compression $\varepsilon = 25\,\%$

Date	Gradient	Time of flow, in min	Mean flow, in 10^{-7} cm/sec		Direction of flow through sample
			inner filters	outer filters	
3/3	25.0	30	3.60	3.97	downward
		60	3.63	3.97	
		90	3.62	3.96	
		120	3.58	3.92	
4/3	20.0	30	2.81	3.09	upward
		60	2.81	3.11	
		90	2.77	3.12	
		120	2.74	3.09	
	3.0	30	0.45	0.53	downward
		60	0.43	0.50	
		90	0.44	0.50	
		120	0.44	0.50	
	10.0	30	1.36	1.53	upward
		60	1.29	1.47	
		90	1.28	1.44	
		120	1.27	1.44	
5/3	0.6	30	0.11	0.10	downward
		60	0.10	0.08	
		90	0.09	0.09	
		120	0.09	0.10	
	1.5	30	0.20	0.25	downward
		60	0.18	0.25	
		90	0.18	0.25	
		120	0.18	0.25	
5/3—6/3	2.7	30	0.34	0.43	downward
		60	0.33	0.45	
		90	0.33	0.44	
		120	0.35	0.45	
		987	0.29	0.41	
6/3	4.5	30	0.34	0.60	downward
		60	0.34	0.58	
		90	0.36	0.57	
		120	0.36	0.57	
	0.0	30	0.16	0.00	downward
		60	0.05	0.06	upward
		90	0.05	0.06	»
		105	0.04	0.06	»
		180	0.03	0.04	»
	20.3	32	2.59	2.93	upward
		62	2.65	3.08	
		92	2.60	3.00	
		122	2.62	3.01	
		152	2.63	3.04	
		185	2.64	3.04	
6/3—7/3	20.3	992	2.82	3.12	upward

Table 3.
Sample No. 9063, taken at a depth of 2 m below ground surface

Data: Shear strength $\tau_f = 1.64$ t/m^2 (fall-cone test)
Initial water content $w_0 = 83\,\%$
Liquid limit $w_L = 100\,\%$
Plastic limit $w_P = 31\,\%$

A. Compression $\varepsilon = 5\,\%$

Date	Gradient	Time of flow, in min	Mean flow, in 10^{-7} cm/sec		Direction of flow through sample
			inner filters	outer filters	
11/3—12/3	0.53	30	0.18	0.13	downward
		60	0.20	0.11	
		120	0.19	0.13	
		180	0.19	0.13	
		240	0.20	0.12	
		1 220	0.18	0.14	
		1 340	0.18	0.14	
12/3—13/3	1.05	30	0.27	0.33	downward
		60	0.30	0.30	
		120	0.29	0.28	
		330	0.30	0.28	
		1 320	0.32	0.21	
		1 530	0.33	0.21	
13/3—14/3	2.0	30	0.52	0.45	downward
		60	0.56	0.43	
		120	0.57	0.40	
		210	0.59	0.38	
		1 220	0.61	0.34	
		1 400	0.60	0.35	
14/3—16/3	0.3	30	0.11	0.05	downward
		2 700	0.12	0.04	
16/3—17/3	4.0	30	1.02	1.08	upward
		60	0.99	1.22	
		120	0.99	1.07	
		240	0.97	1.07	
		360	0.97	1.07	
		1 390	0.98	1.05	
		1 530	0.98	1.05	
17/3—18/3	6.0	30	1.47	1.61	upward
		60	1.51	1.47	
		120	1.54	1.45	
		240	1.54	1.43	
		1 265	1.56	1.41	
		1 385	1.56	1.41	
18/3	10.0	30	2.61	2.59	downward
		60	2.62	2.65	
		120	2.59	2.67	
		210	2.57	2.66	
	20.8	30	5.31	5.58	downward
		60	5.31	5.61	
		90	5.35	5.60	
		120	5.33	5.58	

Date	Gradient	Time of flow, in min	Mean flow, in 10^{-7} cm/sec		Direction of flow through sample
			inner filters	outer filters	
19/3	25.0	30	6.57	6.67	downward
		60	6.55	6.63	
		90	6.53	6.60	
		220	6 48	6.59	
	15.0	30	3.81	4.02	upward
		60	3.81	4.04	
		90	3 82	4.04	
	24.4	30	6.30	6.59	upward
		60	6.25	6.56	

Sample No. 9063

B. Compression $\varepsilon = 15\ \%$

20/3	0.0	33	0.02	0.00	downward
		60	0.02	0.02	
		120	0.01	0.01	
		278	0.01	0.01	
20/3—21/3	0.5	132	0.07	0.05	upward
		162	0.06	0.04	
		1 229	0.05	0.04	
		1 390	0.05	0.04	
21/3—23/3	1.0	30	0.11	0.13	upward
		60	0.11	0.11	
		1 471	0.12	0.11	
		2 715	0.12	0.11	
23/3—24/3	2.0	30	0.27	0.20	upward
		159	0.26	0.23	
		463	0.26	0.23	
		1 423	0.26	0.24	
24/3	4.0	136	0.53	0.49	upward
		265	0.53	0.49	
		325	0.53	0.50	
	7.0	30	0.95	0.93	upward
		67	0.95	1.01	
24/3—25/3	10.0	1 015	1.29	1.38	upward
		1 270	1.29	1.38	
25/3	15.0	31	1.95	2.14	upward
		65	1.95	2.10	
		109	1.95	2.08	
		135	1.95	2.09	
25/3—26/3	20.0	30	2.79	3.12	downward
		260	2.68	2.81	
		964	2.61	2.79	
26/3	25.0	30	3.29	3.42	upward
		90	3.27	3.46	
		130	3.25	3.47	

Table 4.
Sample No. 9095, taken at a depth of 6 m below ground surface

Data: Shear strength $\tau_f = 0.74$ t/m^2 (fall-cone test)
Initial water content $w_0 = 66\,\%$
Liquid limit $w_L = 60\,\%$
Plastic limit $w_P = 22\,\%$

A. Compression $\varepsilon = 5\,\%$

Date	Gradient	Time of flow, in min	Mean flow, in 10^{-7} cm/sec		Direction of flow through sample
			inner filters	outer filters	
3/4—4/4	0.5	30	0.14	0.20	upward
		60	0.14	0.20	
		90	0.12	0.20	
		1 080	0.11	0.21	
		1 200	0.11	0.21	
4/4—6/4	1.0	30	0.27	0.38	upward
		60	0.27	0.42	
		90	0.27	0.42	
		2 820	0.20	0.39	
		2 940	0.20	0.39	
6/4	2.0	30	0.34	0.96	upward
		60	0.34	1.01	
		150	0.38	0.96	
		210	0.38	0.96	
8/4		60	0.49	0.74	
		120	0.48	0.71	
		330	0.39	0.68	
		390	0.38	0.68	
8/4—10/4	0.5	30	0.18	0.05	upward
		1 050	0.04	0.07	
		1 440	0.05	0.07	
		2 490	0.05	0.07	
		2 910	0.05	0.07	
13/4—14/4	4.0	30	1.56	1.18	upward
		60	1.61	1.20	
		120	1.55	1.21	
		1 260	1.29	1.43	
14/4—15/4	0.5	30	0.18	0.20	downward
		60	0.18	0.20	
		1 080	0.16	0.22	
		1 140	0.16	0.22	
15/4	7.0	30	2.54	2.82	downward
		60	2.44	2.79	
		90	2.47	2.85	
		120	2.47	2.85	

Date	Gradient	Time of flow, in min	Mean flow, in 10^{-7} cm/sec		Direction of flow through sample
			inner filters	outer filters	
16/4	10.0	30	4.31	4.48	downward
		60	4.09	4.42	
		120	4.02	4.36	
		330	3.91	4.29	
		420	3.90	4.26	
17/4	15.0	30	6.19	6.34	downward
		60	6.11	6.32	
		120	5.98	6.29	
		330	5.92	6.26	
		390	5.90	6.27	
18/4	25.0	30	9.90	10.53	upward
		60	9.95	10.58	
		120	10.05	10 54	
		210	10.12	10.54	

Sample No. 9095

B. Compression $\varepsilon = 10\ \%$

20/4—21/4	0.5	30	0.16	0.25	upward
		60	0.15	0.19	
		120	0.10	0.16	
		360	0.07	0.14	
		1 410	0.06	0.12	
		1 470	0.06	0.12	
21/4—22/4	1.0	30	0.16	0.25	upward
		60	0.18	0.24	
		120	0.18	0.24	
		330	0.17	0.23	
		1 380	0.16	0.24	
		1 440	0.16	0.24	
22/4—23/4	2.0	30	0.50	0.45	upward
		60	0.48	0.47	
		360	0.44	0.44	
		1 380	0.37	0.48	
		1 440	0.37	0.48	
23/4—24/4	4.0	30	1.11	1.18	downward
		60	1.10	1.19	
		120	1.10	1.18	
		300	1.03	1.20	
		1 320	1.00	1.20	
		1 380	1.00	1.20	

Date	Gradient	Time of flow, in min	Mean flow, in 10^{-7} cm/sec		Direction of flow through sample
			inner filters	outer filters	
24/4	7.0	30	1.81	2.11	downward
		60	1.83	2.11	
		120	1.81	2.08	
		300	1.77	2.09	
24/4 – 25/4	0.5	30	0.14	0.13	downward
		60	0.14	0.15	
		1 080	0.10	0.16	
25/4 – 27/4	0.0	30	0.00	0.00	
		60	−0.01	0.01	downward
		2 910	0 01	0.00	»
27/4	10.0	30	2.59	3.14	upward
		60	2.53	3.08	
		120	2.47	3.04	
		390	2.52	2.98	
27/4 – 28/4	0.5	990	0.07	0.12	upward
28/4	15.0	30	4.08	4.50	upward
		60	4.09	4.48	
		120	4.04	4.50	
		360	4.08	4.45	
28/4 – 29/4	0.5	1 050	0.07	0.15	upward
29/4	25.0	30	7.09	7.30	downward
		60	7.05	7.34	
		120	7.03	7.36	
		240	7.02	7.37	
		30	7.01	7.43	upward
		60	6.95	7.38	

Sample No. 9095

C. Compression $\varepsilon = 20\,\%$

30/4 – 4/5	0.5	30	0.07	0.08	downward
		60	0.08	0.11	
		540	0.08	0.08	
		1 710	0.08	0.08	
		3 180	0.08	0.08	
		4 620	0.08	0.08	
		5 790	0.08	0.08	
4/5 – 5/5	1.0	30	0.16	0.15	downward
		60	0.16	0.14	
		120	0.15	0.16	
		420	0.15	0.16	
		1 410	0.15	0.16	

Date	Gradient	Time of flow, in min	Mean flow, in 10^{-7} cm/sec		Direction of flow through sample
			inner filters	outer filters	
5/5—6/5	2.0	30	0.27	0.28	downward
		60	0.28	0.30	
		180	0.29	0.32	
		450	0.29	0.32	
		1 470	0.27	0.33	
		1 590	0.27	0.33	
6/5—8/5	4.0	30	0.68	0.45	downward
		60	0 64	0.49	
		120	0.64	0.54	
		1 455	0.57	0.61	
		2 790	0.59	0.61	
8/5—9/5	7.0	30	1.00	1.01	upward
		60	1.01	1.02	
		360	1.01	1.02	
		1 350	1.01	1.06	
9/5—11/5	0.5	30	0.07	0.15	upward
		60	0.06	0.10	
		2 880	0.06	0.07	
11/5—12/5	10.0	30	1.59	1.63	downward
		60	1.58	1.66	
		390	1.55	1.66	
		1 410	1.56	1.66	
12/5	15.0	30	2.18	2.42	upward
		60	2.15	2.43	
		120	2.12	2.39	
		420	2.12	2.38	
12/5—13/5	8.5	1 020	1.23	1.32	upward
13/5	25.0	30	3.81	3.95	downward
		60	3.77	3.93	
		120	3.76	3.91	
		390	3.78	3.90	
13/5—14/5	4.1	990	0.58	0.63	downward
14/5	20.0	30	2.86	3.22	upward
		60	2.86	3.19	
		120	2.82	3.18	
		420	2.91	3.13	
14/5—15/5	5.5	1 020	0.74	0.79	upward
15/5	11.0	30	1.61	1.76	downward
		60	1.63	1.74	
		120	1.63	1.73	
		360	1.63	1.70	

Sample No. 9095

D. Compression $\varepsilon = 30\,\%$

Date	Gradient	Time of flow, in min	Mean flow, in 10^{-7} cm/sec		Direction of flow through sample
			inner filters	outer filters	
18/5—19/5	0.5	30	0.05	0.08	downward
		270	0.03	0.05	
		1 290	0.03	0.05	
19/5—20/5	1.0	390	0.06	0.08	downward
		1 440	0.07	0.08	
20/5—21/5	2.0	500	0.13	0.16	downward
		1 440	0.13	0.15	
21/5—22/5	4.0	30	0.27	0.30	downward
		60	0.26	0.31	
		390	0.25	0.29	
		1 380	0.26	0.30	
22/5—23/5	7.0	30	0.45	0.50	downward
		60	0.45	0.53	
		420	0.44	0.50	
		1 500	0.46	0.46	
23/5—25/5	3.0	30	0.23	0.23	downward
		60	0.22	0.24	
		1 560	0.19	0.22	
		2 850	0.19	0.22	
25/5—26/5	10.0	30	0.61	0.73	upward
		60	0.62	0.71	
		360	0.63	0.70	
		1 380	0.63	0.70	
26/5	15.0	30	0.93	1.03	upward
		120	0.92	0.97	
		390	0.92	0.96	
26/5—27/5	8.5	990	0.50	0.52	upward
27/5—28/5	20.0	30	1.27	1.38	downward
		120	1.28	1.35	
		390	1.26	1.34	
		1 380	1.26	1.33	
28/5	25.0	30	1.56	1.66	upward
		60	1.58	1.69	
		120	1.56	1.66	
		330	1.54	1.67	

4. Consolidation of Clay by Drain Wells Based on New Theory of Permeability Presented in Chapter 3

40. Deduction of Consolidation Equation

The law of permeability, as given by Eq. (3:1), will now be applied to the analysis of consolidation of a normally consolidated clay layer by vertical drains only. In this case it is convenient to write the equation of permeability in the form

$$v = \lambda\, m_v\, \gamma_w\, i^n \quad \ldots\ldots\ldots\ldots\ldots\ldots \quad (4:1)$$

where $\lambda\,(L^2T^{-1}) = \varkappa/m_v\,\gamma_w$ corresponds to the coefficient of consolidation c_h, used in the classical theory, $m_v\,(L^2F^{-1})$ is the coefficient of volume compressibility, and $\gamma_w\,(FL^{-3})$ is the unit volume weight of water.

To investigate whether or not λ can be regarded as a constant, the samples were subjected to consolidometer tests in addition to the permeability investigations. In this way it was found that λ slightly increased with pressure. However, the values of m_v obtained from the consolidometer tests were influenced by the sample disturbance, and were largely dependent on the curve fit. Furthermore, a decrease in $\varkappa$ with the time might occur and would neutralize a possible increase in λ caused by m_v. For these reasons it was not possible to draw any definite conclusions as to the true variation in λ. All the same, with the guidance of previous experience regarding the coefficient of consolidation c_h, the error caused by assuming λ to be a constant may be expected to be negligible at small consolidation loads, at least in the case of mineral clays.

The basic assumptions for the following theoretical study are stated below.

(1) Eq. (4:1) is valid; λ is constant.
(2) The clay is saturated and homogeneous.
(3) All compressive strains within the soil mass occur in a vertical direction only.
(4) Horizontal sections remain horizontal throughout the consolidation process (equal strains).
(5) Pore water flow occurs only in a horizontal direction (at right angles to the drain wells).
(6) Settlement is due only to outflow of pore water.
(7) No excess pore water pressure exists in the drain wells.
(8) The zone of influence of each well is a cylinder of unit height.

On these assumptions, the flow condition at radius ϱ, *cf.* Fig. 10, becomes

$$2\,\pi\,\varrho v = -\,\pi\,(R^2 - \varrho^2)\, m_v\, \frac{\partial\, \bar{u}}{\partial\, t} \quad \ldots\ldots\ldots\ldots\ldots \quad (4:2)$$

where v = rate of flow at radius ϱ,
R = ½ D = radius of influence of the drain[1],
m_v = coeffient of elastico-plastic deformability, conventionally defined as coefficient of volume compressibility,
$\bar{u}$ = mean value of excess pore water pressure at the time t.

[1] For a drained area with drain distance = L, $D = 1.13\ L$ when the drains are arranged in a square pattern, and $D = 1.05\ L$ when the drains are arranged in a triangular pattern.

Inserting Eq. (4: 1) into Eq. (4: 2) gives

$$i = \frac{1}{\gamma_w}\frac{\partial u}{\partial \varrho} = \left(-\frac{R^2}{2\lambda\gamma_w}\frac{\partial \bar{u}}{\partial t}\right)^{\frac{1}{n}}\left[\frac{1}{\varrho}\left(1-\frac{\varrho^2}{R^2}\right)\right]^{\frac{1}{n}} \quad \ldots\ldots \quad (4:3)$$

The expression within square brackets can be expanded in the following binomial series:

$$\left[\quad\right]^{\frac{1}{n}} = \varrho^{-\frac{1}{n}}\left[1-\frac{1}{n}\frac{\varrho^2}{R^2}-\frac{n-1}{2!\,n^2}\frac{\varrho^4}{R^4}-\right.$$

$$\left.-\frac{(n-1)(2n-1)}{3!\,n^3}\frac{\varrho^6}{R^6}-\frac{(n-1)(2n-1)(3n-1)}{4!\,n^4}\frac{\varrho^8}{R^8}\ldots\right]$$

Integrating term by term, and inserting the boundary conditions $u = 0$ at $\varrho = r$, the excess pore water pressure u at a given time t becomes

$$u = \gamma_w^{\frac{n-1}{n}}\left(-\frac{R^2}{2\lambda}\frac{\partial \bar{u}}{\partial t}\right)^{\frac{1}{n}}\frac{n}{n-1}\left\{\varrho^{\frac{n-1}{n}}\left[1-\frac{n-1}{n(3n-1)}\left(\frac{\varrho}{R}\right)^2-\frac{(n-1)^2}{2!\,n^2(5n-1)}\left(\frac{\varrho}{R}\right)^4-\right.\right.$$

$$\left.-\frac{(n-1)^2(2n-1)}{3!\,n^3(7n-1)}\left(\frac{\varrho}{R}\right)^6-\ldots\right]-r^{\frac{n-1}{n}}\left[1-\frac{n-1}{n(3n-1)}\left(\frac{r}{R}\right)^2-\ldots\right]\Bigg\} \quad \ldots \quad (4:4)$$

But

$$\bar{u}\,\pi(R^2-r^2) = \int_r^R u\,2\pi\varrho\,d\varrho \quad \ldots\ldots\ldots\ldots\ldots\ldots \quad (4:5)$$

and hence, since $r^2 \ll R^2$,

$$\bar{u} \approx \gamma_w^{\frac{n-1}{n}}\left(-\frac{2^{n-1}}{\lambda}\frac{\partial \bar{u}}{\partial t}\right)^{\frac{1}{n}} R^{\frac{n+1}{n}}\, f\left(n, \frac{r}{R}\right) \quad \ldots\ldots\ldots\ldots \quad (4:6)$$

where the convergent series

$$f\left(n, \frac{r}{R}\right) = \frac{n^2}{n-1}\left\{\left[\frac{1}{3n-1}-\frac{n-1}{n(3n-1)(5n-1)}-\frac{(n-1)^2}{2!\,n^2(5n-1)(7n-1)}-\ldots\right]-\right.$$

$$-\frac{1}{2n}\left(\frac{r}{R}\right)^{\frac{n-1}{n}}+\left[\frac{1}{2n}-\frac{1}{3n-1}+\frac{n-1}{2n^2(3n-1)}\right]\left(\frac{r}{R}\right)^{\frac{3n-1}{n}}+$$

$$\left.+\left[\frac{n-1}{n(3n-1)(5n-1)}+\frac{(n-1)^2}{4n^3(5n-1)}-\frac{n-1}{2n^2(3n-1)}\right]\left(\frac{r}{R}\right)^{\frac{5n-1}{n}}+\ldots\right\}$$

Since $n > 1$, we thus have

$$t = \frac{(2\gamma_w)^{n-1}}{(n-1)\lambda}\, R^{n+1}\,\bar{u}^{1-n}\left[f\left(n, \frac{r}{R}\right)\right]^n + C$$

where C is a constant of integration.

The boundary condition $\bar{u} = \bar{u}_0$ for $t = 0$ gives finally

$$t = \frac{\alpha}{\lambda} D^{n+1} \gamma_w{}^{n-1} \left[\frac{1}{\bar{u}^{n-1}} - \frac{1}{(\bar{u}_0)^{n-1}} \right] \quad \ldots\ldots\ldots\ldots \quad (4:7)$$

where

$$\alpha = \frac{1}{4(n-1)} \left[f\left(n, \frac{r}{R}\right) \right]^n$$

The functions $f(n, \frac{r}{R})$ and α are represented in Fig. 31 for $n = 1.2$, 1.3 and 1.5.

Introducing the average degree of consolidation

$$\bar{U} = \frac{\bar{u}_0 - \bar{u}}{\bar{u}_0}$$

the time t required for a given degree of consolidation $\bar{U}$ is

$$t = \frac{\alpha}{\lambda} \frac{D^{n+1} \gamma_w{}^{n-1}}{(\bar{u}_0)^{n-1}} \left[\frac{1}{(1-\bar{U})^{n-1}} - 1 \right] \quad \ldots\ldots\ldots\ldots \quad (4:8)$$

The excess pore water pressure u at radius ϱ is obtained from Eqs. (4:4) and (4:8). Thus, from Eq. (4:8) we get

$$-\frac{1}{\bar{u}_0} \frac{\partial \bar{u}}{\partial t} = \frac{\lambda (\bar{u}_0)^{n-1}}{\alpha (n-1) D^{n+1} \gamma_w{}^{n-1}} (1-\bar{U})^n \quad \ldots\ldots\ldots \quad (4:9)$$

and hence

$$\frac{u}{\bar{u}_0} = K_1 (1-\bar{U}) \left[F\left(n, \frac{\varrho}{R}\right) - F\left(n, \frac{r}{R}\right) \right] \quad \ldots\ldots\ldots \quad (4:10)$$

in which

$$K_1 = \frac{n}{2(n-1) f\left(n, \frac{r}{R}\right)}$$

$$F(n, x) = x^{\frac{n-1}{n}} \left[1 - \frac{n-1}{n(3n-1)} x^3 - \frac{(n-1)^2}{2! n^2 (5n-1)} x^4 - \ldots \right]$$

(The variable x represents in this case $\frac{\varrho}{R}$ or $\frac{r}{R}$.)

The function $F(n, x)$ for $n = 1.2$, 1.3 and 1.5 is shown in Fig. 32.
The pore water pressure gradient becomes

$$\frac{\partial u}{\partial \varrho} = \frac{(1-\bar{U})\, \bar{u}_0}{D f\left(n, \frac{r}{R}\right)} \left(\frac{R}{\varrho} - \frac{\varrho}{R} \right)^{\frac{1}{n}} \quad \ldots\ldots\ldots\ldots \quad (4:11)$$

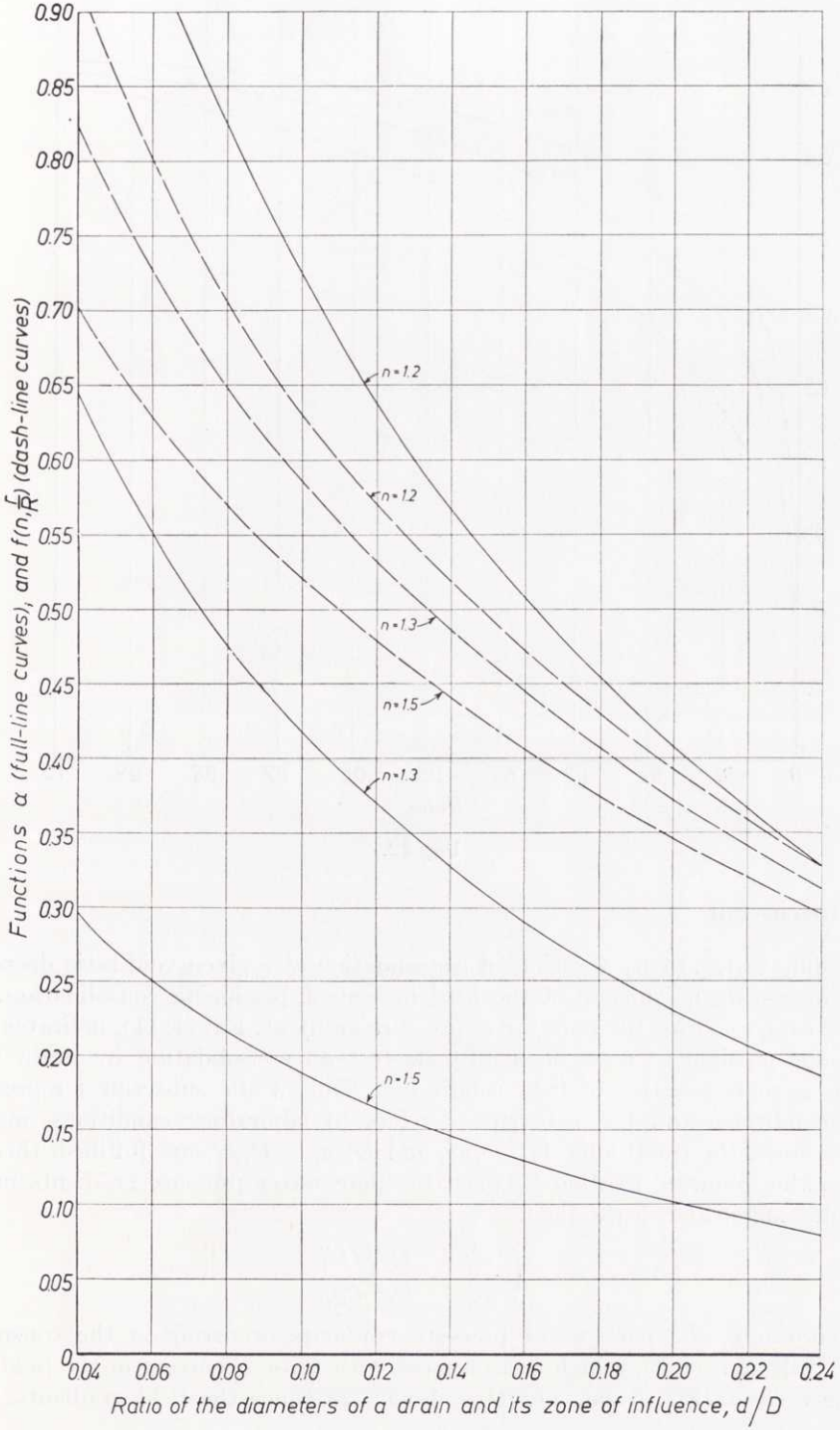
0.90
0.85
0.80
0.75
0.70
0.65
0.60
0.55
0.50
0.45
0.40
0.35
0.30
0.25
0.20
0.15
0.10
0.05
0
0.04
0.06
0.08
0.10
0.12
0.14
0.16
0.18
0.20
0.22
0.24
n=1.2
n=1.2
n=1.3
n=1.5
n=1.3
n=1.5
Functions α (full-line curves), and f(n, r/R) (dash-line curves)
Ratio of the diameters of a drain and its zone of influence, d/D

Fig. 31.

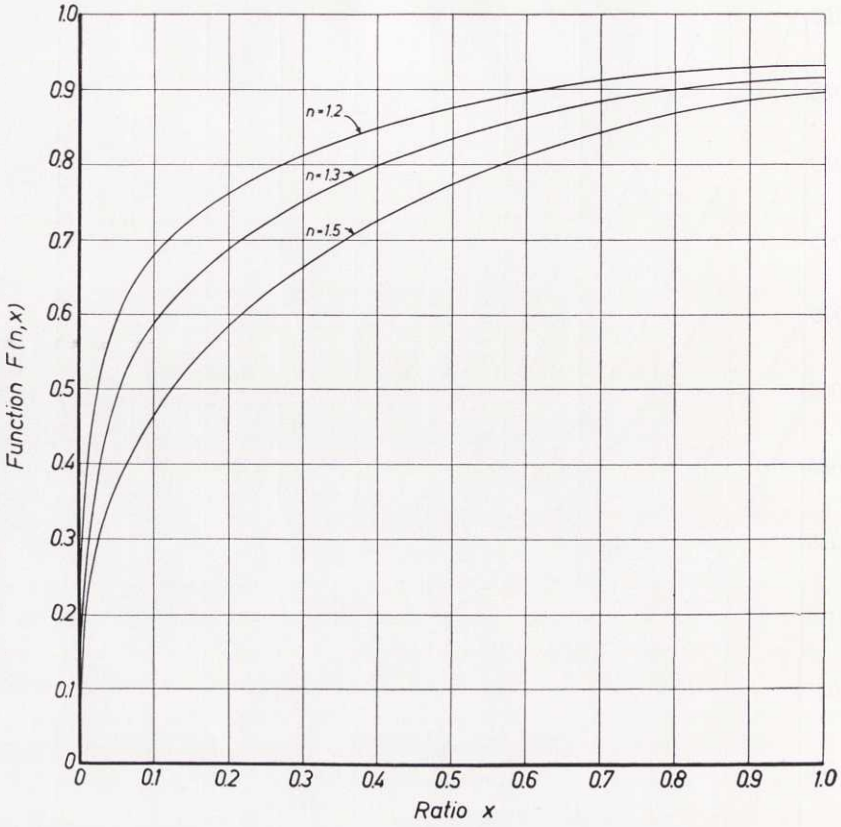

Fig. 32.

41. Discussion

According to Eq. (4: 8), the time of consolidation at a given void ratio decreases with increasing magnitude of the load increment producing consolidation.

The expression for the pore water pressure gradient, Eq. (4: 11), indicates that it is not possible to make a small-scale test on consolidation by drain wells which is representative of field conditions. Thus, if the subscript f represents field conditions and the subscript c refers to laboratory conditions, and if, furthermore, the conditions $\Delta q_f = \Delta q_c$ and $D_f/d_f = D_c/d_c$ are fulfilled, then we obtain the following relation between the pore water pressure gradients in the consolidometer and in the field:

$$\left(\frac{\partial u}{\partial \varrho}\right)_c = \frac{D_f}{D_c}\left(\frac{\partial u}{\partial \varrho}\right)$$

Accordingly, the pore water pressure gradients occurring in the consolidometer will be extremely high as compared with those occurring in the field, *e.g.* in the case of $D_c = 6$ cm, and $D_f = 1.5$ m, 25 times the field gradients. This

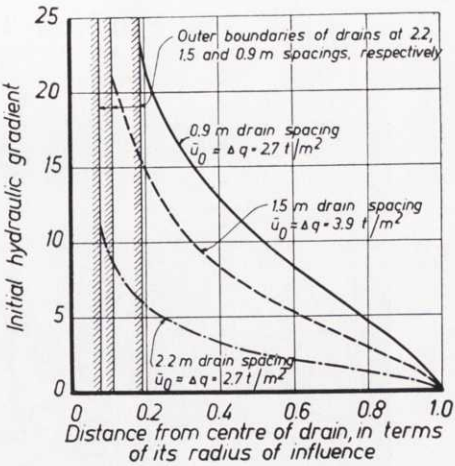

Fig. 33. Initial hydraulic gradients obtained from Eq. (4: 11) for the drain spacings and loads which were used at Skå-Edeby.

difference between laboratory and field conditions can have important practical consequences, if the limit of the given law of pore water flow is exceeded in the consolidometer test but not in the field. This seems undoubtedly to be the case, and the theory presented here is therefore relevant to field conditions only. For example, under the conditions in the test field at Skå-Edeby, the pore water pressure gradients obtained from Eq. (4: 11) for $n = 1.5$ and $\bar{u}_0 = \Delta q$ would reach the maximum values given in Fig. 33. For a drain spacing of 0.9 m and $\bar{u}_0 = 2.7$ t/m², we thus find an initial gradient $i_{t=0} < 10$ within 76 % of the zone of influence of a drain. For a spacing of 1.5 m and $\bar{u}_0 = 3.9$ t/m², we find $i_{t=0} < 10$ within 91 % of the zone, and for a spacing of 2.2 m and $\bar{u}_0 = 2.7$ t/m², $i_{t=0} < 5$ within 94 % of the zone. In this case, during the main part of the period of consolidation, the gradients are obviously within the limits of validity of Eq. (3: 1), as found in Chapter 3, while this is not the case in the laboratory tests.

An approximate value of λ could be found on the basis of the results of the consolidometer test if the limits of validity of Eq. (4: 1) were known. Thus, if DARCY's law of permeability is considered to be valid during the consolidometer test, then, according to Eqs. (3: 2) and (4: 1),

$$n \lambda m_v \gamma_w i_l^{n-1} \left[1 - \frac{i_l (n-1)}{i n} \right] = c_h m_v \gamma_w$$

whence

$$\lambda \approx \frac{c_h}{n i_l^{n-1}}$$

Further comparisons between the theory presented and the results obtained from field and laboratory tests will be made subsequently.

5. Full-Scale Tests at Skå-Edeby

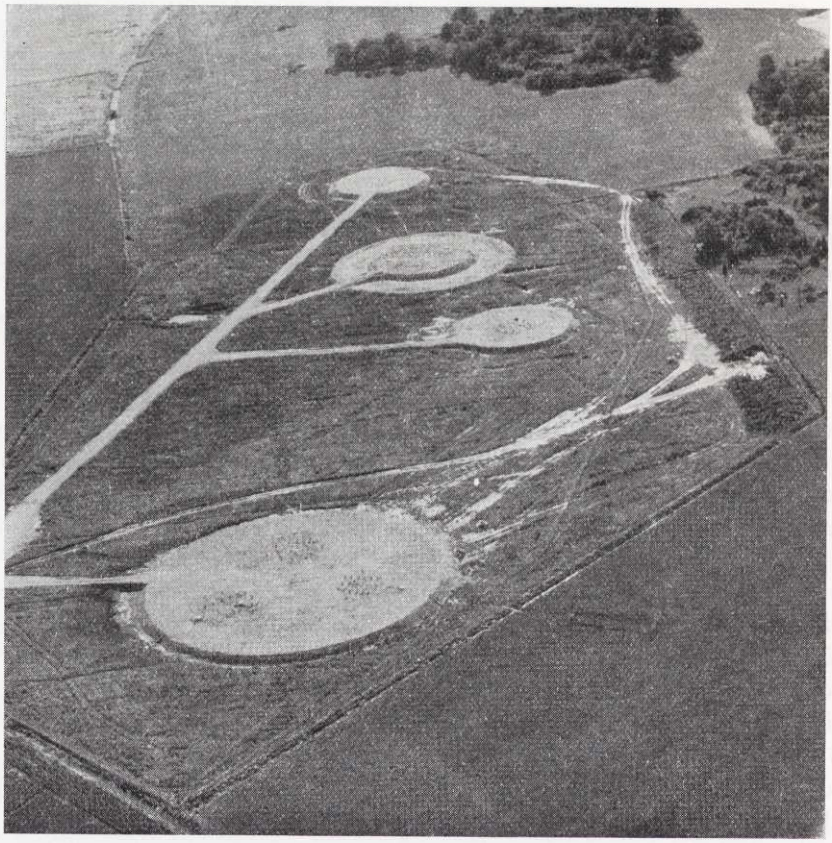

Aerial photo of test field.

50. Description of Test Field and Measuring Equipment

The test field at Skå-Edeby was planned so that it should not interfere with the buildings of a future airfield (*cf.* Section 10). Owing to the limited possibilities of choice, the site conditions are not uniform, and this has complicated the interpretation of the results.

The field comprises four different test areas. Fig. 34 gives their situations and the depth to firm bottom in the field.

The areas were located with the guidance of sounding results so that the depths to firm bottom should be as nearly equal as possible, and so that the

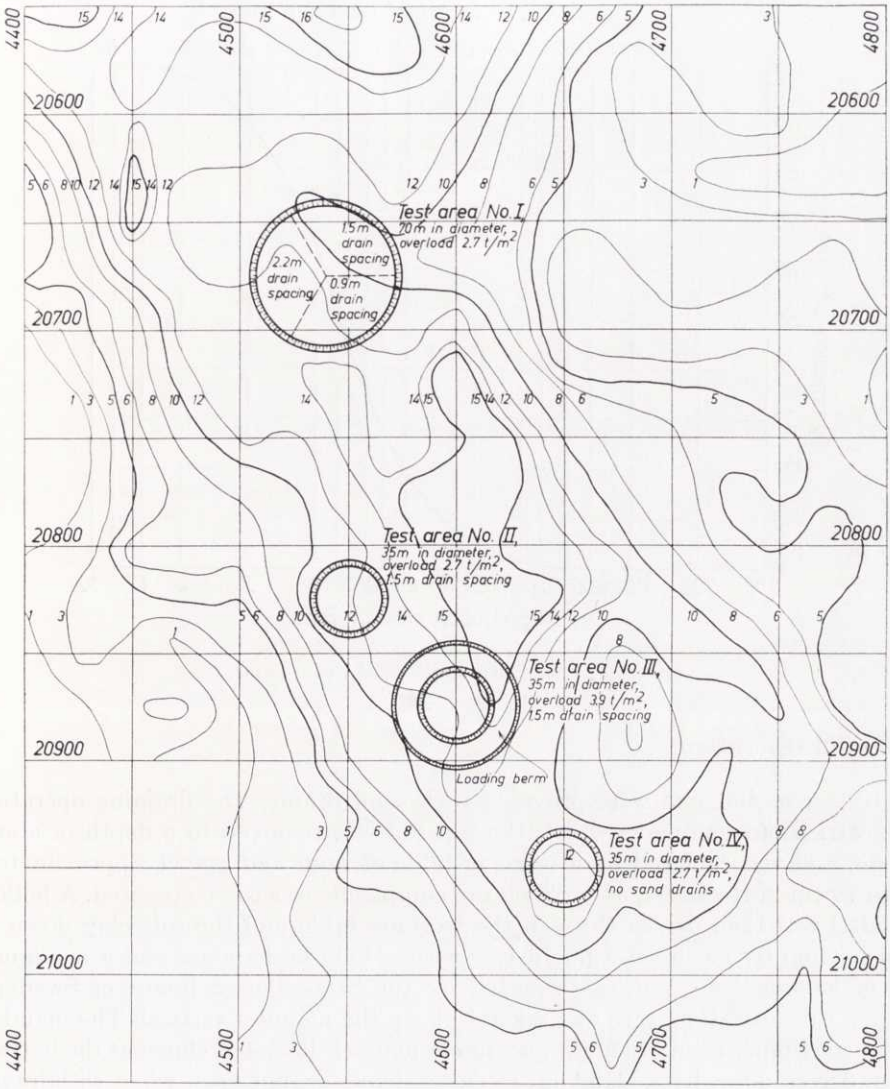

Fig. 34. Test areas and depth from ground surface to firm bottom, in m, in test field at Skå-Edeby. Coordinate system gives horizontal distances, in m.

distances between the areas should be as large as possible in order that the test results obtained in an area might not be appreciably influenced by neighbouring areas. However, owing to irregular bed rock, the depth to firm bottom in the areas varies from 9 to 15 m. The average depth to firm bottom is estimated at 11 m.

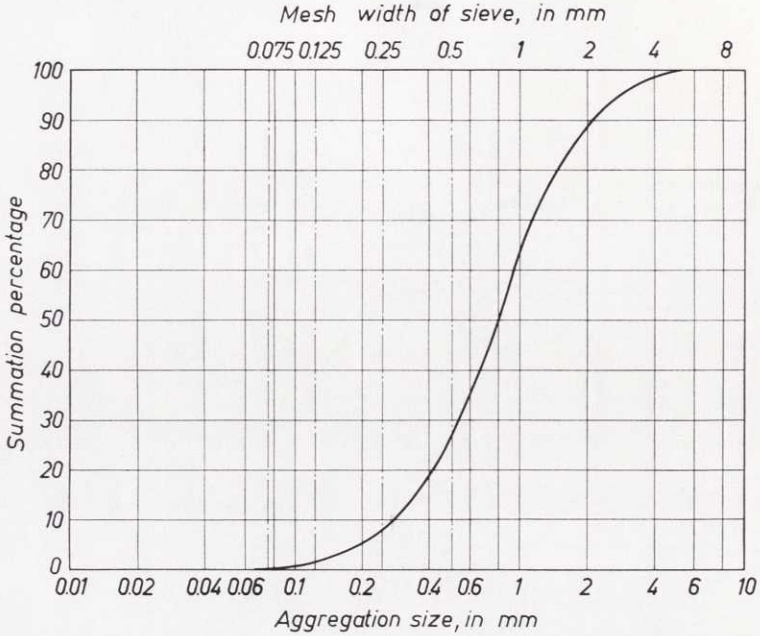

Fig. 35. Grain distribution of drain sand.

Draining Operation

All test areas but one were provided with sand drains. The draining operation was carried out as follows. First, the top soil was removed to a depth of about 25 cm, and was replaced by a working table of sand and gravel, approximately 50 to 70 cm in thickness, over which the equipment was to be operated. A hollow mandrel was then driven through the working table and the soft clay down to firm bottom by means of a pile driver with a 1200 kg hammer and a maximum fall of hammer of 0.5 m (as reported by the State Power Board of Sweden). During this operation, care was taken to keep the mandrel vertical. The mandrel was a steel pipe, 14 m in length and 15 cm in inner diameter, closed at the bottom when driven down by a plane lid, 18 cm in diameter, but open when withdrawn. When the mandrel pipe had reached firm bottom it was filled with saturated sand—grain distribution shown in Fig. 35—to a height of 4 m above the surface of the working table and was then withdrawn, leaving a sand column, about 18 cm in diameter, in the clay. In the places where the depth exceeded 10 m the pipe was first filled with sand, then withdrawn a distance necessary to refill it as described above, and finally withdrawn completely. If the length of the mandrel was insufficient to reach firm bottom, as it proved to be in a minor part of Test Area No. III, then difficulties arose in filling the pipe with sand. Thus the clay at the lower end of the mandrel seemed to be too soft to resist the pressure due to the sand drains. In that case great quantities of sand were

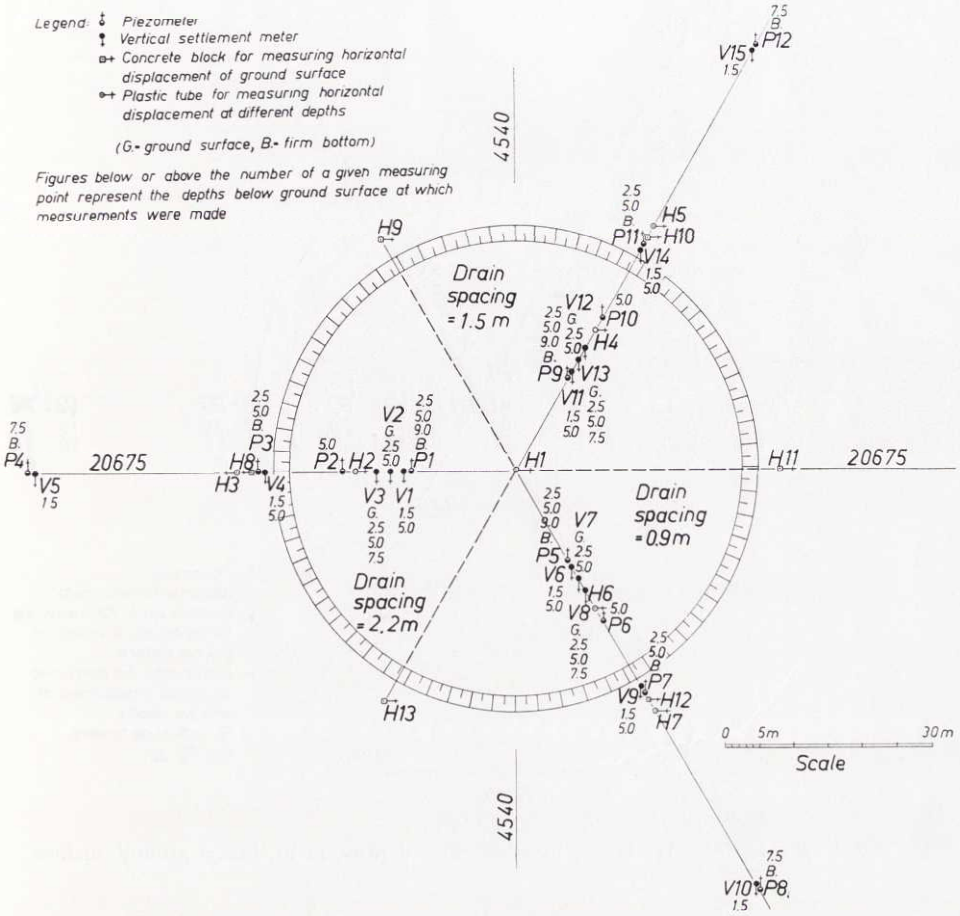

Fig. 36. Test Area No. I: Drain spacings, and meter locations and depths, in m, below ground surface. Settlement meters Nos. V2, V7 and V12 are placed in sand drains.

often used up before sufficiently strong supports were finally obtained for the pipe to be filled.

The drains were arranged in a triangular pattern. In all, 3500 drains were installed, and their average length was 12 m.

Test Areas

The test areas are circular. Area No. I is 70 m in diameter, and is divided into three equal sectors with the respective drain spacings 0.9, 1.5 and 2.2 m. It is loaded by a gravel blanket about 1.5 m in thickness, including the working table.

Area No. II is 35 m in diameter, the drain spacing is 1.5 m, and the total overload, including the working table, is gravel, about 1.5 m in thickness.

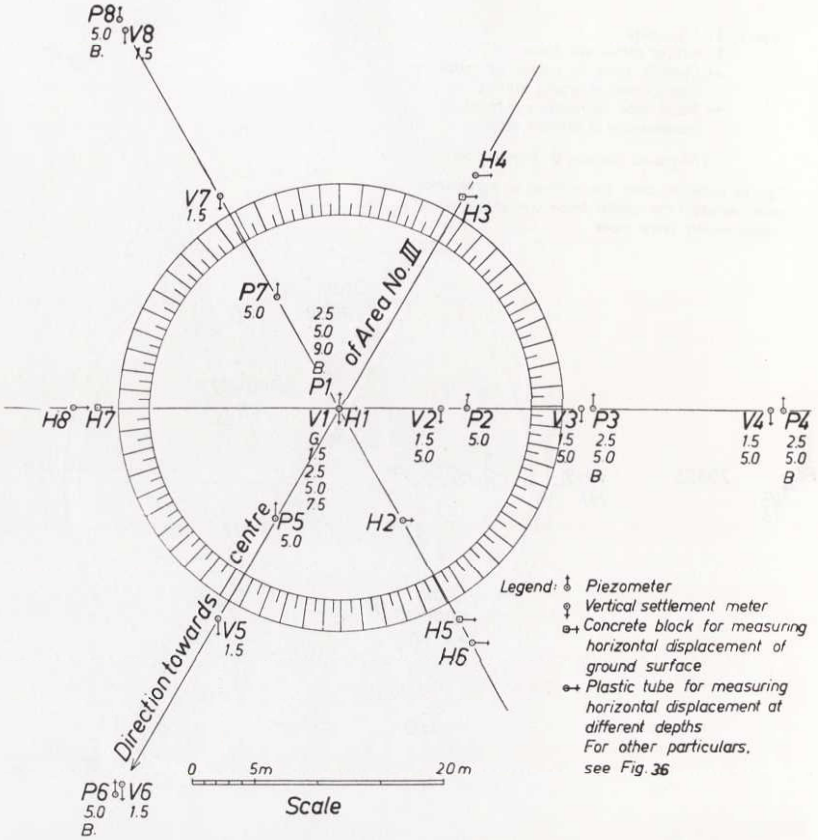

Fig. 37. Test Area No. II: Meter locations and depths, in m, below ground surface.

Area No. III is 35 m in diameter, the drain spacing is 1.5 m, and the total overload, including the working table, is gravel, about 2.2 m in thickness. To take precautions against possible slides, this area was surrounded by a loading berm, 12 m in width and 0.7 m in thickness.

Area No. IV is 35 m in diameter, and the overload is gravel, 1.5 m in thickness. Here no sand drains were installed.

The unit volume weight of the overload material was continuously checked, and was found to be 1.79 t/m^3 on an average.

Vertical Settlement Meters

The settlement of the ground surface and in the interior of the clay, and in Test Area No. I also in sand drains, was observed at different points within and outside the test areas, see Figs. 36 to 39.

The settlement of the ground surface was measured by settlement meters consisting of rods welded to rectangular plates, which were placed directly on the ground below the sand fill.

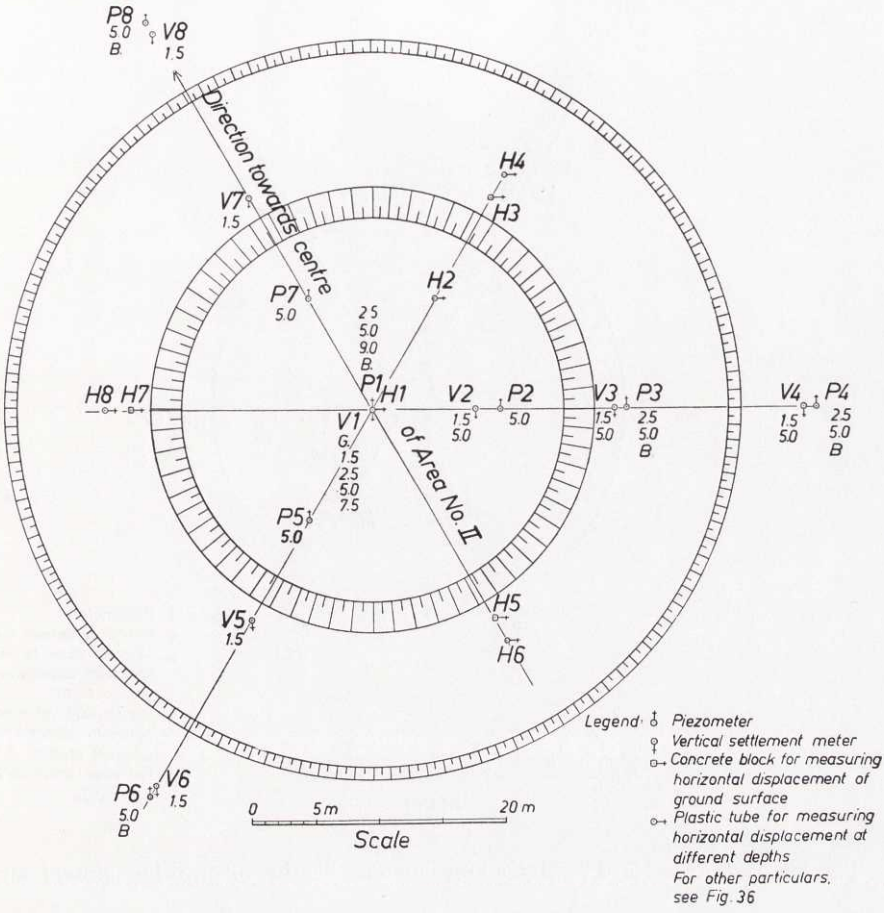

Fig. 38. Test Area No. III: Meter locations and depths, in m, below ground surface.

The settlement in interior parts of the clay and in the drains was measured by means of settlement meters consisting of rods, 19 mm in diameter, welded to earth screws, Fig. 40, which were screwed down to the desired level (*cf.* also KJELLMAN, KALLSTENIUS, and LILJEDAHL, 1955, Fig. 4). The earth-screws used in the drains were smaller in diameter than those used in the clay (125 as compared with 222 mm) and were perforated.

The settlement on top of the drains was measured by settlement meters consisting of rods, 19 mm in diameter, welded to circular, perforated iron plates, 150 mm in diameter.

The rods were coated with asphalt and wrapped in aluminium foil. In the gravel blanket they were protected by a galvanized iron tube, 2 in. in inner diameter. The level of the upper ends of the rods was measured by a precision levelling instrument.

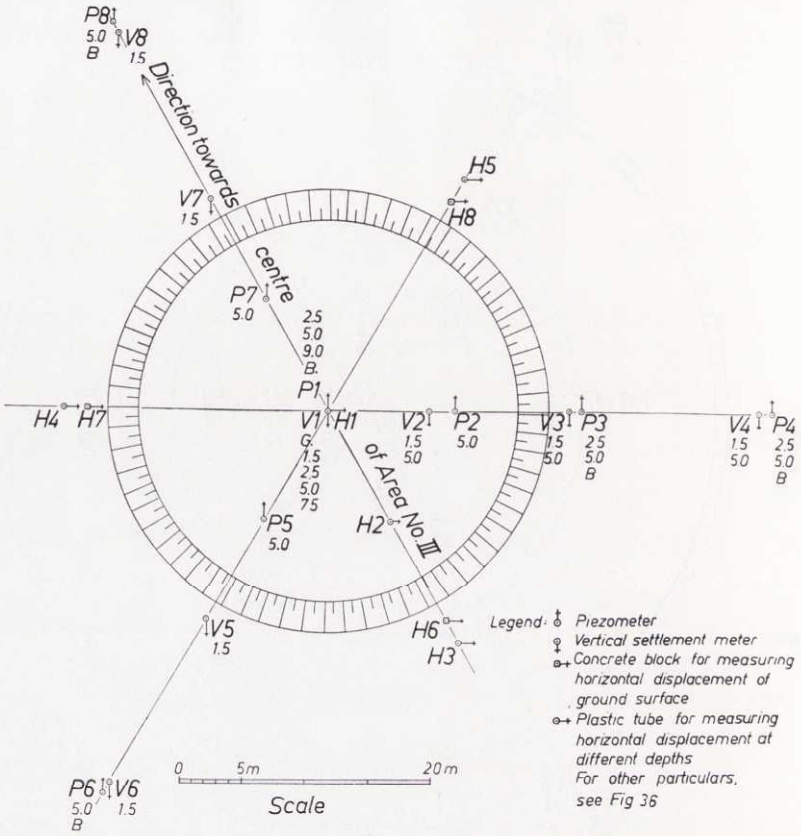

Fig. 39. Test Area No. IV. Meter locations and depths, in m, below ground surface.

Fig. 40. Earth-screw used for settlement observations below ground surface level.

Horizontal Settlement Meters

The horizontal movements of the clay were studied in two different ways.

The displacement of the ground surface was measured by precision measuring tape from iron pins fixed in concrete blocks, which were placed immediately outside the test areas and which followed the movements of the ground surface, to wooden piles placed at great distances from the test areas so as not to be influenced by them. Since the piles might be displaced by accident, the distances between the pins were also measured.

The measurements in the interior of the soil were made by means of plastic tubes, which were driven into the soil down to firm bottom and which were supposed to follow closely the movements of the clay. To begin with, the inclination of the tube at different depths was measured by an inclinometer ordinarily used for measuring bore holes in rock. There were reasons to believe that the inclinometer was affected by vibrations during the first measurements which took place during the driving of drains. Furthermore the inclinometer seemed too long and heavy, and it was suspected that the inclination of the tube at the point of observation due to the soft clay supporting the tube might be affected by the inclinometer itself. These defects were already observed in the second measurements, and the corresponding results are therefore omitted here.

However, at an early stage, a new type of measuring device was installed outside the sectors of Area No. I and also outside Area No. II. A flexible metal tube, 105 mm in inner diameter, was carried down to a depth of 3 to 4 m. A hole for this tube was pre-bored through the dry crust down to a depth of 2 m. The space between the tube and the clay was filled with fine saturated sand, and concrete was poured around the top of the tube.

The inclination of the tube with reference to the ground surface at depths of 1, 2, 3, and, where possible, 4 m was measured with an instrument specially made for this purpose, Fig. 41. This instrument consists of a straight metal rod, 20 mm in diameter, which is guided at the top of the tube and at the point

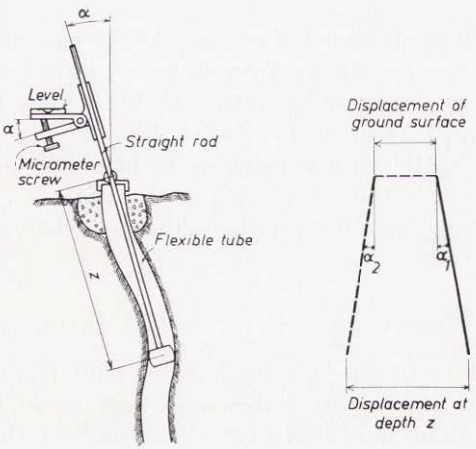

Fig. 41. Sketch of instrument used for determination of horizontal displacement at a given depth, z, below ground surface.

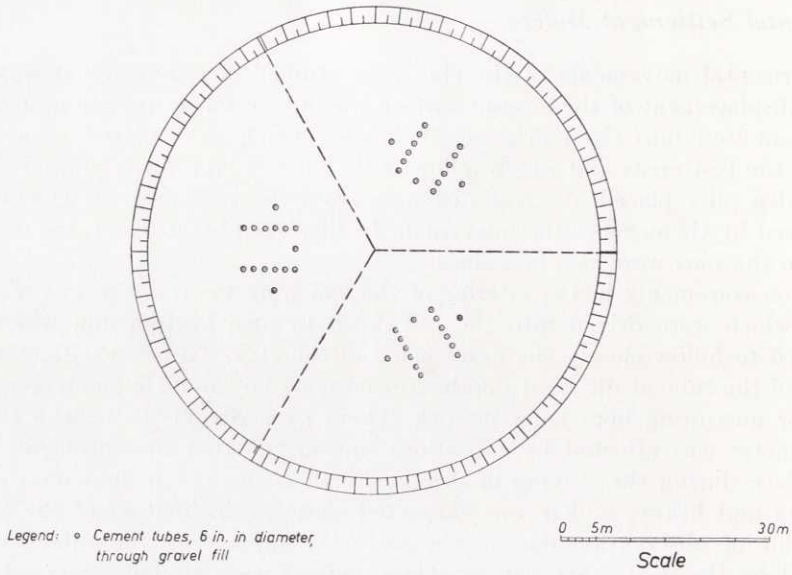

Fig. 42. Locations of cement pipes through gravel fill in Test Area No. I.

of observation. A precision water level is fixed on the top of the rod. The angle between the rod and the water level is measured by a dial gauge by which the inclination of the rod can be determined with an accuracy of 1 in 10000. In practice the accuracy is less, especially when the measurements are carried out at a depth of 4 m. Here the rod must be lengthened, and the apparent inclination can be appreciably different from the true value. However, this source of error was reduced by rotating the rod twice through an angle of 120° and measuring its inclination each time.

Piezometers

The pore water pressures were measured at different levels outside and inside the test areas, Figs. 36 to 39, by means of a Type SGI II piezometer (KALLSTENIUS and WALLGREN, 1956, Figs. 18 a and 20). The accuracy of this type of piezometer is estimated by the above authors at ± 10 cm of water column.

Attempts were made to place the piezometers half-way between the drains, *i.e.* in the centre of a "drain triangle". In reality this attempt will be hindered by difficulties, such as the fact that sand drains are seldom vertical (*cf.* Section 53).

Measures Taken for Future Investigations

For future investigations, cement pipes, 6 in. in diameter, were placed in great numbers within the areas, Figs. 42–43, leaving holes through the fill. In drained areas the tubes were placed half-way between the drains.

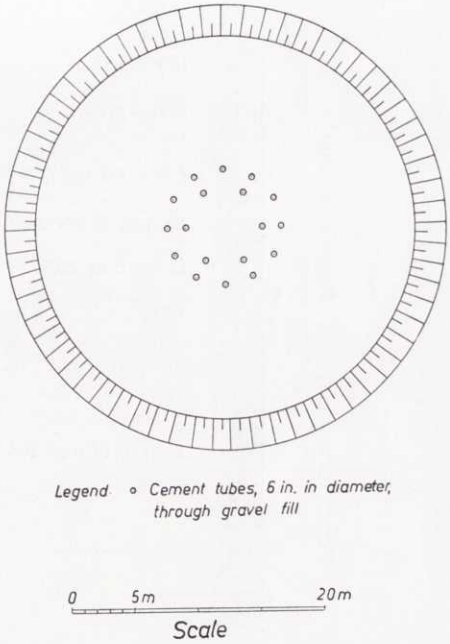

Fig. 43. Locations of cement pipes through gravel fill in Test Areas Nos. II to IV.

51. Geological Description of Site[1]

For the geological investigation, five cores were taken in Area No. I. Two of them were taken immediately before, and the other three approximately one year after, the completion of this test area.

The irregular topography of the site has had important effects on the sedimentation of the clay and also on its stratigraphy.

The soil in the test areas consists of post-glacial clay to a depth of 5 to 6 m. Underneath there is a zone of glacial varved clay, which contains thin layers of sand or silt of varying thickness near the bed rock. Sand or silt is generally found in the immediate neighbourhood of the bed rock but does not continuously cover it (*cf.* also Section 55).

The dry crust has a varying thickness, generally 1 m.

The clay has in some places a high sulphur content. The carbon content, determined according to KOLTHOFF and SANDELL (*cf.* SILFVERBERG, 1957), is approximately 0.4 % both in the post-glacial and late glacial clay.

The clay content (particle size less than 2 μ) varies generally from 60 to 70 %. The grain size distribution in a core taken in Area No. I is shown in Fig. 44.

[1] This description is a brief summary of a report by JÄRNEFORS (1957).

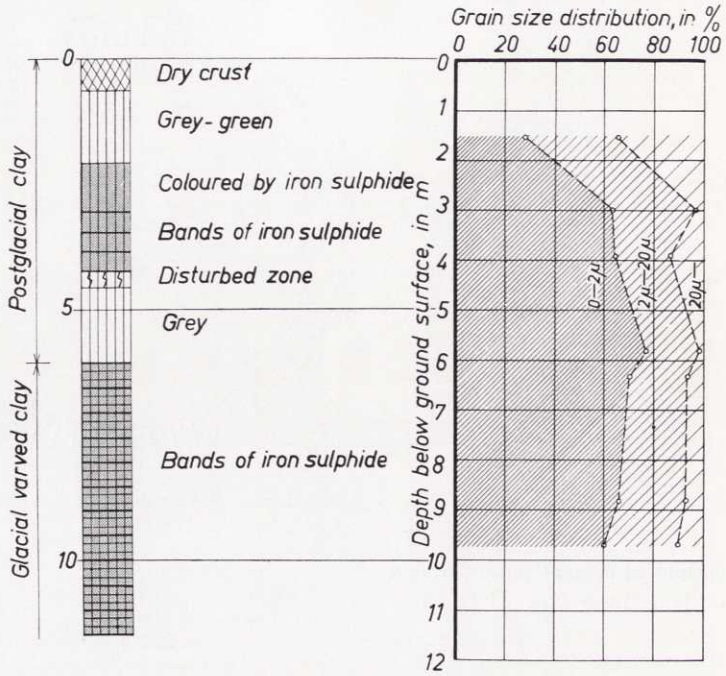

Fig. 44. Geological profile and grain size distribution in core taken in Test Area No. I.

52. Geotechnical Description of Clay

General Details

The preliminary geotechnical investigation was limited by the short time at disposal before the drainage and loading of the test areas had to be carried out. Nevertheless, a rather extensive testing programme was performed, and some of its deficiencies were remedied at a later stage.

The shear strength of the clay was determined *in situ* by the vane borer test (CADLING and ODENSTAD, 1950) and in the laboratory mainly by the fall-cone test (interpreted according to HANSBO, 1957) as well as by the unconfined compression test and by the laboratory vane test (see KALLSTENIUS, 1958).

The sensitivity was determined by the field vane test and by the fall-cone test.

Determinations were also made of the unit volume weight, the water content in per cent of dry weight, and the Atterberg limits. In view of the extensive testing programme, the time-wasting determinations of the Atterberg limits were sometimes replaced by the simple "finlekstal" (fineness number) determinations (STATENS JÄRNVÄGAR, 1922). At a later stage, determinations were also made of the void ratio and specific gravity of clay mineral.

The geotechnical data are shown in Figs. 45 to 50.

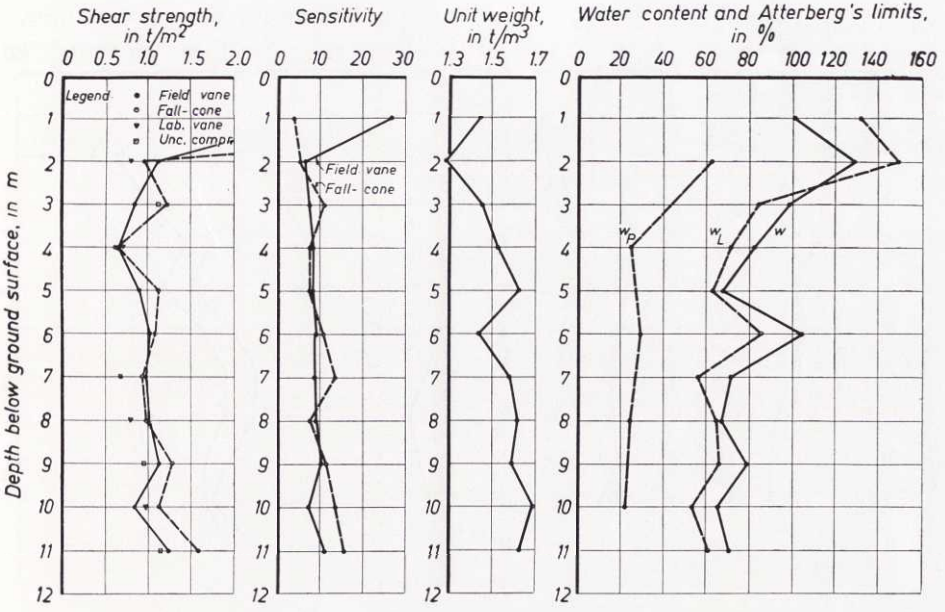

Fig. 45. Geotechnical data on clay. Test Area No. I, drain spacing 0.9 m. Legend for shear strength curves: full-line, field vane tests; dash-line, fall-cone tests.

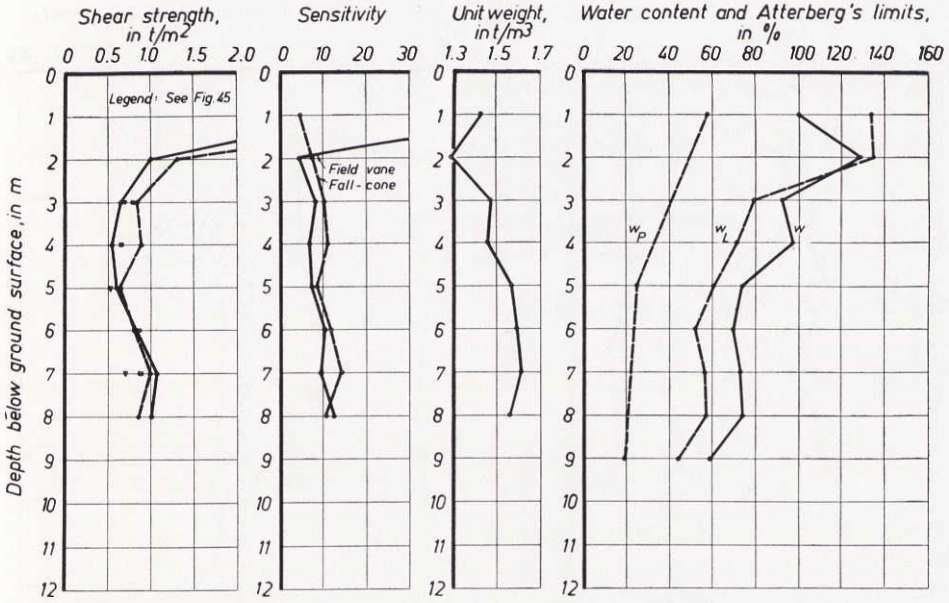

Fig. 46. Geotechnical data on clay. Test Area No. I, drain spacing 1.5 m. Legend, see Fig. 45.

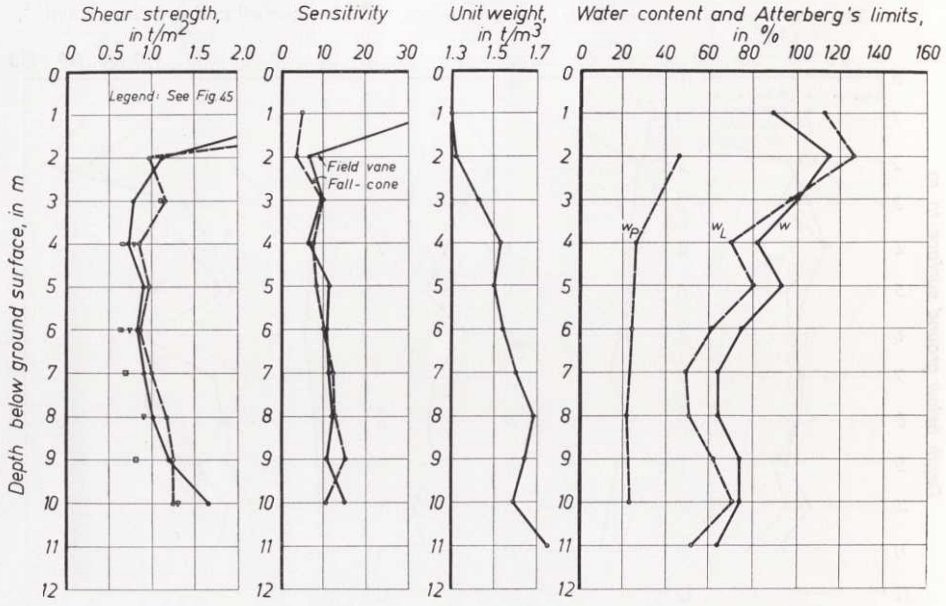

Fig. 47. Geotechnical data on clay. Test Area No. I, drain spacing 2.2 m. Legend, see Fig. 45.

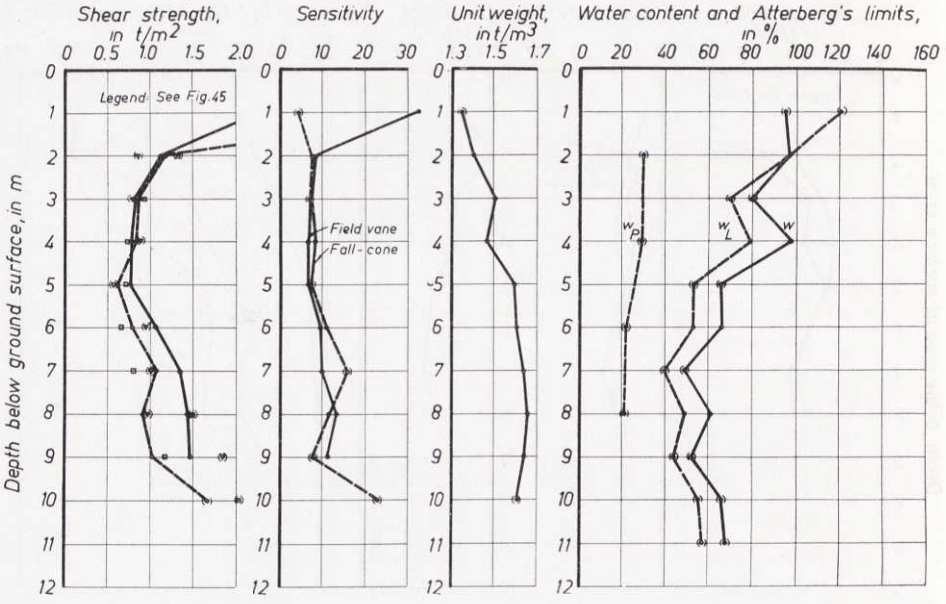

Fig. 48. Geotechnical data on clay. Test Area No. II. (Average of two observations except for points in parentheses, which represent single observations.) Legend, see Fig. 45.

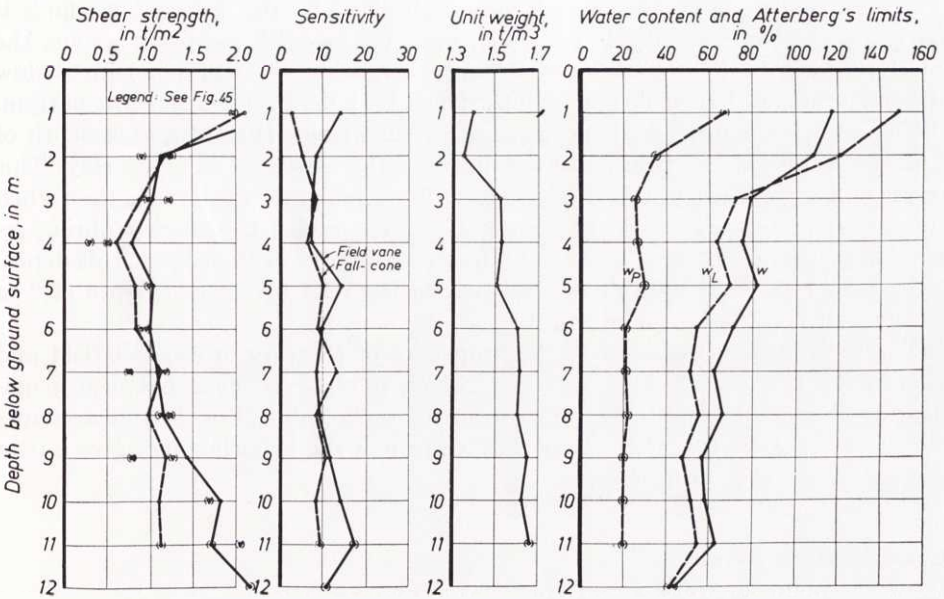

Fig. 49. Geotechnical data on clay. Test Area No. III. (Average of two observations except for points in parentheses, which represent single observations.)
Legend, see Fig. 45.

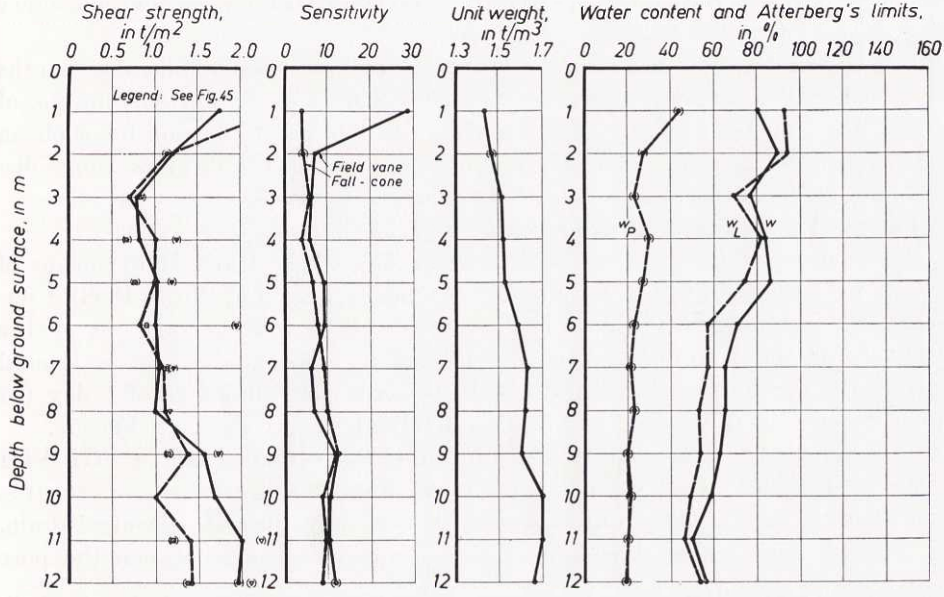

Fig. 50. Geotechnical data on clay. Test Area No. IV. (Average of two observations except for points in parentheses, which represent single observations.)
Legend, see Fig. 45.

The agreement between strength values obtained by the different methods is fairly reasonable. The clay is very soft, even for Swedish conditions. Thus the shear strength is slightly above or around 0.5 t/m^2 (= 0.05 kg/cm^2) just below the dry crust, and then increases with depth to 1 or 2 t/m^2 near firm bottom.

The observed sensitivity is normal for Swedish clays. However, at a depth of 1 m the results of the field vane test indicate the existence of quick clay. This result is not recorded in the fall-cone test. It may be due to the fact that when the test is performed *in situ* free ground water is added to the clay during remoulding. This is rendered possible by frequent fissures in the clay at this depth.

The observed void ratio of the clay varied from 2.1 to 2.3 at a depth of 2 m and from 1.7 to 2.1 at a depth of 8 m.

The results show variation in the properties of the clay in the test field and also in the test areas[1]. This variation, which is observed even between neighbouring borings, makes the interpretation of the results difficult and accounts for the well-known fact that samples taken from a single boring may give a poor picture of the clay properties.

Consolidation Data

The compression characteristics of the clay were originally determined by conventional oedometer tests carried out by AB Orrje & Co. on samples, 60.5 mm in diameter and 20 mm in height, at the successive loads 0.1, 0.2, 0.4, 0.8, 1.6, and 3.2 kg/cm^2. Enough time of compression under each load was allowed for the primary consolidation to be practically completed. Ordinarily a time allowance of 3 days was used, sometimes even more.

The oedometer tests were as a rule carried out on samples taken at depths of 2, 5, and 8 m below ground surface. The samples were taken by means of a SGI IV sampler, no other sampler being available at that time for such an extensive investigation. This sampler is easily handled but gives some disturbance that can be observed in the compression curves.

The results of these tests are given in Figs. 51 to 56.

Later on new samples were taken between Areas Nos. I and II by means of a SGI VIII sampler, which gives better samples (*cf.* KALLSTENIUS, 1958). Conventional oedometer tests, also including unloading, were carried out at the Institute on these samples taken at depths of 3, 4, 6, and 7 m below ground surface. In the tests performed at the Institute a time allowance of 1 day (24 hours) was ordinarily used. The results of these tests are given in Fig. 57.

Consolidometer tests were also made on samples taken with a SGI VIII sampler and with a soil sampler with metal foils (KJELLMAN, KALLSTENIUS, and WAGER, 1950), where drainage was allowed only through a central drain, *cf.* Fig. 58. This rendered possible a better correspondence between the pore

[1] Note, for example, the variation in depth to the high-plasticity layer which is situated at a depth of about 5 m below the ground surface and is about 1 m in thickness. This is even more obvious from Figs. 72 to 74, pp. 115—116.

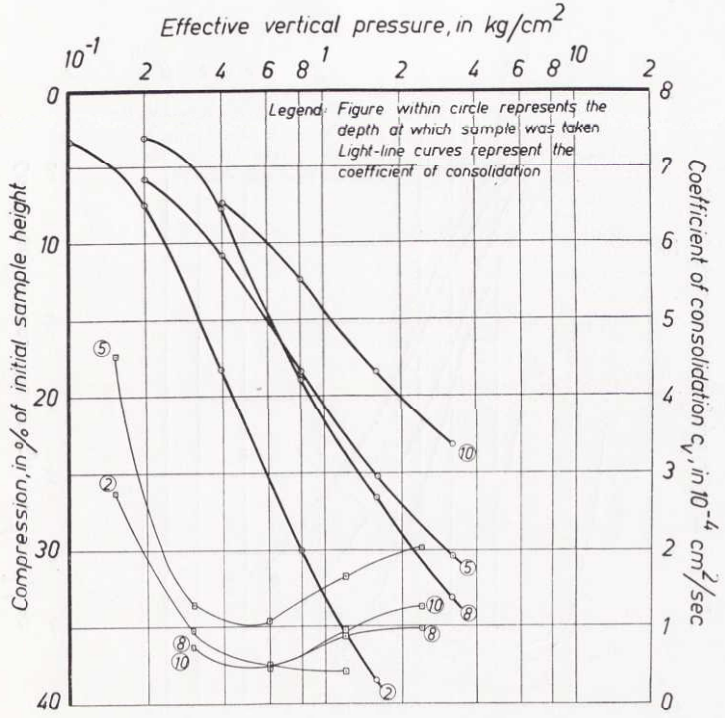

Fig. 51. Data on consolidation of clay. Test Area No. I, drain spacing 0.9 m.

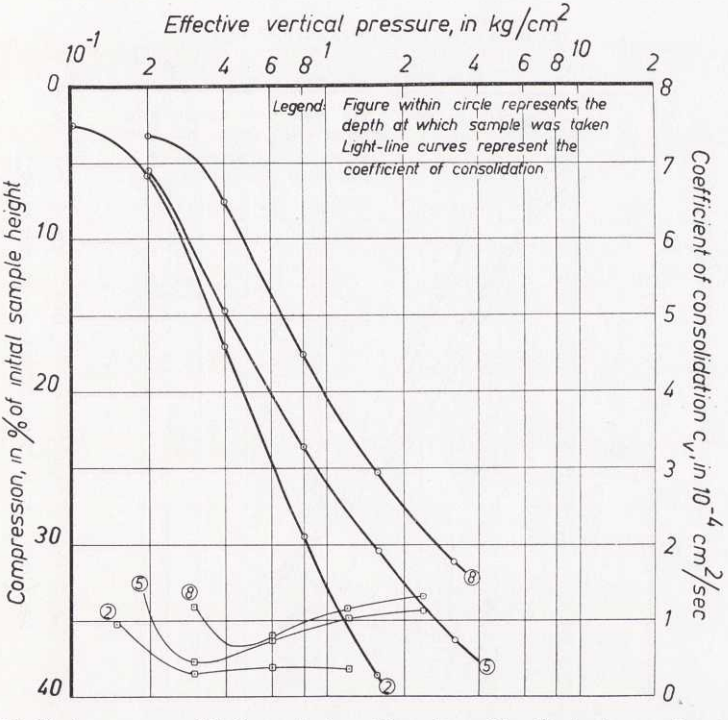

Fig. 52. Data on consolidation of clay. Test Area No. I, drain spacing 1.5 m.

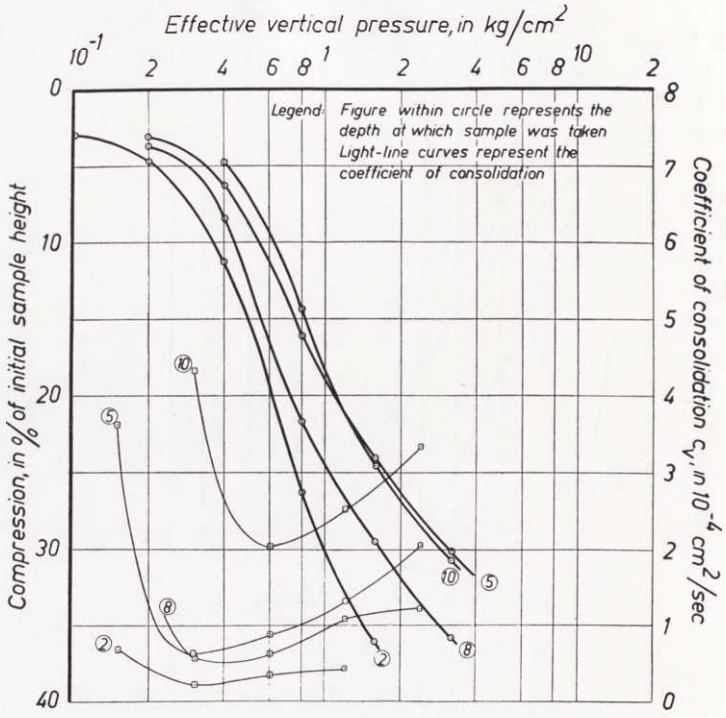

Fig. 53. Data on consolidation of clay. Test Area No. I, drain spacing 2.2 m.

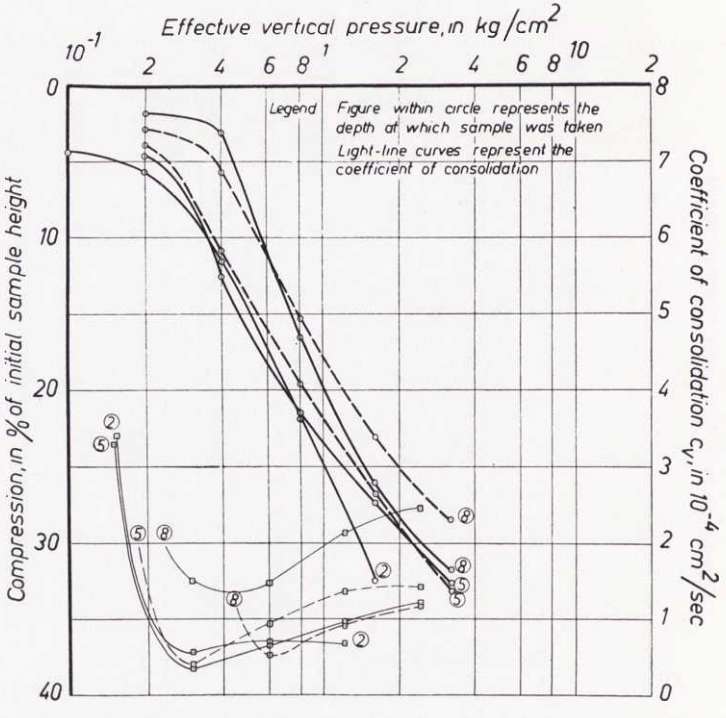

Fig. 54. Data on consolidation of clay. Test Area No. II.

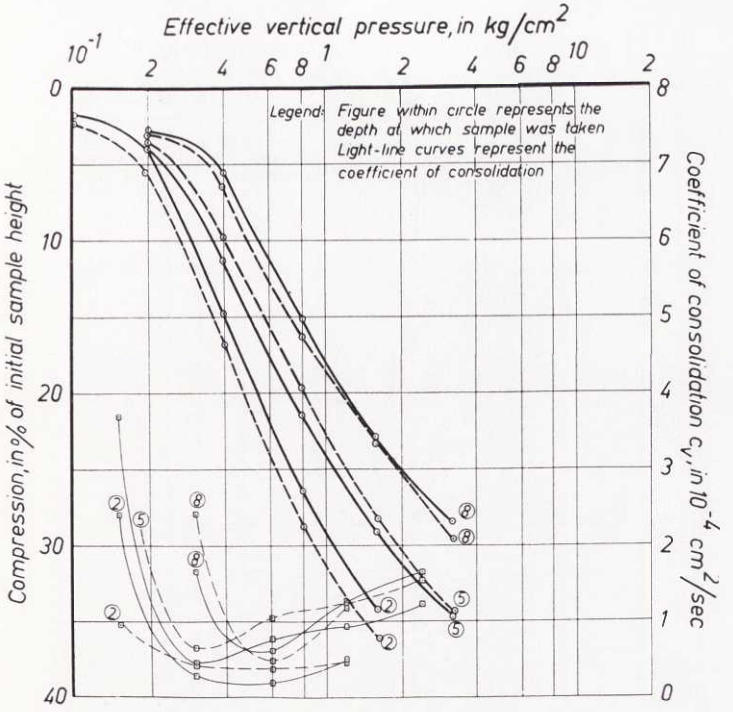

Fig. 55. Data on consolidation of clay. Test Area No. III.

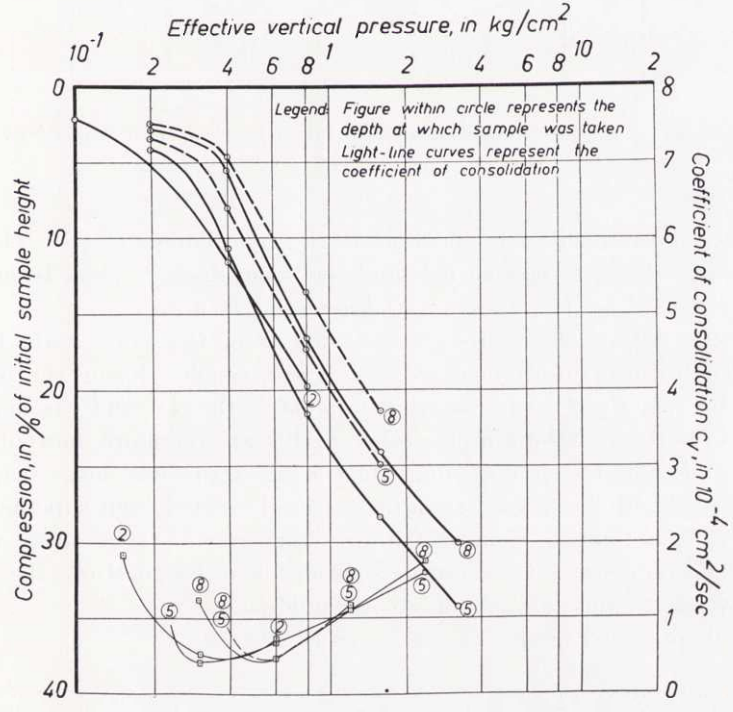

Fig. 56. Data on consolidation of clay. Test Area No. IV.

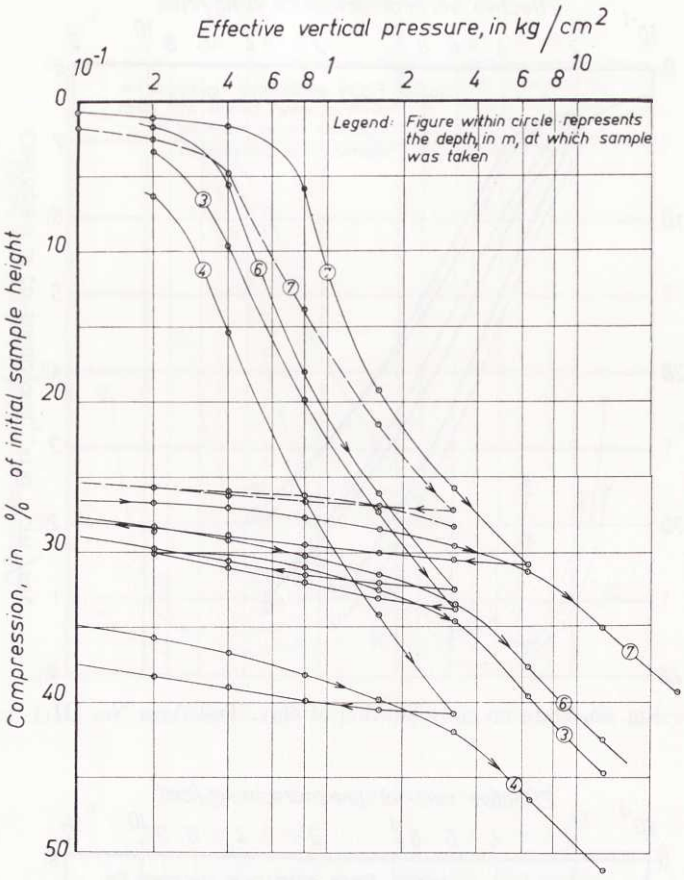

Fig. 57. Data on consolidation of clay samples taken between Test Areas Nos. I and II.

water escape in drained areas and that in the consolidometer test. The sample height used in this case was 40 mm and the drain diameter was 10 or 12 mm. The material used for the drains was either sand or mica.

The interpretation of the results obtained from the mica drain tests was complicated because the drain diameter became smaller during the test. Thus the diameter was about 7 mm on an average after the test and varied generally from top to bottom of the sample. These results are therefore omitted.

In the sand drain tests a stiffening effect of the drains was suspected, but was not to be observed. Sand used as drain material seemed even superior to mica as in the case of sand no change of drain diameter was to be observed during the test. The sand drain tests were also made in order to study the effect on clay behaviour in consolidation due to remoulding.

The result obtained in this case is given in Fig. 59.

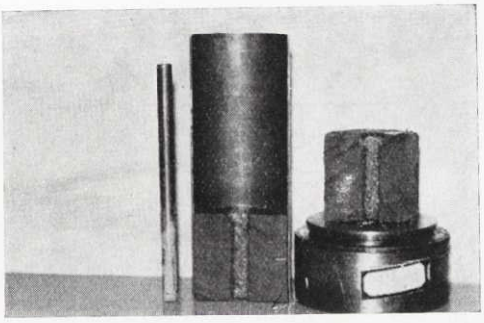

Fig. 58. Specimen prepared for consolidometer test with central drain and split diametrically into two equal parts.

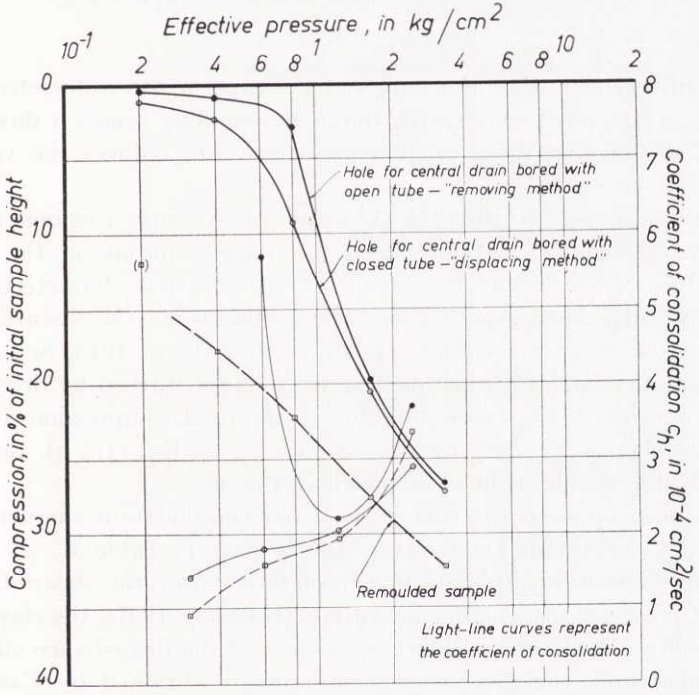

Fig. 59. Consolidation data obtained from consolidometer tests where drainage was allowed through a central sand drain.

An increase in consolidation index is obtained if the pore water escape takes place in a horizontal direction (*i.e.* parallel to the clay strata) and not in a vertical direction ($c_h > c_v$). The results obtained by using central drains agree fairly well with those obtained by consolidation of slices of clay cut out in

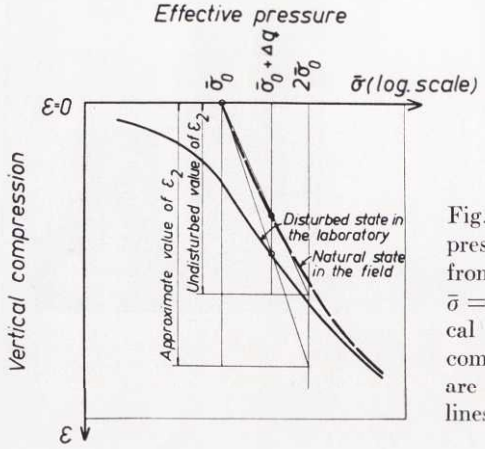

Fig. 60. Graphical determination of ε_2 from compression-pressure curve. The ε_2-lines are drawn from the point of intersection of $\varepsilon = 0$ and $\bar{\sigma} = \bar{\sigma}_0$ to the points of intersection of the vertical through $\bar{\sigma} = \bar{\sigma}_0 + \Delta q$ and the respective compression curves. The respective values of ε_2 are defined by the deformations along the ε_2-lines from $\bar{\sigma} = \bar{\sigma}_0$ to $\bar{\sigma} = 2\ \bar{\sigma}_0$.

a vertical direction so that the pore water escape in the oedometer is parallel to the clay strata (*cf.* LUNDSTRÖM, 1957). Remoulding causes a downward displacement of the void ratio *vs.* pressure curve and reduces the value of the coefficient of consolidation.

The disturbance due to the SGI IV sampler may cause a change in the compression characteristics, and may lead to underestimation of the final compression. However, satisfactory values of the compression characteristics can be obtained by judgement based on experience concerning the disturbance factor for the type of sampler used (*cf.* TERZAGHI and PECK, 1948; SCHMERTMANN, 1955). In practice, at least when dealing with clay disturbed by driving of sand drains, an acceptable approximate value of the final compression for normally consolidated clay is obtained by choosing for ε_2, *cf.* Eq. (1: 5 b), the value determined by the graphical method shown in Fig. 60.

A comparison between the compression and consolidation characteristics obtained by the conventional oedometer tests is made in Table 5.

From the relationship between preconsolidation pressure, shear strength and liquid limit previously stated by the Author (HANSBO, 1957), the clay was found to be normally consolidated. However, in spite of the disturbance effects of the sampling operation, the preconsolidation pressure obtained by CASAGRANDE's method (CASAGRANDE, 1936) is often found to be higher than that corresponding to the calculated value for normally consolidated clay. This seemingly peculiar phenomenon can partly be ascribed to friction in the oedometer, but this does not explain the whole discrepancy. Thus, LEONARDS and RAMIAH (1959) found from oedometer tests with and without secondary consolidation that after a period of rest a quasi-preconsolidation pressure was developed in the clay, which was considerably higher than the maximum previous consolidation pressure. Such a quasi-preconsolidation pressure developed in clay with the time of rest was also mentioned by LAMBE (1958).

Table 5.

Area	Drain spacing, in m	Conventional[1] ε_2 in %			Modified[1] ε_2 in %			Minimum of c_v in 10^{-4} cm²/sec			Estimated average between depths of 2.5 and 7.5 m	
		depth 2 m	depth 5 m	depth 8 m	depth 2 m	depth 5 m	depth 8 m	depth 2 m	depth 5 m	depth 8 m	ε_2 in %	$c_v/10^{-4}$ cm²/sec
I	0.9	11	8	12	12	15	25	0.4	1.0	0.5	17	0.7
	1.5	13	10	10	11	19	23	0.3	0.5	0.7	18	0.5
	2.2	16	11	14	8	10	28	0.2	0.6	0.5	14	0.5
II	1.5	10	9—13	10—14	8	15—17	20—21	0.6	0.3—0.4	0.5—1.4	15—16	0.4—0.7
III	1.5	12—13	10—11	10—11	10—11	13—15	18—19	0.2—0.4	0.5—0.6	0.5—0.6	13—15	0.4—0.6
IV	no drains	8	10—11	9—11	7	13—16	17—21	0.5	0.4—0.5	0.4—0.5	13—15	0.4—0.5

[1] "Conventional" refers to the method of determining ε_2 by the inclination of the virgin compression curve, whereas "modified" refers to the method of determining ε_2 which is demonstrated in Fig. 60.

53. Pore Water Pressures

Introductory Remarks

The piezometers used in the test field at Skå-Edeby have no doubt generally given reliable pore water pressure values. However, some difficulties can be met with in the interpretation of the results.

The main difficulty appears in drained areas where the observed initial pore water pressure and the rate of pore water pressure dissipation (see Section 11 and Fig. 11) depend on the distance from a drain to the point of observation. Now the exact position of the piezometers between the drains is not known. Observations made at a given single point in a drained area may therefore give a misleading conception of the pore water pressure caused by the loading and draining operations or of the average pore water pressure dissipation. To give comparable values of the pore water pressure in a drained area, the measurements should thus be carried out at a number of comparable points.

The interpretation of the test results in some places is rendered difficult owing to the irregular bed rock, or to the sand and silt layers near firm bottom, or to the fissures which have also been found at great depths. Thus the filter stone, which is continuously driven downwards, might come to pass a fissure or a sand layer, and this would no doubt influence the measurements.

Of course, instrument errors may in exceptional cases influence the measurements. However, these errors are generally easy to detect.

For example, instrument errors might be due to stresses in the rubber membrane of the piezometer pick-up, to the fact that a filter stone might become blocked, to air bubbles in the measuring system, *etc.*

Furthermore, some part of the oil-filled measuring system may occasionally not be sufficiently heat-insulated. In such a case, a change of temperature in the tube causes a pressure, which may influence the measurements if the change is appreciably quicker than the time lag of the piezometer[1]. This effect can be studied in Table 6. Here the tubes were intentionally left uninsulated for 20 to 30 cm of their lengths, from the extension pipe to the insulating box protecting the manometers. The greatest change of pore pressure due to the change in temperature has occurred in piezometer No. P1: 9.0. However, the filter stone of this piezometer may have been nearly blocked or surrounded by a clay lense of extremely low permeability.

With satisfactory heat-insulation no similar temperature effects were to be observed.

[1] An expression for the time lag was given in KALLSTENIUS and WALLGREN (1956). However, this expression was based on the validity of DARCY's law of permeability. If this law is replaced by the new equation of permeability, Eq. (3: 1), we obtain the corresponding time lag

$$T = \frac{K_2}{\varkappa}\left[\frac{1}{(\Delta u_T)^{n-1}} - \frac{1}{(\Delta u_0)^{n-1}}\right]$$

where $K_2 = \dfrac{\Theta_v \gamma_w^{\,n}}{4\pi(n-1)}\left(\dfrac{2}{n}-1\right)^{-n} r_0^{-(2-n)}$

Θ_v = volume factor of piezometer

Table 6.

Area No. I Piezometer No.	Observed manometer pressure, in t/m²		
	11/9 1958; 01 p.m. temp. + 18° C	12/9 1958; 04 a.m. temp. + 6° C	15/9 1958; 02 p.m. temp. + 18° C
P 1: 2.5	0.79	0.75	0.79
5.0	0.70	0.60	0.75
9.0	2.18	1.60	2.23
B.	−0.83	−0.90	−0.82
P 7: 2.5	1.28	1.18	1.31
5.0	1.83	1.75	1.84
B.	0.25	0.19	0.24
P 9: 2.5	0.90	0.70	0.88
5.0	1.45	1.40	1.41
9.0	0.59	0.55	0.58
P 10: 5.0	0.90	0.85	0.86

Finally it is important for the connection between the nozzle and the sealing cap to be tight. If this is not the case, the piezometric head corresponds to the water level in the tube.

In May 1958, all piezometers were removed from the field and overhauled in the laboratory in order that possible instrument errors might be detected and eliminated.

The observed pore water pressures sometimes seem strange. However, the problem of variation in pore water pressure, *e.g.* with the ground water level and the time of the year, is a complex one, and has not yet been finally solved.

Test Results

The observed pore water pressures are given in Figs. 61 to 66 and in Table 7. Detailed information about all results of the measurements would require too much space.

---

r_0 = $\sqrt{A_f/4\pi}$ (A_f = filter area)
γ_w = unit volume weight of water
Δu_T = accuracy of piezometer
Δu_0 = difference between recorded and true pore water pressure

Choosing, for example, n = 1.5 we thus find

$$T = \frac{K_3}{\varkappa \sqrt{\Delta u_0}} \left(\sqrt{\frac{\Delta u_0}{\Delta u_T}} - 1 \right), \text{ where } K_3 = 0.828 \frac{\Theta_v \, \gamma_w^{1.5}}{\sqrt{r_0}}$$

The importance of this new expression for the time lag is particularly great where high accuracy is needed.

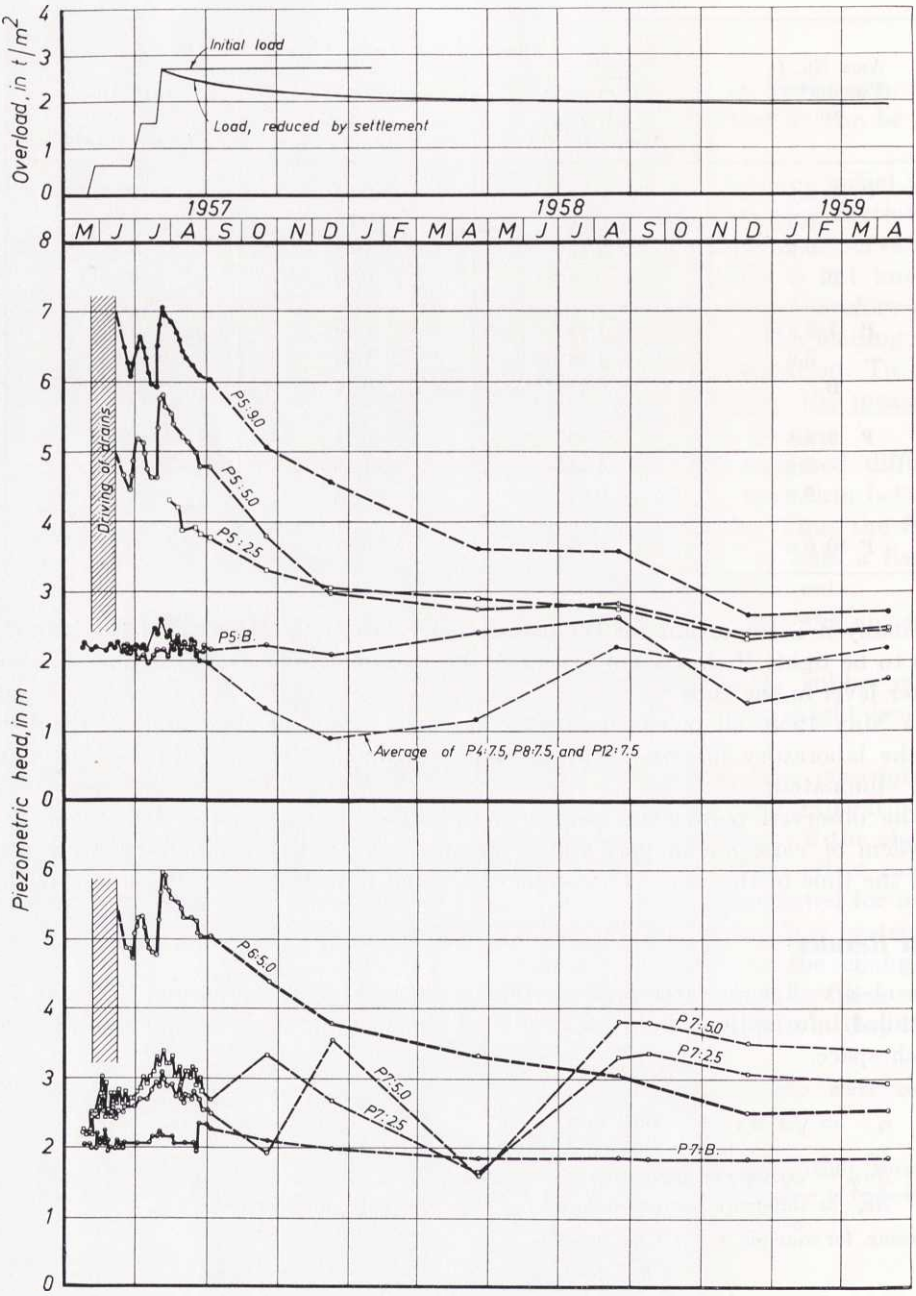

Fig. 61. Overload and observed pore water pressures. Test Area No. I, drain spacing 0.9 m. *Cf.* Fig. 36.

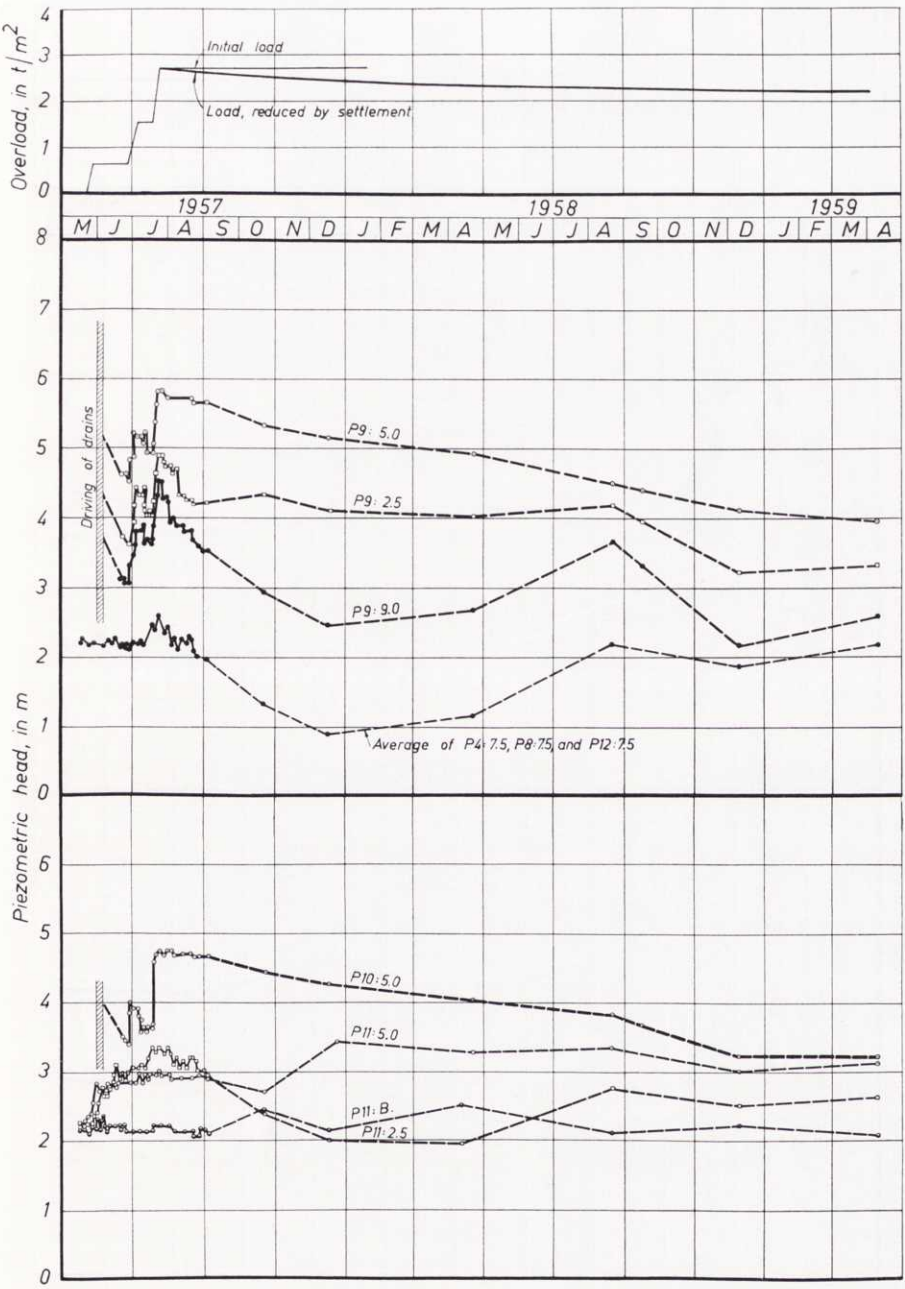

Fig. 62. Overload and observed pore water pressures. Test Area No. I, drain spacing 1.5 m. *Cf.* Fig. 36.

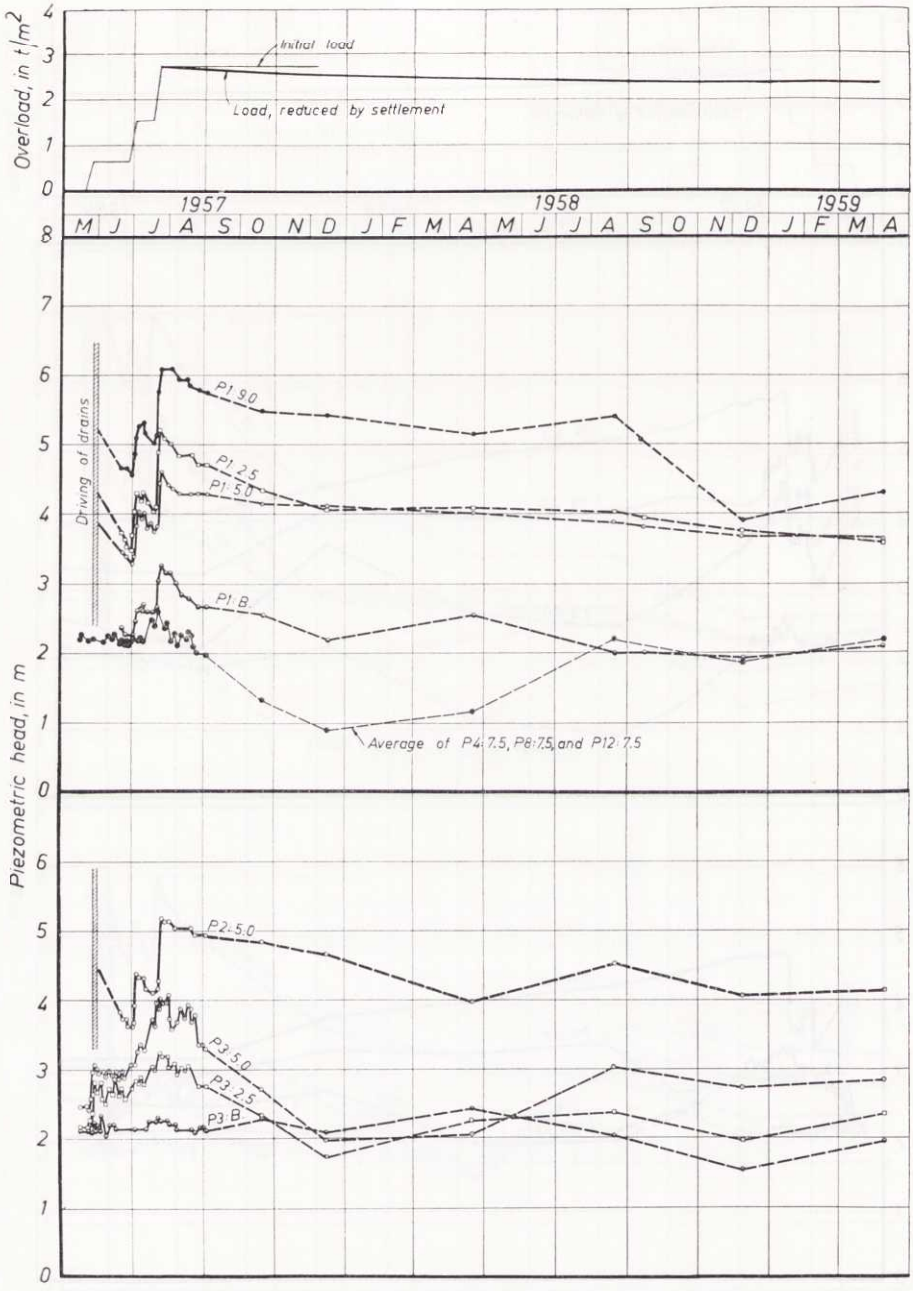

Fig. 63. Overload and observed pore water pressures. Test Area No. I, drain spacing 2.2 m. *Cf.* Fig. 36.

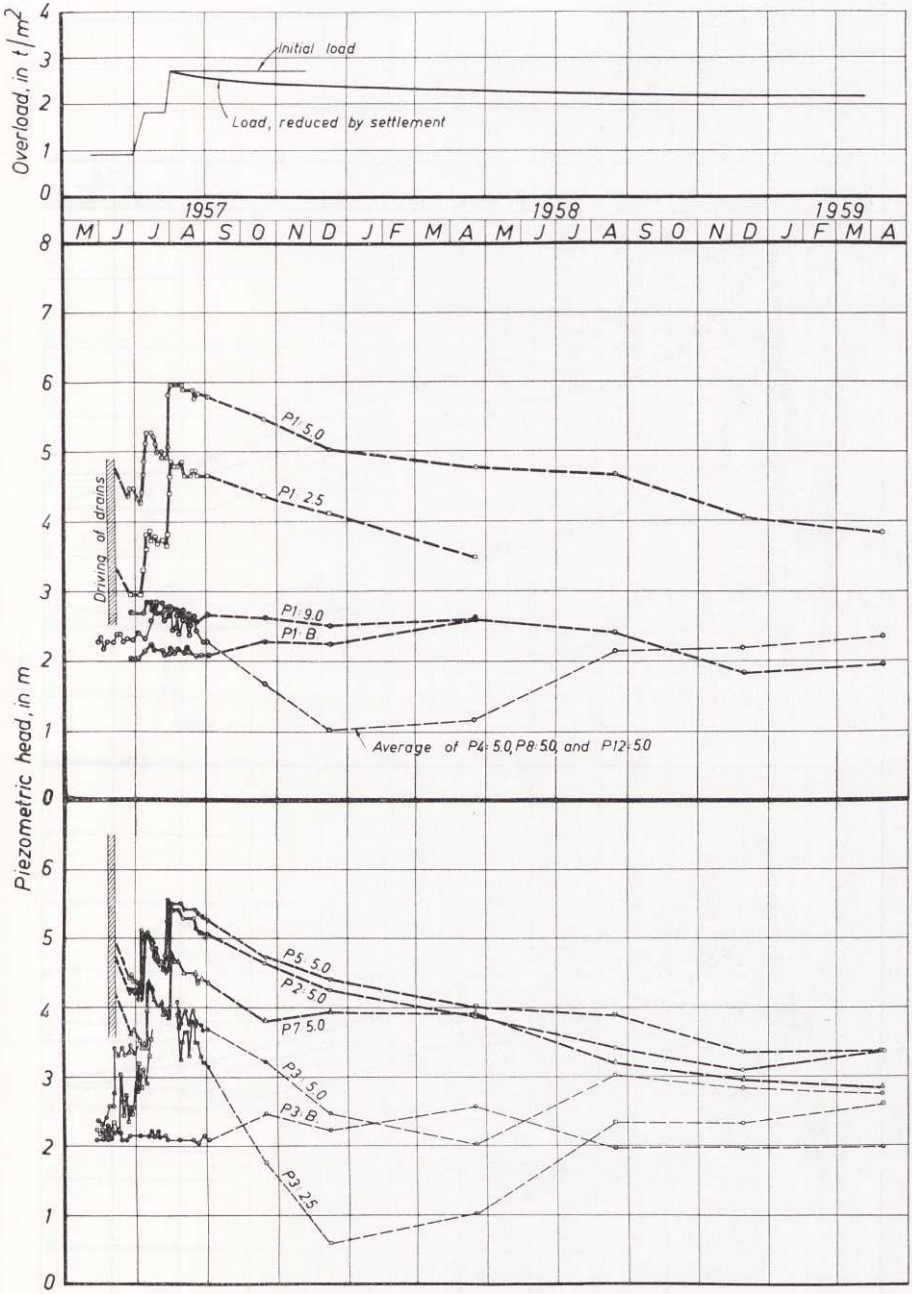

Fig. 64. Overload and observed pore water pressures. Test Areas No. II. *Cf.* Fig. 37.

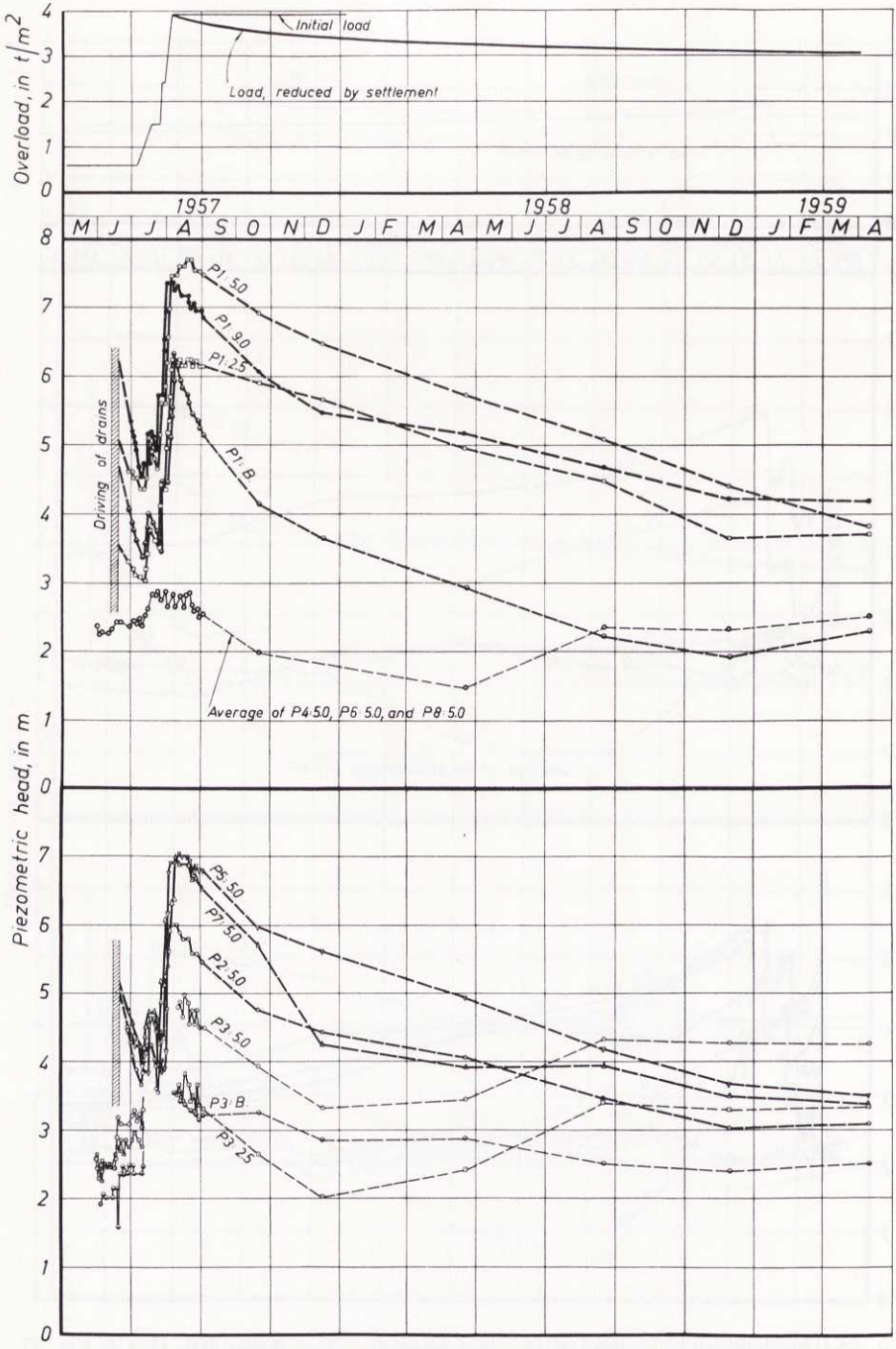

Fig. 65. Overload and observed pore water pressures. Test Area No. III. *Cf.* Fig. 38.

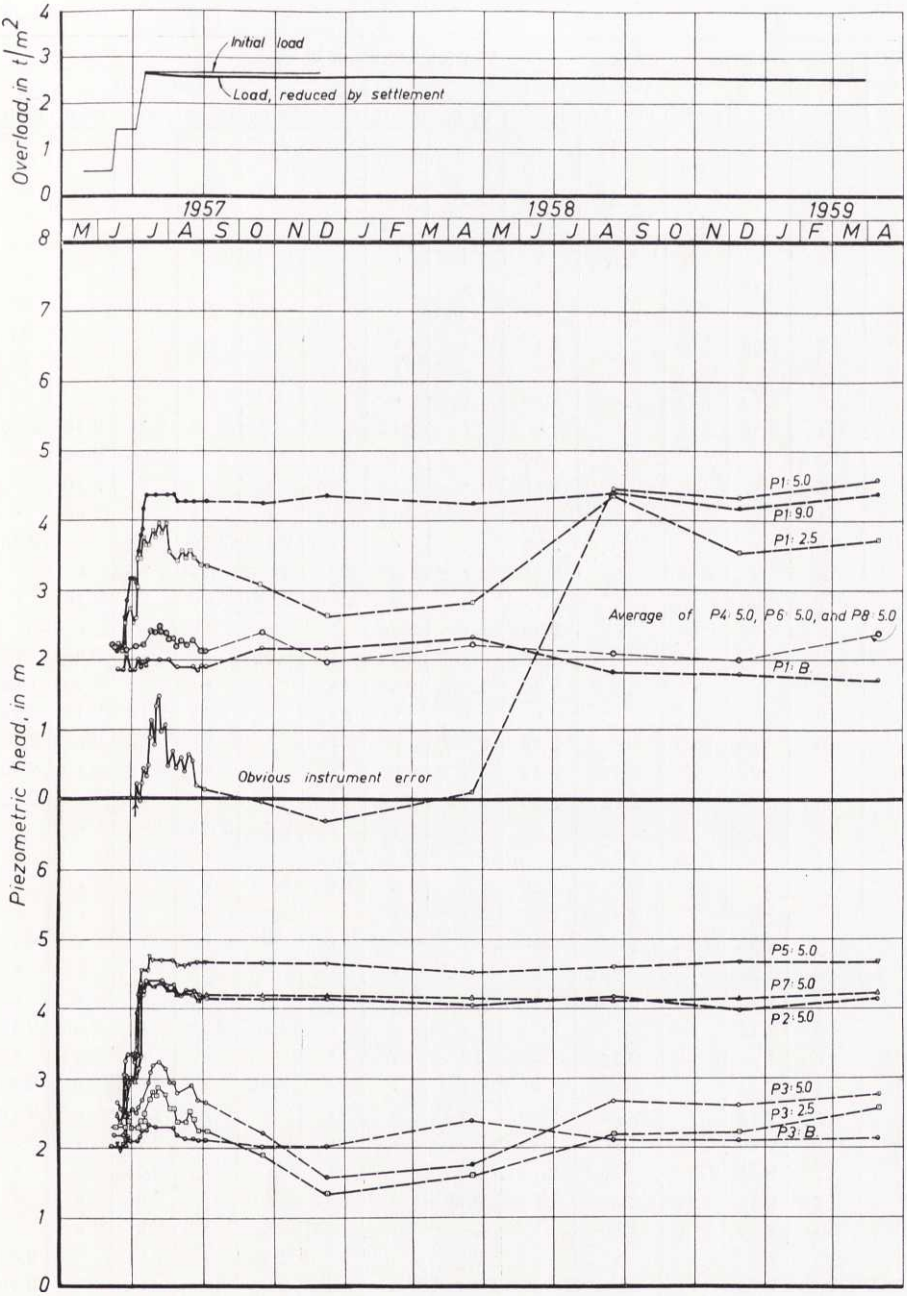

Fig. 66. Overload and observed pore water pressures. Test Area No. IV. *Cf.* Fig. 39.

Table 7.

Date	Temp. in °C	Piezometric head, in m											
		Test Area No. I						Test Area No. II					
		P4:7.5	P8:7.5	P12: 7.5	P4:B.	P8:B.	P12:B.	P4:5.0	P6:5.0	P8:5.0	P4:B.	P6:B.	P8:B.
1957													
17/5	+11	2.10	2.25	2.20	2.20	2.15	2.10						
18	13	2.35	2.20	»	»	»	»						
20	16	»	»	2.15	»	2.10	»						
21	10	2.25	»	»	»	»	»						
23	10	»	2.25	2.10	»	2.20	»						
24	7	2.20	2.20	»	2.15	»	»						
25	6	»	2.25	»	»	»	»						
27	8	»	2.15	»	2.20	»	»						
28	11	2.25	2.20	»	»	»	2.15				2.05	2.10	2.20
29	8	»	»	»	2.30	»	2.20	2.30	2.25	2.30	2.00	2.05	»
30	18	»	»	»	2.20	»	2.10	2.25	»	»	»	2.10	»
31	11	»	»	»	2.35	2.15	2.15	2.20	»	2.25	»	2.05	»
1/6	13	»	»	»	2.20	»	»	»	2.30	2.20	»	»	2.15
2	13	»	2.15	»	2.15	»	2.05	2.25	2.35	2.15	»	»	»
3	17	2.30	»	»	2.25	»	2.20	2.20	2.20	»	»	2.10	»
4	13	2.25	2.20	»	2.35	»	2.30	»	»	»	»	»	»
5	8	2.15	»	»	2.25	»	2.20	»	2.25	»	»	2.05	»
6	9	»	»	»	2.20	2.20	2.10	»	»	»	»	2.20	1.95
7	10	»	2.25	»	»	»	»	2.25	»	2.35	2.10	2.10	2.25
8	10	»	»	»	2.15	»	»	»	»	»	2.05	2.05	2.15
10	16	2.25	»	2.20	2.20	»	»	»	»	»	2.10	2.10	2.20
11	12	2.20	»	2.15	2.25	»	2.20	»	»	»	»	»	2.25
12	18	»	»	2.20	»	»	»	»	2.35	2.25	»	»	»
13	11	»	2.20	2.15	»	»	2.15	2.35	»	»	»	»	»
14	16	»	2.25	»	2.20	»	»	»	2.40	»	»	»	»
15	19	2.25	»	2.20	2.25	»	»	»	2.55	»	»	»	»
16	19	2.35	2.20	2.25	2.20	»	2.10	»	»	»	»	»	»
17	23	2.30	»	2.20	»	»	»	»	»	»	»	»	»
18	7	2.25	2.15	2.15	»	»	»	»	»	2.20	»	»	»
19	9	2.15	»	»	2.15	»	»	»	2.50	2.15	»	2.05	2.15
20	13	»	»	2.10	»	2.15	»	»	»	»	»	2.10	»
22	14	2.25	»	»	»	»	»	»	2.45	»	2.00	2.05	2.25
24	14	2.15	»	2.05	2.10	2.10	»	»	»	»	2.05	»	2.10
25	17	»	»	»	2.15	»	»	»	»	»	2.10	»	»
26	17	2.20	2.20	2.10	2.10	2.15	»	»	»	»	2.05	»	»
27	17	2.15	2.15	2.05	»	2.10	»	2.30	»	»	2.00	»	»
28	15	2.20	2.20	2.10	»	2.15	»	2.35	»	»	2.05	»	»
29	15	»	»	»	»	2.10	»	»	2.40	»	»	»	2.05
1/7	20	2.25	»	2.15	»	2.15	»	2.40	2.45	2.20	»	»	2.15
2	15	»	»	»	»	2.10	»	»	»	2.25	»	»	»
3	16	»	»	2.10	»	2.15	»	2.35	2.50	»	»	»	»
4	20	2.20	2.25	»	2.15	»	»	2.45	»	»	»	»	»
5	15	2.25	2.20	»	2.10	»	»	2.35	»	»	2.00	»	2.00
6	16	2.20	2.25	»	»	»	»	2.45	2.45	2.20	2.10	2.00	2.10
8	15	2.25	»	2.15	2.15	2.20	»	»	2.55	2.35	2.05	»	2.15
9	15	»	»	2.10	2.10	2.15	»	»	2.50	2.20	»	»	2.05

Table 7 (continued).

Date	Temp. in °C	Piezometric head, in m											
		Test Area No. I						Test Area No. II					
		P4:7.5	P8:7.5	P12: 7.5	P4:B.	P8:B.	P12:B.	P4:5.0	P6:5.0	P8:5.0	P4:B.	P6:B.	P8:B.
10	16	2.20	2.20	2.10	2.15	2.15	2.10	2.40	2.45	2.15	2.05	2.00	2.05
11	18	2.25	2.25	»	»	»	»	»	2.50	2.25	»	2.05	2.15
12	18	2.30	»	2.15	»	2.20	»	2.45	2.55	2.35	2.10	2.00	»
13	17	»	»	»	»	»	»	»	»	»	»	2.05	»
14	20	2.35	2.35	2.25	2.10	2.30	»	2.55	2.65	2.40	»	2.10	2.25
15	21	»	»	»	2.30	2.35	»	»	2.70	2.50	»	»	»
16	21	2.40	»	2.30	»	»	»	2.60	2 85	2.55	»	»	»
17	20	2.45	2.40	2.40	2.35	2.45	2.15	2.70	2.90	2.65	2.15	»	2.35
18	24	2.50	2.45	2.45	2.40	»	2.20	2.75	»	2.75	»	2.15	2.45
19	24	2.45	»	2.40	2.35	»	»	»	2.95	»	»	2.20	»
20	21	2.40	2.40	2.35	2.30	»	2.15	»	»	2.70	»	2.15	2.40
22	25	2.50	2.45	2.50	2.40	2.55	2.20	»	»	»	2.20	2.20	2.45
23	25	2.55	2.55	2.65	2.45	2.65	»	»	»	»	2.15	»	2.40
24	20	2.45	2.50	2.50	2.40	2.55	»	»	»	2.75	2.10	»	2.45
25	19	2.50	2.45	»	»	2.50	2.15	»	»	»	»	»	2.40
26	22	2.45	»	2.40	2.85	2.45	2.10	»	2.90	2.60	»	2.15	2.25
27	18	2.40	2.40	2.30	2.30	2.35	»	»	2.80	2.50	»	2.10	»
29	19	»	2.35	»	»	»	»	»	2.90	»	»	»	»
31	23	2.45	2.45	2.40	2.35	2.45	»	»	2.95	»	»	»	2.35
1/8	19	»	2.40	2.35	»	2.35	»	»	»	»	»	»	»
2	15	2.35	2.30	»	2.20	2.25	»	2.70	2.85	2.80	»	2.05	2.15
3	13	2.30	2.15	2.05	2.15	2.10	2.05	2.50	2.75	2.05	2.05	2.00	1.95
5	18	»	»	»	2.10	»	»	»	»	2.10	2.10	»	2.00
7	17	2.35	2.30	2.20	2.20	2.25	»	2.60	2.95	2.30	»	2.10	2.20
8	15	2 25	2.15	1.90	2.10	2.10	»	2.45	2.70	2.00	»	2.00	1.80
10	19	»	»	»	»	2.15	2.00	»	2.75	2.10	2.05	»	1.95
12	19	2.35	2.30	2.15	2.20	2.20	2.05	2.55	2 90	2.30	2.00	2.05	2.10
14	16	»	»	2.10	»	»	»	»	»	»	»	»	2.15
15	17	»	»	»	2.15	»	»	2.50	2.75	2.15	»	2.00	1.90
17	19	2.30	2.20	»	2.20	»	»	2.55	2.80	2.20	»	»	2.05
19	17	2.35	2.35	2.20	»	2.25	»	2.60	2.95	2.35	»	2.05	2.15
21	17	»	2.30	2.10	»	»	2.00	2.55	»	2.25	»	»	2.10
22	15	2.20	2.15	1.95	2.05	2.15	»	2.45	2.75	2.05	»	2.00	1.95
24	18	2.30	»	1.85	2.15	»	»	»	»	»	»	»	1.75
26	15	2.20	2.00	»	2.00	2.05	»	2.35	2.70	1.90	2.05	1.95	1.70
28	15	2.25	2.05	»	2.10	2.10	»	»	2.60	1.85	2.10	2.00	»
31	14	2.20	1.95	1.80	2.05	»	»	—	—	—	—	—	—
3/9	13	2.15	»	»	»	2.05	2.05	»	»	»	»	1.95	1.60
21/10	8	1.80	1.30	0.90	2.10	1.90	2.40	1.90	1.95	1.20	2.35	2.05	1.50
16/12	1	1.50	0.95	0.30	1.55	1.35	2.15	1.15	1.15	0.75	2.15	1.60	1.00
1958													
21/4	4	1.80	1.45	»	2.00	1.65	2.45	1.20	1.35	1.00	»	2.00	1.75
Piezometers replaced by new ones													
20/8	19	2.25	2.15	2.20	1.90	1.90	1.85	2.15	2.40	1.95	1.90	1.90	1.95
9/12	1	1.80	1.90	1.95	»	1.95	»	»	2.35	2.05	»	»	2.55
1959													
9/4	6	2.15	2.05	2.25	2.00	1.85	1.90	2.25	2.55	2.25	1.85	2.00	2.00

Date	Temp. in °C	Piezometric head, in m											
		Test Area No. III						Test Area No. IV					
		P4:5.0	P6:5.0	P8:5.0	P4:B.	P6:B.	P8:B.	P4:5.0	P6:5.0	P8:5.0	P4:B.	P6:B.	P8:B.
1957													
1/6	+16	2.25	2.55		1.70	1.45							
2	13	»	2.30		2.10	2.00							
3	18	»	2.25		»	»							
4	13	»	»		»	»							
5	8	»	»		»	»							
6	9	2.30	2.20		»	2.10							
7	10	2.25	2.25		»	2.05							
8	11	2.30	»		»	»							
10	16	2.25	»		»	2.10							
11	12	»	»		»	2.05							
12	18	2.30	»		2.15	2.10							
13	11	2.25	»		2.10	»							
14	16	»	»		»	»							
15	20	2.30	2.30		2.15	2.15		2.20	2.25	2.20	2.05	2.20	—
16	19	2.25	»		»	»		2.10	»	»	»	2.10	—
17	23	2.30	»		»	»		»	»	»	»	2.15	—
18	7	2.35	2.35		2.10	2.10		»	»	»	»	2.10	2.35
19	9	2.45	2.30		2.15	»		»	»	2.10	»	»	2.25
20	13	»	»		2.20	»		»	»	2.20	»	»	2.35
22	14	»	»		2.10	»		»	»	»	»	»	2.20
24	14	»	2.25		2.15	»		»	2.20	2.15	»	»	2.25
25	17	»	»		»	»		2.15	2.25	2.20	»	2.20	2.15
26	18	2.40	»		»	»		2.10	»	»	»	2.15	2.20
27	17	2.45	»		»	»		»	»	»	»	»	2.15
28	15	2.40	»		»	»		»	»	»	»	2.20	2.20
29	16	»	2.30		2.15	2.05		»	»	»	»	2.10	2.15
1/7	21	»	2.35		»	»		»	»	»	»	2.15	2.20
2	16	»	2.30		»	»		»	»	»	»	»	»
3	18	»	2.35		»	»		»	»	»	»	2.20	2.15
4	21	»	2.40		»	»		»	2.30	»	»	2.15	»
5	17	»	2.35		»	»		»	2.35	»	»	2.20	»
6	17	»	»		»	»		»	»	»	»	»	»
8	15	»	2.40		»	»		»	2.30	»	»	2.10	»
9	16	»	2.35		»	»		»	2.25	»	»	»	2.10
10	18	2.35	2.30		»	»		»	2.35	»	»	2.20	»
11	20	2.45	2.35		»	»		»	2.45	»	2.10	»	»
12	20	»	2.40		»	»		»	»	»	2.15	»	»
13	19	2.60	»		»	»		»	2.40	»	»	2.25	2.15
14	20	»	2.45		»	2.10		»	2.50	»	»	»	»
15	21	2.65	»		»	»		2.15	2.55	2.30	2.25	2.30	»
16	24	»	2.50		»	2.15		»	2.65	»	2.30	2.35	2.20
17	22	2.70	2.65		»	2.25		»	2.70	»	»	»	»
18	25	2.75	2.70		2.10	2.30		»	2.80	»	2.35	»	»
19	23	»	2.75		»	»		»	2.75	»	»	2.30	»

Same as P6:5.0 in Test Area No. II

Same as P6:B. in Test Area No. II

Table 7 (continued).

Date	Temp. in °C	Piezometric head, in m											
		Test Area No. III						Test Area No. IV					
		P4:5.0	P6:5.0	P8:5.0	P4:B.	P6:B.	P8:B.	P4:5.0	P6:5.0	P8:5.0	P4:B.	P6:B.	P8:B.
20	24	2.75	2.70		2.10	2.25		2.15	2.70	2.35	2.30	2.30	2.20
22	26	2.80	2.75		»	2.30		»	2.90	2.30	2.40	»	»
23	24	»	2.70		»	2.25		—	—	—	—	—	—
24	22	2.85	2.75		»	»		»	2.95	2.35	2.50	»	»
25	20	2.80	2.70		»	2.20		—	—	—	—	—	—
26	24	»	»		»	»		»	2.80	2.30	2.40	»	»
27	19	2.75	2.65		»	»							
29	20	»	»		»	2.25							
30	24	2.85	»		»	»		»	2.75	»	2.35	»	»
31	25	2.90	2.75		»	»							
1/8	19	2.80	2.65		»	2.20							
2	17	2.50	2.60		2.40	2.30		»	2.50	»	2.25	2.25	»
3	14	2.75	»		2.10	2.25							
5	21	2.80	2.65	Same as P6:5.0 in Test Area No. II	2.15	2.30	Same as P6:B. in Test Area No. II						
6	22	2.85	»		»	»		»	»	»	»	»	»
7	18	»	»		»	»							
8	16	2.75	2.50		»	2.25							
9	18	»	»		»	»		2.20	2.20	2.25	2.05	2.10	»
10	20	2.80	»		2.10	»							
12	19	»	2 60		»	»							
13	19	2.85	2.65		»	2.30		»	2.45	2.20	2.10	»	2.15
14	16	2.80	2.60		»	»							
15	19	»	2.55		»	»							
16	16	2.70	2.50		»	2.25		»	2.30	»	2.05	»	»
17	20	2.85	2.60		»	2.30							
19	18	»	2.65		»	»							
20	16	2.90	»		»	»		»	»	»	2.15	»	»
21	17	2.85	»		»	»							
22	18	2.75	2.50		»	2.25							
23	15	»	»		»	»		»	»	2.35	2.05	»	2.10
24	18	»	»		»	2.30							
26	16	2.70	2.40		»	2.25		2.10	2.25	2.25	1.90	2.25	2.05
28	18	2.75	2.45		2.15	2.30							
30	16	2.65	2.35		»	»		2.05	2.15	2.20	1.85	2.15	2.00
2/9	13	»	»		»	2.25		»	»	»	»	»	»
21/10	8	2.25	1.80		2.50	2.55		2.10	1.85	»	1.80	1.85	2.30
16/12	2	1.75	1.45		2 60	2.40		2.20	1.55	2.10	1.30	1.55	»
1958													
21/4	4	1.70	1.40		2.55	3.70		2.25	1.70	2.70	1.60	1.70	2.40
Piezometers replaced by new ones													
21/8	17	2.45	2.25		2.20	2.50		2.05	2.10	2.15	1.95	2.10	2.20
9/12	1	2.35	2.30		1.95	2.00		»	1.90	2.05	1.85	1.90	»
1959													
9/4	7	2.45	2.50		»	2.15		2.20	2.25	2.70	2.40	2.30	2.05

Disturbance Due to Driving of Drains

The pore water pressures observed within the areas were extrapolated in order to estimate the maximum "disturbance pressures" u_d reached after completion of drainage, see Table 8. The corresponding disturbance pressures remaining after completion of the loading operation are also given in this table.

Table 8.

Area No.	Drain spacing, in m	Maximum disturbance pressure after completion of drainage, in t/m²	Maximum disturbance pressure after completion of loading, in t/m²	Pressure observed at depth, in m
I	0.9	4	2	9
I	1.5	2	1	5
I	2.2	2	1½	9
II	1.5	2	1	5
III	1.5	3½	1½	9

However, although these maximum disturbance pressure values were selected among all the values observed within the respective areas, the real maximum disturbance pressure may naturally be higher.

Obviously, the excess pore water pressure created by the drainage operation is considerable.

The disturbance will reach its maximum in the vicinity of a drain. Furthermore, the disturbance is assumed to increase to a certain extent with depth (*cf.* KALLSTENIUS, 1958), and this seems to be confirmed in our investigation. Thus the fact that the excess pressures measured at a depth of 9 m in the 1.5 sector of Area No. I and in Area No. II are lower than those observed at a depth of 5 m may be due to contact between the filter stone and a neighbouring drain at a depth of 9 m or to sand layers in the former case and instrument errors in the latter.

The average disturbance is to some extent a function of the displaced clay volume, *i.e.* of the drain spacing and the average drain length[1]. This effect can

Table 9.

Area No.	Drain spacing, in m	Average drain length, in m	Average disturbance pressure $\bar{u}_d$ in t/m²	Maximum deviation $\Delta\bar{u}_d$ in t/m²	Number of observation points
I	0.9	11	2.1	0.2	2
I	1.5	9	1.5	0.6	2
I	2.2	11	1.1	0.3	2
II	1.5	11	1.7	0.5	4
III	1.5	13	2.1	0.1	4

[1] Of course, other factors, such as sensitivity and type of clay, would have an influence on the disturbance pressure but the influence of these factors will not be discussed here.

be studied in Table 9, where $\bar{u}_d$ represents the observed average disturbance pressure at a depth of 5 m, obtained by extrapolation as before.

As was to be expected, the disturbance pressure increases with decreasing drain spacing and also with increasing drain length. We should not venture to draw further conclusions from these values, but it may be worth mentioning that, within the limits given in Table 9, $\bar{u}_d$ at a given depth is nearly proportional to the average drain length and to $(3.9 - L)$, where L represents the actual drain spacing in metres.

A study of individual pore pressure values shows that the disturbance tends to increase towards the centres of the areas.

Driving of drains caused a rise of pore water pressure also outside the areas and this was indicated even by the piezometers situated farthest away. Thus, excess pore water pressures were observed at a distance of 35 m from the periphery of Area No. I (approximately 0.05 t/m² on the average at a depth of 7.5 m), and at a distance of 17½ m from the peripheries of Areas Nos. II and III (approximately 0.1 t/m² on the average at a depth of 5 m). The maximum rise of pressure observed at the observation points situated at a distance of 2 m from the periphery of Area No. I and at a distance of 2½ m from the peripheries of Areas Nos. II and III is given in Table 10.

Table 10.

Area No.	Drain spacing, in m	Excess pore water pressure, in t/m²	Pressure observed at depth, in m
I	0.9	0.8	5
I	1.5	0.6	5
I	2.2	0.6	2.5 and 5
II	1.5	1.0	5
III	1.5	0.8	5

These values are single observations. For a given clay, the disturbance ought to increase to a certain extent with increasing displaced volume (see above and Section 54).

Influence of Loading on Pore Water Pressure

During the loading operation the step-by-step rise of pore water pressure observed within the areas corresponds fairly well with the step-by-step application of the gravel loads. However, the rise observed outside the areas in the course of load application is also considerable. Thus, at a distance of 35 m from the periphery of Area No. I an average maximum rise of about 0.4 t/m² was obtained at a depth of 7.5 m, and at a distance of 17½ m from the periphery of Area No. II a rise of about 0.5 t/m² was observed at a depth of 5 m. This corresponds to approximately 15 % of the load in the former case and 20 % in the latter.

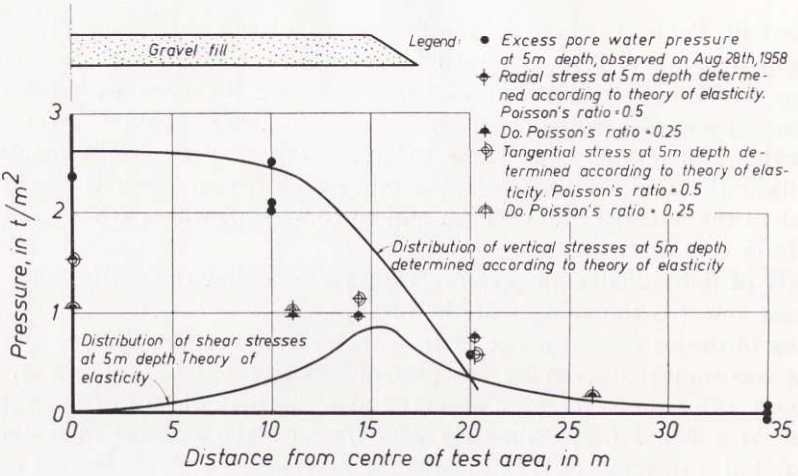

Fig. 67. Observed excess pore water pressure distribution at a depth of 5 m below ground surface in Test Area No. IV compared with distribution of theoretical stresses produced at the same depth by overload. *Cf.* pp. 143–146.

The theoretical distribution of stress under a loaded area (see Appendix) is compared in Fig. 67 with the results of the pore water pressure measurements carried out in the undrained Area No. IV. One of the piezometers in this area, No. P1: 5.0, was no doubt incorrect to start with. Therefore, the pore pressure values used for the above comparison were those taken after this piezometer had been replaced. This was not done until more than a year had passed since the completion of loading. However, during this period—with the exception of the first two months—the pore water pressure dissipation was practically of no importance. During the first two months a rapid decrease of pressure, similar to that occurring in the pore pressure measurements carried out in the laboratory, *cf.* Section 21, was detected at the points of observation outside the areas and also inside the undrained area. This decrease seems to be different in nature from that characterized by the hydrodynamic law of pore water pressure dissipation[1]. However, it is small (0.1 to 0.4 t/m^2), and has an appreciable influence only on the results obtained outside the areas.

In Fig. 67, the average excess pore water pressure at a distance of 35 m from the centre of Area No. IV has been put equal to zero. This means that the previously mentioned "non-hydrodynamic" decrease is estimated at 0.3 t/m^2, *i.e.* the same value as the original excess pore water pressure observed at a distance of 35 m from the centre of Area No. IV.

These results can be used in determining SKEMPTON's pore pressure coefficient A (SKEMPTON, 1954). Thus the observations made inside the periphery of the loaded area gave $A = 0.77$, provided that POISSON's ratio $\nu = 0.5$ and that the

[1] This phenomenon was discussed in Section 21.

coefficient $B = 1$. At the periphery of the area the pore water pressure may have been influenced by creep of the clay. Thus the theoretical shearing stresses at the periphery equalled or even exceeded the observed shear strength of the clay.

Seasonal and Daily Variations in Pore Water Pressure

The observed pore water pressures are at some places considerably influenced by the time of the year. This might be due in some degree to the above-mentioned difficulties and errors in measurements, but in a case where the temperature at, or not too far from, the point of observation is influenced by the seasonal variation of temperature (*cf.* p. 123), the pore water pressure should also be influenced. This phenomenon can partly be attributed to the difference in thermal expansion between pore water and mineral grains (*cf.* BARBER and STEFFENS, 1958). Since the pore water has a higher coefficient of thermal expansion than the clay mineral, a decrease of temperature would result in pore water pressure decrease[1]. A possible seasonal or daily variation in ground water level would also influence the pore water pressure. Furthermore, differences in ground water level in the sand drains and in surrounding clay may occasionally occur, and this would likewise influence the pore water pressure.

A daily variation of pore pressure due to the influence of the moon or of the height of the barometer would probably be negligible.

Influence of Load and Drain Spacing on Rate of Consolidation

According to the equations advanced in Chapter 4, the time of consolidation depends on the initial excess pore water pressure. This effect was studied by comparing the rates of consolidation within Areas II and III, which have the same dimensions and drain spacings, but are submitted to different loads. At a depth of 2.5 m the results might be influenced by fissures and at a depth of 9 m by sand or silt layers[2]. Thus, to compare are the values observed at a depth of 5.0 m. The consolidation at this depth is here considered to be caused solely by the drains. This is justified by the fact that a "hydrodynamic" decrease of excess pore water pressure was not to be detected at a depth of 5 m in the undrained area, or was found to be negligible as compared with the accuracy in measurements.

The results of the comparison are given in Table 11[3] and Fig. 68.

[1] The problem of thermal influence on the pore water is intricate (*cf. e. g.* STEGMÜLLER, 1958) and a complete explanation of a pore pressure change because of a change in temperature is hard to give.

[2] In Area No. II the piezometer at a depth of 9 m (No. P1: 9.0) seems to give incorrect values or is in contact with an adjacent sand drain.

[3] The initial excess pore water pressures u_0 given in Tables 11 and 12 represent the values obtained after completion of loading (equal to observed maximum u_0). This might be disputable, considering that part of consolidation has then undoubtedly taken place. However, this seems to be the only practicable interpretation and does not depend on mere intuition. The error introduced might have a visible effect in the u_0-values obtained at a close drain spacing, particularly 0.9 m spacing. *Cf.* also p. 111.

In Areas II and III the initial piezometric head existing before drainage is estimated at 2.3 m on an average.

Table 11.

Area No.	Piezometer No.	Δq t/m²	u_0 t/m²	$U_h = 100\,(1 - \frac{u}{u_0})$ %					
				21.10 1957	16.12 1957	21.4 1958	20.8 1958	9.12 1958	9.4 1959
II	P 1: 5.0	2.7	3.7	14	26	33	36	52	58
	P 2: 5.0		3.2	27	39	51	65	75	67
	P 5: 5.0		3.2	24	34	47	50	67	67
	P 7: 5.0		2.5	40	34	36	64	74	78
			3.2	26	34	42	54	67	68
III	P 1: 5.0	3.9	5.4	14	23	36	48	61	72
	P 2: 5.0		3.7	33	42	52	68	80	79
	P 5: 5.0		4.7	22	29	44	60	70	74
	P 7: 5.0		4.7	28	58	65	65	75	77
			4.6	24	38	49	60	72	76

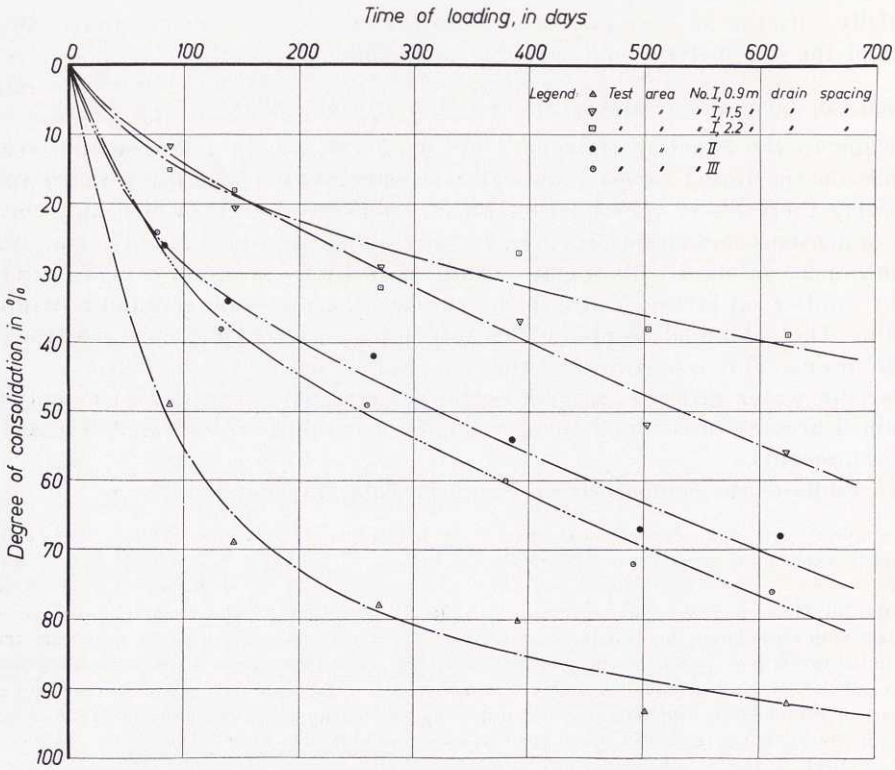

Fig. 68. Average rates of consolidation in Test Areas Nos. I to III obtained from the pore water pressure observations which are given in Tables 11 and 12.

As was shown in Chapter 4, the relation between the times of consolidation of two clay layers provided with equally spaced drains and acted upon by loads of different magnitude is

$$\frac{t_1}{t_2} = \frac{\lambda_2}{\lambda_1}\left(\frac{\bar{u}_{02}}{\bar{u}_{01}}\right)^{n-1} \quad \ldots\ldots\ldots\ldots\ldots\ldots\ldots \quad (5{:}1)$$

In this case the values of λ may be considered to be equal for the two Areas Nos. II and III, and the probable value of n, as deduced from Fig. 68, becomes[1]

$$n = 1 + \frac{\log\left(\frac{t_{II}}{t_{III}}\right)}{\log\left(\frac{\bar{u}_{0III}}{\bar{u}_{0II}}\right)} \approx 1.5 \text{ to } 1.6$$

We also find from Table 11 that the ratio of the initial excess pore water pressures, $\bar{u}_{0III}/\bar{u}_{0II}$, in this case happens to be nearly equal to the ratio of the loads, $\Delta q_{III}/\Delta q_{II}$. Probably, this is merely accidental, but it may also be due to the previously discussed effect of different drain lengths in these two areas.

The individual values given in Table 11 apparently speak against the above theory. Thus, the lower the individual initial excess pore water pressure, the higher the rate of consolidation. This contradiction to the result obtained when studying the average values of pore water pressure may probably be ascribed to differences in distance from the piezometer to the adjacent drains. The rate of excess pressure dissipation thus increases considerably when the distance to a sand drain decreases, *cf. e.g.* Fig. 11. Consequently, since the piezometers were installed about or more than a week after completion of drainage, the initial excess pressure observed in the immediate vicinity of a drain will be small while the rate of consolidation will be high. Now it must be remembered that *the equations advanced in Chapter 4 refer to the average consolidation,* and hence not to the consolidation occurring at a given point between adjacent drains. Therefore, when studying the validity of the given consolidation equations, average values have to be considered.

The small number of comparable piezometers within Test Area No. I—only 2 in each sector—makes it difficult to check the validity of the above consolidation theory for different drain spacings. Nevertheless, the values given in Table 12[2] and Fig. 68 may furnish some information.

[1] In determining u regard has been paid to the vertical settlement of the filter stones of the piezometers.

The progressive reduction of excess pore water pressure caused by the reduction of load due to settlement (part of the load sinking down below ground water level) is neglected here, since it amounts in both cases to the same percentage of the initial values. This is easily seen from the relation $\Delta\bar{u} = \gamma'\delta_g = \gamma'\Delta q\, h\, m_v\, \bar{U}$, in which $\Delta\bar{u}$ is the average reduction of pore water pressure due to settlement δ_g of ground surface and γ' is the reduction of weight per unit volume of submerging part of load. Thus, at two different loads Δq_1 and Δq_2, we obtain, at the same degree of consolidation ($\bar{U}_1 = \bar{U}_2$), the relation

$$\frac{\Delta\bar{u}_1}{\Delta\bar{u}_2} \approx \frac{\Delta q_1}{\Delta q_2} \approx \frac{\bar{u}_{01}}{\bar{u}_{02}}$$

[2] In Area No. I the initial piezometric head before drainage is estimated at 2.2 m on an average. See also footnote 3, p. 105.

Table 12.

Area No.	Drain spacing, in m	Piezometer No.	u_0 t/m²	$U_h = 100\,(1 - \frac{u}{u_0})$ %					
				21.10 1957	16.12 1957	21.4 1958	20.8 1958	9.12 1958	9.4 1959
I	0.9	P 5:5	3.6 | 3.7	56 | 49	78 | 69	85 | 78	82 | 80	95 | 93	93 | 92
		P 6:5	3.8 |	42 |	59 |	70 |	77 |	91 |	91 |
	1.5	P 9:5	3.6 | 3.1	13 | 12	25 | 21	36 | 29	39 | 37	46 | 52	51 | 56
		P 10:5	2.5 |	10 |	17 |	22 |	34 |	58 |	60 |
	2.2	P 1:5	2.4 | 2.7	18 | 15	20 | 18	24 | 32	30 | 27	37 | 38	41 | 39
		P 2:5	3.0 |	12 |	17 |	40 |	23 |	38 |	36 |

As is seen from Fig. 68, the relation between times of consolidation for different drain spacings as obtained hitherto becomes

$$5.7 \leqq \frac{t_{1\,5}}{t_{0.9}} \leqq 6.5 \; (6.4 \text{ at } \overline{U} = 50\,\%)$$

and

$$0.9 \leqq \frac{t_{2.2}}{t_{1.5}} \leqq 1.6 \; (1.5 \text{ at } \overline{U} = 40\,\%)$$

By comparing the rates of excess pore pressure dissipation at drain spacings of 0.9 m and 2.2 m in Test Area No. I with that obtained at a drain spacing of 1.5 m in Test Area No. II, Fig. 68, we obtain

$$2.1 \leqq \frac{t_{1\,5}}{t_{0.9}} \leqq 4.0 \; (3.8 \text{ at } \overline{U} = 50\,\%)$$

and

$$2.2 \leqq \frac{t_{2.2}}{t_{1\,5}} \leqq 3.2 \; (3.0 \text{ at } \overline{U} = 40\,\%)$$

According to the classical theory, the relation between the times of consolidation is

$$\frac{t_{1.5}}{t_{0.9}} = 4.4 \frac{c_{h.\,0\,9}}{c_{h,\,1.5}}$$

and

$$\frac{t_{2.2}}{t_{1.5}} = 2.7 \frac{c_{h,\,1.5}}{c_{h,\,2.2}}$$

For equal values of c_h, these results agree fairly well with the latter two results (3.8 and 3.0) given above on this page.

According to Eq. (4:8), for $n = 1.5$, the above relation becomes

$$\frac{t_{1.5}}{t_{0\,9}} = 5.65 \sqrt{\frac{3.7}{3.1}} \frac{\lambda_{0\,9}}{\lambda_{1\,5}} = 6.2 \frac{\lambda_{0.9}}{\lambda_{1.5}}$$

and

$$\frac{t_{2\,2}}{t_{1.5}} = 3.24 \sqrt{\frac{3.1}{2.7}} \frac{\lambda_{1\,5}}{\lambda_{2\,2}} = 3.5 \frac{\lambda_{1.5}}{\lambda_{2.2}}$$

For equal values of λ, these results are closely in agreement with the first and last results (6.4 and 3.0) given above on this page.

If we choose $n = 1.6$, then this relation becomes

$$\frac{t_{1.5}}{t_{0.9}} = 6.04 \sqrt[5]{\left(\frac{3.7}{3.1}\right)^3} \frac{\lambda_{0.9}}{\lambda_{1.5}} = 6.7 \frac{\lambda_{0.9}}{\lambda_{1.5}}$$

and

$$\frac{t_{2.2}}{t_{1.5}} = 3.47 \sqrt[5]{\left(\frac{3.1}{2.7}\right)^3} \frac{\lambda_{1.5}}{\lambda_{2.2}} = 3.8 \frac{\lambda_{1.5}}{\lambda_{2.2}}$$

Experience has shown that c_h decreases with increasing disturbance (*cf.* Fig. 59), and so does no doubt λ. Therefore, the theoretical time ratios are actually smaller than those obtained for equal values of c_h and of λ. If we take this into consideration, we still find acceptable agreement with the classical theory, though not so good as that with the new theory. Thus, for the classical theory, we find the following conditions which must be satisfied in order that the theoretical time ratios shall fit in with the observed mean time ratio:

$$\frac{c_{h,\,0.9}}{c_{h,\,1.5}} = \begin{cases} 1.45^{1)} \\ 0.86 \end{cases} \quad \text{and} \quad \frac{c_{h,\,1.5}}{c_{h,\,2.2}} = \begin{cases} 0.56 \\ 1.11 \end{cases}, \text{ respectively}$$

Similarly, for the new theory we find the following conditions:

for $n = 1.5$, $\quad \frac{\lambda_{0.9}}{\lambda_{1.5}} = \begin{cases} 1.03 \\ 0.61 \end{cases}$ and $\frac{\lambda_{1.5}}{\lambda_{2.2}} = \begin{cases} 0.43 \\ 0.86 \end{cases}$, respectively

and for $n = 1.6$, $\quad \frac{\lambda_{0.9}}{\lambda_{1.5}} = \begin{cases} 0.96 \\ 0.57 \end{cases}$ and $\frac{\lambda_{1.5}}{\lambda_{2.2}} = \begin{cases} 0.42 \\ 0.84 \end{cases}$, respectively

In practice, the difference in results for $n = 1.5$ and $n = 1.6$ is small.

Since the above ratios ought to be smaller than unity the new theory is obviously in better agreement with the practical results than the classical theory.

Another way of treating the disturbance effects on the coefficient of consolidation would be to introduce a zone of smear (*cf.* BARRON, 1948). However, this meets with practical difficulties and does not seem to be more in accordance with reality than the method used above.

Comparison between Theoretical and Observed Time-Consolidation Curves

According to the classical theory, the time of consolidation, t, may be obtained from Eq. (1:29), which gives, for drain spacings:

$$L = 0.9 \text{ m}, \qquad t = \frac{0.102 \cdot 10^4 \,(\text{cm}^2)}{c_h} \ln \frac{1}{1 - \bar{U}}$$

$$L = 1.5 \text{ m}, \qquad t = \frac{0.444 \cdot 10^4 \,(\text{cm}^2)}{c_h} \ln \frac{1}{1 - \bar{U}}$$

$$L = 2.2 \text{ m}, \qquad t = \frac{1.20 \cdot 10^4 \,(\text{cm}^2)}{c_h} \ln \frac{1}{1 - \bar{U}}$$

[1] The top figures in the right-hand members of these equations refer to the time ratios observed at 50 and 40 % degrees of consolidation, respectively, in Test Area No. I alone, while the bottom figures refer to the corresponding time ratios observed in Test Areas No. I (0.9 and 2.2 m drain spacing) and No. II (1.5 m drain spacing).

By comparing the tc_h-values thus obtained with the time-consolidation curves observed in Areas I and II, Fig. 68, we find the c_h-values given in Table 13.

Table 13.

$\bar{U}$ %	tc_h in cm²			c_h in cm²/sec		
	Area No. I $L = 0.9$ m	Area No. II $L = 1.5$ m	Area No. I $L = 2.2$ m	Area No. I $L = 0.9$ m	Area No. II $L = 1.5$ m	Area No. I $L = 2.2$ m
20	230	1 000	2 680	$0.99\ 10^{-4}$	$2.03\ 10^{-4}$	$1.90\ 10^{-4}$
40	520	2 270	6 140	$0.99\ 10^{-4}$	$1.29\ 10^{-4}$	$1.17\ 10^{-4}$
70	1 230	5 330	14 400	$0.81\ 10^{-4}$	$1.03\ 10^{-4}$	
90	2 350	10 200	27 600	$0.50\ 10^{-4}$		

According to the new theory, we find the corresponding values from Eq. (4:8), which gives for $n = 1.5$ and

$$L = 0.9 \text{ m}, \qquad t = \frac{0.0935 \cdot 10^5\ (\text{cm}^{2.5})}{\lambda \sqrt{\frac{\bar{u}_0}{\gamma_w}}} \left(\frac{1}{\sqrt{1 - \bar{U}}} - 1 \right)$$

$$L = 1.5 \text{ m}, \qquad t = \frac{0.547 \cdot 10^5\ (\text{cm}^{2.5})}{\lambda \sqrt{\frac{\bar{u}_0}{\gamma_w}}} \left(\frac{1}{\sqrt{1 - \bar{U}}} - 1 \right)$$

$$L = 2.2 \text{ m}, \qquad t = \frac{1.77 \cdot 10^5\ (\text{cm}^{2.5})}{\lambda \sqrt{\frac{\bar{u}_0}{\gamma_w}}} \left(\frac{1}{\sqrt{1 - \bar{U}}} - 1 \right)$$

By comparing the $t\lambda$-values with the time-consolidation curves observed in Areas I and II, we find the λ-values given in Table 14.

Table 14.

$\bar{U}$ %	$t\lambda$ in cm²			λ in cm²/sec		
	$L = 0.9$ m $\bar{u}_0 = 3.7$ t/m²	$L = 1.5$ m $\bar{u}_0 = 3.2$ t/m²	$L = 2.2$ m $\bar{u}_0 = 2.7$ t/m²	Area No. I $L = 0.9$ m $\bar{u}_0 = 3.7$ t/m²	Area No. II $L = 1.5$ m $\bar{u}_0 = 3.2$ t/m²	Area No. I $L = 2.2$ m $\bar{u}_0 = 2.7$ t/m²
20	57	361	1 270	$0.25\ 10^{-4}$	$0.73\ 10^{-4}$	$0.90\ 10^{-4}$
40	141	890	3 130	$0.27\ 10^{-4}$	$0.50\ 10^{-4}$	$0.60\ 10^{-4}$
70	401	2 530	8 900	$0.26\ 10^{-4}$	$0.49\ 10^{-4}$	
90	1 050	6 610	23 300	$0.22\ 10^{-4}$		

Obviously, the phenomenon of decrease in c_h with the time of consolidation, *cf.* Chapter 1, can to a certain degree be explained by the non-validity of DARCY's law of permeability for clays at small hydraulic gradients. Thus, the

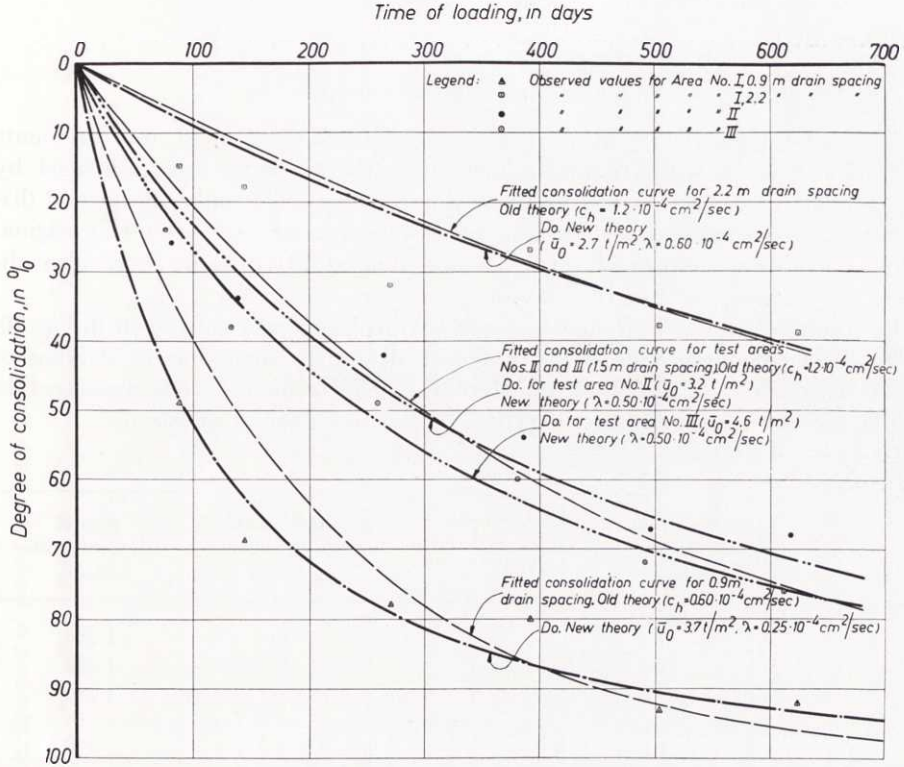

Fig. 69. Theoretical time-consolidation curves compared with observed consolidation values based on pore pressure investigations in Test Areas Nos. I to III. *Cf.* Fig. 68.

agreement between observed and theoretical rates of excess pore water pressure dissipation in the new consolidation theory is far closer than in the classical theory. However, we also find that λ slightly decreases with the time of consolidation. This might be ascribed to the assumption that $\varkappa/m_v$ is a constant but also, for example, to the above-mentioned non-hydrodynamic decrease of excess pore pressure (thixotropy). Furthermore, if the values of U_h in Tables 11 and 12 were reduced to constant load values (*cf.* footnote 1, p. 107), then the decrease of λ with the time would be greater. On the other hand, the circumstance that part of the consolidation had taken place when the loading was completed does not affect the λ-values in our case, where the observed average excess pore water pressures were used[1].

The comparison made in Fig. 69[2] between theoretical time-consolidation curves corresponding to the classical and the new theory ($n = 1.5$) and the results obtained in the test field gives more obvious evidence of the superiority of the new consolidation equation.

[1] The influence of secondary effects on the pore water pressures occurring during the period of primary settlement is probably negligible.

[2] The expression "fitted consolidation curve" used in Fig. 69 refers to the values of c_h and λ which were fitted to the field observations.

54. Flow of Clay in Lateral Direction

Direct Measurements of Horizontal Displacements

For the subsequent interpretation of the results of settlement measurements (Section 55), it is useful to know how much these results are influenced by lateral outflow of clay. As has previously been mentioned, only the lateral displacement of the ground surface was accurately measurable. After the original methods had been improved, some results of qualitative value were also obtained for interior parts of the clay.

The results of the measurements of surface displacements are shown in Fig. 70.

The displacements obtained at different drain spacings due to driving of drains are compared in Table 15. Here the displacements were measured in a radial direction, away from the centre of the test area in question.

Table 15.

Area No.	Drain spacing, in m	Distance from drained surface to observation point, in m	Horizontal displacement, in cm	Size of drained area, in m^2
I	0.9	3	9	1 280
	1.5	3	5	1 280
	2.2	3	1/2	1 280
II	1.5	1 1/2	3	960
III	1.5	1 1/2	3 1/2	960

As was to be expected, the displacement of the ground surface increases with increasing volume of displaced clay, *i.e.* with decreasing drain spacing and increasing drain length and, within certain limits, also with increasing size of drained area.

The approximate values of displacements due to a load q applied in drained areas after completion of drainage are given in Table 16.

Table 16.

Area No.	Drain spacing, in m	q in t/m^2	Total load, in t/m^2	Displacement, in cm
I	0.9	2.3	2.7	4 1/2
	1.5	2.3	2.7	3
	2.2	2.3	2.7	2 1/2
II	1.5	1.8	2.7	1 1/2
III	1.5	2.4	3.9	2 1/2
IV	No drains	2.1	2.7	1 1/2

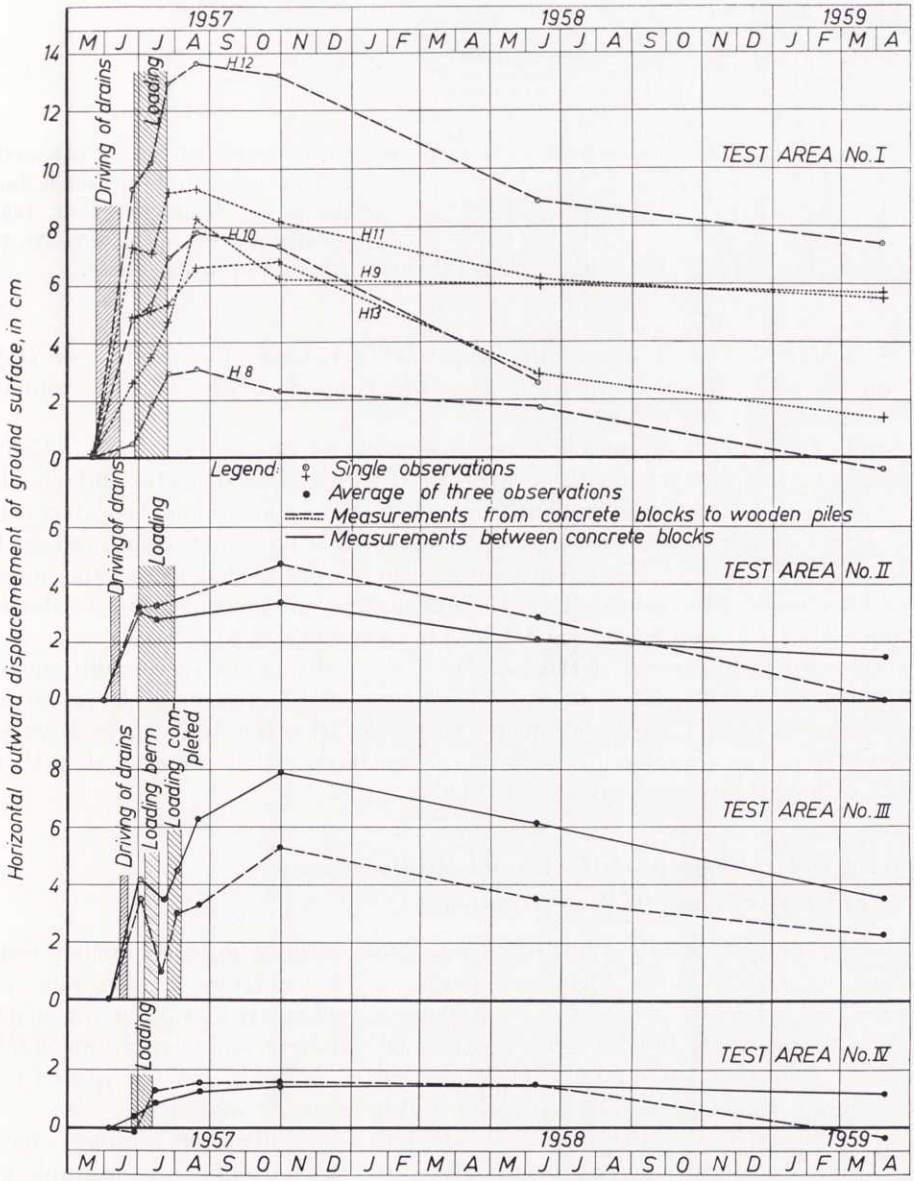

Fig. 70. Observed lateral displacements of ground surface at the distances from drained surfaces given in Table 15.

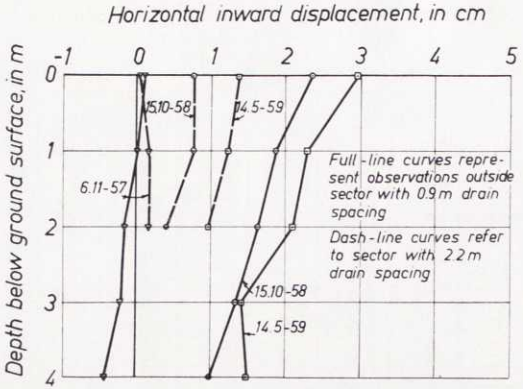

Fig. 71. Lateral displacement of boundary of Test Area No. I, measured during the period from Oct. 24th, 1957 (represented by zero-displacement), to the dates given in the figure.

Obviously, driving of drains also appreciably reduced the rigidity of clay outside the areas. Again we find that the disturbance increases with the volume of displaced clay.

During the process of consolidation, the points of observation were initially displaced further away from the centres of the areas (visco-elastic and plastic deformations), but were subsequently moved in the opposite direction, towards the centres of the areas. The latter phenomenon is no doubt connected with increasing curvature of the ground surface under the loaded areas, and must necessarily occur if the continuity of the soil surface is maintained. For an elastic medium, this is tantamount to a decrease of POISSON's ratio ν.

The lateral displacement of the interior of the soil was not successfully measured until October 24, 1957, after the beginning of the inward displacement of the ground surface. The displacements measured after the above date have so far occurred in a direction towards the areas, though they were smaller than in the case of the ground surface, *cf.* Fig. 71.

Indirect Determination of Horizontal Displacements by Control of Change in Water Content

The volume displacements could be checked, for example, by continuously controlling the change in water content of the clay layer. However, the value of this method is limited owing to the scattering caused partly by the heterogeneity of the soil and partly by the increasing rate of consolidation when approaching a drain (*cf.* Section 53 and Fig. 11). An extensive investigation is required for the method to be accurate. Otherwise, it will be mere estimation.

A continuous control of the water content has been made on samples which were taken as nearly half-way between the drains as possible. An example of the results obtained at a given time in Area No. I is given in Figs. 72 to 74. A comparison of the results obtained at different time intervals is made in Figs. 75 and 76. All values given here are mean values for the clay layer originally situated between depths of 2.5 and 7.5 m below ground surface. The observed

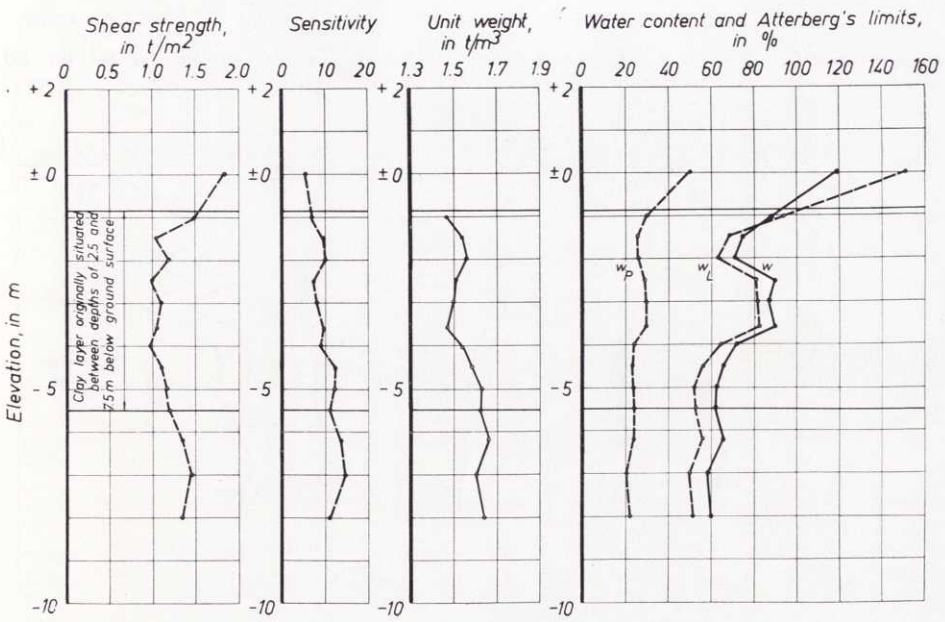

Fig. 72. Geotechnical data of clay. Test Area No. I, drain spacing 0.9 m. June, 1958.

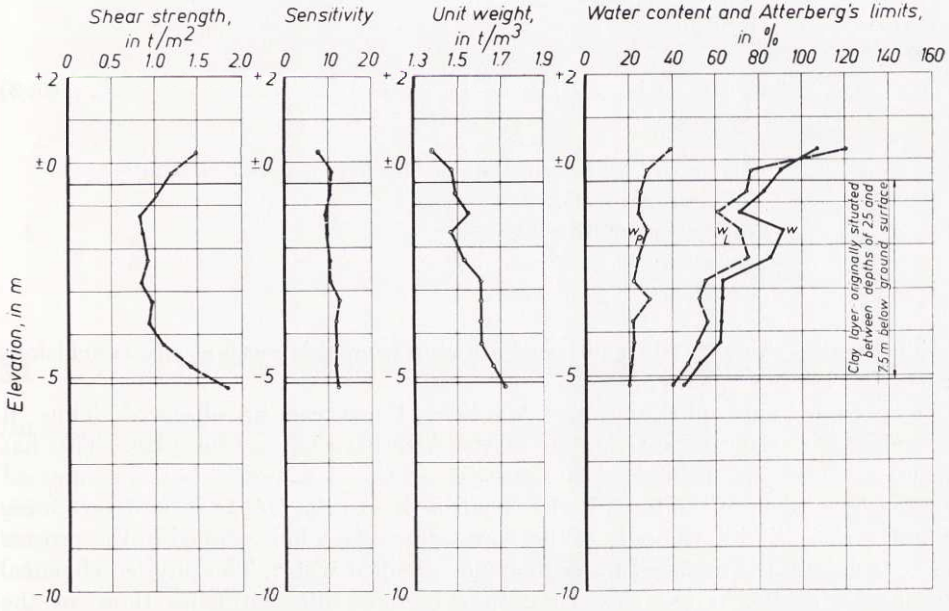

Fig. 73. Geotechnical data of clay. Test Area No. I, drain spacing 1.5 m. June, 1958.

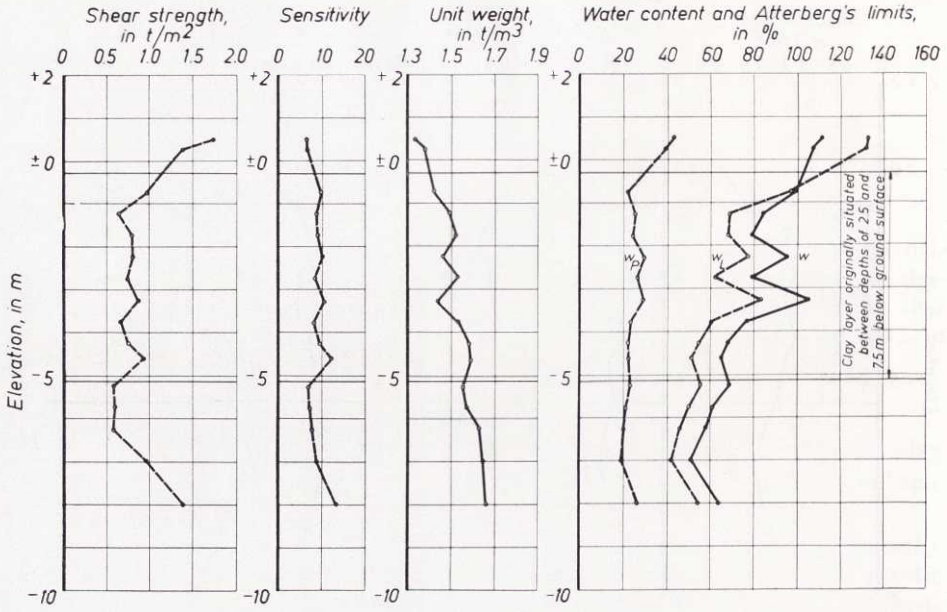

Fig. 74. Geotechnical data of clay. Test Area No. I, drain spacing 2.2 m. June, 1958.

values are compared with that theoretical water content curve in which the effect of horizontal displacement is neglected. This curve is obtained, for a saturated clay, from the equation

$$\overline{w} = \overline{w}_0 - \frac{\Delta h}{h}\left(\frac{\gamma_w}{\gamma_s} + \overline{w}_0\right) \quad \ldots\ldots\ldots\ldots\ldots\ldots \quad (5:3)$$

where $\overline{w}_0$ = initial mean water content of the investigated clay layer,
h = thickness of the layer,
Δh = compression of the layer,
γ_w = specific gravity of pore water,
γ_s = specific gravity of solids.

The results show the difficulties of drawing from this method any conclusions as to the lateral outflow.

A phenomenon concerning the Atterberg limits can be observed. Thus, it seems as if a progressive reduction of the Atterberg limits took place. This has been observed on specimens consolidated in the oedometer, but was not expected to happen in the field. Perhaps this is due to the fact that, in determining the Atterberg limits, the part of the pore water which has escaped in the process of consolidation is replaced by ordinary or distilled water. The physico-chemical properties of the tested clay have thus become different from those of the original clay.

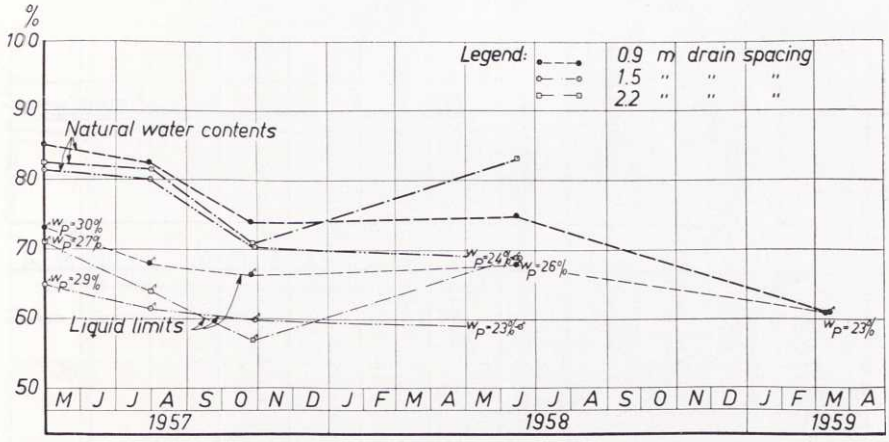

Fig. 75. Results of water content investigations performed at different time intervals in Test Area No. I.

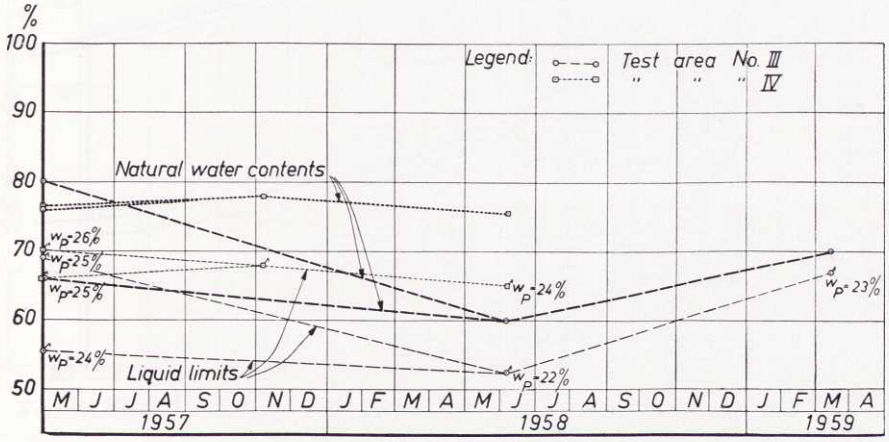

Fig. 76. Results of water content investigations performed at different time intervals in Test Areas Nos. III and IV.

55. Vertical Settlements

Introductory Remarks

The measurements of settlements were carried out with great accuracy. Nevertheless, errors might appear in the results on account of the human factor but they are generally easy to observe, and do not cause difficulties in the interpretation of the results. Other difficulties will be discussed in what follows.

As has been mentioned previously, the thickness of the dry crust is approximately 1 m on an average, while the depth to firm bottom varies from 9 to

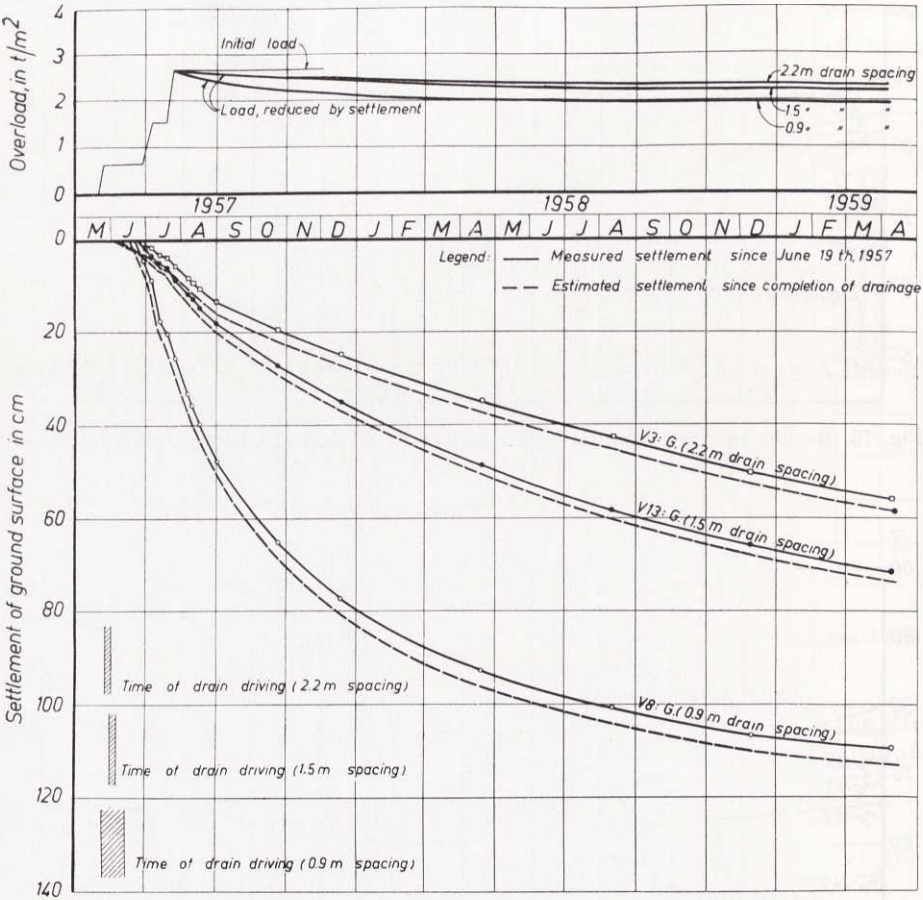

Fig. 77. Settlement observations in Test Area No. I. *Cf.* Fig. 36.

more than 15 m. When studying the consolidation, it is convenient to consider a clay layer which is not influenced by the above-mentioned factors. In our case, settlement measurements have been made at the ground surface and at depths of 1.5, 2.5, 5.0 and 7.5 m below the ground surface. The settlements of the ground surface and those at a depth of 1.5 m are certainly influenced by the dry crust. It is therefore advantageous to study the consolidation of one or both of the two layers, 2.5 m in thickness, situated at depths of 2.5 to 5.0 m and 5.0 to 7.5 m, respectively. If comparisons are to be made between the magnitudes or the rates of compression of a certain definite layer in the different test areas, then the best result is surely obtained from the layer, 5.0 m in thickness, situated at a depth of 2.5 to 7.5 m. In this way the high-plasticity layer mentioned in Section 52 will be included with certainty, while this is not the case if each one

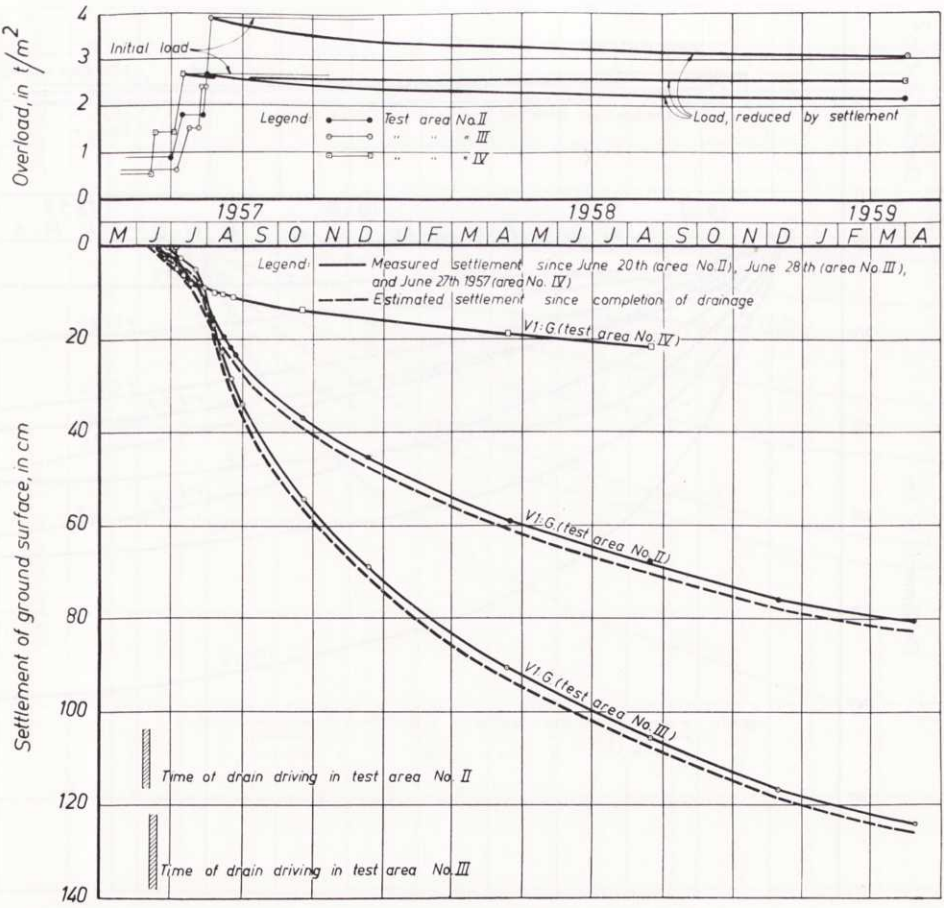

Fig. 78. Settlement observations in Test Areas Nos. II to IV. *Cf.* Figs. 37 to 39.

of the two 2.5 m layers forming an integral part of the 5.0 m layer is studied separately, *cf.* Figs. 72 to 74.

The consolidation of the layer, situated at a depth of 1.5 to 5.0 m, will be considered in the case where settlement measurements have been carried out at depths of 1.5 and 5.0 m below the ground surface only.

Test Results

The results of the measurements are given in the form of diagrams. The settlements at the ground surface and at the 2.5, 5.0 and 7.5 m levels at given points within the different areas are represented in Figs. 77 to 80. The corresponding compression of the 5 m layer situated originally between depths of 2.5 and 7.5 m below ground surface is given in Figs. 81 to 82.

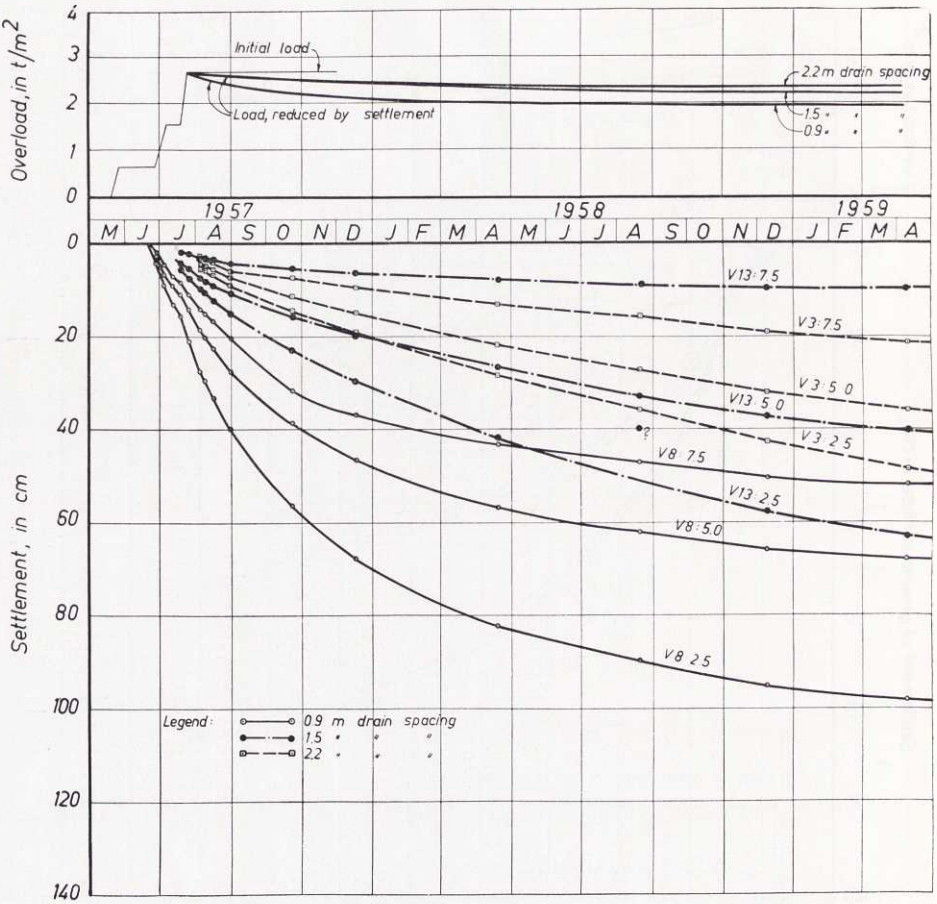

Fig. 79. Settlement observations in Test Area No. I. *Cf.* Fig. 36.

Elevation of Ground Surface Caused by Driving of Drains

The soil removed by driving of drains caused a rise of the ground surface that was to be observed in the settlement meters which are nearest to the test areas. Thus, at a distance of 1.5 m outside the drained surfaces of Test Areas Nos. II and III the observed rise was approximately 1½ cm on an average at depths of 1.5 m (6 observation points) and 5 m (2 observation points) below ground surface. At a distance of 1 m outside the different sectors of Area No. I, the respective values of the rise observed at depths of 1.5 and 5 m were:

8½ and 4 cm at 0.9 m drain spacing
3½ „ 1 cm „ 1.5 m „ „
1 „ ½ cm „ 2.2 m „ „

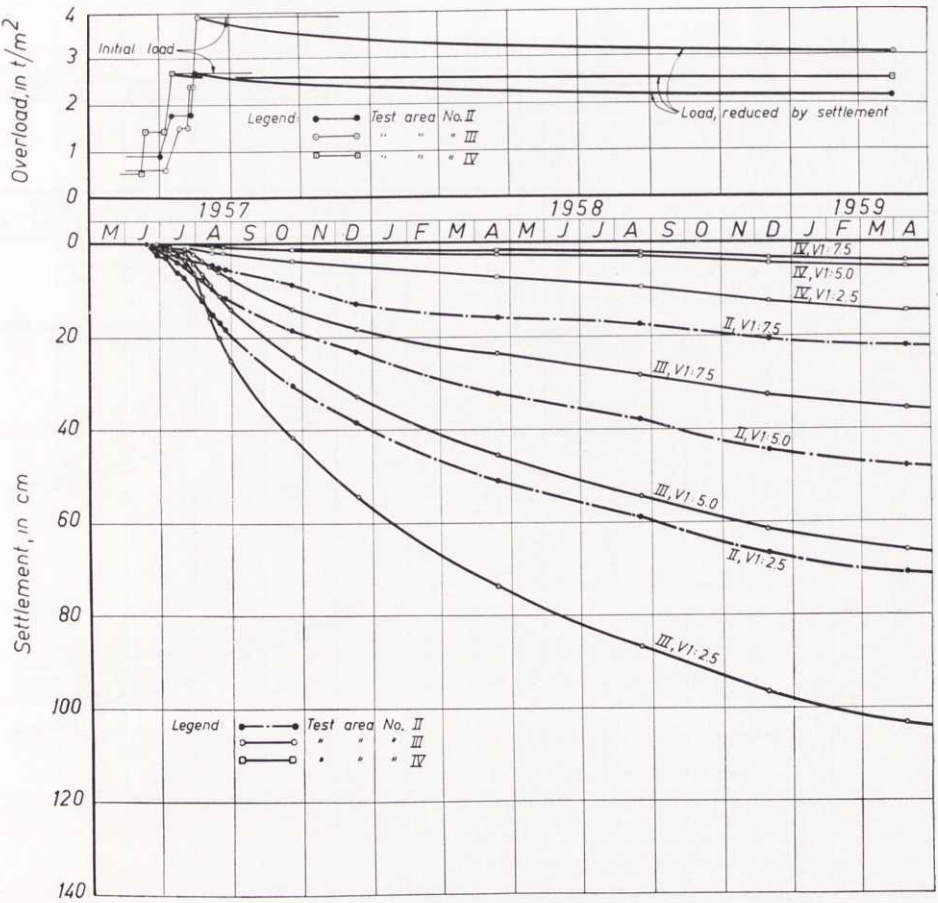

Fig. 80. Settlement observations in Test Areas Nos. II to IV. *Cf.* Figs. 37 to 39.

These values were single observations, and consequently, the statistical deviations are not known.

The observations made farthest away from the test areas showed an average elevation of the ground surface of 2 mm (9 observation points). However, this value is close to the limit of accuracy of the measuring method, and is comprised within the natural range of variation in ground surface level, *e.g.* due to the variation of gravitation caused by the influence of the moon and the sun (*cf. e.g.* TOMASCHEK, 1957), to varying soil temperature, *etc.*

Seasonal Variation in Rate of Settlement

The influence of seasonal variation in temperature on the rate of settlement is complicated since a change in the soil temperature may have the opposite effects stated in what follows.

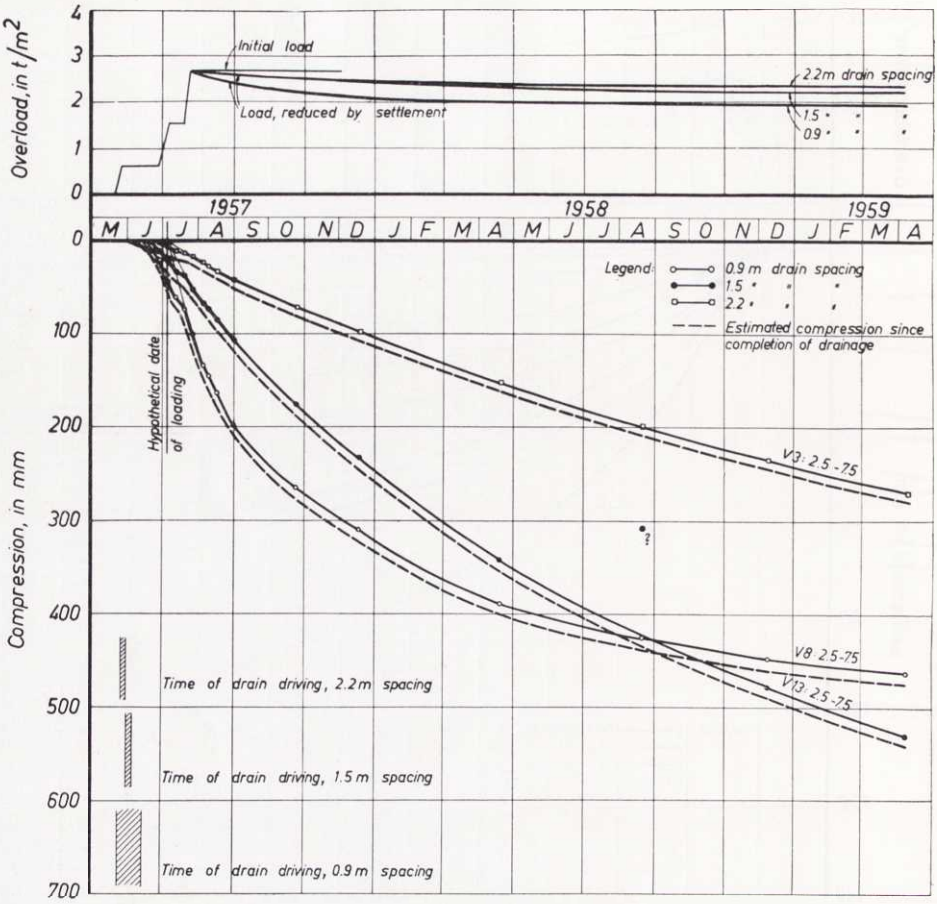

Fig. 81. Compression of the 5 m layer situated originally between depths of 2.5 and 7.5 m below ground surface. Test Area No. I.

Firstly, a decrease of temperature increases the viscosity of pore water and, according to LAMBE (1958), is assumed to expand the double layer. These effects cause a decrease in rate of settlement[1].

Secondly, a decrease of temperature reduces the thickness of the clay layer in direct proportion to the coefficient of thermal expansion of the clay and to the change in temperature. This causes an apparent increase in rate of settlement. In this connection (*cf.* also Section 53) it should be mentioned that the decrease of temperature also causes a reduction of the excess pore water pressure

[1] The temperature effects on the consolidation behaviour have been studied in the laboratory, *e.g.* by FINN (1951) and BURMISTER (1951). Thus, according to FINN, a decrease of temperature reduces the coefficient of consolidation of remoulded clay and causes a vertical downward displacement of the void ratio *vs.* pressure curve. According to BURMISTER, a temperature drop (rise) makes the slope of the void ratio *vs.* pressure curve of undisturbed clay flatter (steeper).

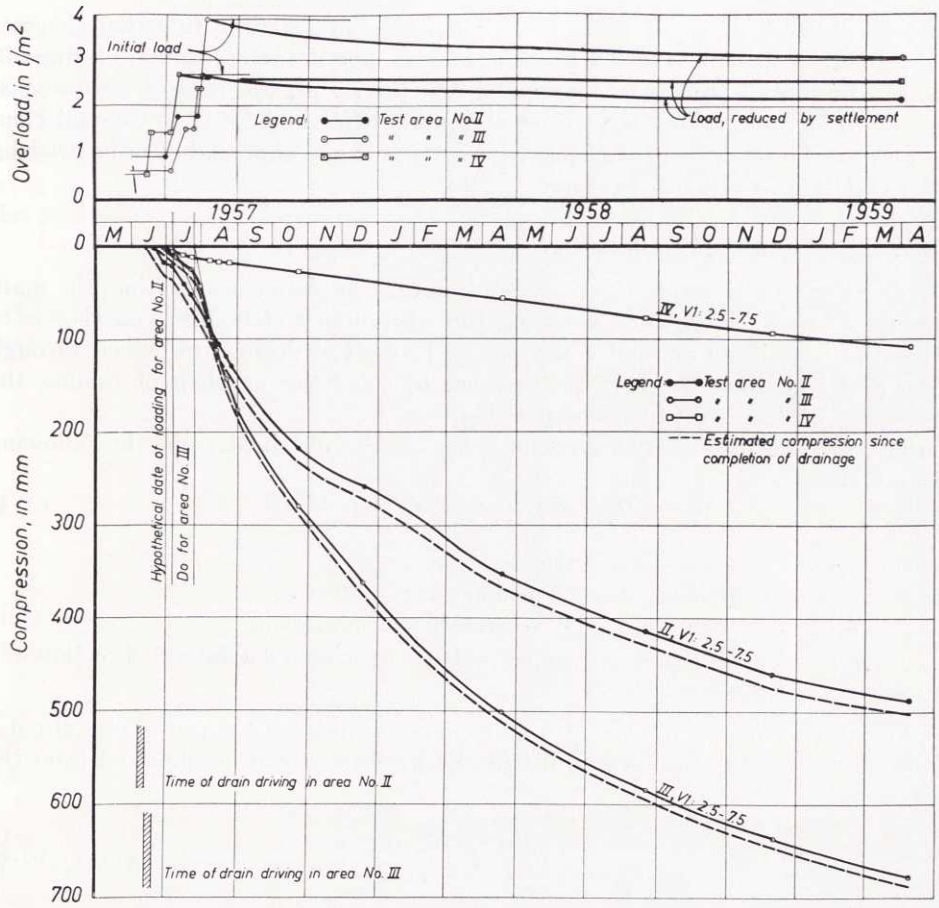

Fig. 82. Compression of the 5 m layer situated originally between depths of 2.5 and 7.5 m below ground surface. Test Areas Nos. II to IV.

and, according to the new theory, this decrease leads to an increase in time of consolidation.

Thirdly, seasonal variations in load, *e. g.* variations in ground water level and, during the winter, in snow load, will influence the rate of settlement.

Moreover, frost has an influence on the rate of settlement in the interior and in the immediate neighbourhood of the frozen zone of the soil. Frost might also reduce the effectiveness of drainage by clogging the pores of the sand fill on the top of the drains (or on the ground surface).

It is probable that a variation in soil temperature does not occur at a greater depth than 7 to 8 m below ground surface (*cf.* MOUM and ROSENQVIST, 1957). Nevertheless, we find in general that the rate of settlement of the clay underneath a depth of 7.5 m increases in the late autumn. This may be caused by

a lowering of the ground water level. Similarly, we generally find that the rate of settlement at depths of 2.5 and 5 m increases in the late autumn, *cf.* Figs. 79 to 80. In the layer between depths of 2.5 and 7.5 m, the rate of compression seems to increase during the winter season. This might be due to thermal compression. The settlement of the ground surface is not appreciably influenced by the variation in soil temperature.

Estimation of Final Compression

In addition to estimating the time required for complete consolidation, the main problem to be solved when assessing the advisability of building on clay is to find the magnitude of final compression. If vertical drains are driven through the clay bed, then we have furthermore to solve the problem of finding the influence of drains on final compression.

The final settlement (compression) δ_{tot} can be obtained from the following equation

$$\delta_{tot} = \delta_i + \delta_p + \delta_s + \delta_{fl} \quad \ldots\ldots\ldots\ldots\ldots\ldots \quad (5:4)$$

where δ_i = instantaneous settlement,
δ_p = settlement due to primary consolidation,
δ_s = settlement due to secondary consolidation,
δ_{fl} = settlements caused by outflow of clay in a lateral direction (*cf.* Section 54).

For an elastic medium, the instantaneous settlement of the centre of a circular area submitted to a uniformly distributed pressure q can be obtained from the equation

$$\delta_i = I \frac{R_A \, q}{E} \quad \ldots\ldots\ldots\ldots\ldots\ldots\ldots\ldots \quad (5:5)$$

where R_A = radius of loaded area A,
E = modulus of elasticity,
I = influence value, determined by the value of H/R_A, where H is the depth to firm bottom.

Although the assumption of elastic behaviour is not fulfilled in the case of soil (*cf.* Section 12), Eq. (5:5) may nevertheless be expected to give sufficiently accurate results in practice. However, the practical use of this equation is complicated as the apparent modulus of elasticity E is difficult to find by conventional laboratory investigations (*cf. e.g.* BERGSTRÖM and LINDERHOLM, 1946). Thus, for example, at Skå-Edeby, the value of E obtained from unconfined compression tests on samples which were taken at a depth of 4 m (*cf.* KALLSTENIUS, 1958) by means of a sampler SGI IX was less than, or about, 5 kg/cm^2. For other sampler types, E was found to be considerably lower. The correct apparent value of E must be higher than that which is obtained from this type of test. Thus, at Skå-Edeby, the instantaneous settlement of the centre of Area No. IV at a load increment of 1.2 t/m^2 is approximately $\delta_i = 4.5$ cm.

If this value is inserted into Eq. (5: 5), we find, for the depth and the loading conditions in this case ($H/R_A \approx 2/3$) and $\nu = 0.5$ (TERZAGHI, 1944, Fig. 138), the apparent modulus of elasticity $E \approx 16$ kg/cm^2.

The value of δ_i for a given clay layer is most easily found from measurements made at the instant of load application. In this manner we obtain, for the clay layer situated between depths of 2.5 and 7.5 m in the undrained Area No. IV, the following compression:

$$\delta_i \approx 6 \text{ mm for a load increment of } 1.2 \text{ t/m}^2$$

Consequently, the minimum instantaneous compression by which the observed total compression should be reduced is

$$\begin{aligned} &\text{for Area No. I, approximately } \frac{2.3}{1.2} \cdot 6 = 12 \text{ mm,} \\ &\text{„ „ „ II, „ } \frac{1.8}{1.2} \cdot 6 = 9 \text{ mm,} \\ &\text{„ „ „ III, „ } \frac{3.3}{1.2} \cdot 6 = 17 \text{ mm.} \end{aligned}$$

However, these values may be increased considerably owing to the effect of disturbance (*cf.* MÉNARD, 1957), and it is therefore difficult to give accurate values.

The primary part of the long-time settlements will be estimated by means of two methods, *viz.*, firstly, by using as a starting-point the compression characteristics found in the laboratory, and secondly, by comparing the excess pore water pressures and settlements observed most recently.

In the calculation of the primary consolidation settlement by the aid of the first method, account must be taken of the reduction of load caused by the part of the load sinking down below the ground water level. The ground water at Skå-Edeby is often found 50 cm below the original ground surface, of which 25 cm had been taken away before the gravel blanket was laid out. Thus, the ground water level is situated only about 25 cm below the gravel blanket, and, with the requisite accuracy, the reduction of weight can be put roughly equal to 0.7 times the settlement of the ground surface. In this case, the final primary compression δ_p of a clay layer of thickness h can approximately be expressed by the value given by the equation (*cf.* Eq. 1: 5 b)

$$\delta_p \approx h \frac{\varepsilon_2}{\log 2} \log \frac{\bar{\sigma}_0 + \Delta q - \gamma' \delta_g}{\bar{\sigma}_0} \quad \ldots\ldots\ldots\ldots \quad (5:6)$$

where ε_2 = additional deformation due to doubling the load,
$\bar{\sigma}_0$ = effective preconsolidation pressure (average value for the layer in question),
Δq = pressure increment (average value for the layer in question) under which consolidation takes place,
δ_g = final settlement of ground surface,
γ' = 0.7 t/m^3 (average for total settlement period).

The results of these calculations relating to the clay layer situated between depths of 2.5 and 7.5 m are given in Table 17. In these calculations, the effect of the disturbance caused by the drainage operation as well as the lateral outflow and a possible stiffening effect of the sand drains on the clay are disregarded.

Table 17[1].

Area No.	Drain spacing, in m	ε_2 %	$\bar{\sigma}_0$ t/m²	Δq t/m²	$\gamma' \delta_g$ t/m²	δ_p cm
I	0.9	17	2.8	2.7	0.8	63
	1.5	18	2.8	2.7	0.7	70
	2 2	14	2 8	2.7	0.9	50
II	1.5	15—16	2.8	2.7	0.9	54 - 57
III	1.5	13—15	2.8	3.9	1 1	65—75
IV	No drains	13—15	2.8	2.7	0.9	47—54

In the second method, the final primary compression is determined from the equation (*cf.* Eq. 1: 3)

$$\delta_p \approx \delta_1 + \frac{\delta}{\bar{U}} \quad \ldots\ldots\ldots\ldots\ldots\ldots\ldots \quad (5:7)$$

where δ_1 = consolidation settlement at the instant of completion of loading,
δ = consolidation settlement after completion of loading,
$\bar{U}$ = degree of consolidation obtained by observing excess pore pressure dissipation.

Several approximations are involved in this method.

Firstly, the observed values of δ will have to be reduced by the part of compression δ_{fl} which is due to lateral outflow of clay.

Secondly, $\bar{U}$ refers to the total consolidation of the clay layer, *i.e.* to the combined action of horizontal and vertical drainage.

As has previously been mentioned, the excess pore water pressure at a depth of 5 m in the undrained area had not changed since the instant of loading. No consolidation in a vertical direction was therefore observed at this depth. However, the settlement measurements show a certain amount of compression of the investigated clay layer in the undrained area also. This compression might be due solely to the effect of vertical drainage or, which is more probable, to the combined effects of vertical drainage and outflow of clay in a horizontal lateral direction. Owing to the shortcomings of the measurements of horizontal displacement of clay (*cf.* Section 50), no direct information has been obtained about the influence of this factor at a greater depth than about 3 m. However, indirect

[1] The value of ε_2 given in Table 17 was determined by means of the method suggested in the above, *cf.* p. 89, Table 5.

information may be obtained from other observations. Thus, as has already been mentioned, judging by the pore water pressure measurements, the effect of vertical drainage is negligible at a depth of 5 m, and the main part of compression occurring at that depth is consequently due to outflow. Furthermore, by comparing the magnitudes of compression of the upper and lower clay layers situated between depths of 2.5 to 5.0 and 5.0 to 7.5 m, respectively, we find that at least the upper layer is influenced by vertical drainage.

For the undrained area, the relation between the vertical average compression δ_{fl} of a layer, 5 m in thickness, and the average lateral outflow $\delta_{h,fl}$ at the periphery of the area is obtained from the equation

$$\frac{\pi 35^2}{4} \delta_{fl} = \pi \cdot 35 \cdot 5 \, \delta_{h,fl}$$

and hence $\delta_{fl} = 0.57 \, \delta_{h,fl}$

If we assume that the upper and lower layers have the same amount of outflow of clay[1] and that only the upper layer has so far been influenced by vertical drainage[2], then we obtain on April 8, 1959, *i.e.* after 635 days of loading, $\delta_{fl} \approx 2\,½$ cm, corresponding to an outflow of $\delta_{h,fl} = 4\,½$ cm. This value refers to the clay layer, 5 m in thickness, situated between depths of 2.5 and 7.5 m. In consideration of the results given in Section 54, this value seems reasonable.

If the above assumption is accepted as true, the effect of vertical drainage on the layer in question can be estimated at $\overline{U}_v = 16\,\%$ on the above-mentioned day. On the other hand, if no regard is paid to lateral outflow, $\overline{U}_v$ is equal to 22 %. If we take for $\overline{U}_h$ the corresponding values given in Tables 11 and 12, the corresponding total consolidation $\overline{U}$ is obtained from the equation (*cf.* CARRILLO, 1942)

$$\overline{U} = \overline{U}_h + \overline{U}_v - \overline{U}_h \, \overline{U}_v \quad \ldots\ldots\ldots\ldots\ldots\ldots \quad (5{:}8)$$

The values of $\overline{U}$ calculated from this equation are given in Table 18 without correction and in Table 19 with correction for outflow.

If we take for δ the values observed in the field[3] and for δ_1 the observed values reduced by the previously estimated minimum values of δ_i, then we find the final compression values without correction for outflow given in Table 18.

Except for Test Area I/0.9 and I/2.2, the values of δ_p given in this table are mostly considerably greater than the values of δ_p given in Table 17. However, if the values of δ in Table 18 are reduced so as to take account of the outflow δ_{fl}, they will agree more closely with the corresponding values in Table 17.

[1] In reality, the upper layer is likely to have a greater amount of outflow than the lower layer.

[2] This assumption is justified by the pore pressure measurements carried out at a depth of 9 m in the undrained area, *cf.* Fig. 66. No decrease of excess pressure has been observed at this depth.

[3] The values used in this connection refer to given points within the areas. The distribution of compression underneath the loaded area is discussed below, p. 134.

Table 18.

Area No.	Drain spacing, in m	δ_1 cm	δ cm	$\bar{U}$ %	δ_p cm
I	0.9	9	37	94	48
	1.5	5	48	66	78
	2.2	1	26	52	51
II	1.5	7	42	75	63
III	1.5	6	61	81	81

For example, let us examine the effect of outflow on the assumption that the deduced value of $\delta_{fl} = 2\,½$ cm, *i.e.* $\delta_{h,fl} = 4\,½$ cm, for the undrained area is correct. Let us proceed by making the working hypothesis that, for a given load, the outflow under a drained area, compared with that under the undrained area, is proportional to the corresponding instantaneous lateral displacement of loading. This may be estimated from the data given in Table 16. For Areas Nos. II and III, $\delta_{fl} \approx 0.58\ \delta_{h,fl}$ and for Area No. I, $\delta_{fl} \approx 0.29\ \delta_{h,fl}$. By simple proportioning, we find the following effect of lateral outflow in April 1959:

Area No.	I/0.9	I/1.5	I/2.2	II	III
δ_{fl} cm	3	2	2	3	6

If the values of δ in Table 18 are reduced by these values, we obtain δ_p as given in Table 19.

Table 19.

Area No.	Drain spacing, in m	δ_1 cm	δ cm	$\bar{U}$ %	δ_p cm
I	0.9	9	34	93	46
	1.5	5	46	63	78
	2.2	1	24	49	50
II	1.5	7	39	73	60
III	1.5	6	55	80	75

The agreement between the values of δ_p in Tables 17 and 19 is good, particularly since the values of ε_2 in Table 17 are rough approximations and in consideration of the fact that the estimated value of δ_1 in Table 19 may be too high and that the values of δ_{fl} deduced in the above are uncertain. However, a disagreement is found for those sectors in Area I in which the drain spacings

are 0.9 and 1.5 m. Thus, for a spacing of 0.9 m, the value of δ_p given in Table 19 is considerably lower than that given in Table 17, whereas for a spacing of 1.5 m it is considerably higher. In the former case, the reduction of compression from the value given in Table 17 to the value given in Table 19 is probably caused by a stiffening effect of the closely spaced drains on the clay, which prevails over the contrary effect of remoulding. In the latter case, the difference between the values in Tables 17 and 19 is probably due to two reasons. Firstly, the value of $\overline{U}$ seems very low. Since $\overline{U}$ is taken from two piezometers only, the real average might just as well be considerably higher (*cf.* Section 53). Secondly, the settlement meter placed at a depth of 7.5 m in Area I/1.5 has been subjected to small settlements, and this indicates that it is placed at a small distance from firm bottom or, possibly, from a large erratic block. Such erratic blocks are found here and there on the visible part of the bed rock cropping up above the clay plain. Likewise, at least at one point, an erratic block or, possibly, a rock peak has undoubtedly been observed on the bed rock at a great depth in connection with electrical resistance sounding carried out in the test field (OSTERMAN, 1959, Fig. 15). Naturally, in such a case, the real average compression of the clay layer could be completely different from the observed compression.

It is even possible that the low value of $\overline{U}$ and the corresponding large compression of the layer in Area I/1.5 are mutually related. An erratic block or rock peak would act like a wedge which is continuously pressed from below into the clay layer when it settles. If, then, the block or rock is not covered with a continuous layer of sand or silt[1], new pore water pressures would be created in the process of settling, and would add to the existing excess pressures.

The values obtained in Areas II and III are slightly higher than those given in Table 17. This might be due to the effect of remoulding, but also to underestimation of δ_{fl} or δ_i or both. For example, if δ_{fl} is put equal to 5 and 10 cm, then the final primary compression is 58 cm at Area II and 70 cm at Area III, respectively. If, on the other hand, $\delta_i = 3$ cm at Area II ($\delta_1 = 5$ cm) and 6 cm at Area III ($\delta_1 = 2$ cm), then we get $\delta_p = 58$ and 73 cm, respectively. Neither of these applied values of δ_{fl} and δ_i seems unreasonable.

Rate of Consolidation as Determined by Rate of Compression

The rate of consolidation is currently determined from settlement measurements by means of the relation $\overline{U} = \delta/\delta_p$. It will be shown here that this method, though seemingly simple, is difficult, and requires knowledge of several important phenomena which are generally disregarded. Thus, if the time-consolidation curve obtained by the aid of this method is not correctly adjusted, then this curve may differ appreciably from that which is obtained from pore pressure measurements.

[1] That this might be the case is obvious from the above-mentioned electrical resistance sounding. The erratic block (or rock peak) can be situated at the sounding hole No. 3. At this place, no increase of electrical resistance, which would indicate the existence of a continuous high-permeable layer, has been observed.

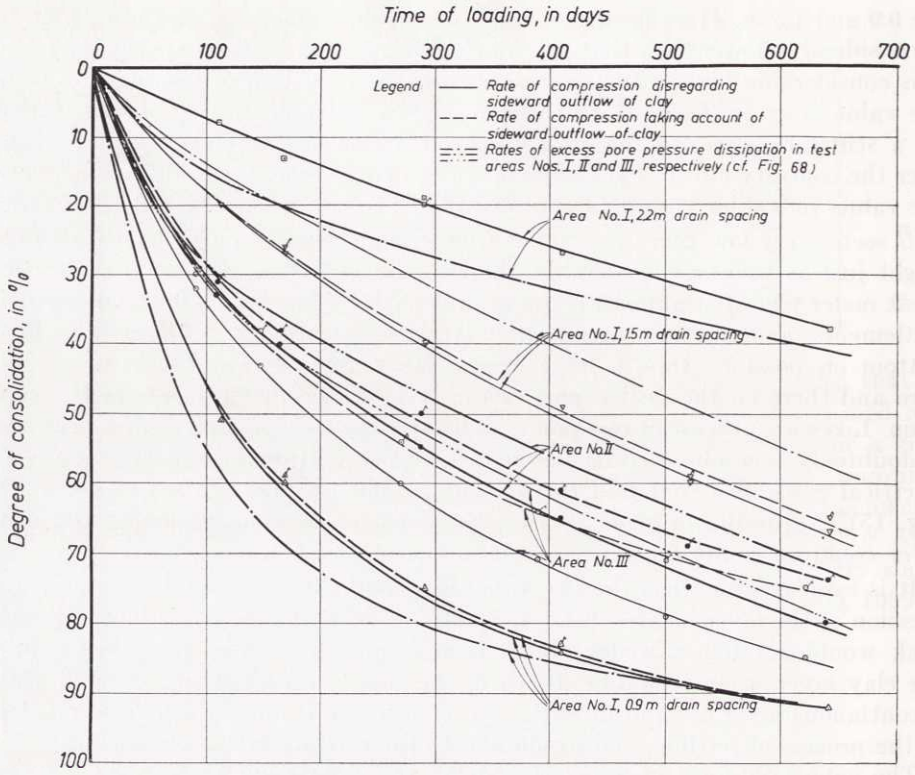

Fig. 83. Time-consolidation curves as determined, on the one hand, by the rate of compression and, on the other hand, by the rate of pore water pressure dissipation.

The first, and perhaps main, difficulty has already been met with in determining the final primary compression. As has just been shown, this compression can be determined with accuracy only if the pore water pressures and lateral outflow of soil are measured at the same time as vertical settlements, and not until the observed excess pore water pressure tends to zero. As a matter of fact, the primary compression is not known even then, as the settlement occurring up to that moment involves a certain amount of secondary settlement, whose magnitude cannot be determined on the basis of present knowledge. It is therefore obvious that this method of determining the degree of consolidation has serious shortcomings.

Secondly, a problem arises owing to the previously mentioned fact that the load is gradually reduced by the part of the load sinking down below the ground water level. This reduction will be reflected in the slope of the time-settlement curve, which is smaller than in the case where the load is constant throughout the consolidation process.

The difference in character between, on the one hand, the rate of compression obtained without and with correction for the estimated lateral outflow and, on the other hand, the rate of excess pore water pressure dissipation, appears from Fig. 83.

In order to be comparable, the rate of compression is here reduced so as to take account of vertical drainage by means of Eq. (5: 8). In this case the effects of vertical drainage have been assumed to be equal in all test areas, and this is of course a rough approximation. However, the resulting errors in $\bar{U}_h$ may be regarded as negligible.

In determining $\bar{U}$, the compression δ_p has as a rule been estimated at the values given in Table 17 on the basis of the highest values of ε_2 obtained in the drained areas and the lowest value of ε_2 observed in the undrained area. For Test Area I/0.9, the value given in Table 17 undoubtedly involves a large error. For this reason, we have chosen the final compression in this case on the assumption that $\bar{U}_h$ given in Table 12 is correct.

The values of $\bar{U}$, $\bar{U}_v$ and $\bar{U}_h$ thus obtained since a hypothetical date of completion of loading[1] are given in Table 20.

Table 20.

Date	23.10.-57		18.12.-57		18.4.-58		20.8.-58		8.12.-58		8.4.-59	
Consolidation / Area No.	$\bar{U}_v = 4$ %		$\bar{U}_v = 6$ %		$\bar{U}_v = 11$ %		$\bar{U}_v = 15$ %		$\bar{U}_v = 18$ %		$\bar{U}_v = 22$ %	
	$\bar{U}$	$\bar{U}_h$	$\bar{U}$	$\bar{U}_h$	$\bar{U}$	$\bar{U}_h$	$\bar{U}$	$\bar{U}_h$	$\bar{U}$	$\bar{U}_h$	$\bar{U}$	$\bar{U}_h$
I/0.9	53	51	62	60	78	75	86	84	91	89	94	92
I/1.5	23	20	31	27	47	40	57	49	67	60	74	67
I/2.2	12	8	18	13	28	19	38	27	44	32	52	38
II	36	33	44	40	58	55	70	65	79	75	84	80
III	35	32	46	43	64	60	75	71	83	79	88	85

If, on the other hand, the effect of lateral displacements is taken into account, then we obtain the values given in Table 21. Here, the displacements have been assumed to vary according to the same time function as the vertical settlements. If we chose the same final compression as in the above (except for Test Area I/0.9, see below), then the values of $\bar{U}$ in Table 20 would have to be multiplied

[1] Since the load is gradually applied, part of consolidation has already taken place at the time of actual completion of loading, *cf.* also p. 105. A fairly good approximation of the time-consolidation relationship may be obtained by introducing a hypothetical loading time. The total load is thus supposed to act from the date indicated by extrapolation of the compression curves as shown in Figs. 81 and 82.

in this case by a coefficient χ, whose magnitude is determined by the estimated effect of outflow. This coefficient is determined in our case on the basis of the values of δ_{fl} given on p. 128, and is

Area	I/1.5	I/2.2	II	III
χ	0.96	0.92	0.93	0.90

For Area I/0.9, the final compression was estimated at the value given in Table 19 by analogy with the above (same $\bar{U}_h$ as in Table 20).

Table 21.

Date	23.10.-57		18.12.-57		18.4.-58		20.8.-58		8.12.-58		8.4.-59	
Consolidation / Area No.	$\bar{U}_v = 3\ \%$		$\bar{U}_v = 5\ \%$		$\bar{U}_v = 8\ \%$		$\bar{U}_v = 11\ \%$		$\bar{U}_v = 13\ \%$		$\bar{U}_v = 16\ \%$	
	$\bar{U}$	$\bar{U}_h$	$\bar{U}$	$\bar{U}_h$	$\bar{U}$	$\bar{U}_h$	$\bar{U}$	$\bar{U}_h$	$\bar{U}$	$\bar{U}_h$	$\bar{U}$	$\bar{U}_h$
I/0.9	52	51	61	59	77	75	85	83	90	89	93	92
I/1.5	22	20	30	26	45	40	55	49	64	59	71	65
I/2.2	11	8	17	13	26	20	35	27	41	32	48	38
II	33	31	41	38	54	50	65	61	73	69	78	74
III	32	30	41	38	58	54	68	64	75	71	79	75

As was to be expected, the time-consolidation curves obtained from settlement measurements differ quantitatively from those obtained from pore water pressure measurements, but a more interesting fact is that there is also a qualitative difference between them. The possible causes of the discrepancies observed have already been discussed in this subsection. In this case, too, the shape of these curves agrees with the shape of the theoretical consolidation curves in the new theory better than in the classical theory. By using this method, we also find that the rate of consolidation increases with increasing load, and this contradicts the classical theory.

Stiffening Effect of Drains

The presence of a stiffening effect of the drains has already been observed previously in estimating the final compression of the 5 m layer, *cf.* p. 129. It was found that the compression in the sector of Area I having a drain spacing of 0.9 m was smaller than expected. For drain spacings of 1.5 and 2.2 m, however, no such effect was observed.

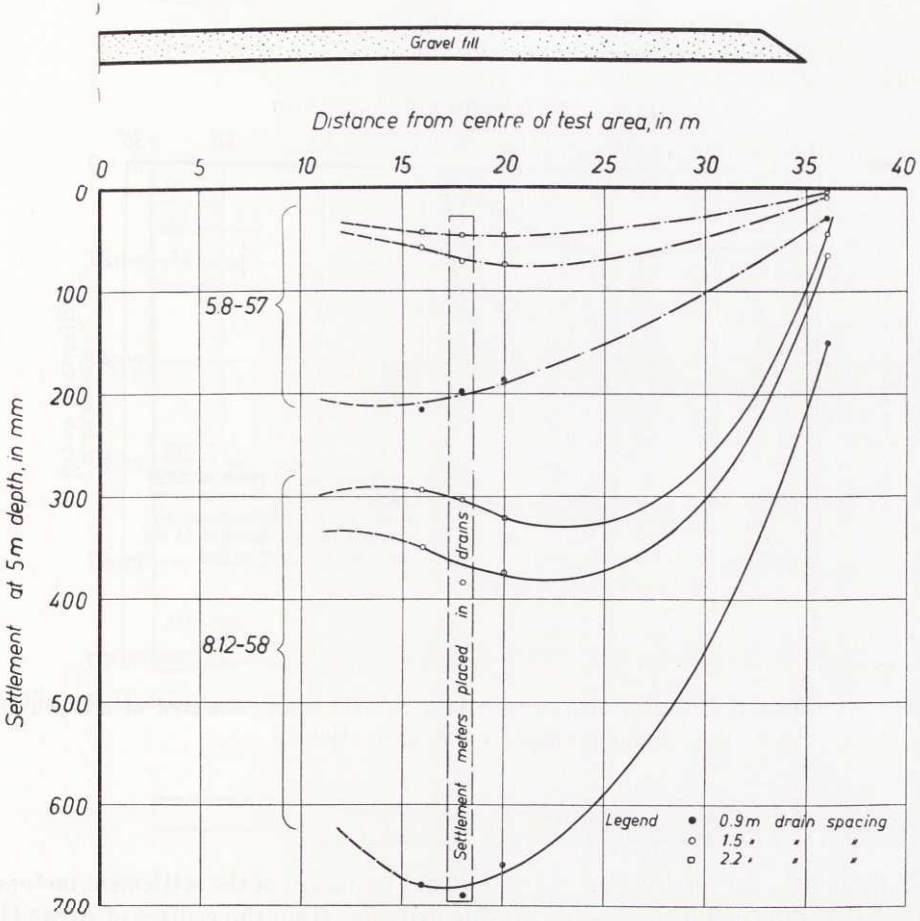

Fig. 84. Settlement in sand drains compared with settlement in surrounding clay. Curves represent, for the two measuring dates in question, from top to bottom: 2.2, 1.5, and 0.9 m drain spacings. Test Area No. I.

In order to study more closely the distribution of settlements in and around the drains, each sector of Test Area I was furnished with settlement meters at different depths, also inside a drain, see Fig. 36. The results of these measurements are compared in Fig. 84 with those of the settlement measurements carried out on surrounding clay.

In the case of 0.9 and 1.5 m drain spacings the results indicate that the rate of settlement near the drains is higher than it is at a greater distance from them, in accordance with the "free strain" hypothesis. However, on the whole, the results agree fairly well with the equal strain hypothesis. A column effect, in the sense that the drains are less compressible than the surrounding clay, as it is often assumed to exist, cannot be observed.

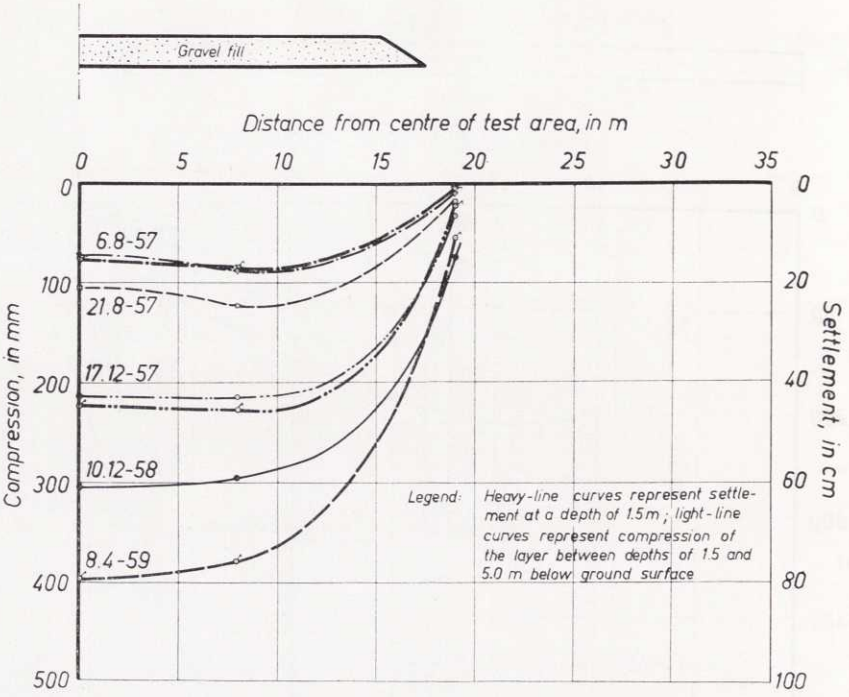

Fig. 85. Distribution of settlements in Test Area No. II. Values observed at a depth of 1.5 m are marked with short strokes.

Distribution of Settlements underneath Loaded Area

The distribution of settlements can be studied by means of the settlement meters placed at depths of 1.5 and 5 m at varying distances from the centres of Areas II to IV. The results of this part of the investigation are given in Figs. 85 to 87.

In the first measurements, the distribution of settlements (compression) corresponds fairly well to that in an elastic medium having POISSON's ratio ν ranging from 0.3 to 0.5 (*cf.* TERZAGHI, 1944, Fig. 138 c).

In drained areas, the redistribution of internal stresses in the course of consolidation causes a change in the distribution of settlements, which corresponds to a decrease in ν. As a rule, the observed distribution of settlements does not differ appreciably from that which corresponds to $\nu = 0$, but a further increase in the curvature of the settlement surface seems to take place in the course of time. The latter effect may be attributed to lateral outflow of clay.

In the undrained area, the change in the distribution of settlements has not occurred in the manner just described above, but has rather taken place in the opposite direction. This is no doubt due to the escape of pore water in a horizontal radial outward direction, and this escape has an appreciable influence on the settlements in the present case (*cf.* HELENELUND, 1951).

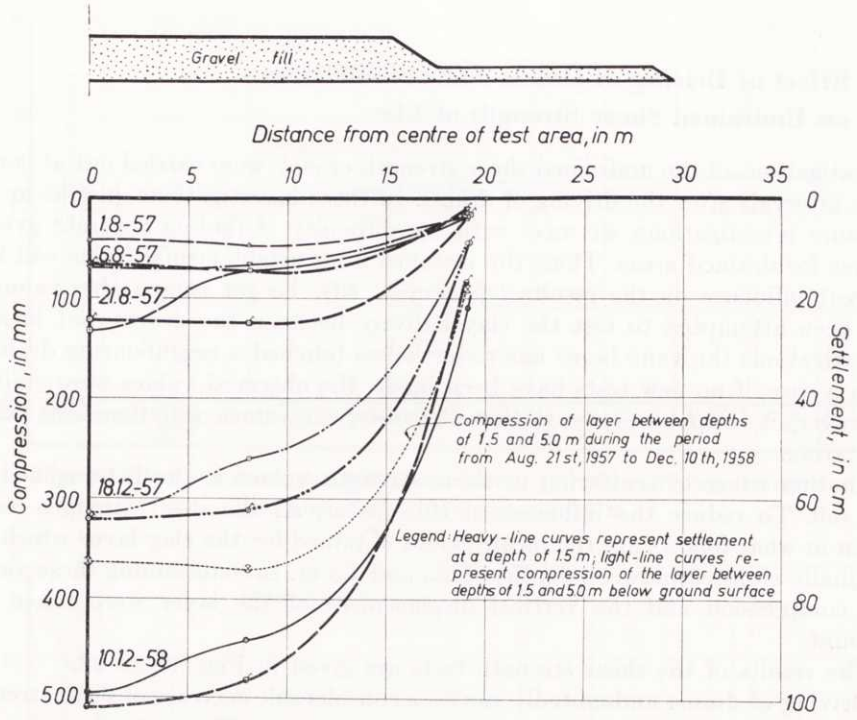

Fig. 86. Distribution of settlements in Test Area No. III. Values observed at a depth of 1.5 m are marked with short strokes.

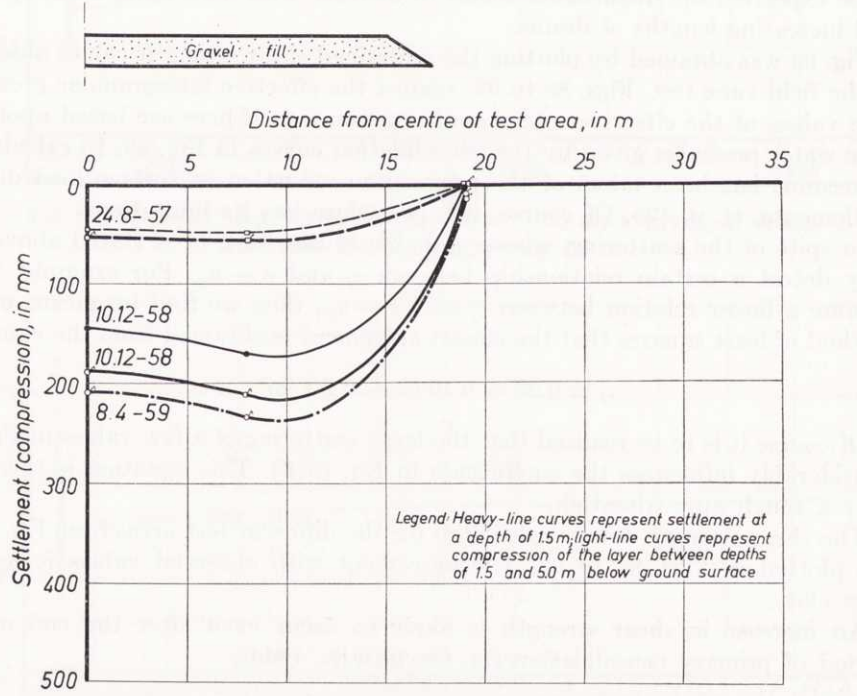

Fig. 87. Distribution of settlements in Test Area No. IV. Values observed at a depth of 1.5 m are marked with short strokes.

56. Effect of Driving of Drains and Consolidation on Undrained Shear Strength of Clay

Investigations of the undrained shear strength of clay were carried out at certain time intervals after the driving of drains. In these investigations, just as in pore pressure investigations, we meet with the difficulty of finding accurate average values for drained areas. Thus, the distance from neighbouring drains will have a great influence on the results (*cf.* Section 53). To get comparable values, it has been attempted to test the clay halfway between the drains, but in some investigations the vane borer has nevertheless touched a neighbouring drain. In such a case, if no new tests have been made, the observed values were omitted. However, it is to be expected that the observed values will therefore exhibit scattering.

Another cause of scattering in shear strength values is the heterogeneity of the soil. To reduce the influence of this factor, all the shear strength values given in what follows are the mean values obtained for the clay layer which was originally situated between depths of 2.5 and 7.5 m. In determining these values, the compression and the vertical displacement of the layer were taken into account.

The results of the shear strength tests are given in Figs. 88 to 92.

Driving of drains undoubtedly causes a considerable decrease of shear strength, in our case 20 to 40 % of the original shear strength. The scattering of values is too great to allow an exact statement concerning the disturbance, but, as was to be expected, the disturbance seems to increase with decreasing drain spacing and increasing lengths of drains.

Fig. 93 was obtained by plotting the undrained shear strength values observed in the field vane test, Figs. 88 to 92, against the effective intergranular pressure. The values of the effective intergranular pressure used here are based upon the pore water pressures given by the consolidation curves in Fig. 68. In calculating σ, account has been taken of the progressive reduction in surface load due to settlements, *cf.* p. 125. Of course, this procedure has its limitations.

In spite of the scattering, whose probable causes have been stated above, we may detect a certain relationship between τ_f and $\sigma - u_w$. For example, if we assume a linear relation between τ_f and $\sigma - u_w$, then we find by means of the method of least squares that the closest agreement is obtained from the equation

$$\tau_f = 0.26 + 0.19\,(\sigma - u_w)\ \mathrm{t/m^2} \quad \ldots\ldots\ldots\ldots\ldots\ldots \quad (5{:}9)$$

Of course it is to be realized that the large scattering of a few values in Fig. 93 considerably influences the coefficients in Eq. (5:9). This equation is therefore only a rough approximation.

The shear strength curves calculated for the different test areas from Eq. (5:9) are plotted in Figs. 88 to 92. The agreement with observed values is reasonably close.

An increase in shear strength is likely to occur even after the end of the period of primary consolidation (*cf.* OSTERMAN, 1960).

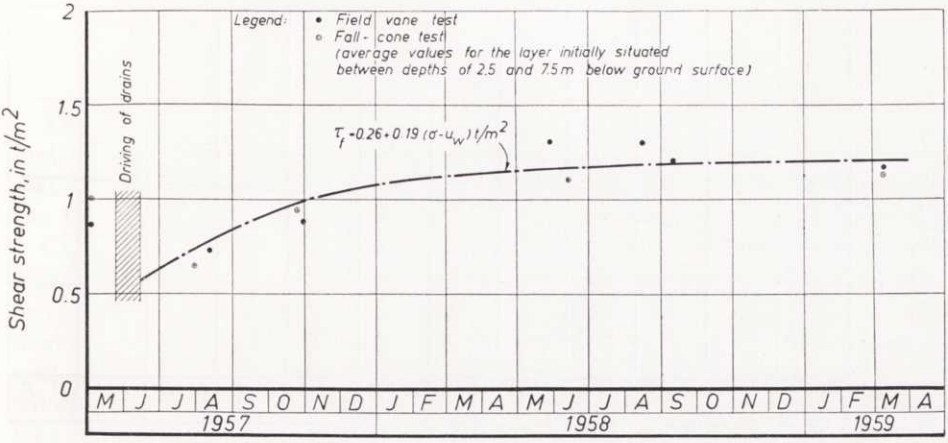

Fig. 88. Observed shear strength values before and after driving of drains. Test Area No. I, drain spacing 0.9 m.

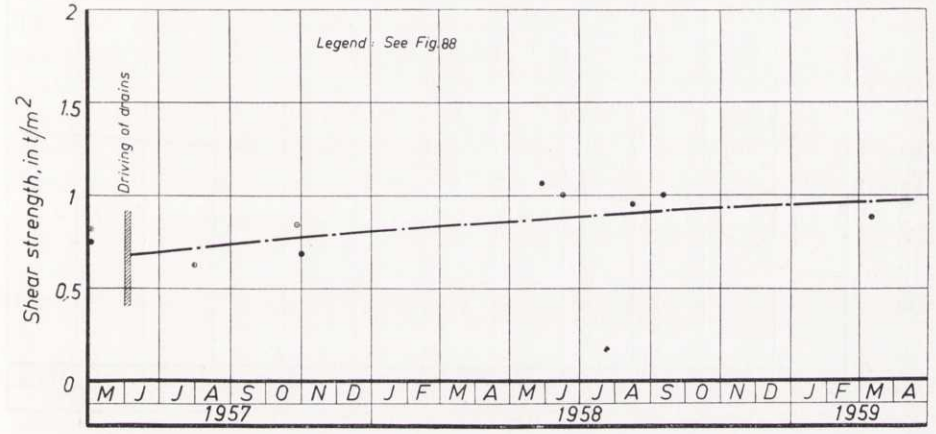

Fig. 89. Observed shear strength values before and after driving of drains. Test Area No. I, drain spacing 1.5 m.

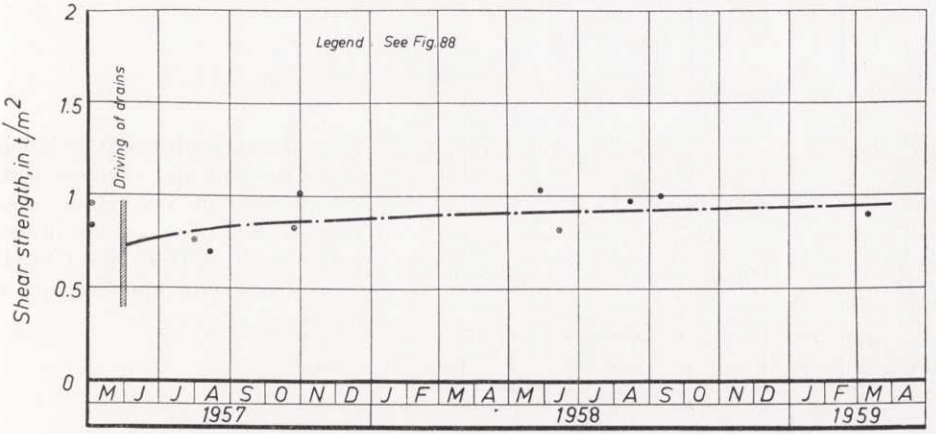

Fig. 90. Observed shear strength values before and after driving of drains. Test Area No. I, drain spacing 2.2 m.

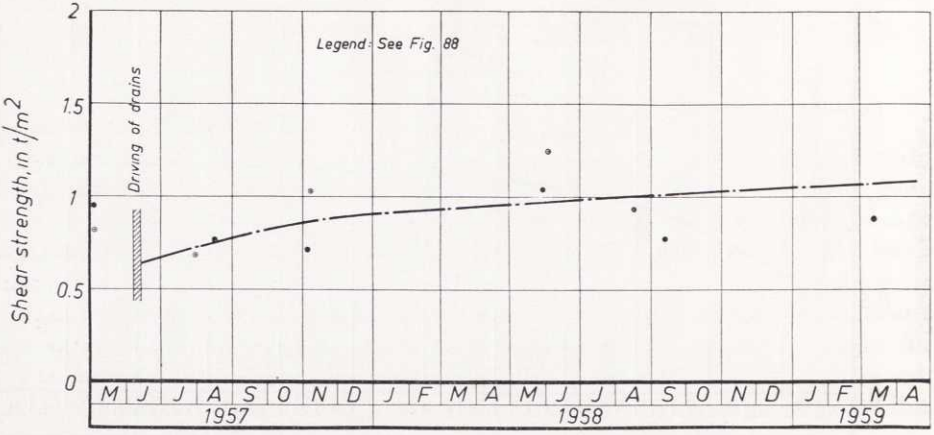

Fig. 91. Observed shear strength values before and after driving of drains. Test Area No. II.

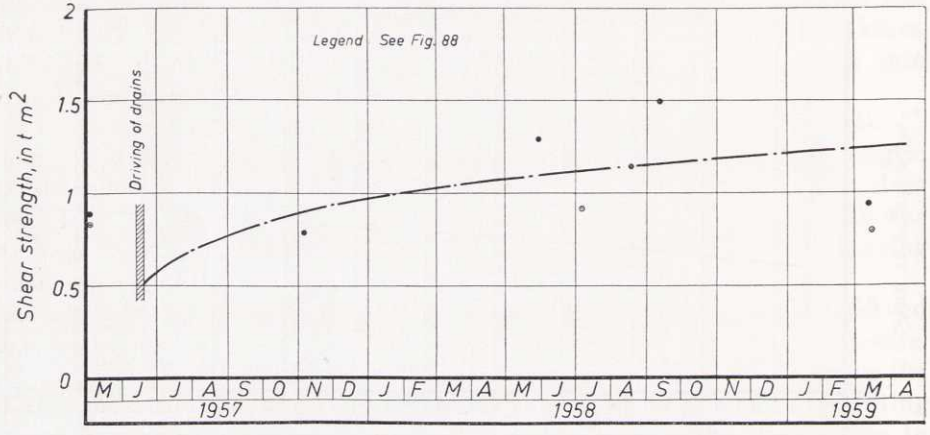

Fig. 92. Observed shear strength values before and after driving of drains. Test Area No. III.

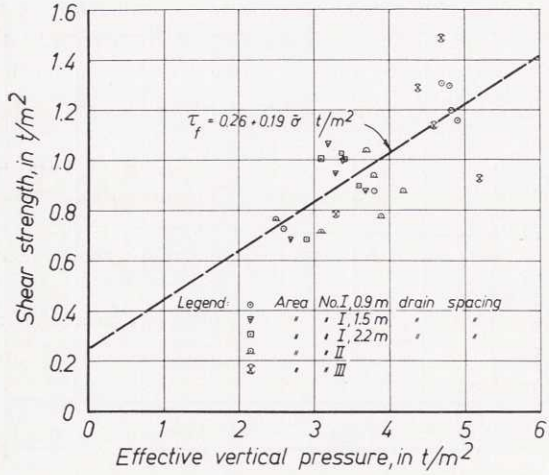

Fig. 93. Relation between undrained shear strength and effective vertical pressure obtained from shear strength and pore pressure investigations in Test Areas Nos. I to III. Values observed after driving of drains.

6. Summary

The present paper deals with the special problems of consolidation which are met with when vertical sand drains are used in order to accelerate the rate of settlement of clay. Furthermore, certain particular phenomena connected with the consolidation problem as a whole are also treated.

Chapter 1 contains a review of some important theories of consolidation. Chapter 2 gives some results of research on pore water pressures and "friction", or rather, "bond", between the ring and the clay in the oedometer test. Chapter 3 deals with the permeability of clay. The results of permeability tests are presented and a new theory of permeability is suggested. A new equation of consolidation is advanced in Chapter 4. Finally, in the light of the new findings, Chapter 5 gives the results obtained in connection with full-scale investigations in a test field, established in 1957 at Skå-Edeby, 25 km west of Stockholm.

Laboratory Research

The investigations dealt with in Chapters 2 and 3 were made on saturated clay samples from the test field at Skå-Edeby. Their results are stated in what follows.

(1) During the oedometer test the distribution of pore water pressure over the impermeable base of the clay specimen (in a conventional oedometer with drainage at top and bottom corresponding to the "midplane" of the specimen) was fairly uniform when the preconsolidation load had been exceeded. In this case the oedometer test can therefore be considered representative of the theoretical case of an infinitely extended, uniformly loaded clay layer submitted to consolidation. However, when the load was below the preconsolidation load, the pore water pressure in the vicinity of the cylindrical boundary of the specimen was about zero. Accordingly, this case did not fulfil the conditions stated in the above theoretical case.

The pore water pressure caused in the loading operation corresponded fairly well with the magnitude of the load increment. However, a rapid decrease of pore water pressure occurred, which did not seem to be due to escape of pore water and which, consequently, did not obey TERZAGHI's consolidation theory. Thus it seemed as if some of the pore water released by the application of the load were bound again to the soil in the course of time (thixotropy). The observed decrease of pressure was of varying order of magnitude, and seemed to bear a certain relationship to the magnitude of the compression increment due to consolidation.

(2) The "friction" between the clay specimen and the oedometer ring was reduced when the preconsolidation load was exceeded. An immediate fall of friction took place after the application of a new load increment. This indicates that the loading operation involved a decrease of effective intergranular pressure.

The coefficient of friction during unloading of a sample was considerably higher than that during loading.

A variation of friction was observed.

(3) The permeability tests were made in order to find out whether or not DARCY's law of permeability could be applied to clays subjected to small hydraulic gradients. For the investigated clays, the flow of water was then found to follow a revised law of permeability, given by Eqs. (3: 1) and (3: 2), with the exponent n varying from 1.0 to 1.5. For sufficiently small hydraulic gradients, which corresponded to those occurring in practice in the field, the permeability obeyed Eq. (3: 1).

During a permeability test the pores in the clay were sometimes partly clogged and sometimes partly widened. This may indicate the existence of particles that were free, or were bound loosely enough to be moved even by extremely small hydraulic gradients.

The observed deviation from DARCY's law was assumed to depend on the character of the clay. Thus, for example, for a clay which obeyed DARCY's law, the titre curve obtained by pH-metric titration was different from those obtained for the clays which deviated from DARCY's law of permeability.

On the basis of the new theory of permeability the Author advanced an equation of consolidation in the case of vertical sand drains on the simplified assumption of "equal strains". The time of consolidation thus obtained is defined by Eq. (4: 8), and differs from that determined by the classical equation of consolidation, *e.g.* in being dependent on the initial excess pore water pressure. From the expressions for the pore pressure gradient, Eq. (4: 11), and the permeability, Eqs. (3: 1) and (3: 2), it was found that a consolidometer test with central drain cannot be made so as to be representative of field conditions.

Field Investigations

In planning the field investigations, it was originally intended to study, among other things, the influence exerted on consolidation by varying drain spacing and varying load, and to examine the disturbance of clay caused by driving of drains. For this purpose, four test areas were established. Three of these areas were furnished with vertical sand drains, about 18 cm in diameter. One of these areas, 70 m in diameter, was divided into three equal sectors with the respective drain spacings 0.9, 1.5 and 2.2 m. In the other two, 35 m in diameter each, a drain spacing of 1.5 m was used throughout. The fourth area, 35 m in diameter, was left "undrained" in order that the effect of sand drains alone might be segregated in the results obtained from drained areas. All the areas were equally loaded, except one of the smaller, drained areas, which was more heavily loaded than the others (2.7 and 3.9 t/m^2, respectively). The areas were provided with an extensive measuring equipment.

The clay properties were subjected to a thorough investigation of conventional type. The clay was found to be saturated. It was fairly soft even for Swedish conditions (shear strength varying from about 0.05 kg/cm^2 below the dry crust to 0.1 or 0.2 kg/cm^2 near firm bottom), and had normal sensitivity (in general varying from 5 to 15).

The depth to firm bottom varied in the four test areas, and was 11 m on an average. The ground water table was located just below the dry crust. Layers

of silt or sand were generally found near firm bottom. In the consolidation studies it has been attempted to avoid the influence of these layers or of the dry crust near the ground surface. Therefore, a special study was made of that clay layer which had originally been situated between the depths of 2.5 and 7.5 m below the ground surface. The compressibility of this layer, defined by the deformation caused by doubling the load, varied from 13 to 18%. The coefficient of consolidation, as found from the conventional oedometer test, varied from $0.4 \cdot 10^{-4}$ to $0.7 \cdot 10^{-4}$ cm^2/sec. However, the consolidometer tests which allowed pore water escape in a direction parallel to the clay strata gave considerably higher values of the coefficient of consolidation.

In the other investigations made in the test field, the following phenomena were mainly considered:

(1) Disturbance due to driving of drains.
(2) Distribution of excess pore water pressure under loaded area.
(3) Distribution of settlement under loaded area.
(4) Rates of consolidation obtained from observed excess pore water pressures and settlement.
(5) Stiffening effect produced on clay by sand drains.
(6) Increase in shear strength due to consolidation.

The following observations were made.

(1) Driving of drains caused a considerable disturbance of the clay inside and immediately outside the drained areas. This disturbance was directly visible both in pore water pressure measurements and in shear strength observations.

The resulting excess pore water pressure increased with decreasing drain spacing and also with increasing average drain length. The maximum "disturbance pressures" obtained inside the areas after completion of drainage varied from about 0.2 kg/cm^2 at 2.2 m drain spacing to about 0.4 kg/cm^2 at 0.9 m spacing. The observed average disturbance pressures amounted to about half the above values. The disturbance tended to increase towards the centres of the areas.

Furthermore, driving of drains caused a decrease of about 20 to 40 % in the original shear strength values. In this case, too, the disturbance tended to increase with decreasing spacing and increasing length of drains.

The above disturbance was also visible indirectly, *e.g.* in observations of horizontal displacements of the ground surface at the peripheries of the areas. It was found that driving of drains also appreciably reduced the rigidity of the clay outside the areas.

Furthermore, the displaced soil caused a heave of the ground surface.

(2) The distribution of excess pore water pressure due to loading was studied in the undrained area at a depth of 5 m below ground surface. The results were compared with the theoretical stress distribution under a circular load on an elastic isotropic semi-infinite body. By inserting these stresses (POISSON's ratio = $= 0.5$) into SKEMPTON's pore pressure equation (assuming that the pore pressure coefficient $B = 1$), a good agreement was obtained with the observed excess pore pressures inside the area, provided that the pore pressure coefficient A was equal

to 0.77. The pore water pressures observed at the periphery of the area may have been influenced by creep of the clay. Thus the theoretical shearing stresses at the periphery equalled or even exceeded the observed shear strength of the clay.

In the drained areas the momentary increase of excess pore water pressures during loading corresponded fairly well with the load increments.

The loading operation also caused an excess pore water pressure that was observed in the piezometers placed as far as 35 m outside the periphery of that loaded area which is 70 m in diameter.

(3) The distribution of settlement observed just after the application of the load corresponded fairly well with that in an elastic medium having POISSON's ratio ν of 0.3 to 0.5. In the drained areas the gradual redistribution of intergranular pressure in the process of consolidation changed the settlement distribution in a way corresponding to a decrease in ν. The settlement distribution was also influenced by sideward outflow of clay.

In the undrained area the distribution of settlement was influenced by escape of pore water in an outward radial direction.

(4) The rates of consolidation obtained from the pore water pressure and settlement observations were compared with one another and with those computed from the classical and new consolidation equations. The average pore pressure dissipation observed inside the drained areas were in close agreement with the new consolidation equation, see Eq. (4: 8), and gave a probable value of the exponent n of 1.5 to 1.6. The agreement with the classical consolidation equation, see Eq. (1: 29), was not equally good. The main argument in favour of the new equation is the fact that the rate of pore pressure dissipation increased with increasing magnitude of consolidation load.

The coefficient of consolidation had to be reduced in view of the disturbance caused by driving of drains. Thus, for example, the value of the coefficient of consolidation to be used in the theory for 0.9 m drain spacing was only half the value corresponding to 1.5 m spacing.

The rate of settlement differed appreciably from the rate of pore pressure dissipation. In this case, too, the new equation of consolidation was in closer agreement with the results.

The conventional method of determining the degree of consolidation by settlement observation was shown to be difficult. Thus, the settlement was influenced by lateral outflow of clay, whose magnitude was difficult to find with the types of measuring equipment available at that time. Furthermore, the final settlement value to be used in this method will not be known with certainty until the settlement is completed or, at least, nearly completed.

A certain seasonal influence was exerted on the rate of settlement and on the excess pore water pressures.

(5) A stiffening effect of the sand drains on the clay was observed only in the case of 0.9 m drain spacing. It is often assumed that, during consolidation, the drains act like columns, which are less compressible than the surrounding clay, and which therefore carry part of the load. This assumption was not

confirmed in practice. On the contrary, for drain spacings of 0.9 and 1.5 m, the settlement was more advanced in the vicinity of a drain, and this is in agreement with BARRON's "free strain" hypothesis.

(6) The average increase of undrained shear strength due to consolidation was found to follow approximately Eq. (5: 9). Great scattering in shear strength values was obtained. This was probably due to varying distance from the investigated clay to neighbouring sand drains.

7. Appendix

70. Equations of Stress Distribution under Circular Loaded Area Based on Assumption of Elastic Body

The problem of stress distribution in a semi-infinite elastic body submitted to a concentrated external load was originally solved by BOUSSINESQ (1885). His solution is general, and can formally be applied to any law of distribution of pressure over an area having a boundary of any form.

In the case of uniform pressure q over a circular area with radius a on a semi-infinite body having a constant value of modulus of elasticity, E, a solution was given by LOVE (1929). The following stress equations are obtained from his solution, *cf.* Fig. 94.

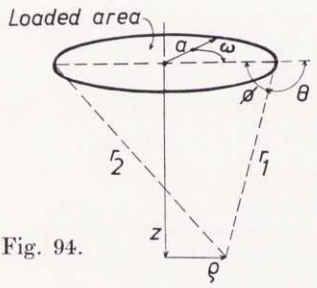

Fig. 94.

If $\varrho < a$, $0 \leqq \phi \leqq \frac{\pi}{2}$, we have

$$\sigma_z = -\frac{q}{\pi}\left[\pi - K'E(\phi) + (K' - E')F(\phi) - \frac{z}{r_2}\left(K' - \frac{r_1^2 + r_2^2 - 4a^2}{2r_1^2}\right)E'\right] \quad .. \quad (7:1)$$

$$\sigma_\varrho = -\frac{q}{\pi}\left\{2\nu\left[\pi - K'E(\phi) + (K' - E')F(\phi) - K'\frac{z}{r_2}\right] + \frac{1-2\nu}{2}\left[\pi - \frac{z r_2}{\varrho^2}E' + \right.\right.$$
$$+ \frac{z(2a^2 + z^2)}{r_2 \varrho^2}K' - \frac{a^2 + \varrho^2}{\varrho^2}\left(K'E(\phi) - (K' - E')F(\phi)\right)\Big] +$$
$$\left. + \frac{z}{2}\left[\left(\frac{r_1^2 + r_2^2 - 4a^2}{r_1^2 r_2} - \frac{2r_2}{\varrho^2}\right)E' - \frac{2K'}{r_2} + \frac{r_2}{\varrho^2}(1 + k^2)K'\right]\right\} \quad .. \quad (7:2)$$

$$\sigma_\omega = -\frac{q}{\pi}\left\{2\nu\left[\pi - K'E(\phi) + (K'-E')F(\phi)\right] + \frac{1-2\nu}{2}\left[\pi + \frac{z\,r_2}{\varrho^2}E' - \right.\right.$$
$$- \frac{z(2a^2+2\varrho^2+z^2)}{r_2\varrho^2}K' + \frac{a^2-\varrho^2}{\varrho^2}\left(K'E(\phi) - (K'-E')F(\phi)\right)\Big] -$$
$$\left. - \frac{z\,r_2}{2\varrho^2}\left[(1+k^2)K' - 2E'\right]\right\} \quad \ldots\ldots\ldots\ldots\ldots \quad (7:3)$$

where
$$K' = \int_0^{\pi/2} \frac{d\phi_1}{\sqrt{1-k'^2\sin^2\phi_1}} \qquad k = \frac{r_1}{r_2} = \sin\alpha$$
$$E' = \int_0^{\pi/2} \sqrt{1-k'^2\sin^2\phi_1}\; d\phi_1 \qquad k' = \sin\left(\frac{\pi}{2} - \alpha\right)$$
$$F(\phi) = \int_0^{\phi} \frac{d\phi_1}{\sqrt{1-k^2\sin^2\phi_1}}$$
$$E(\phi) = \int_0^{\phi} \sqrt{1-k^2\sin^2\phi_1}\; d\phi_1$$

K' and E' are complete elliptic integrals of first and second order, respectively, whereas F and E are incomplete elliptic integrals of first and second order.

If $\varrho > a$, $0 \leqq \Theta \leqq \frac{\pi}{2}$, we have

$$\sigma_z = -\frac{q}{\pi}\left[K'E(\Theta) - (K'-E')F(\Theta) - \frac{z}{r_2}\left(K' - \frac{r_1^2+r_2^2-4a^2}{2r_1^2}\right)E'\right] \quad .. \quad (7:4)$$

$$\sigma_\varrho = -\frac{q}{\pi}\left\{2\nu\left[K'E(\Theta) - (K'-E')F(\Theta) - \frac{K'z}{r_2}\right] + \frac{1-2\nu}{2}\left[-\frac{\pi a^2}{\varrho^2} - \frac{z\,r_2}{\varrho^2}E' + \right.\right.$$
$$+ \frac{z(2a^2+z^2)}{r_2\varrho^2}K' + \frac{a^2+\varrho^2}{\varrho^2}\left(K'E(\Theta) - (K'-E')F(\Theta)\right)\Big] +$$
$$\left. + \frac{z}{2}\left[\left(\frac{r_1^2+r_2^2-4a^2}{r_1^2\,r_2} - \frac{2\,r_2}{\varrho^2}\right)E' - \frac{2}{r_2}K' + \frac{r_2}{\varrho^2}(1+k^2)K'\right]\right\} \ldots\ldots \quad (7:5)$$

$$\sigma_\omega = -\frac{q}{\pi}\left\{2\nu\left[K'E(\Theta) - (K'-E')F(\Theta)\right] + \frac{1-2\nu}{2}\left[\frac{\pi a^2}{\varrho^2} + \frac{z\,r_2}{\varrho^2}E' - \right.\right.$$
$$- \frac{z(2a^2+2\varrho^2+z^2)}{r_2\varrho^2}K' - \frac{a^2-\varrho^2}{\varrho^2}\left(K'E(\Theta) - (K'-E')F(\Theta)\right)\Big] -$$
$$\left. - \frac{z\,r_2}{2\varrho^2}\left[(1+k^2)K' - 2E'\right]\right\} \ldots\ldots\ldots\ldots\ldots \quad (7:6)$$

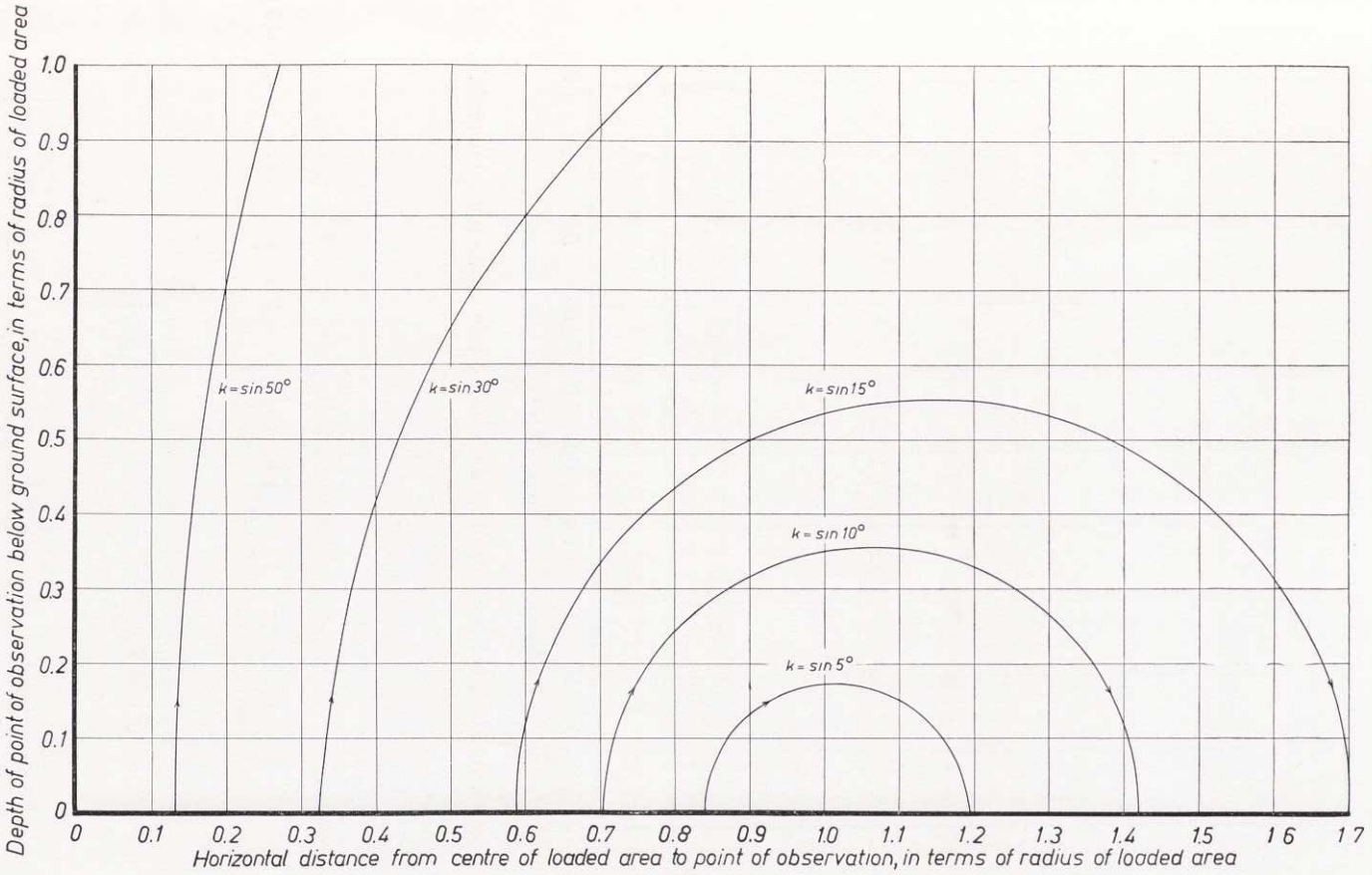

Fig. 95. Relation between z and ϱ for various values of elliptic integrals.

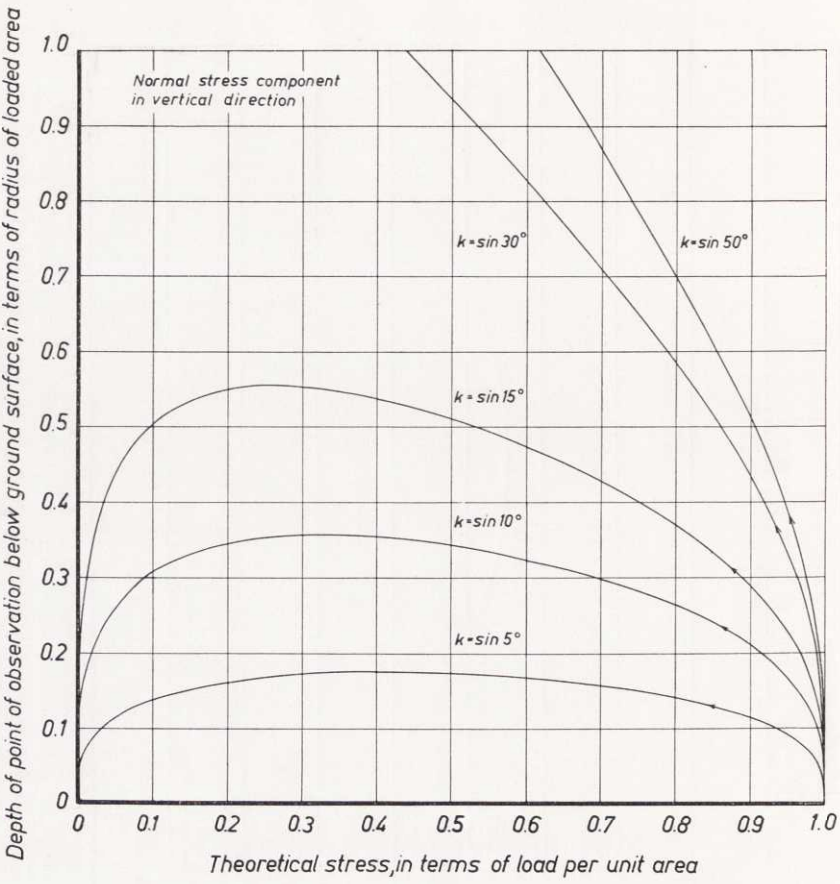

Fig. 96. Relation between z and σ_z for various values of elliptic integrals.

Finally, we have

$$\tau_{\varrho z} = -\frac{q}{\pi}\,\frac{z^2}{2\,r_2\,\varrho}\left[\left(1+\frac{1}{k^2}\right)E' - 2\,K'\right] \qquad (7:7)$$

If $\varrho = 0$, we have

$$\sigma_z = q\left[-1+\frac{z}{\sqrt{a^2+z^2}} - \frac{a^2\,z}{(a^2+z^2)^{3/2}}\right]$$

$$\sigma_\varrho = \sigma_\omega = q\left[\frac{1+2\,\nu}{2}\left(-1+\frac{z}{\sqrt{a^2+z^2}}\right) + \frac{a^2\,z}{2\,(a^2+z^2)^{3/2}}\right]$$

$$\tau_{\varrho z} = 0$$

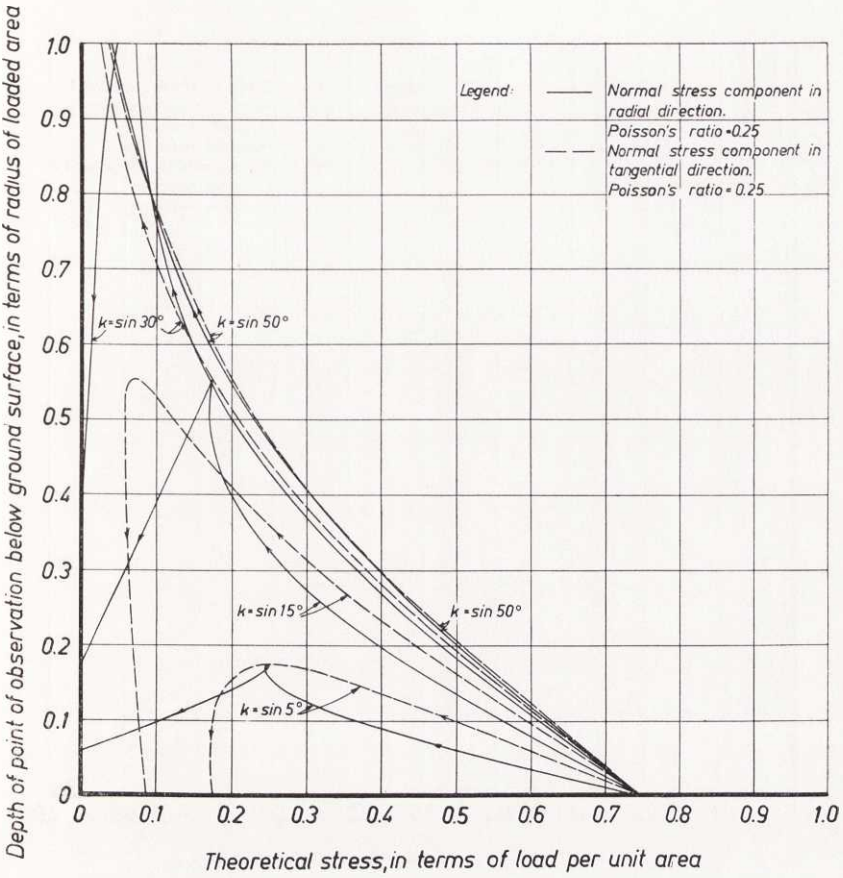

Fig. 97. Relation between z and σ_ϱ, and z and σ_ω for various values of elliptic integrals. POISSON's ratio $\nu = \frac{1}{4}$.

To give LOVE's solution a more practical form for our purpose, it has been represented in diagrams, Figs. 95 to 98.

The maximum error due to the assumption of a semi-infinite body can be estimated by comparing a given stress at a certain definite depth under the centre of a loaded area with that calculated on the assumption of firm bottom at this depth (CUMMINGS, 1941). As the actual depth to firm bottom in the present cases varies from 9 m to more than 15 m, and is approximately 11 m on an average, the difference in stress between these two cases is considerably greater than in reality. By using this method (assuming POISSON's ratio $\nu = 0.5$), the maximum error is found to be, for example, about 10 % at a depth of 10 m, 7 % at a depth of 7.5 m, and 1 % at a depth of 5 m below ground surface. The real error can obviously be neglected (*cf.* also GRANHOLM, 1956).

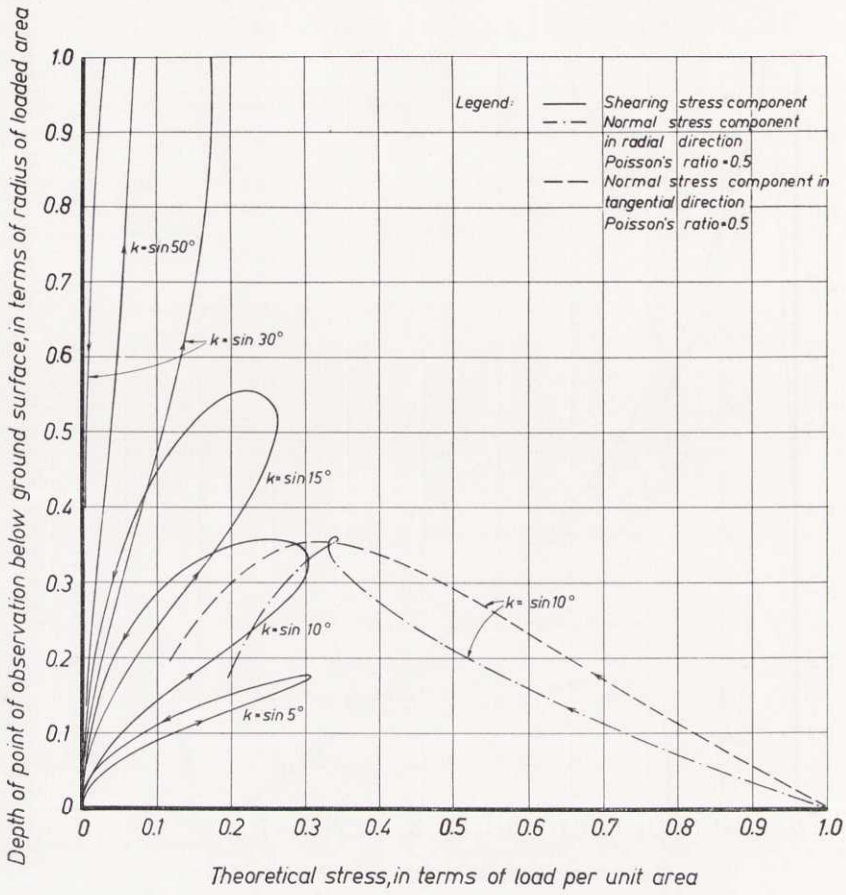

Fig. 98. Relation between z and $\tau_{\varrho z}$, z and σ_{ϱ}, and z and σ_{ω} for various values of elliptic integrals.

σ_{ϱ} and σ_{ω} determined on the assumption that POISSON's ratio $\nu = \frac{1}{2}$.

The assumption that the modulus of elasticity is constant throughout the soil is justifiable in our case, where the soil consists of clay of high plasticity (*cf.* FRÖHLICH, 1934, p. 89).

Notations

A	SKEMPTON's first pore pressure coefficient.
A_f	Filter area of piezometer.
a	Coefficient of total compressibility. TAYLOR. Also root of equation. Also radius of circular load area.
a_f	Final compressibility. BIOT.
a_i	Instantaneous compressibility. BIOT.
a_v	Coefficient of primary compressibility. TERZAGHI.
B	SKEMPTON's second pore pressure coefficient.
B.	Firm bottom.
b	Coefficient.
C	Constant of integration.
C_c	Compression index.
c_a	Coefficient of consolidation for varying permeability in two-dimensional consolidation by the use of drain wells. SCHIFFMAN.
c_f	Final coefficient of consolidation for varying permeability in two-dimensional consolidation by the use of drain wells. SCHIFFMAN.
c_h	Coefficient of consolidation in two-dimensional consolidation by the use of drain wells.
c_V	Coefficient of consolidation for varying permeability in one-dimensional vertical consolidation. SCHIFFMAN.
c_v	Coefficient of consolidation in one-dimensional vertical consolidation. TERZAGHI.
c'_v	Coefficient of consolidation in one-dimensional vertical consolidation. BIOT.
c_p	Coefficient of consolidation in one-dimensional vertical consolidation taking account of secondary consolidation. TAYLOR.
D	Diameter of zone of influence of a drain well (sand drain).
D_f	Diameter of zone of influence of a drain well (sand drain) under field conditions.

D_c	Diameter of zone of influence of a drain well (sand drain) under laboratory conditions.
d	Diameter of drain well (sand drain).
d_f	Diameter of drain well under field conditions.
d_c	Diameter of drain well under laboratory conditions.
E	Modulus of elasticity.
E'	Complete elliptic integral of second order.
$E(\phi)$, $E(\Theta)$	Incomplete elliptic integrals of second order.
e	Void ratio (ratio of volume of voids to volume of solids).
e_0	Initial void ratio before application of a pressure increment.
e_1, e_2	Void ratios at beginning and end of a pressure increment. TAYLOR.
e'_1, e'_2	Void ratios at beginning and end of primary compression. TAYLOR.
erfc	Complementary error function.
exp	$\exp x = e^x$.
$F(\phi)$, $F(\Theta)$	Incomplete elliptic integrals of first order.
F, f	Functions.
G	Modulus of shear.
G.	Ground surface.
g	Function of Poisson's ratio. TAN.
H	Depth from ground surface to firm bottom.
h	Thickness of clay layer.
h_s	That part of thickness h which corresponds to solid substance.
I	Influence value.
i	Hydraulic gradient.
i_0, i_l	Characteristic values of hydraulic gradient.
J	Variable used by TAYLOR.
J_0, J_1	Bessel functions of first kind of zero and first order.
K_1, K_2, K_3	Functions.
K'	Complete elliptic integral of first order.
k	Coefficient of permeability. Also modulus of elliptic integral.
$\bar{k}$	Average coefficient of permeability.
k'	Complementary modulus of elliptic integral.
k_0	Initial value of coefficient of permeability.

k_f	Final value of coefficient of permeability.
L	Drain spacing.
ln	Natural logarithm.
log	BRIGG's logarithm.
m	Positive integer 0, 1, 2, . . ., ∞.
m_v	Coefficient of volume compressibility. TERZAGHI.
N	$\frac{\pi}{2}, \frac{3\pi}{2}, \frac{5\pi}{2}, \ldots, \frac{(2m+1)\pi}{2}, \ldots, \infty$.
n	Exponent in new permeability equation.
n'	Porosity (ratio of volume of voids to total volume).
n'_0	Initial porosity.
P	Piezometer.
P1: 2.5, *etc.*	Piezometer No. 1 placed at a depth of 2.5 m below ground surface, *etc.*
p	$\partial/\partial t$, HEAVISIDE's operator. TAN.
Q	Coefficient determined by the degree of saturation of a clay. BIOT.
q	Load.
R	Radius of zone of influence of a drain well (sand drain).
R_A	Radius of loaded area.
R_u	Rate of imposed excess pore water pressure. SCHIFFMAN.
r	Radius of drain well (sand drain).
r_0	Equivalent radius of filter area of piezometer.
r_1/r_2	Modulus of elliptic integral.
r_p	Ratio of primary compression to total compression (primary compression ratio). TAYLOR.
r'_p	Primary compression ratio on previous secondary compression basis. TAYLOR.
T	Time lag of piezometer.
T_f	Final time factor for varying permeability in two-dimensional consolidation. SCHIFFMAN.
T_h	Time factor in two-dimensional consolidation by the use of drain wells.
T_k	Time factor in one-dimensional vertical consolidation. TAYLOR.

T_V	Time factor for varying permeability in one-dimensional vertical consolidation. SCHIFFMAN.
T_v	Time factor in one-dimensional vertical consolidation. TERZAGHI.
t	Metric ton (= 1000 kg).
t	Time.
t_a	The time when the rates of settlement for primary and secondary consolidation are equal. ZEEVAERT.
U	Consolidation ratio (general expression).
$\bar{U}$	Average of U.
U'	Excess pore pressure dissipation ratio. TAYLOR.
U_a	"Aggregate" consolidation ratio. TAYLOR and MERCHANT.
U_h	Consolidation ratio in two-dimensional consolidation by the use of drain wells.
U_v	Consolidation ratio in one-dimensional vertical consolidation.
u	Excess pore water pressure.
$\bar{u}$	Average of u.
u_0	Initial value of u.
u_2	Characteristic value of u. SCHIFFMAN.
u_d	Excess pore water pressure caused by disturbance.
u_h	Excess pore water pressure at impermeable base of a single-drained clay layer.
u_w	Total pore water pressure.
V	Vertical settlement meter.
V1: 1.5, *etc.*	Vertical settlement meter No. 1 placed at a depth of 1.5 m below ground surface, *etc.*
v	Rate of flow (flow per unit area per unit time).
w	Natural water content. Also displacement in z-direction.
$\bar{w}$	Average water content.
w_0	Initial water content.
w_L	Liquid limit.
w_P	Plastic limit.
x	Variable.
Y_0, Y_1	Bessel functions of second kind of zero and first order.
z	Vertical coordinate. Also depth below ground surface.

a	Function. Also angle.
a_b	Coefficient determined by the degree of saturation of a clay. BIOT.
a_c	Constant. SCHIFFMAN.
a_e	Coefficient. ŠUKLJE.
a_p, a_s	Constants. BUISMAN.
β	Constant. SCHMID-SCHIFFMAN.
γ'	Unit volume weight of submerged soil.
γ_s	Specific gravity of solids.
γ_w	Unit volume weight of water.
Δ	Increment.
Δh	Compression of a clay layer of thickness h.
Δq	Pressure (load) increment under which consolidation takes place.
$\Delta\sigma$	Normal pressure increment.
$\Delta\bar{\sigma}$	Effective intergranular pressure increment.
δ	Settlement (compression) at the time t due to consolidation.
δ_1	Characteristic part of settlement.
δ_f	Final settlement (compression). TAYLOR and MERCHANT.
δ_{fl}	Settlement (compression) due to lateral outflow of soil.
δ_g	Settlement of ground surface.
$\delta_{h,fl}$	Horizontal displacement due to lateral outflow.
δ_i	Instantaneous settlement.
δ_p	Primary settlement (compression).
δ_s	Secondary settlement (compression).
δ'_s	Undeveloped part of secondary settlement (compression). TAYLOR and MERCHANT.
δ_t	Settlement (compression) taking account of primary and secondary effects. BUISMAN.
δ_{tot}	Total settlement.
ε	Strain.
ε_2	Compression index often used in Sweden. ODENSTAD.
η	Shear viscosity of soil skeleton. TAN.
$\bar{\eta}$	Viscosity constant. TAYLOR.

Θ	Constant. TAN. Also angle.
$\varkappa$	Coefficient of permeability.
λ	Coefficient of consolidation.
λ_s	Coefficient. TAN.
μ	Coefficient. SKEMPTON and BJERRUM.
μ_c	Constant. TAYLOR and MERCHANT.
μ_s	Coefficient. TAN.
ν	POISSON's ratio.
ν_c	Constant. SCHIFFMAN.
ϱ	Radius vector from the central axis (cylindrical coordinates).
σ	Normal pressure.
$\bar{\sigma}$	Effective intergranular pressure.
$\bar{\sigma}_0$	Effective preconsolidation pressure.
$\bar{\sigma}_b$	Bond resistance. TAYLOR.
$\bar{\sigma}_v$	Viscous structural resistance. TAYLOR.
σ_z	Normal stress component in vertical direction.
σ_ϱ	Normal stress component in radial direction.
σ_ω	Normal stress component in tangential direction.
τ_f	Shear strength.
$\tau_{\varrho z}$	Shearing stress component.
Φ_1, Φ_2, Φ_3	Functions. TAYLOR.
ϕ	Angle.
χ	Coefficient of lateral outflow.
ψ	Function. TAN.
ω	Function. TAN. Also vectorial angle.

Bibliography

Arai, H., 1955. Pore Water Pressure Measurements during Consolidation Tests. *Rep. Transp. Techn. Res. Inst., Japan.*

Barber, E. S. and Steffens, G. P., 1958. Pore Pressures in Base Courses. *Public Roads, Vol. 30 No. 3 p. 53—62.*

Barron, R. A., 1944. The Influence of Drain Wells on the Consolidation of Fine-Grained Soils. *(R. I.) Diss. Providence, U. S. Engng. Office.*

— 1948. Consolidation of Fine-Grained Soils by Drain Wells. *Amer. Soc. Civ. Engrs. Paper No. 2346* (with discussions).

Bergström, S. G. and Linderholm, S., 1946. A Dynamic Method for Determining Average Elastic Properties of Surface Soil Layers. *Swed. Cem. a. Concr. Res. Inst. Proc. No. 7.*

Biot, M. A., 1935. Le problème de la consolidation des matières argileuses sous une charge. *Ann. Soc. Scient. Bruxelles, Vol. 55.*

— 1941. General Theory of Three-Dimensional Consolidation. *J. Appl. Phys. Vol. 12.*

Bishop, A. W. and Henkel, D. J., 1957. The Measurement of Soil Properties in the Triaxial Test. *London.*

Bodman, G. B., 1937. The Variability of the Permeability »Constant» at Low Hydraulic Gradients during Saturated Water Flow in Soils. *Proc. Soil Sci. Soc. Amer. Vol. 2, pp. 45—53.*

Boussinesq, J., 1885. Application des potentiels à l'étude de l'équilibre et du mouvement des solides élastiques. *Paris.*

Brenner, Th., 1946. Om mineraljordarternas hållfasthetsegenskaper (On the Strength Properties of Mineral Soils). *Bull. Géol. Finlande No. 139, Helsinki.*

Brinch Hansen, J., 1957. Calculation of Settlements by Means of Pore Pressure Coefficients. *Acta Polytechnica. Civ. Engng. Build. Constr. Vol. 4. No. 8.*

Buisman, A. S. K., 1936. Results of Long Duration Settlement Tests. *Proc. 1. Internat. Conf. Soil Mech. a. Found. Engng., Vol. 1.*

Buisson, M., 1953. Fondations des constructions et des barrages, charge admissible, observation des tassements, affaissements régionaux. *General Report, Proc. 3. Internat. Conf. Soil Mech. a. Found. Engng., Vol. 2.*

Burmister, D. M., 1951. General Discussion. *Symposium on Consolidation Testing of Soils. Amer. Soc. Test. Mat., Spec. Techn. Publ. No. 126.*

Cadling, L. and Odenstad, S., 1950. The Vane Borer. An Apparatus for Determining the Shear Strength of Clay Soils Directly in the Ground. *Swed. Geot. Inst. Proc. No. 2.*

Carillo, N., 1942. Simple Two and Three Dimensional Cases in the Theory of Consolidation of Soils. *J. Math. Phys., Vol. 21 No. 1.*

Casagrande, A., 1936. The Determination of the Pre-Consolidation Load and its Practical Significance. Discussion. *Proc. 1. Internat. Conf. Soil Mech. a. Found. Engng. Vol. 3.*

Casagrande, A. and Fadum, R. E., 1940. Notes on Soil Testing for Engineering Purposes. *Harv. Soil. Mech. Ser. No. 8.*

Churchill, R. V., 1944. Modern Operational Mathematics in Engineering. *New-York.*

Cummings, A. E., 1941. Foundation Stresses in an Elastic Solid with a Rigid Underlying Boundary. *Civ. Engng. Vol. 11 No. 11.*

Darcy, H., 1856. Les fontaines publiques de la ville de Dijon. *Paris.*

Дерягин, Б. В., и Крылов, Н. А., 1944. Аномальные явления при течении жидкостей через жесткие узкопористые фильтры. (Предварительное сообщение). *Академия наук СССР.*

(Deryagin, B. V. and Krylov, N. A., 1944. Anomalies Observed in the Flow of Liquids through Hard Fine-Porous Filters. (Preliminary Paper.) *Academy of Sciences, USSR.)*

Finn, F. N., 1951. The Effect of Temperature on the Consolidation Characteristics of Remoulded Clay. *Symposium on Consolidation Testing of Soils. Amer. Soc. Test. Mat., Spec. Techn. Publ. No. 126.*

Флорин, В. А., 1959. Основы механики грунтов, Том I. *Ленинград и Москва.*
(Florin, V. A., 1959. Basic Soil Mechanics, Vol. I. *Leningrad & Moscow.)*

Fröhlich, O. K., 1934. Druckverteilung im Baugrund. *Wien.*

Gibson, R. E. and Mc Namee, J., 1957. The Consolidation Settlement of a Load Uniformly Distributed over a Rectangular Area. *Proc. 4. Internat. Conf. Soil Mech. a. Found. Engng. Vol. 1.*

Glover, R. E., 1930. Temperature Movements in Concrete and Other Materials with Special Reference to Boulder Dam. *Techn. Mem. No. 158. Bur. Reclam, Denver, Colo.*

Goldschmidt, V. M., 1926. Undersökelser over lersedimenter. (Investigations on Clay Sediments). *Nordisk jordbrugsforskning, No. 4—7.*

Granholm, Hj., 1956. Boussinesq's problem. En approximativ beräkningsmetod. (Boussinesq's Problem. An Approximative Method of Calculation). *Bygningsstatiske Meddelelser. XXVII. No. 2.*

Grisel, F., 1936. Sur les écoulements d'eau, sous pression constante, à travers une masse de béton. *Compt. Rend. Séanc. Acad. Sci.*

Hansbo, S., 1957. A New Approach to the Determination of the Shear Strength of Clay by the Fall-Cone Test. *Swed. Geot. Inst. Proc. No. 14.*

Helenelund, K. V., 1951. Om konsolidering och sättningar av belastade marklager. (On Consolidation and Settlement of Loaded Soil-Layers). *Medd. Järnv.styr. Geot. Sekt. No. 3, Helsinki.*

de Josselin de Jong, G., 1957. Application of Stress Function to Consolidation Problems. *Proc. 4. Internat. Conf. Soil Mech. a. Found. Engng. Vol. 1.*

Järnefors, B., 1957. Utlåtande ang. lerlagerföljden vid Skå-Edeby flygfält. (Report on the Clay Stratigraphy at the Skå-Edeby Airport). *Not printed.*

Kallstenius, T., 1958. Mechanical Disturbances in Clay Samples Taken with Piston Samplers. *Swed. Geot. Inst. Proc. No. 16.*

Kallstenius, T. and Wallgren, A., 1956. Pore Water Pressure Measurements in Field Investigations. *Swed. Geot. Inst. Proc. No. 13.*

Kézdi, A., 1958. Cinq ans de mécanique du sol en Hongrie. *Ann. Inst. Techn. Bât. et Trav. Publ. Nos. 127—128, p. 866. Sols et Fond. No. 29. Paris.*

Kjellman, W., 1948. Consolidation of Fine-Grained Soils by Drain Wells. *Trans. Amer. Soc. Civ. Engrs., Vol. 113. Contribution to the Discussion.*

Kjellman, W., Kallstenius, T. and Liljedahl, Y., 1955. Accurate Measurement of Settlements. *Swed. Geot. Inst. Proc. No. 10.*

Kjellman, W., Kallstenius, T. and Wager, O., 1950. Soil Sampler with Metal Foils. Device for Taking Undisturbed Samples of Very Great Length. *Swed. Geot. Inst. Proc. No. 1.*

Koppejan, A. W., 1948. A Formula Combining the Terzaghi Load-Compression Relationship and the Buisman Secular Effect. *Proc. 2. Internat. Conf. Soil Mech. a. Found. Engng. Vol. 3.*

Lambe, T. W., 1958. The Structure of Compacted Clay. *Proc. Amer. Soc. Civ. Engrs. Vol. 84 No. SM2 Paper No. 1654.*

Leonards, G. A. and Ramiah, B. K., 1959. Time Effects in the Consolidation of Clays. *Symposium on Time-Rate of Loading in Testing Soils, ASTM, Annual Meeting. Preprint.*

Love, A. E. H., 1929. The Stress Produced in a Semi-Infinite Solid by Pressure on Part of the Boundary. *R. Soc. Phil. Trans. Vol. 228.*

Lundström, R., 1957. Grundförhållanden och sättningskalkyler för storflygplats vid Skå-Edeby. (Soil Conditions and Settlement Analyses for Intercontinental Airport at Skå-Edeby). *Väg- o. Vattenbyggaren No. 3.*

Ménard, L., 1957. Mesures in situ des propriétés physiques des sols. *Ann. Ponts et Chaussées. May-June.*

Moum, J. and Rosenqvist, I. T., 1957. Jordtemperaturen i Öst-Norge. (Ground Temperature in Eastern Norway). *Norw. Geot. Inst. Publ. No. 23.*

Muhs, H. and Kany, M., 1954. Einfluss von Fehlerquellen bei Kompressionsversuchen. *Fortschr. u. Forsch. im Bauwesen. R. D. H. 17, Grundbau, Vorschriften u. Versuche, T. 1.*

Murayama, S. and Shibata, T., 1959. On the Secondary Consolidation of Clay. *Proc. Jap. Soc. of Testing Materials.*

Odenstad, S., 1947. Jämförelse mellan olika metoder att beräkna sättningens tidsförlopp vid djupdränering. (Comparison between Different Methods of Calculating the Time-Settlement Relation in Deep Drainage). *Swed. Geot. Inst. Not published.*

— 1954. Beräkning av sättningens slutbelopp ur den jungfruliga kurvan. (Calculation of the Final Value of Settlement from the Virgin Curve.) *Swed. Geot. Inst. Not publ.*

Osterman, J., 1959. Geotekniska utredningar i anslutning till frågan om Stockholms storflygplats vid Skå-Edeby. (Geotechnical Investigations in Connection with the Project of the Stockholm Intercontinental Airport at Skå-Edeby). *Rakennusinsinööri 15: 4.*

— 1960. Notes on the Shearing Resistance of Soft Clays. *Acta Polytechnica Scandinavica. Ci 2 (263/1959).*

Reiner, M., 1960. Deformation, Strain and Flow. *London.*

Rendulic, L., 1935. Der hydrodynamische Spannungsausgleich in zentral entwässerten Tonzylindern. *Wasserw. u. Techn. Nos. 23—24 p. 250—253. Nos. 25—26 p. 269—273.*

— 1936. Porenziffer und Porenwasserdruck in Tonen. *Bauingenieur Nr 51/52.*

Richart, F. E., 1957. A Review of the Theories for Sand Drains. *Jour. Soil Mech. Found. Div., Proc. Amer. Soc. Civ. Engrs., Vol. 83, No. SM3, Paper 1301.*

Rosenqvist, I. T., 1958. Remarks to the Mechanical Properties of Soil Water Systems. *Geol. Fören. Stockholm Förh. Bd. 80 H. 4.*

Rutledge, P. C., 1939. Compression Characteristics of Clays and Application to Settlement Analysis. *Doctor's thesis, Harv. Univ. Mass. U.S.A.*

Scheidegger, A. E., 1957. The Physics of Flow through Porous Media. *London.*

Schiffman, R. L., 1958. Consolidation of Soil under Time-Dependent Loading and Varying Permeability. *Proc. Highw. Res. Board, Vol. 37.*

— 1959. Flow of Visco-Plastic Fluids through Porous Media. *Dep. Civ. Engng. Div. Soil Mech. Rensselaer Polytechn. Inst. Troy, N. Y.*

Schmertmann, J. H., 1955. The Undisturbed Consolidation Behaviour of Clay. *Trans. Amer. Soc. Civ. Engrs. Vol. 120 Paper No. 2775.*

Schmid, W. E., 1957. The Permeability of Soils and the Concept of a Stationary Boundary-Layer. *Proc. Amer. Soc. Test. Mat. Vol. 57 p. 1195—1218.*

Silfverberg, L., 1957. Chemical Determination of Soil Organic Matter. *Swed. Geot. Inst., Proc. No. 15.*

Skempton, A. W., 1954. The Pore Pressure Coefficients A and B. *Géotechnique Vol. 4 No. 4 p. 143—147.*

Skempton, A. W. and Bishop, A. W., 1954. Soils (Chapter 10, Building Materials. Their Elasticity and Inelasticity. Ed. by M. Reiner.) *Amsterdam.*

Skempton, A. W., and Bjerrum, L., 1957. A Contribution to Settlement Analysis of Foundations on Clay. *Géotechnique Vol. 7 No. 4.*

Statens Geotekniska Institut (Swedish Geotechnical Institute), 1949. *Medd. No. 2.*

Statens Järnvägar: Geotekniska Kommissionen, 1914—1922. 1922. Slutbetänkande. (Swedish State Railways: The Geotechnical Commission, 1914—1922. Final Report.) *Geotekn. Medd. Nr. 2. Stockholm.*

Stegmüller, L., 1958. Beeinflussung der Frosthebung an Strassendecken durch chemisch-physikalische Behandlung des Bodens. *Forschungsarb. aus dem Strassenwesen, H. 37.*

Šuklje, L., 1955. Influence de l'épaisseur de la couche compressible sur le caractère et la vitesse de la consolidation. *5. Congrès des Grands Barrages, Vol. 1.*

— 1957. The Analysis of the Consolidation Process by the Isotaches Method. *Proc. 4. Internat. Conf. Soil Mech. a. Found. Engng. Vol. 1.*

Tan, Tjong Kie, 1954. Onderzoekingen over de rheologische eigenschappen van klei. (Investigations on the Rheological Properties of Clay). *Doctor's Thesis. Univ. of Technology, Delft.*

— 1957. Secondary Time Effects and Consolidation of Clays. *Academia Sinica, Harbin, China.*

Taylor, D. W., 1942. Research on Consolidation of Clays. *Mass. Inst. Techn. Publ. Dep. Civ. a. Sanit. Engng. Ser. 82.*

Taylor, D. W., and Merchant, W., 1940. A Theory of Clay Consolidation Accounting for Secondary Compressions. *J. Math. a. Phys., No. 1.*

Terzaghi, K., 1923. Die Berechnung der Durchlässigkeitsziffer des Tones aus dem Verlauf der hydrodynamischen Spannungserscheinungen. *Akad. Wissensch., Wien, Sitzungsber. Bd. 132, H. 1, Mat.-Naturwissensch. Klasse.*

Terzaghi, K., 1925. Erdbaumechanik, *Leipzig u. Wien.*

— 1944. Theoretical Soil Mechanics. *New York.*

Terzaghi, K. and Fröhlich, O. K., 1936. Theorie der Setzung von Tonschichten. *Leipzig u. Wien.*

Terzaghi, K. and Peck, R. B., 1948. Soil Mechanics in Engineering Practice. *New York and London.*

Tomaschek, R., 1957. Die Flut der festen Erde. *Umschau H. 21.*

Utlåtande angående Stockholms storflygplats, alternativen vid Halmsjön respektive Skå-Edeby, avgivet den 4 september 1957. (Report on the Stockholm Intercontinental Airport, Halmsjön and Skå-Edeby Alternatives, Submitted on September 4th, 1957.)

Virgin, Ä., 1918. Markytans höjdförändringar hos lösa jordlager. (Variations in Ground Surface Level of Soft Soil Layers.) *Tekn. Tidskr., V. o. V. Vol. 48 H. 6.*

Winterkorn, H. F., 1954. Water Movement through Porous Hydrophilic Systems under Capillary, Electrical, and Thermal Potentials. *ASTM Spec. Techn. Publ. No. 163. Symp. on Permeability of Soils, Chicago, Ill., June 15th.*

Zeevaert, L., 1957. Consolidation of Mexico City Volcanic Clay. *Proc. Joint Comm. D-18 of ASTM and SMMS. Preprint.*

van Zelst, Th. W., 1948. An Investigation of the Factors Affecting Laboratory Consolidation of Clay. *Proc. 2. Internat. Conf. Soil Mech. a. Found. Engng. Vol. 7.*

Acknowledgements

I am greatly indebted to the Swedish Geotechnical Institute for its kind permission to publish this doctor's thesis in the Proceedings of the Institute. Furthermore, I wish to express my deep gratitude to Mr. Justus Osterman for his active interest in my work. His vast experience and his constant encouragement were of invaluable help in the preparation of this thesis. In addition, I wish to express my heart-felt thanks to Mr. Alf Wallgren and Mr. Jan Goldschmidt for their devoted cooperation in the design of the laboratory equipment and in the performance of the laboratory tests. Credit is also due to Mr. Ilya Cyon for his valuable linguistic collaboration. The clarifying discussions with Dr. Erik Forslind and the generous assistance of Professor Hjalmar Granholm have been most helpful in my work.

Moreover, I wish to express my sincere appreciation of the help given by all those who have contributed to this work. In particular, I wish to thank Mr. Torsten Kallstenius, who made many useful suggestions in connection with piezometer measurements, Mr. Egon Norén, who carried out the main part of the field investigations, Mr. Nils Flodin, who assisted in editing work, Mr. Oleg Wager, who helped in translating Russian quotations, Mr. Rolf Söderblom, who made the pH-metric titration tests, Mrs. Ingegerd Olofsson and Mrs. Nelly Bengtsson, who typed the manuscript, Mrs. Dagny Alm-Sjöberg, who prepared the drawings for reproduction, and the staff of the Consulting Laboratory of the Institute, who made the routine laboratory investigations.

Stockholm, March, 1960.

Sven Hansbo

GÖTEBORG 1960
ELANDERS BOKTRYCKERI AKTIEBOLAG